Molecular Angiogenesis Laboratory
Faculty of Sciences
University of Liège

Cell communication via microRNA exchange between endothelial and tumour cells during anti-cancer neoadjuvant chemotherapy

Stella Dederen

Thesis submitted in partial fulfilment of the requirements for the degree of Doctor in Sciences by the University of Liège

Supervisor: Dr. Ingrid Struman

Academic year 2018-2019

LIÈGE université
GIGA institute

Molecular Angiogenesis Laboratory

Coming back to where you started is not the same as never leaving

Terry Pratchett

Avant tout, je tiens à remercier ma promotrice, Ingrid Struman. Pour m'avoir accueillie dans le laboratoire, bien sûr. Mais surtout pour avoir cru en ce projet jusqu'au bout, et m'avoir accompagnée jusqu'à la dernière seconde. Merci pour ces 4 (5 ?) années intéressantes et bien remplies. Merci pour ton soutien et tes conseils. J'aurais décidément beaucoup appris.

Alors, Nico. C'est tout à fait clair que sans ton enthousiasme et ta guidance, je n'en serais pas là. Merci de m'avoir transmis tes techniques, tes protocoles, ton bureau, ton bench et tes pipettes... Pour la folle ambiance dans le bureau et tes précieux conseils. Et tous les ragots !

Merci Mimi, pour ces années où tu as été la première personne que je saluais en arrivant au labo. Heureusement que tu n'es pas partie trop loin ! A qui aurions-nous posé toutes nos questions ? A toi qui a tout testé, merci pour ton écoute et tes conseils techniques.

Merci à Oli, ma deuxième paire de mains ! Merci pour ton aide tout au long de ma thèse. Toujours là pour me donner un coup de main pour changer mes milieux ou charger une PCR. Et en plus, on se sera quand même souvent bien marré. Et ça, c'est pas faux.

Thomas, mon voisin de bench, de bureau, de thèse. On y sera finalement arrivé tous les deux ! J'ai été contente de travailler à tes côtés, même si tu me piquais parfois mes pipettes.

Merci, Cécile, pour les soirées à discuter politique seules au labo en fin de soirée. Marie, pour les conseils profiling et les histoires de chat fou. Jenn, I haven't forgotten that you were the one to welcome me in the lab when everybody was out having fun in a congress in the USA ! Thanks for the help with bioinformatics.

Amandine, dernière arrivée. Ça a été un plaisir de t'encadrer au cours de ton stage et de ton mémoire. Et une joie que tu restes me tenir compagnie pour la fin de ma thèse. C'est vraiment gentil de ta part, j'apprécie. Blague à part, nos discussions dans tous les coins du labo vont me manquer. Je te souhaite bon vent, et bon courage pour la suite. Tu sais où me trouver.

Un grand merci à Claire et Sébastien, nos français pas si loin de chez eux. Bon, quand même désolée pour la météo, Séba. Tu verras, on s'y fait. Merci pour m'avoir fait bénéficier de votre expérience. Claire, merci pour les analyses bio-info, et Séba, pour tes conseils exo. Et puis, pour nos discussions éclairantes sur la vie et le monde académique.

Steph, bien joué. Tu as réussi à partir en Italie juste avant que je n'arrive, et à en revenir quand je pars… Était-ce bien nécessaire de se donner cette peine si c'était quand même pour relire un bout de ma thèse ? En tout cas, moi, je suis vraiment contente d'avoir fini par faire la connaissance de la légende, l'être mythique du LAM ! Encore un tout grand merci pour tes précieux conseils.

Aux membres des ZDDM, LOR, MBPEL, SQCHQ, GUIHVQPIU HGQ VHJDXDFG, CVCXVDFGHU, bref, le BMGG ! A vous tous, les déjà partis, les toujours là, et les

récemment arrivés, un énorme merci ! Ensemble, vous créez cette atmosphère si agréable au 1er étage. Et individuellement, vous êtes de fantastiques personnes. Alice, et ton enthousiasme lumineux pour organiser plein de trucs. Anne-So, et les conseils et comparaison en matière d'organisation d'evjf. Arnaud, bravo pour avoir si bien tenu le coup pendant nos temps de midi remplis de conversation « de filles ». Mais de toute façon, ça finissait quand même par parler de chats. Jojo, pour ta gentillesse et ta bonne humeur. Claudia et ton merveilleux accent espagnol qui mettait tout de suite du soleil dans une journée pluvieuse.

Merci aux nouvelles arrivées au 1er, les filles du PSI, pour tous vos rires ! Céline, Guilia, Amandine et Sarah, vous avez apporté un peu d'aventure et de nouvelles distractions dans le labo. Grâce à vous, je connais maintenant la distinction entre un extincteur à gaz et un extincteur à poudre…

D'une manière générale, merci à tous ceux qui ont contribué à la réalisation de ce travail, au sein du GIGA et du CHU. Je remercie en particulier Christine Gilles et Marc Thiry pour vos explications et conseils avisés, et les membres de mon comité de thèse pour leurs encouragements.

Un très grand merci à mes amis de sbim ! Sophie, 9 ans qu'on n'est jamais très loin. Le sevrage va être difficile. Mais est-ce vraiment nécessaire ? Megan, toi qui soigne si bien la conjonctivite, à nos envies de voyage ! Justine, qui me précède dans mes voyages, avec tes expressions bien particulières et ton enthousiasme pour certains bouquins. Justine, Odile, Yasmine, et tes photos du bout du monde. A vous qui m'avez toujours rendu le sourire et la motivation les jours gris. Je me serai levée juste pour vos rires. Ça, on n'en manque jamais avec vous. A nos pause-thé et nos nombreuses soirées ! Je sais que je peux compter sur vous, c'est que le début ! Merci aussi à Loïc, Matthias, Cédric et Vincent (notamment pour les coups de main en informatique).

Fio et Margot, mes pharmaciennes préférées. Merci pour les soupers, et toutes les anecdotes de vos aventures en officines, avec vos patients…particuliers.

Alors parce qu'il y a une vie en dehors de la thèse (si si…), un énorme merci à Claire, Nadège, Mélanie, Audrey, Hélène, Yasmine K, Manu. En particulier, merci à Sophie L et Gaëtan pour avoir relu ce travail, et corrigé cet anglais scientifique, imbuvable pour qui n'est pas du domaine ! C'est toujours un plaisir de vous voir et de se plonger dans de nouveaux horizons avec vous. Pour tous les délires, passés et à venir, merci !

Nicolas, silicate chanteur et humain formidable. Pour tout.

Mes parents, qui ont toujours cru en moi, parfois plus que moi-même. Maman, qui me pousse en avant quand j'hésite, m'a appris qu'il n'y a pas d'âge pour apprendre. Papa, qui m'aide à relativiser et m'a montré comment m'émerveiller de tout. Et ma famille, Mamy, Françoise et Ady, pour m'avoir encouragée tout au long. Papy, je te l'avais dit.

Résumé

Les interactions entre les cellules tumorales et leur microenvironnement sont essentielles au développement tumoral. C'est pourquoi la compréhension des mécanismes de communication entre les différents types cellulaires est cruciale pour le développement de nouvelles thérapies anti-cancers. Les exosomes, de petites vésicules libérées par les cellules dans l'environnement extracellulaire, interviennent dans la communication intercellulaire, notamment via leur contenu spécifique. En effet, ils transportent diverses molécules, dont des microARN. Ces microARN sont quant à eux capables de réguler une large gamme de fonctions cellulaires. Dans le cadre du cancer, les exosomes sont potentiellement sécrétés par tous les types cellulaires composant le microenvironnement tumoral, et participent à la réponse aux traitements.

Au cours de ce travail, nous avons mis en évidence que les traitements par deux agents chimiothérapeutiques, l'épirubicine et le paclitaxel, sont capables d'influencer le contenu en microARN des exosomes produits par les cellules endothéliales. Nous avons identifié quatre microARN dont la sécrétion est augmentée dans les exosomes de cellules traitées : miR-373-3p, miR-887-3p, miR-122-5p et miR-129-5p. Des tests fonctionnels réalisés avec ces miARN dans des cellules de cancer du sein ont montré que miR-373-3p provoquait une réduction de l'agressivité des cellules tumorales en diminuant l'invasion et en augmentant leur capacité d'adhésion. Nous avons ensuite réalisé une analyse transcriptomique des cellules tumorales surexprimant miR-373-3p. Nous avons ainsi remarqué que le miARN inhibait la transcription de facteurs importants de la transition épithélio-mésenchymateuse (TEM), tels que CD44, SLUG et ZEB1. De plus, miR-373-3p régulait également RELA (NFκB/p65) et le TGFβR2, lesquels interviennent dans de nombreuses fonctions au sein des cellules, et ont été reliés à la TEM. Les exosomes de cellules endothéliales traitées ont pu induire une diminution des niveaux de ces deux dernières cibles. Ensuite, les fonctions des miARN ont été testées dans des cellules de cancer du sein résistantes à l'épirubicine ou au paclitaxel. Nous avons découvert que les cellules ne répondaient plus à la surexpression des miARN. Nous avons donc réalisé la même analyse transcriptomique sur les cellules résistantes à l'épirubicine surexprimant miR-373-3p, et avons remarqué que les cibles n'étaient plus régulées.

En conclusion, les résultats suggèrent que les cellules endothéliales jouent un rôle indirect dans la réponse aux drogues de chimiothérapie, en sécrétant des exosomes chargés en miR-373-3p. Le miARN va à l'encontre de la TEM et diminue l'agressivité des cellules.

Cependant, les effets régulateurs du miARN semblent perdus lorsque les cellules sont résistantes aux traitements.

Abstract

The interaction between tumour cells and their microenvironment is an essential aspect of tumour development. Therefore, understanding how this tumour microenvironment communicates with tumour cells is crucial for the development of new anti-cancer therapies. Exosomes, small vesicles released by cells into the extracellular environment, mediate cell-cell communication by their specific content. Interestingly, they carry miRNAs, which are able to regulate a wide range of functions in cells. In the context of cancer, exosomes are potentially secreted by all cell types that compose the tumour microenvironment, and participate in the tumour response to treatment.

In this work, we showed that epirubicin and paclitaxel, two common drugs against breast cancer, influenced the miRNA content of exosomes secreted by endothelial cells. We identified four miRNAs, miR-373-3p, miR-887-3p, miR-122-5p and miR-129-5p, as increased in exosomes secreted by drug-treated cells. Analysis of the functions of those miRNAs in breast cancer cells revealed that miR-373-3p was able to decrease the aggressiveness of the tumour cells by decreasing invasion and increasing adhesion. We then performed a transcriptomic analysis on the tumour cells overexpressing miR-373-3p, and noticed that the miRNA was inhibiting the transcription of important regulator of epithelial-mesenchymal transition (EMT), such as CD44, SLUG and ZEB1. Moreover, miR-373-3p also targeted RELA (NFκB/p65) and TGFβR2, which regulate many functions in the cells and have been linked to EMT. Exosomes from drug-treated endothelial cells could induce a downregulation of the two last targets. Then, the functions of the miRNAs were tested on breast cancer cells resistant to epirubicin or paclitaxel. Interestingly, we discovered that the cells were not responding anymore to the overexpression of the miRNAs. We performed the same transcriptome analysis on the cells resistant to epirubicin overexpressing miR-373-3p, and saw that the targets that were regulated in sensitive cells were almost not inhibited in resistant cells.

Taken together, these results suggest that endothelial cells are indirect players in the response to chemotherapy by secreting exosomes loaded with miR-373-3p. The miRNA promotes the inhibition of invasion and the increase of adhesion of breast cancer cells, potentially via the downregulation of RELA, TGFβR2, CD44, SLUG and ZEB1. However, the regulatory potential of miR-373-3p appears to be lost when the cells are already resistant to the drugs.

Abbreviations

ABCB1	ABC transporter B1
AGO	Argonaute
bp	Base pair
BRCA	BReast CAncer
BrdU	Bromo-deoxyuridin
BSA	Bovine Serum albumin
CAF	Cancer-associated fibroblast
cDNA	Complementary DNA
DGCR8	DiGeorge syndrome Critical Region gene 8
DLS	Dynamic light scattering
DMEM	Dulbecco's modified eagle medium
DNA	Deoxyribonucleic acid
DPBS	Dulbecco’s phosphate buffered saline
dsRNA	Double strand RNA
EGFR	Epidermal growth factor receptor
EGM2	Endothelial cell growth media 2
EMT	Endothelial-mesenchymal transition
ER	Oestrogen receptor
ESCRT	Endosomal sorting complex required for transport
EV	Extracellular vesicles
EXP5	Exportin 5
FBS	Foetal bovine serum
GADD45A	Growth arrest and DNA-damage-inducible protein
GW	glycine-tryptophan
HDL	High-Density Lipoproteins
HER2	Human Epidermal Growth Factor Receptor-2
HRP	Horseradish peroxydase
HUVEC	Human umbilical vein endothelial cell
ILV	Intra-luminal vesicles
LNA	Locked nucleic acid
lncRNA	Long non coding RNA
MDA-MB-231/epi	MDA-MB-231 resistant to epirubicin
MDA-MB-231/pacli	MDA-MB-231 resistant to paclitaxel
MDH2	Malate dehydrogenase 2
MDR1	Multidrug resistance 1
miRNA	Micro RNA
mRNA	Messenger RNA
MV	Microvesicles
MVB	Multi-vesicular body
NGS	Next generation sequencing
nt	nucleotide
PACT	protein activator of PKR
PARP	poly(ADP-ribose) polymerase
PAZ	Piwi-Ago-Zwille domain
PBS	Phosphate buffered saline
PCNA	Proliferating cell nuclear antigen
PFA	Paraformaldehyde
P-gp	P-glycoprotein

PI	Propidium iodide
PIWI	P-element Induced WImpy testis
POR	Cytochrome P450 reductase
PR	Progesterone receptor
qRT-PCR	Quantitative reverse transcription polymerase chain reaction
RISC	RNA-Induced Silencing Complex
RLC	RISC loading complex
RNA	Ribonucleic acid
RNA pol II	RNA polymerase II
SDS-PAGE	Sodium dodecyl sulfate polyacrylamide gel electrophoresis
shRNA	Short hairpin RNA
SIRT6	Sirtuin 6
ssRNA	Single strand RNA
TDE	Tumour cell-derived exosome
TNBC	Triple-negative Breast Cancer
TOP2A	Topoisomerase 2 a
TRBP	Transactivation Response RNA Binding Protein
UTR	Untranslated region
ZEB	zinc-finger E-box-binding homeobox

Table of contents

List of figures

List of tables

Introduction

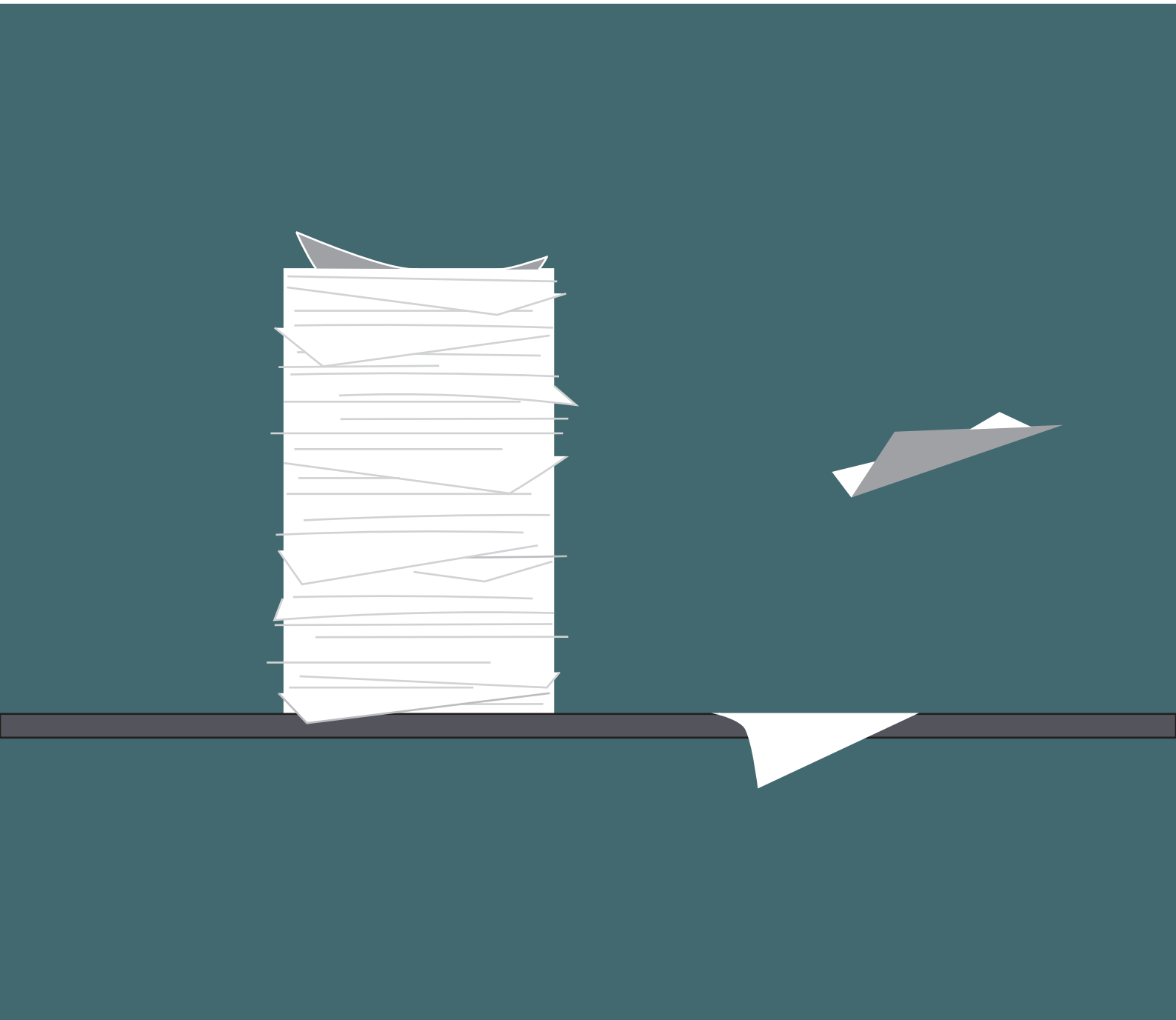

Introduction

I. Breast Cancer

In Belgium in 2015, breast cancer was the most prevalent cancer in women, representing over 30% of all malignancies. The number of newly diagnosed breast cancer in Belgium is expected to rise from 10,466 in 2014 to 12,125 in 2025, an increase mainly attributed to the aging of the population. Indeed, the majority of the breast cancers are diagnosed in elderly women. It is also the first cause of cancer death in women in Belgium (Silversmit et al. 2017).

As for many other types of cancer, the development of breast cancer has many causes. Breast cancer, however, presents distinct features. It is a heterogeneous disease, and the prognosis and treatments vary with the subtypes and the category of the tumour. The first classification was based on histological characteristics. Nowadays, tumours are also sub-classified depending on their molecular profile. The combination of clinical and mechanistic characterisations are used in an attempt to discover a better medical care and adapt the treatment strategy to the patient. The existence of distinct biological subtypes emphasizes the need for a better understanding of the molecular mechanisms, and for more specific biomarkers and treatment strategies.

1.1 Risk factors

Some risk factors are hereditary. Women diagnosed with breast cancer occasionally have a relative carrying the disease. The risk depends on the genetic proximity, the number of women diagnosed with breast cancer, and the age of detection. About 5% of the women diagnosed with breast cancer carry a mutation on the genome of either BRCA1 or BRCA2 (BReast CAncer 1 or 2). Those proteins are involved in major functions: DNA repair, chromatin remodelling, cell-cycle checkpoints and, in case of BRCA1, transcription factor related to the regulation of oestrogen receptor activity. The risk inherent to their mutation can be modified by a second mutant gene, or by an environmental factor. Women carrying a mutation in BRCA1 or 2 have an 80% risk of developing breast cancer during their lifetime (Narod 2006; Malone et al. 2006).

Reproductive factors are preponderant risks in women cancer. The term “reproductive factors” usually comprises risks linked to the age of first full-term pregnancy, age of first menstruation, whether or not the children were breastfed, etc. Long term (>5 years) use of

oral contraceptives are included, since a prolonged exposure to oestrogen or progesterone has been linked to a slightly higher prevalence of breast cancer (Mørch et al. 2018). Reproductive factors have been mainly associated with hormone receptor–positive tumours. Moreover, lifestyle factors such as stress, obesity, the lack of physical exercise, and alcohol consumption are well-known risk factors of cancer (Colditz & Bohlke 2014).

Exposure to environmental factors increases the risk of developing various types of cancers, including breast cancer. These factors notably include exposure to pesticides (dioxin,…), heavy metals (lead, mercury,…), endocrine disruptive compounds (chemicals able to interfere with any aspect of hormone action, e.g. bisphenol A, phthalates, parabens) or radiations (Dumalaon-Canaria et al. 2014; Gray et al. 2017).

1.2 Carcinogenesis

Carcinogenesis cannot be imputed to one cause or mechanism only. It is a multistep phenomenon leading to the acquisition of tumour features such as immortality, the capacity to evade cell death, the activation of metastasis, a sustained proliferation, the evasion from growth suppression and the induction of angiogenesis (Hanahan & Weinberg 2011). Loss of tumour-suppressor genes or activation of oncogenes are the foundations of tumorigenesis. As a particularity of breast cancer, hormones (oestrogens and progesterone) exert a major effect on breast carcinogenesis. Œstradiol, via its action on its receptor, stimulates cell proliferation and inhibits apoptosis. Moreover, oestrogens metabolites have been shown to present genotoxic effects by causing DNA point mutations (Yager & Davidson 2006; Yue et al. 2013).

1.3 Classification

Today, different methods of classification are used to characterise the various kind of breast cancer. These characteristics provide various information, useful to establish treatment regimens adapted to the heterogeneity of the disease.

1.3.1 Histology, grade and stage

The main classification of breast cancer in use today is based on **histopathologic features**. It relies on analysis by the pathologist of stained slides from the tumour biopsy. The ductal carcinoma derived from duct cells and are the most common. In situ breast carcinoma are not invasive and localized at their site of origin. Invasive carcinomas can be sub-classified too, and the infiltrating ductal carcinoma accounts for about 80% of breast

cancers. Other types include lobular carcinoma (in situ or invasive), inflammatory breast cancer, and other rare types of disease (Eliyatkin et al. 2015; Rakha & Green 2017; Malhotra et al. 2010).

The **grade** of the cancer is given by the Elston-Ellis classification system (itself adapted from the Scarff Bloom and Richardson classification system), based on the percentage of tubule formations on the tumour, the degree of nuclear pleomorphism, and the mitotic count and rate. A numeral scoring is attributed to each criterion, and their sum defines the grade of the tumour, from grade I to III. The grading system is correlated to the prognosis: patients with a grade I, i.e., more differentiated tumour, have better survival rates than grade III patients, carrying a less differentiated cancer (**fig. I 1**) (Elston & Ellis 1991; Viale 2012).

Feature		Score
Tubule formation		
Majority of tumour (>75%)		1
Moderate degree (10-75%)		2
Little or none (<10%)		3
Nuclear pleomorphism		
Small, regular uniform cells		1
Moderate increase in size and variability		2
Marked variation		3
Mitotic counts (dependent on microscope field area)		
Ex: Leitz Ortholux		
0-9		1
10-19		2
>20		3
Score		
grade I	3-5 points, well-differentiated	
grade II	6-7 points, moderately differentiated	
grade III	8-9 points, poorly differentiated	

Figure I 1. ***Elston-Ellis grading system for breast cancer****. Figure adapted from "AJCC. Cancer staging Atlas 7th edition".*

The **stage** of a breast cancer is the most important classification system in regards to prognosis and treatments. The staging system, called TNM, is based on the size of the primary tumour (T), lymph node invasion (N), and the presence of metastasis (M) (**fig. I 2**)(Eliyatkin et al. 2015).

Breast Cancer Staging	
Primary tumour (T)	
TX	Primary tumour cannot be assessed
T0	No evidence of primary tumour
Tis	Carcinoma in situ
T1-3	Tumour size: T1≤20 mm; 20 mm<T2<50 mm; T3<50 mm
T4a-d	Tumor of any size with direct extension to the chest wall and/or to the skin
Regional Lymph Nodes (N)	
NX	Regional lymph nodes cannot be assessed
N0	No regional lymph node metastases
N1mi	Micrometastases
N1-3	Size, location and number of regional lymph nodes with detected tumour cells
Distant Metastases (M)	
M0	No clinical or radiographic evidence of distant metastases
M1	Distant detectable metastases

ANATOMIC STAGE/PROGNOSTIC GROUPS			
Stage 0	Tis	N0	M0
Stage IA	T1	N0	M0
Stage IB	T0	N1mi	M0
	T1	N1mi	M0
Stage IIA	T0	N1	M0
	T1	N1	M0
	T2	N0	M0
Stage IIB	T2	N1	M0
	T3	N0	M0
Stage IIIA	T0	N2	M0
	T1	N2	M0
	T2	N2	M0
	T3	N1	M0
	T3	N2	M0
Stage IIIB	T4	N0	M0
	T4	N1	M0
	T4	N2	M0
Stage IIIC	Any T	N3	M0
Stage IV	Any T	Any N	M1

Figure I 2. ***TNM staging system for breast cancer****. Figure adapted from "AJCC. Cancer staging Atlas 7th edition".*

1.3.2 Molecular classification on breast cancer

A more recent approach focuses on the molecular profile of breast tumours, especially invasive ductal carcinomas. This relatively new classification system has been made possible thanks to the development of technologies allowing to evaluate the expression of thousands of genes, such as microarray chips or Next Generation Sequencing (NGS). The subsequent subtypes reflect the biological features of the neoplasms, but can also be used to predict their responses to treatments and clinical behaviours (Perou et al. 2000; van 't Veer et al. 2002).

The most discriminating factor is the expression status of Oestrogen Receptor (ER). It allows the segregation of tumours into two main clusters, based on their luminal (ER+) or basal (ER-) characteristics.

The luminal subtype (ER+) accounts for about 75% of invasive carcinomas. Such tumours possess the characteristics of breast luminal cells, expressing ER, PR and cytokeratines 8 and 18. They are further discriminated between Luminal A and Luminal B. The **Luminal A** subtype is associated with the best outcome. Tumours in this group are usually low-grade and present a good survival rate. This subtype has a negative receptor status for HER2, and the proliferation index is low. The **Luminal B** tumours are slightly more aggressive than the A, have a higher proliferation rate, and can be either HER2+ or HER2-.

ER- tumours present basal cells characteristics. They typically do not express ER and PR. When the neoplasm overexpresses the HER2, they are sub-classified as **HER2+**

neoplasms. **Triple-negative Breast Cancers** (TNBC) are the ones lacking the overexpression of all three markers (ER-, PR-, HER2-). This subtype is the most heterogeneous. The molecular mechanisms underlying this subtype are less understood. They represent about 15 to 20% of all breast carcinomas and are associated with poor prognosis and reduced long-term survival. TNBC are predominantly found in young patients and are linked to hereditary mutations in BRCA1 genes. In term of morphology, clinical presentation, prognosis, association with BRCA1 and therapeutic options, TNBCs largely overlap in 70-80% of cases with **basal-like** carcinomas. This last subtype is triple-negative, but still has specific markers as the neoplasms express cytokeratin 5/6 and/or EGFR (**fig. I 3**)(Sotiriou et al. 2003; Sandhu et al. 2010; Lam et al. 2014).

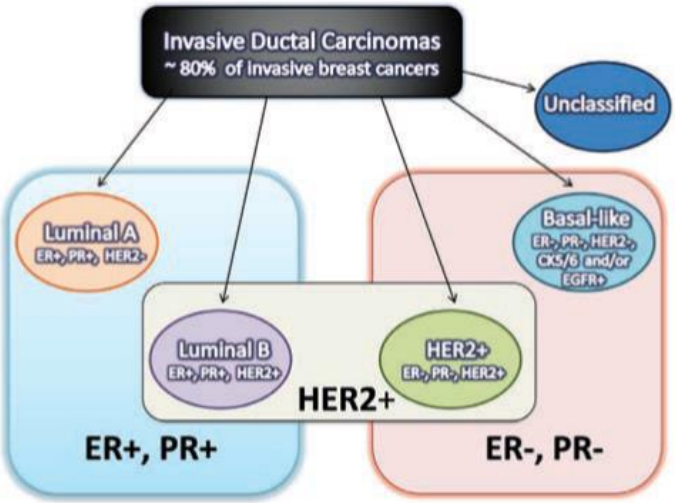

Figure I 3. ***Diagram of the breast cancer molecular classification****. In blue and pink: subtypes based on the expression of ER/PR. In blue, the hormone-receptor positive (Luminal A and Luminal B) and the hormone-receptor negative (HER2+ and basal-like) in pink. In the central grey rectangle, presence of HER2 amplification in Luminal B and HER2+ subtypes. Figure from Sandhu et al. 2010*

A few other molecular subtypes have been described, e.g., claudin-low, basal-like immune suppressed, basal-like immune-activated.

This classification, however, remains usually the prerogative of research labs or clinical trials. A few multigene assays are already available, but they are not routinely used in clinics. It is hoped that the large-scale techniques will help optimise chemotherapy regimens and identify potential targets, especially in the case of TNBCs (Rakha & Green 2017). However, specific immunochemistry markers assessing the overexpression of Oestrogen Receptor (ER), Progesterone Receptor (PR) and Human Epidermal Growth Factor Receptor-2 (HER2), as well as the Ki67 proliferation index can be used to help determine if the patient is likely to respond to targeted therapy.

1.4 Treatments

1.4.1 Surgery

Surgical removal is still the treatment of choice for breast cancer (**fig. I 4**). Over the past thirty years, surgery has shifted towards breast-conservation treatments. Total mastectomy is still unavoidable in some patients due to tumour size, tumour multicentricity, prior radiation to the chest, recurrence after a conservation treatment, or even patient choice. It can also be prophylactic in case of BRCA1/2 mutation carriers (Senkus et al. 2015). Radio or chemotherapy can be given prior to surgical resection to reduce the size of the tumour and facilitate breast-conservation treatment. This kind of treatment is called neoadjuvant therapy. In case of breast-conservation surgery, the margin status of the tumour must be assessed, and a histological analysis is performed on the resected tissue. Furthermore, the surgeon performs a sentinel lymph node biopsy to evaluate the potential presence of micro or macrometastases. The status of regional lymph node is a strong predictor of long-term prognosis (Senkus et al. 2015).

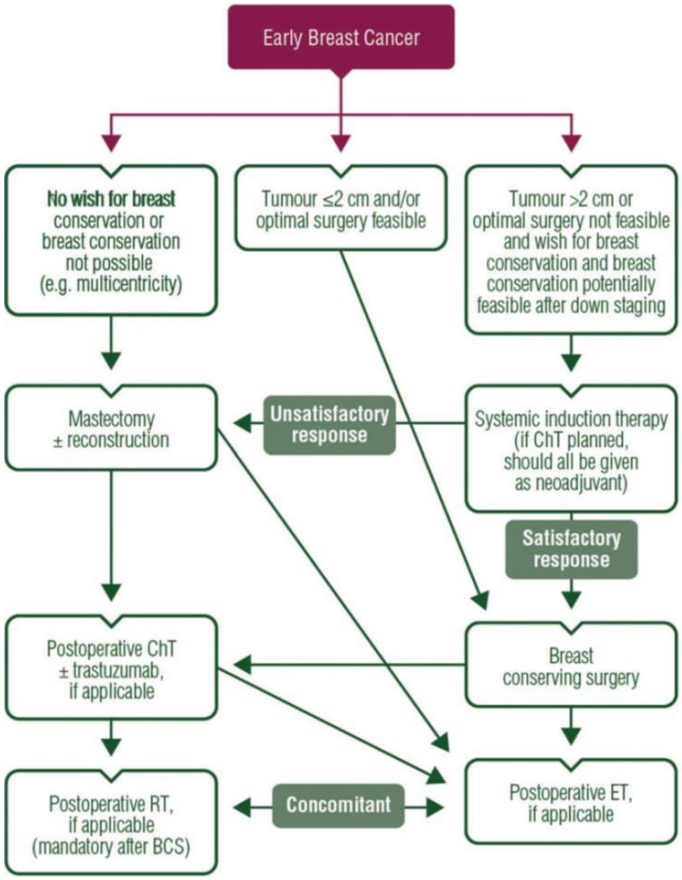

Figure I 4. ***Decision algorithm for the treatment of early breast cancer****. Cht, chemotherapy; BCS, breast-conserving surgery; ET, endocrine therapy; RT, radiotherapy. Figure adapted from Senkus et al. 2015*

1.4.2 Radiotherapy

A breast-conservation surgery is generally followed by adjuvant radiotherapy. Whole breast radiation therapy alone has been demonstrated to significantly reduce the 10-year risk of recurrence, and to decrease the 15-year risk of breast-cancer mortality (Early Breast Cancer Trialists' Collaborative Group (EBCTCG) et al. 2011). Regional lymph node radiation improves long-term survival in patients as well. Radiotherapy can be considered to treat unresectable disease, followed by surgery if the tumour becomes resectable (Senkus et al. 2015).

1.4.3 Targeted therapy

In some cases, a targeted therapy can be added to the treatment. This is the case for breast cancers overexpressing ER. They are said to be hormone-dependent because oestrogens promote their growth by binding to their receptors. It is thus beneficial to block the action of those receptors. Tamoxifen is the most widely used blocker among hormone-dependent breast cancer patients. This drug is a modulator of oestrogen receptors. Among post-menopausal patients, aromatase inhibitors have also shown good results. Aromatase is an enzyme responsible for the endogenous production of oestrogen. By inhibiting its activity, the drug can greatly reduce oestrogen concentration (Early Breast Cancer Trialists' Collaborative Group (EBCTCG) 2015; Senkus et al. 2015).

As previously mentioned, some carcinomas overexpress the HER2 oncogene. As a growth factor receptor, its presence is associated with a poor prognosis and resistance to some chemotherapeutics. A specific monoclonal antibody (Trastuzumab) has been manufactured to block this receptor. Since its commercialisation in the late 1990's, other molecules have been developed, e.g., Pertuzumab and Lapatinib (Matsen & Neumayer 2013).

With a better knowledge of the biology and chain of events happening in neoplasm, therapies are designed to specifically target mutated proteins. Patients carrying germline BRCA1 or BRCA2 mutation can for example benefit from the synthetic lethality induced by olaparib, a PARP inhibitor. PARP is also an enzyme implicated in DNA repair, especially in detecting single-strand DNA break. Synthetic lethality is described as "a mechanism using a combination of genetic and induced effects (for example, by a therapeutic agent) working together to induce cell death, where any single one of these effects is non-lethal" (Sondka et al. 2018). In metastatic breast cancer, inhibiting PARP in tumour cells already deficient for

BRCA induced death by failure in DNA breaks repair pathways (Robson et al. 2017; Sondka et al. 2018).

Development of new diagnosis and therapeutic procedures requires a good understanding of the molecular processes involved in oncogenesis. Moreover, the tumour microenvironment is another important player, which should not be ignored when studying cancer development. Furthermore, targeted therapies are also under scrutiny for their ability to fight drug resistance. Further work is still needed to develop a truly personalised medicine (Sondka et al. 2018; Masoud & Pagès 2017).

1.4.4 Chemotherapy

Chemotherapy is one of the major treatments for cancer, along with radiotherapy and surgery. Researchers keep trying to discover new drugs and new ways to potentiate or repurpose existing ones (Sun et al. 2017). There is a wide range of molecules currently used as chemotherapeutic agents (**fig. I 5**). Some are used only in one type of cancer, others can treat a large number of tumours. They can be given as single agent, or in a combination of different molecules. Adjuvant chemotherapy can be given after surgery or radiotherapy to lower the risks of recurrence or metastasis. Alternatively, some chemotherapeutic treatments are prescribed as neoadjuvant prior to surgery in order to reduce the size of the tumour and facilitate its resection. Neoadjuvant chemotherapy also allows the physician to monitor the response of the tumour to the drugs, and leaves the possibility to stop an inefficient treatment (Ithimakin & Chuthapisith 2013). Chemotherapy is indicated for the majority of TNBC and HER2+ tumours. The treatments are mainly based on taxanes and anthracyclines (Masoud & Pagès 2017). One of the goals behind the molecular analysis of tumours is notably to optimize chemotherapy regiments for different breast cancers. TNBC, especially, have only a few molecular targets today. The antineoplastic drugs are classified into different families: anthracyclines, alkylating agents, kinase inhibitors, anti-microtubule agents, antimetabolites,

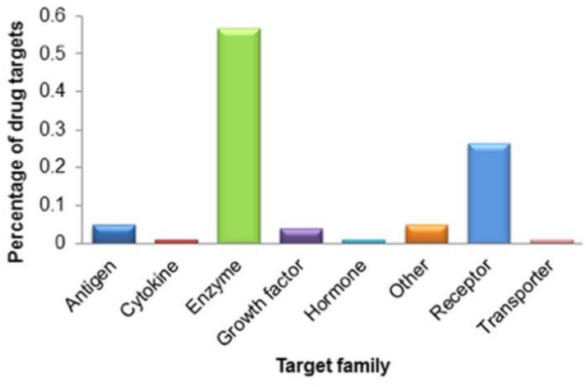

Figure I 5. ***Anticancer drugs target different subcellular function families****. Figure from Sun et al. 2017.*

aromatase inhibitors, topoisomerase inhibitors, mTor inhibitors, and retinoids (Corrie 2008; Chabner & Roberts 2005).

This work will focus on the effects of two drugs that are currently used for the treatment of breast cancer: epirubicin (Epi), an anthracycline, and paclitaxel (Pacli), an anti-microtubule agent from the taxane family.

1.4.4.1 Epirubicin

Epirubicin is a member of the anthracycline drug family. Anthracyclines started to be used in treatment of metastatic breast cancer in the 1970's (Conte et al. 2000). The fact that they are still some of the most common anti-cancer agents today illustrates how potent they are.

a. Mechanisms of action

Anthracyclines interfere with cell biology at different levels. Their main mechanism of action occurs through the intercalation of the molecule between adjacent DNA base pairs (**fig. I 6**). This will impair the DNA replication and RNA transcription. Moreover, the intercalating agent can stabilize the covalent bonds between the Topoisomerase II and the DNA strands, which in turn causes double-strand DNA breaks. They are two isoforms of topoisomerase II, topoisomerase IIα and IIβ. They are differentially regulated and involved in distinct biological functions. The anthracyclines preferentially target topoisomerase IIα, which is implicated in replication (Chikamori et al. 2010; Eijdems et al. 1995). Additionally, some anthracyclines (daunorubicin, aclarubicin) have also been shown to be able to evict histones from the chromatin, including the histone H2AX, leading to some epigenetic damages (Pang et al. 2015). Another significant mechanism is the generation of free radicals, which, in addition to DNA damages, can also create membrane alterations by lipid peroxidation (Minotti 2004). These past few years, it has been showed that anthracyclines can improve anticancer immune responses, by activating tumour-infiltrated lymphocytes and Natural Killers (Ma et al. 2013; Feng et al. 2016). All those effects contribute to the inhibition of cell growth and lead towards tumour cell death.

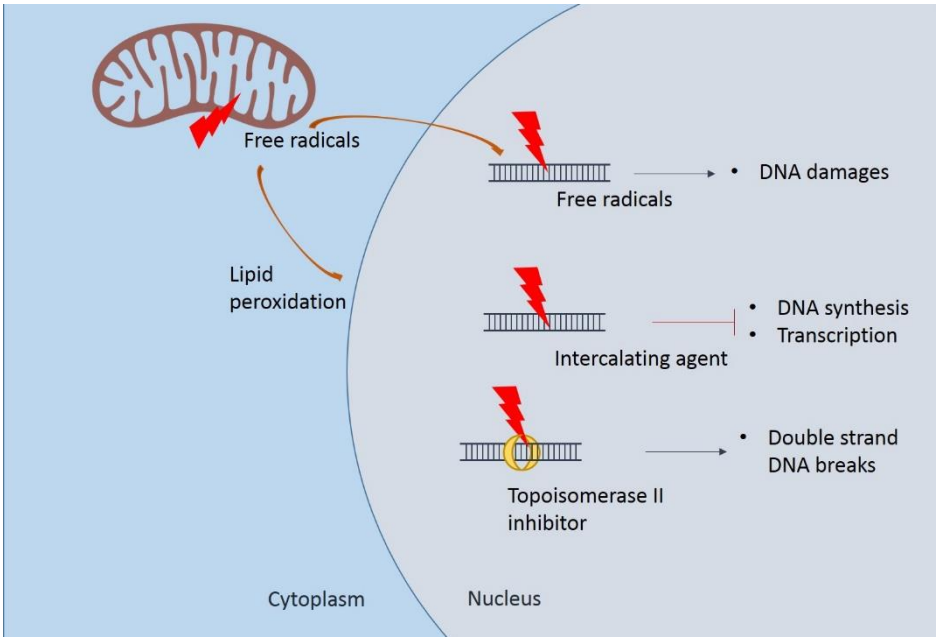

Figure I 6. ***Principal mechanisms of action of epirubicin****. Epirubicin main toxicity is related to DNA damages as intercalating agent and inhibitor of topoisomerase II. Moreover, epirubicin induces the release of free radicals, which increase DNA damages and lipid peroxydation.*

b. Doxorubicin vs epirubicin

The first anthracyclines were discovered in *Streptomyces peucetius* and named Doxorubicin. This molecule was soon used to treat solid and haematological tumours. Unfortunately, the adverse effects linked to the cardiotoxicity were significant enough to trigger a search for new analogues, with superior activity or less toxicity. Epirubicin is one of the newly designed anthracycline, with different kinetic and metabolic properties (Minotti 2004). Comparative studies showed that, for equimolar dose, the cytotoxic activity remained the same between the two drugs. However, the cardiac toxicity was significantly reduced in the case of the second generation drug. Epirubicin and its metabolites are eliminated faster than doxorubicin, reducing the total body exposure to the drug. Interestingly, it has also been shown that the administration of paclitaxel with epirubicin induced an increase of urinary elimination and a decrease of plasma levels of epirubicinol, the cardiotoxic metabolite of epirubicin (Paul Launchbury & Habboubi 1993). The only criteria used to predict toxicity of Doxorubicin is the total cumulative dose. As the effects of anthracycline are dose-dependent, a lower associated toxicity allows the use of larger doses of epirubicin with an improved outcome for the patient (Paul Launchbury & Habboubi 1993; Jain et al. 1985; Senkus et al. 2015).

c. Epirubicin-related toxicity

Epirubicin-related toxicity can be divided between short term and long term toxicity. Short term adverse effects are common for cytotoxic agents, which cannot specifically target tumour cells. These include alopecia, leucopenia, gastrointestinal toxicity and mucositis. They are reversible (Anampa et al. 2015; Bontenbal et al. 1998).

Cardiotoxicity is the major long term toxicity related to anthracyclines. The principal risk factor for anthracyclines being the total cumulative dose, limited to 900 mg/m² for epirubicin. The causes of this toxicity implicate a partial loss of mitochondrial function and impaired cellular respiration in cardiomyocytes. Formation of free radicals due to anthracyclines metabolism causes the disruption of the mitochondrial membrane and the release of cytochrome c and inhibition of the mitochondrial chain reaction. Moreover, anthracyclines can interfere with the mitochondria genome, disturb the calcium homeostasis and interfere with the metabolism of iron (Volkova & Russell 2012; Sandhu & Maddock 2014; Kwok & Richardson 2002). Cardiomyocytes are particularly sensitive to reactive oxygen species, and the combination of those mechanisms could trigger permanent cardiomyocyte apoptosis and necrosis.

1.4.4.2 Paclitaxel

Paclitaxel is a member of the taxane family, a class of mitotic inhibitors. It was first isolated in 1971, from the tree *Taxus brevifolia* (Pacific yew) (Wani et al. 1971). Since that particular species was already scarce, semi-synthetic pathway to produce paclitaxel were developed with other yew species. Due to the difficulty of production and its poor solubility, it was approved for cancer treatment only 21 years later (Rowinsky & Donehower 1995).

a. Mechanisms of action

The taxane family is composed of products that stop mitosis, usually interacting with and perturbing the microtubule spindle machinery facilitating mitosis (De Brabander et al. 1981). The taxanes have a peculiar mode of action: they bind to the N-terminal 31 amino acids of the beta-tubulin subunit in the microtubule. There, they promote the polymerization of tubulin, inhibiting the disassembly of microtubules (**fig. I 7**) (Rao et al. 1994). It has notably for effect to induce arrest in the G2 and M phases (De Brabander et al. 1981; Schiff et al. 1979; Jordan et al. 1993). It has also been shown to induce TNFα expression (Burkhart et al. 1994).

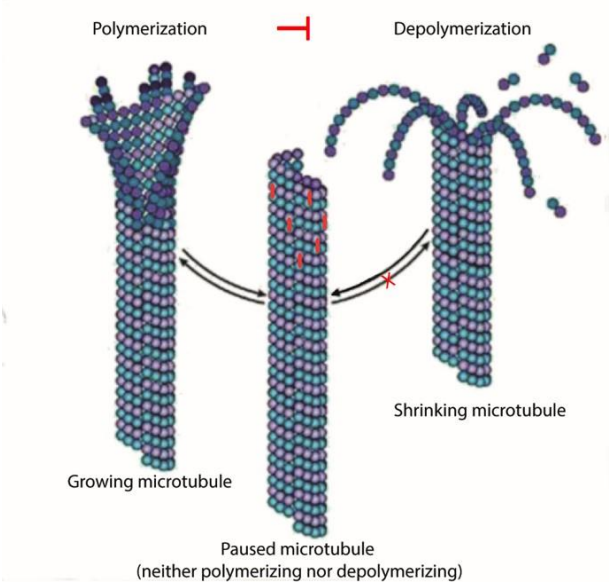

Figure I 7. ***Effect of paclitaxel on microtubule dynamic****. Paclitaxel (in red) stabilizes microtubules and prevents the depolymerisation. Figure adapted from Kaur et al. 2014.*

b. Paclitaxel-related toxicity

Its main dose-limiting toxicities are neutropenia and peripheral neuropathy, but these are generally manageable (Rowinsky et al. 1993). Neutropenia tends to be more severe with longer infusions, and depends on previous myelotoxic therapy. To prevent severe depletion of neutrophils, granulocyte colony-stimulating factor is often given with the treatment (Hashiguchi et al. 2015). Hypersensitivity is a problem caused, mainly, by its castor oil vehicle (Cremophor EL) (Gelderblom et al. 2001). Less common toxicities include gastrointestinal effects and disturbance in cardiac rhythm. The latter may potentiate the adverse cardiac effects of anthracycline (Rowinsky & Donehower 1995; Lombardi et al. 2004).

c. Paclitaxel and its derivatives

In order to improve the clinical results and lower the toxicity, paclitaxel-derivative and new formulations have been developed. Docetaxel and Cabazitaxel (Paller & Antonarakis 2011) are semi-synthetic, highly related analogues of paclitaxel. Docetaxel possesses the same mechanisms of action as paclitaxel, but has different pharmacokinetics and side effects (Crown 2004). Cabazitaxel has a poor affinity for the P-glycoprotein (P-gp), one of the main protein responsible for multi-drug resistance (Paller & Antonarakis 2011). Nab-paclitaxel (nanoparticle albumin–bound paclitaxel) is a recent formulation of paclitaxel. It uses

albumin to enhance its solubility and has shown good clinical results (Von Hoff et al. 2013; Neesse et al. 2014).

1.4.4.3 Epirubicin and paclitaxel in breast cancer treatment.

Chemotherapy is recommended in the majority of Triple-Negative Breast Cancer, HER2+ (Senkus et al. 2015) and metastatic breast cancer. Epirubicin is efficient as first-line single agent in the treatment of breast cancer (Michelotti et al. 2000), as well as paclitaxel (Bishop et al. 1997). However, they are mainly used today in combination regimen. The purpose of such association is to mix drugs with different modes of action to target a maximum of tumour cells and avoid the development of resistance. Epirubicin is often used in combination with fluorouracil and/or cyclophosphamide, followed by taxane. It has been shown that the addition of taxanes improves the efficacy of chemotherapy, but increases non-cardiac toxicity. Nevertheless, chemotherapy regimens based on anthracyclines and taxanes reduce breast cancer mortality by about 30% (Senkus et al. 2015; Gnant et al. 2017; Early Breast Cancer Trialists' Collaborative Group (EBCTCG) et al. 2012).

1.4.4.4 Mechanisms of acquired resistance

a. Common mechanisms of resistance

One of the most studied mechanism of acquired resistance implicates ABC transporters: membrane phosphoglycoproteins functioning as drug-efflux pumps. These molecules are able to limit the accumulation of drug within the cytoplasm by evacuating it outside. The best known molecule of this family is P-glycoprotein (encoded by *MDR1*, aka *ABCB1*). P-gp can detect and bind a large variety of hydrophobic natural-product drugs when they enter the plasma membrane, including anthracyclines and taxanes. This mechanism is responsible for cross-resistance between several chemotherapy agents, known as multidrug resistance (Gottesman 2002). Resistant cells are able to transfer resistance to sensitive cells via microparticles. Those microparticles were carrying P-gp, survivin (another protein implicated in resistance), and miR-21, which was able to activate the NFκB pathway (de Souza et al. 2015).

There are also some more indirect and less specific mechanisms of resistance, which rather focus on evading apoptosis by interfering with the cell death signalling pathways or modulating the transcription of key genes. For instance, resistance to taxane has been linked with changes in the levels or post-translational modifications of proteins from the BCL-2 family (Ferlini et al. 2003). Likewise, the cytotoxity of Doxorubicin can be impaired by the

status of the protein p53. If p53 is lost or mutated, cells are less likely to respond to the drug (Aas et al. 1996).

b. Specific to taxanes

Cells have various mechanisms to avoid the effects of taxanes (**fig. I 8**). Some tumours have a- and b-tubulin with impaired capacity to polymerize into microtubules. Paclitaxel-resistant cells may shift the balance towards the depolymerized form of tubulin. Their slow rate of assembly is then normalized by the taxanes, making the cells dependant on paclitaxel for growth (Yin et al. 2007). Another mechanism implicates changes in tubulin isoform expression, towards expression of isoform βIII or βIV tubulin (Kavallaris et al. 1997). Resistance can also be mediated by alterations in Microtubule-Associated Proteins (MAPs). For instance, a decrease of expression or an increased phosphorylation of MAP-4 shifts the microtubule towards a more destabilized state. By opposition, stathmin would destabilize

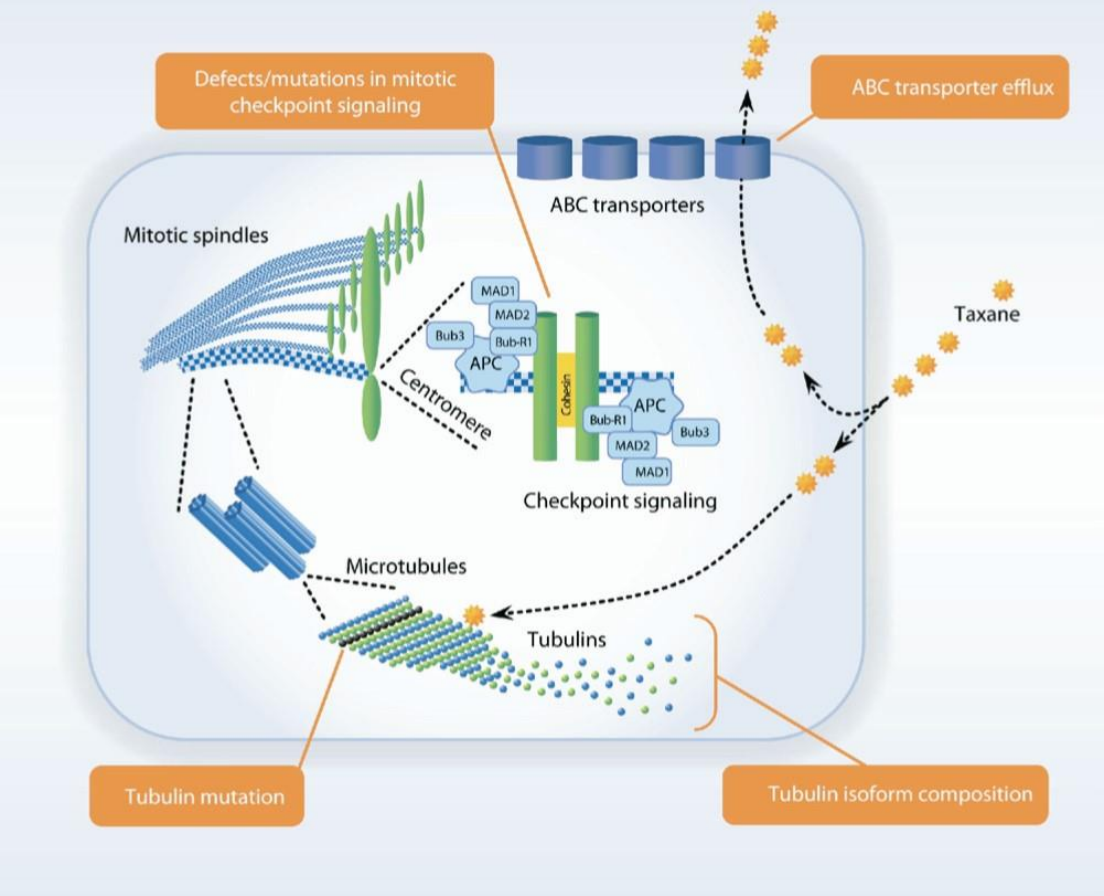

Figure I 8. ***Proposed mechanisms of resistance to taxanes****. Resistance specific to taxanes can happen via mutation of α- or β-tubulin, or the selection of tubulin isoforms less susceptible to be targeted by taxanes. Common drug-resistance mechanisms include the export of the drug by ABC transporters to lower its intracellular concentration, and mutations or defects in checkpoint signalling, minimizing the effect of taxane-induced microtubule stabilization. Figure adapted from Chien et al. 2008.*

the microtubules. Therefore, overexpression or dephosphorylation of this protein can induce resistance (Martello et al. 2003).

c. Specific to anthracyclines

Alterations in both gene expression and activity of topoisomerase II affect the sensitivity of cells to anthracyclines (Chien & Moasser 2008). It has been demonstrated that, when cells are selected for resistance to doxorubicin, they present a decreased level of Topoisomerase IIα mRNA and protein levels. Moreover, post-translational modifications of the protein seems to also contribute to the resistance in human lung cancer cells (Eijdems et al. 1995).

1.4.4.5 miRNAs and epirubicin/paclitaxel

Chemotherapy treatments can modulate the expression of some miRNAs, with various effects. As previously mentioned, epirubicin and paclitaxel have been shown to induce the export of the tumour suppressor miR-503-5p in exosomes (Bovy et al. 2015). In patients having received neoadjuvant chemotherapy (epirubicin with/without docetaxel), miR-200c was found down-regulated in non-responders as compared to responders. The transfection of doxorubicin-resistant cells with a miR-200c mimic was able to enhance the chemosensitivity to epirubicin (Chen et al. 2012). In a study on MDA-MB-231 resistant to epirubicin, docetaxel or vinorelbine, Zhong and colleagues found 22 miRNAs increasingly secreted into exosomes, potentially implicated in the transfer of resistance (Zhong et al. 2016).

1.5 Tumour microenvironment

Breast tumours are not only composed of breast cancer cells, they also include a variety of other cell types and extracellular matrix component, which are known as the tumour microenvironment. The cell types comprise fibroblasts, pericytes, endothelial and immune cells and bone-marrow derived cells (Hanahan & Weinberg 2011). The crosstalk between the microenvironment and the cancer cells influences the tumour progression and evolution towards eradication, metastasis or resistance or response to therapy. Fibroblasts are major cellular components of the tumour microenvironment. Once they are activated by cancer cells, they are called tumour-associated fibroblasts (CAFs) and their interactions are frequently studied (Maia et al. 2018). For instance, it has recently been shown that the CAFs play a role in determining the molecular subtype of breast cancer. Researchers demonstrated

that the paracrine crosstalk between basal-like carcinoma cells expressing the platelet-derived growth factor (PDGF)-CC and the CAFs expressing its receptor was controlling the subtype of the tumour. Impairing the PDGF-CC led to the conversion towards a hormone receptor-positive subtype (Roswall et al. 2018). Exosomes from pancreatic CAFs present in pancreas cancers, resistant to gemcitabine, were shown to transfer miR-146a to cancer cells, promoting drug resistance (Richards et al. 2017). The stroma can be shaped to receive metastatic cells by tumour-promoting pro-inflammatory cells, but also by circulating factors. Extracellular vesicles (EVs) were also shown to participate to the metastatic process by preparing a pre-metastatic niche, an environment that prepare the tissue to received metastasis (Peinado et al. 2012).

Endothelial cells play a crucial role in the tumour progression as they are responsible for the blood supply and the access to oxygen and nutrient necessary for the tumour expansion. Blood vessels are used by metastatic cells to disseminate thorough the organism. Tumour vascularization is however poorly organized, with differences in vascular maturity, leading to hypoxic area lacking nutrients within the tumour. This influences the heterogeneity of the tumour and the distribution of drugs to the cells, and thus the efficiency of therapies (Carmeliet & Jain 2000; Junttila & De Sauvage 2013). The main factors implicated in angiogenesis are the vascular endothelial growth factor (VEGF) and the angiopoietin family. In addition to cytokines and growth factors, EVs have recently emerged as important regulators of angiogenesis. Tumour-derived EVs were shown to promote endothelial cell migration and tube formation (Zhuang et al. 2012; Umezu et al. 2013). Under hypoxia, glioblastoma-derived microvesicles were able to induce the proliferation of endothelial cells (Skog et al. 2008). The communication is also observed in the reverse direction. Indeed we and other have shown that endothelial EVs could impact tumour cell behaviour (Bovy et al. 2015). These examples illustrate the complexity of the tumour-stroma interactions, and the need for a better understanding of the crosstalk between various cell types.

The implication of the small non coding RNAs microRNAs (miRNAs) in the development of human breast cancer is developed in the next chapter

II. MicroRNAs

MicroRNAs (miRNAs) are small non-coding RNAs of 20 to 24 nucleotides. They play important roles in the regulation of target genes by binding to complementary regions of messenger transcripts, and repress their translation or regulate their degradation.

The first miRNA was discovered in 1993 in the nematode *C. elegans*, and it revolutionized the field of molecular biology (Lee et al. 1993). Coming from regions previously considered as "Junk DNAs" of unknown function, more than 2000 miRNAs have been identified in human. It is now known that they are highly conserved between species and they are considered as important regulatory sequences. MiRNAs are predicted to regulate up to 60% of the coding genes, and have been implicated in most of the physiological processes, but also in pathologies. Depending on the availability of mRNAs and the level of expression of the miRNAs in a given cell type, miRNAs provide a unique combination of effects. Some are expressed in a tissue-specific manner, or depending of the developmental stage. Moreover, they are secreted into extracellular fluids. Since the biogenesis and structure of miRNAs are different between plants, viruses, and animals, in this work we will focus on miRNAs in animals only (Krol et al. 2010; Macfarlane & Murphy 2010; O'Brien et al. 2018).

2.1 Nomenclature

Basically, the nomenclature of miRNAs is made of several elements:

- The prefix is given depending on the organism. For instance, *hsa* for humans, *mmu* for mice.
- *miR* is used for mature sequences, while the precursor hairpins are written *mir*.
- A sequential numerical identifier is added (miR-21, miR-503, miR-3085). Homologous sequences in different species receive the same number.
- The suffix -5p or -3p is assigned for sequences derived from the 5' or 3' arms of the hairpin precursor.

MiRNAs can receive a letter suffix when they are part of the same family, but contain sequence differences, such as hsa-miR-301a and hsa-miR-301b.

Additional numbered suffix can be given to the name of paralogous sequences, when the mature sequences are identical but the hairpin loci is distinct. For example: hsa-miR-16-1 and hsa-miR-16-2.

Previously, the non-expressed miRNA of a duplex was designated with an asterisk mark, as in miR-302a, aka miR-302a-5p, vs miR-302a*, standing for miR-302a-3p. However, deep sequencing analysis have demonstrated that many miRNAs were indeed expressed and thus wrongly annotated (Kozomara & Griffiths-Jones 2014; Griffiths-Jones et al. 2006).

2.2 Biogenesis

The biogenesis of miRNAs is a highly regulated process, taking place in 5 steps (**fig. I 9**).

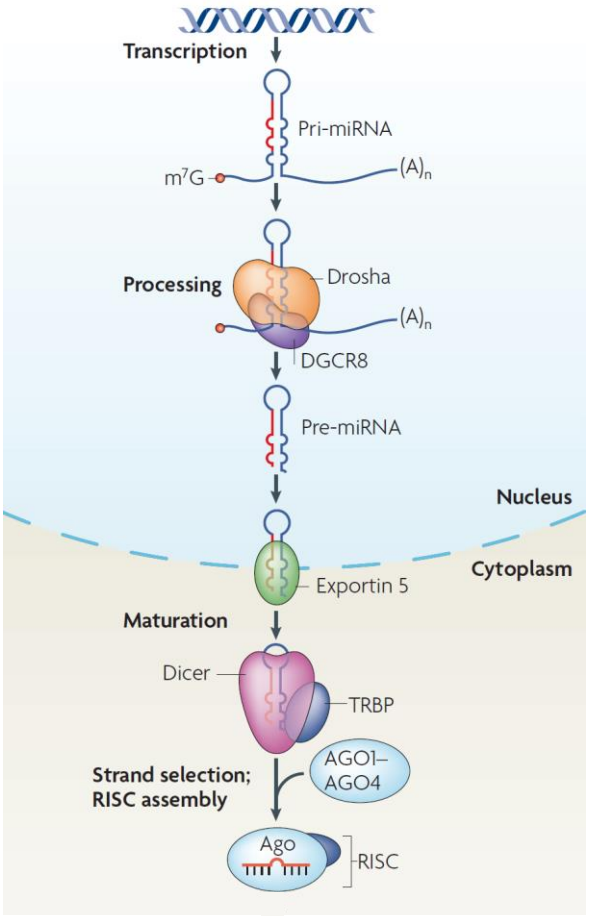

Figure I 9. ***MiRNA biogenesis****. miRNAs are transcribed by an RNA polymerase into an primary transcript (pri-miRNA). The hairpin structure is recognized by the enzyme Drosha and its co-factor DGCR8, which cleaves the pri-miRNAs and releases pre-miRNAs. After their export into the cytoplasm by the Exportin-5, the enzyme Dicer and its co-factors TRBP and/or PACT cleaves the precursor, generating a mature miRNA duplex. One strand is selected, the other one is degraded, and the mature miRNA is loaded to an Ago protein to form the RISC. Figure adapted from Inui et al. 2010.*

2.2.1 Transcription

Most of miRNAs are first transcribed by an RNA polymerase II (RNA Pol II), although some can be targeted by RNA Pol III. Around 50% of the miRNA loci are located in introns

of protein coding genes, and only few in exon. Then they share the promotor of their host gene. The remaining miRNAs are intergenic, transcribed independently of coding genes and regulated by their own promotor. The transcripts are called primary miRNAs (pri-miRNAs). When the loci are close, it often happens that several pri-miRNAs are transcribed together, forming a cluster. Those miRNAs may later be regulated individually at post-transcriptional level. Usually of more than 1 kb, the pri-miRNAs are capped in their 5' end (M^7GpppG) and are provided with a poly-adenylated tail in 3' (Lee et al. 2004). A cluster contains a number of stem-loop structures where the future miRNAs are paired in double stranded RNA (dsRNA). A typical pri-miRNA consists of one or more stems of 33–35 dsRNA, a terminal loop and single-stranded RNA (ssRNA) segments at both sides (Ha & Kim 2014; O'Brien et al. 2018). Transcription of miRNA genes is regulated the same way as protein coding genes, under the control of various transcription factors.

2.2.2 Nuclear cleavage

The maturation of the miRNA starts in the nucleus, when the hairpin is cleaved by the Microprocessor complex. The latter is a large protein complex formed by the RNase III endonuclease Drosha and its cofactor, the double-stranded RNA-binding protein DGCR8 (DiGeorge syndrome Critical Region gene 8). DGCR8 is responsible for recognizing and binding the pri-miRNA. DGCR8 interacts with the pri-miRNA and determines the cleavage site. The flanking ssRNAs and the dsRNA are the critical segments for this processing. Drosha is in charge of cleaving the 3' and 5' arms of the pri-miRNA, eleven bases away from the junction between the ssRNA and dsRNA. This process releases a pre-miRNA hairpin of about 65 nt (Han et al. 2006; Macfarlane & Murphy 2010). Interestingly, Drosha and DGCR8 control the level and stability of each other (Krol et al. 2010).

2.2.3 Nuclear export

The next steps in the maturation process happen in the cytoplasm. The pre-miRNAs are exported outside the nucleus by the nucleocytoplasmic transporter factor Exportin 5 (EXP5) and its cofactor Ran. Once in the cytoplasm, Ran hydrolyses GTP and the pre-miRNA is released. EXP5 recognizes the dsRNA stem bigger than 14 bp with a short 3' overhang. Through this mechanism, only the correctly processed pre-miRNAs are exported (Lund et al. 2004; Kim et al. 2009).

2.2.4 Cytoplasmic cleavage

Once in the cytoplasm, the pre-miRNA undergoes a second cleavage by the RNase III endonuclease Dicer. The enzyme removes the terminal loop, resulting in a miRNA duplex of around 22 nt, with 2 nt protruding as overhangs at each 3' end (Winter et al. 2009). Dicer is a highly conserved multi-domain protein comprising two tandem RNase III nuclease domains, an N-terminal helicase domain which interact with the terminal loop of the pre-miRNA, facilitating its recognition, and the PAZ (PIWI-AGO-ZWILLE) domain, which binds the 3' and 5' end of the pre-miRNA. Dicer interacts with two cofactors: TRBP (Transactivation Response RNA Binding Protein) and PACT (protein activator of PKR). These two facilitate Dicer activity, but are not essential. TRBP, a double-stranded RNA-binding domain protein, also helps stabilizing Dicer (Winter et al. 2009; Ha & Kim 2014; Chendrimada et al. 2005).

2.2.5 Formation of the RNA-Induced Silencing Complex (RISC)

The miRNA duplex is finally loaded in a complex with an Argonaute (AGO) protein, usually AGO2, generating the effector complex, RISC. This process happens thanks to a RISC-Loading Complex (RLC), composed of Dicer, its cofactor TRBP (and/or PACT) and AGO. The RLC assembles spontaneously, the miRNA hairpin joining only after the formation of the ternary complex. Some reports indicate that Dicer may stay associated with the RISC (Gregory et al. 2005). The miRNA duplex is loaded on AGO, which also requires chaperone activity of Hsc70/Hsp90. It is composed of the future mature miRNA, or guide strand, and of its complementary sequence, the passenger strand. The relative thermodynamic stability of the two ends of the duplex determines which strand is degraded. The strand with the weakest stability of base pair at the 5' end is selected. The other strand is degraded via the endonucleolytic activity of AGO2. Since other human AGO (AGO1, 3 and 4) lack the slicer activity, another RNA helicase may mediate the removal of the passenger strand. After the loading, Dicer dissociates from the RISC. The mature miRNA and AGO associate with other proteins to form the RISC, the ribonucleoprotein structure effector of the miRNA activity (Khvorova et al. 2003; Winter et al. 2009; Kim et al. 2009).

2.2.6 Non canonical biogenesis pathways

There are multiple non-canonical miRNA biogenesis pathways. These pathways usually involve proteins from the canonical pathway, such as Drosha, Dicer, EXP5 and AGO2. For instance, mirtrons, miRNAs derived from introns of mRNAs during splicing, are

produced in a Drosha/DGCR8-independent way. They are directly exported to the cytoplasm without Drosha cleavage, and become substrate for Dicer. Alternatively, small hairpin RNAs (shRNAs) are cleaved by the Microprocessor complex but are further processed in a Dicer-independent manner, relying on AGO2 for their cleavage (O'Brien et al. 2018).

2.3 Mechanism of action

2.3.1 Composition of RISC

In addition to its role in selecting the guide strand, RISC is the multiprotein complex responsible for the RNA interference mediated by miRNAs. The minimal component of RISC is one miRNA and one AGO protein. The miRNA is the guide which allows the RISC to select its target by base-pairing with a complementary mRNA. Other auxiliary proteins can act as regulators or modify its function, and the binding of RNP (ribonucleoprotein) to the target mRNA can either counteract or facilitate RISC activity (Krol et al. 2010).

2.3.2 Argonaute proteins

This family of proteins is highly conserved among eukaryotes. It is composed of two subfamilies: AGO and Piwi. The Piwi proteins bind only to piwiRNAs and are only expressed in germ lines, while the AGO subfamily is ubiquitous and binds to miRNAs and siRNAs. Humans have four AGO proteins, AGO1-4. They all bind to miRNAs with few differences in miRNAs repertoire (Azuma-Mukai et al. 2008). AGO proteins are bilobal, one N-terminal lobe with an N-terminal domain and a PAZ domain, and the other C-terminal lobe containing a MID (middle) and a PIWI domain. The 5' monophosphate of the guide miRNA is anchored at the interface between the MID and PIWI domains, while the 2 nt 3'end overhangs is recognised and bound by the PAZ domain (**fig. I 10**). The PIWI domain is similar to that of RNase H, capable of slicing target mRNAs. In humans, only AGO2 is able to slice perfectly complementary target mRNAs through its catalytic triad in the PIWI domain (two aspartates and one histidine). However, all AGO can induce translational repression and mRNA degradation (Huntzinger & Izaurralde 2011; Petri et al. 2011; Nakanishi 2016; Wilson & Doudna 2013).

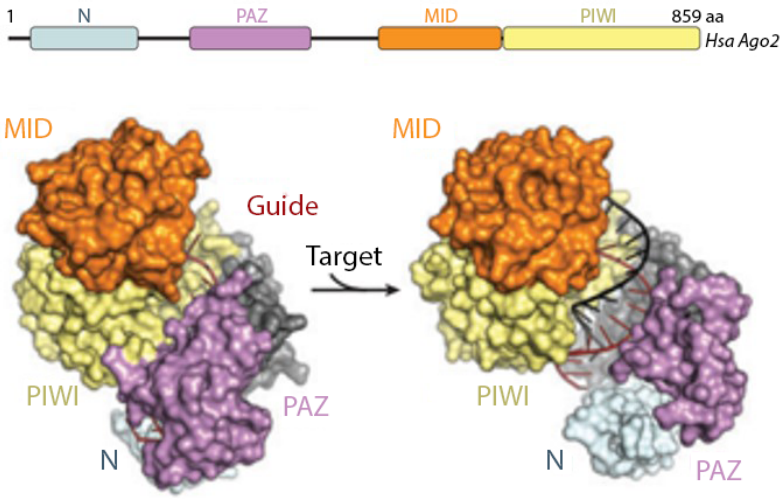

Figure I 10. ***Tridimensional structure of a AGO protein linked to a miRNA****. The N-terminal and PAZ domain link to the 3' end of the miRNA, while the 5' end is bound by the MID domain. The binding of the miRNA to a target mRNA induces a change in conformation: the 3'end of the miRNA is released from the Paz domain, and the two lobes of the protein open. The Piwi domain contains the catalytic site of Ago Figure adapted from Wilson & Doudna 2013.*

2.3.3 *GW182 and P-bodies*

Among the cofactors of AGO, GW182 appears as protein essential for RISC-mediated silencing. As its name indicates, the protein is characterized by a high number of glycine-tryptophan (GW) repeats. These repeats enable the interaction of GW182 with AGO. The C-terminal of the protein can bind directly to mRNA, which, together with the MID domain, promotes the mRNA degradation. GW182 acts as a scaffold for effector protein (Behm-Ansmant et al. 2006). The protein also possesses a glutamine- rich domain, regulating its localization to Processing-bodies (P-bodies). P-bodies are functional cytoplasmic domains specialized in reversible mRNA repression and mRNA decay. They contain a variety of enzymes and RNP necessary for mRNA decapping, deadenylation, RNA degradation and translational repression (Cougot et al. 2004; Eulalio et al. 2007). P-bodies are strongly linked to the activity of RISC, and the inhibition of miRNA biogenesis prevents their formation (Pauley et al. 2006; Nakanishi 2016; Macfarlane & Murphy 2010).

2.3.4 Identification of target mRNA

The identification of target mRNAs by a miRNA depends on the rules of base pairing. The miRNA sequence is complementary to some transcripts, to a sequence usually located in the 3'UTR (untranslated region) of the mRNA. MiRNAs can also bind to sequences in the 5' or coding region of an mRNA, but it is more singular and usually less effective. On the miRNA side, the target recognition relies strongly on the complementarity with the **seed**, the nucleotides 2 to 8 of the 5' end (**fig. I 11**). Particularly conserved, those sequences

determine families of paralog miRNAs (Lewis 2005). One miRNA can target several mRNAs, and conversely a single mRNA can be regulated by multiple miRNAs (Bartel 2004). The complementarity of the other bases can potentially play a role, especially when the seed pairs with imperfect complementarity. The degree of complementarity between the miRNA and the target determines the silencing mechanism (Macfarlane & Murphy 2010).

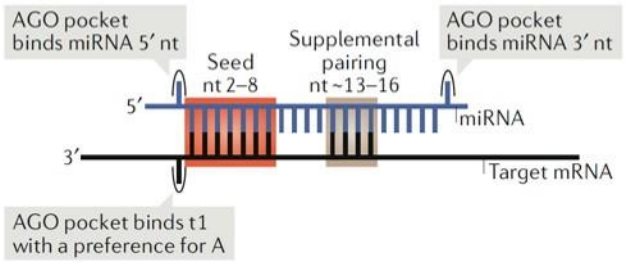

Figure I 11. ***Interaction between a miRNA and its target mRNA****. The seed region (nucleotides 2-8 from the 5'end) are crucial for target mRNA recognition. An adenine in the target mRNA opposite miRNA nucleotide 1 also increases the specificity and affinity of the binding to Ago, as well as additional base pairing along the miRNA. Figure adapted from Gebert & MacRae 2018.*

2.3.5 mRNA cleavage

A direct cleavage of the target mRNA can be catalysed by AGO2. For that to happen, it requires an extensive and near-perfect base-pairing between the mRNA and the seed (Yekta et al. 2004; Bartel 2009). This is usually the case in plants. In animals, however, another mechanism is preferentially responsible for target repression. AGO2 thus tends to act like the other non-endonucleolytic AGO and mediate translational repression. It has been shown that a strong interaction between the miRNA and its target destabilizes the association between AGO and the miRNA, promoting its degradation (Krützfeldt et al. 2005).

2.3.6 Translation repression and mRNA decay

When the interaction between the miRNA and its mRNA target is not fully complementary, the mRNA is not directly cleaved but rather goes through a translational repression. Different mechanisms exist that leads to RNA decay (**fig. I 12**). RISC can inhibit the translation of mRNA in several ways. AGO can bind to the 5' cap of mRNAs, hence interfering with the binding of the translation initiation factors. RISC has also been reported to cause the ribosomes to dissociate prematurely, leaving the translation incomplete. But miRNAs not only repress target translation, they can also trigger target degradation. Indeed, RISC can provoke the degradation of mRNA even before the initiation. GW182 has the capacity to recruit deadenylases complexes such as the PAN2/3, followed by the CCR4–

NOT. By deadenylating the poly-A tail, RISC prevents the circularization of the mRNA (Christie et al. 2013). Then the miRNA promotes the decapping of mRNAs by the DCP1:DCP2 complex. Removing the cap and the tail enables the access of exonucleases to nucleotides, leading to the mRNA exonucleolytic digestion at both ends (Behm-Ansmant et al. 2006; Braun et al. 2012; Eulalio et al. 2007). Today, it seems that the major mechanism of silencing by miRNAs in animals is the target degradation (Huntzinger & Izaurralde 2011).

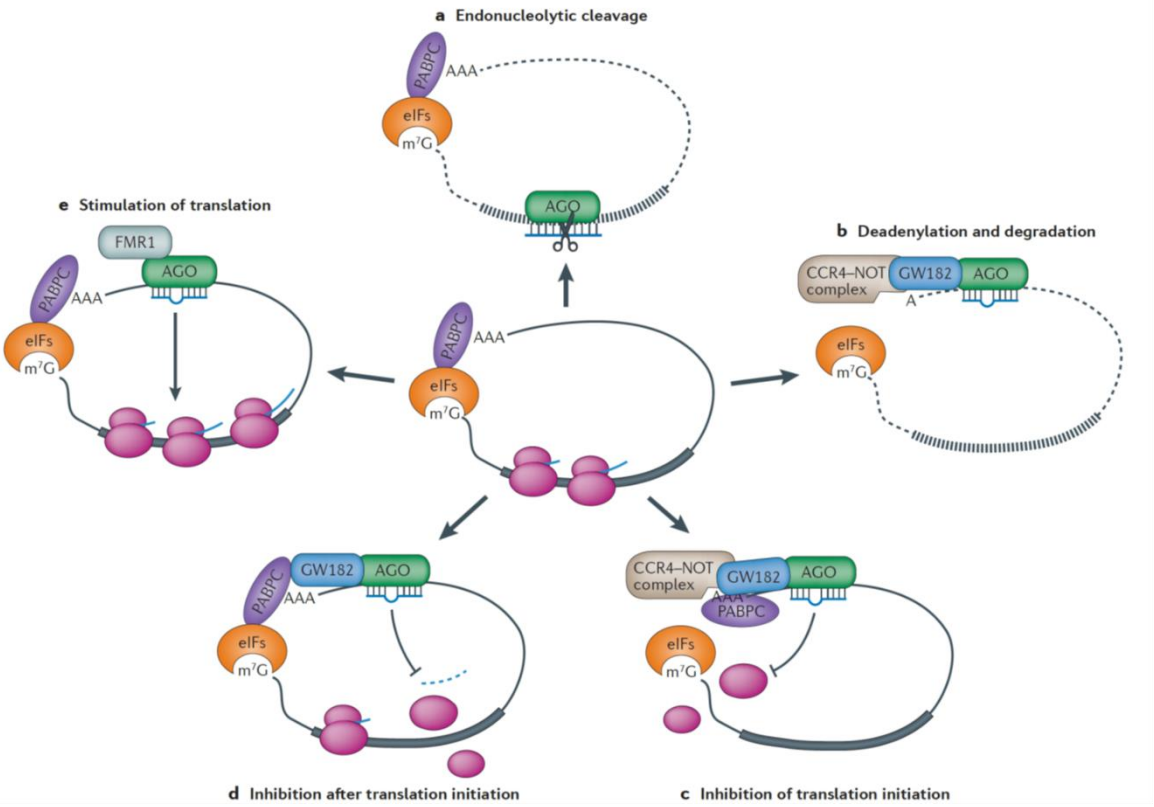

Figure I 12. ***Mechanisms of target regulation by miRNAs.*** *miRNAs regulate gene expression through multiple pathways. A complex of eukaryotic initiation factors (eIFs) binds the 5′ cap and the cytoplasmic poly(A)-binding protein (PABPC), connecting the 5′ and 3′ ends of mRNAs and stimulating their translation by the ribosome (in pink). A. Perfect pairing between a miRNA and its target site induces endonucleolytic cleavage by Argonaute (AGO), leading to rapid degradation of the mRNA. B. Partial pairing of the miRNA complex to target 3′ untranslated region (UTR) sites can result in deadenylation of the mRNA through recruitment of the CCR4–NOT complex by the RISC-associated GW182 proteins. Loss of the poly(A) tail causes dissociation of PABPC and leads to degradation of the mRNA. C. The RISC can also induce translational repression by blocking initiation via recruitment of CCR4–NOT by GW182. D. Translational repression can also be induced by the RISC by inhibiting a step after initiation, such as promoting ribosome drop-off or stimulating proteolysis of the nascent peptide. E. miRNAs have also been shown to upregulate target expression under certain conditions through a mechanism that involves Argonaute and fragile X mental retardation protein 1 (FMR1). Figure adapted from Pasquinelli et al. 2012*

2.3.7 Translation stimulation

Surprisingly, some studies have reported an up-regulation of gene expression via miRNAs. It seems to happen under specific conditions. AGO2 has been shown to activate

the translation of some transcripts in serum-starvation condition (Vasudevan & Steitz 2007). During amino-acid starvation, miR-10a could favour the activation of the translation of mRNAs encoding ribosomal proteins (Ørom et al. 2008). In another study, miR-122-5p was able to stimulate the translation of genes of the Hepatitis C Virus by interacting directly with two target sites in the 5'UTR of the viral genome (Henke et al. 2008).

2.4 miRNAs in cancer

MiRNAs are important actors of tumour development. Depending on the type of cancer, miRNAs can play the role of oncogenes or tumour suppressors. They are intensively studied in cancer, considering that they can take part in tumour growth, metastasis or drug resistance. They are also considered for their potential as biomarkers of prognosis or diagnosis, and even therapy. Here are a few examples of their roles in tumour processes.

A global depletion of miRNAs by inhibiting key components of their biogenesis was proven to be oncogenic, promoting cellular transformation and tumorigenesis (Kumar et al. 2007). Dicer expression, for instance, is frequently dysregulated in cancer. In ovarian cancer, a downregulation of Dicer expression leads to cell proliferation, migration and cell cycle progression (Kuang et al. 2013). Likewise, miRNA expression in tumour cells is globally decreased compared to normal tissues (Lu et al. 2005). Indeed, many miRNA genes are located in regions of the genome that are frequently deleted, amplified or translocated in cancer (Calin et al. 2004). The dysregulation of miRNA level can also be due to alterations of the proteins that control their expression. For instance, the miR-34 family members are direct transcriptional targets of p53 and act as part of the p53 suppressive network of aberrant cell proliferation (He et al. 2007). MiRNA promotor can also be epigenetically regulated (Lin & Gregory 2015). Single-nucleotide polymorphisms (SNPs) of the miRNA seed region can affect its capacity to recognize mRNA targets (G. Sun et al. 2009). Conversely, mutations at the 3'UTR of mRNAs have been observed in tumour cells, modifying or removing the regulatory capacity of miRNAs (Ziebarth et al. 2012). Eventually, other RNA sequences with multiple RNA binding sites may compete with the target and act as sponges for the miRNA. Those RNAs can be long non-coding RNAs (lncRNAs), pseudogenes, circular RNAs or even mRNAs (Hayes et al. 2014).

2.4.1 miRNAs in metastasis

One of the main process in the development of metastasis is the epithelial–mesenchymal transition (EMT), which gives the cell the capacity to migrate. The role of

miRNAs in regulating EMT is fundamental. Some are considered as anti-metastasis by blocking the transition. For example, the miR-200 family members target the transcription factors ZEB1 and ZEB2 (zinc-finger E-box-binding homeobox). Those transcription factors favour the EMT through the inhibition of the expression of epithelial genes (Gregory et al. 2008). The level of the miR-200 family members are lower in metastatic triple-negative breast cancer when compared to other types of breast cancer cells and tumours (Humphries et al. 2014). Interestingly, ZEB1 represses the miR-200 family and other miRNA anti-EMT, thus creating a feedback loop towards tumorigenicity (Wellner et al. 2010). On the contrary, other miRNAs mostly promote EMT. For instance miR-10b is considered as a mediator of motility and invasiveness, and its level is increased in metastatic breast cancer (Ma et al. 2007; Piasecka et al. 2018).

2.4.2 miRNAs in drug resistance

Since miRNAs are implicated in cancer, they have been studied for their potential role in the development of resistance to anti-cancer therapies. Depending on the target mRNAs available for the miRNAs, one miRNA can be considered an oncogene in one context, and a tumour-suppressor in another. MiR-15b and miR-16 have been shown to repress the expression of the anti-apoptosis protein BCL2, hence restoring chemosensitivity in gastric cancer cell lines (Xia et al. 2008). In MDA-MB-231 cell line, overexpression of miR-130a-3p and miR-451a also restores the chemosensitivity to doxorubicin (Ouyang et al. 2014). On the other hand, some miRNAs are overexpressed in different resistant cancer types and their knockdown restores the response to various drugs. For instance, it is the case for miR-221 and miR-222 in castration resistant prostate cancer (T. Sun et al. 2009) or miR-21 in clear renal cell carcinoma (Gaudelot et al. 2017). It has been described that miR-21 could protect pancreatic cancer cells from gemcitabine, among other things by targeting the pro-apoptosis protein FasL (Wang et al. 2013). In breast cancer overexpressing HER2, the inhibition of miR-375 has been demonstrated to be partly responsible for the development of resistance against trastuzumab (a monoclonal antibody against HER2). As a miRNA acting as a tumour suppressor, it inhibits IGF1R expressing. Losing miR-375 means activating another growth factor receptor (Ye et al. 2014).

2.4.3 miRNAs in diagnosis and therapy

Every tumour presents a specific profile of miRNAs. Since they can be released into extracellular fluids, miRNAs are potential biomarker candidates for a large variety of

diseases, including cancers. They can help discriminate between healthy and cancer patients, or act as prognosis markers. All in one, they could be used as efficient, non-invasive and cheap biomarkers. As marker of different cancers, they can assist more usual techniques. For instance, the classification of breast cancer into molecular subtypes is an important factor for the medical care of the patients. Distinct expression patterns of miRNAs have been identified for each type of breast cancer (Farazi et al. 2014). Moreover, miRNAs can discriminate between benign and malignant lesion, for example in prostate cancer (Mahn et al. 2011). MiRNAs can also be used to predict the response to treatment. In pancreatic cancer patients, high serum level of miR-21 was correlated to poor prognosis and a lower overall survival. Moreover, this could also serve to predict the chemosensitivity of the tumour to gemcitabine (Wang et al. 2013). MiR-21 (overexpressed) is one of the most common miRNA associated with cancer and patient outcome (Pan et al. 2010).

If the majority of studies focuses on biomarkers, some researchers are looking for a way to exploit miRNAs as therapeutic agents. A phase I clinical trial has already successfully assessed the feasibility and safety of injecting a liposomal miR-34a mimic (MRX34). The goal is to restore the lost suppressor function of endogenous miR-34a. This miRNA is involved in the regulation of many oncogenes, in processes like chemoresistance, metastasis or tumour immune evasion (Beg et al. 2017). Other strategy would be to downregulate the level of harmful miRNAs. This method has been applied in a phase II trial by targeting miR-122 with an antisense *locked-nucleic acid* (LNA) DNA. The miRNA inhibitor (antimiR) acts by forming a duplex with its miRNA target, therefore inhibiting its action (Janssen et al. 2013). The major obstacle is to guarantee the efficient delivery of RNA to cells, i.e., avoiding degradation in body fluids and allowing them to pass the lipid membrane. Lipid carriers such as liposomes or exosomes are an efficient way to overcome those hurdles (Lieberman 2018). Other concerns regard the danger of off-target effects, the accuracy of the dosing, and the possible activation of innate immune nucleic acid sensors, such as Toll-like receptors. Indeed, miRNAs can act as ligand of the Toll-like receptor and trigger the activation of an inflammation response (Christopher et al. 2016; Fabbri et al. 2012).

2.5 Circulating miRNAs

As mentioned in the previous section, miRNAs are secreted into the extracellular milieu and can be found in virtually all biological fluids (Webber et al. 2010). MiRNAs in plasma are highly stable and protected from degradation (Mitchell et al. 2008). Once in the circulation, they can be delivered to other cells where they are able to perform their

regulatory role (Montecalvo et al. 2012). They appear as a new mode of cell-cell communication. Their stability in biological fluids is due to their association with either proteins, lipoproteins, or extracellular vesicles (EVs). If miRNAs in EVs are currently the most studied, it is still unclear which fraction is the most predominant (Arroyo et al. 2011; Gallo et al. 2012). It could be a mechanism dependent on the miRNA or the cell of origin (O'Brien et al. 2018).

2.5.1 In complex with proteins

MiRNAs have been found bound to proteins in the circulation. The first study to identify miRNAs outside EVs in cultured cells supernatants suggested that they could be involved with RNA-binding proteins such as nucleophosmine-1 (Wang et al. 2010). Other studies have found non-vesicular miRNAs in plasma that were protected from degradation by the protein AGO2 (Turchinovich et al. 2011; Arroyo et al. 2011). By forming complexes with AGO2, miRNAs remained resistant to RNaseA degradation in a dose- and time-dependent way (Li et al. 2012). Plasma miRNAs have also been shown in complex with AGO1. The profile of miRNAs associated with AGO1 or AGO2 inside MCF7 cells was different regarding one protein or the other. However, those differences disappeared in circulating miRNAs (Turchinovich & Burwinkel 2012). Turchinovich and colleagues have hypothesized that miRNAs-AGO2 complexes are the remains of dead cells. However, no significant cell lysis was found in Wang's experiment. The role of such miRNA-protein complexes in cell communication is still unknown (Turchinovich et al. 2011; Wang et al. 2010).

2.5.2 In complex with lipoproteins

Circulating miRNAs can also be carried by High-Density Lipoproteins (HDL). HDL are lipoproteins implicated in the transport of lipids, such as cholesterol, from cells to the liver, where they will be eliminated. HDL have been shown to carry miRNAs and deliver them to recipient cells. Moreover, in the same study, scientists demonstrated that the miRNA-HDL profile was different between normal patients and patients suffering from familial hypercholesterolemia (Vickers et al. 2011). In another study, miR-486 and miR-92a were associated with HDL. Together, these studies allowed the identification of subjects suffering from stable or vulnerable coronary artery disease (Niculescu et al. 2015). Circulating miR-223 was shown to transfer from HDL to endothelial cells, where it would inhibit its target ICAM-1 (Tabet et al. 2014). Conversely, another group of scientists could

not discriminate patients suffering from the same disease using miR-223 circulating with HDL, and they weren't able to transfer miRNAs to endothelial cells, smooth muscle cells, or peripheral blood mononuclear cells (Wagner et al. 2013). Differences in the concentration of miR-223 in the HDL might be responsible for the discrepancies (Michell & Vickers 2016).

2.5.3 In extracellular vesicles

Transfer of information via EVs in now considered as a new mode of intercellular communication. They can carry proteins, lipids and nucleic acids, from producing to receiving cells, via the extracellular milieu and the blood circulation. As potential biomarkers, studies tend to find miRNAs contained in EVs more efficient to discriminate between conditions. However, some miRNAs have disclosed better diagnostic performances when tested in the whole plasma (van Eijndhoven et al. 2016; Endzeliņš et al. 2017). Today, it is considered that cells secrete three main classes of EVs, based upon their biogenesis (**fig. I 13**). They also have different composition and function. The microvesicles (MVs) are formed by direct budding from the plasma membrane. Then the apoptotic bodies, as their name implies, are derived from cells undergoing programmed cell death. Last but not least, exosomes are small vesicles originating from the endocytic pathway. This aspect will be developed in the next chapter.

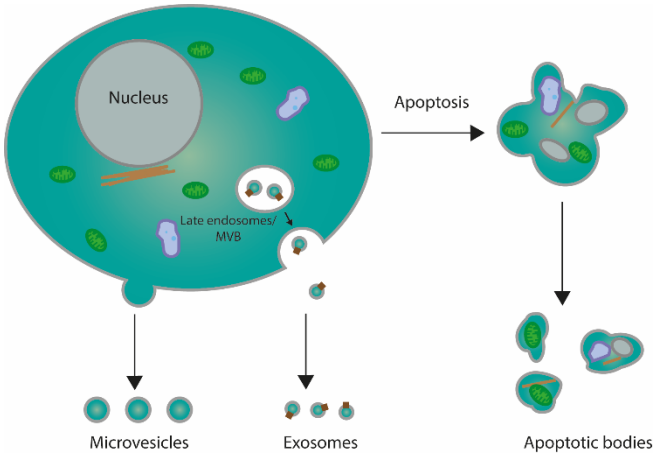

Figure I 13. ***Types of extracellular vesicles****. Currently, three main types of extracellular vesicles can be discriminated based on their biogenesis. Figure adapted from Akers et al. 2013.*

2.5.3.1 Microvesicles

Microvesicles come from the direct budding of the plasma membrane and are released directly into the extracellular space. Their biogenesis relies mainly on rearrangement of the plasma membrane. Their size varies between 50 to 1000 nm, but can be even larger (up to 10 µm) when they are produced by cancer cells. In that case, they are called oncosomes (Minciacchi et al. 2016). The lipid and protein composition of their membrane is close to the

one of their cell of origin, but enriched in cholesterol (van Niel et al. 2018). Although MVs are preferentially studied for their protein content, they still carry miRNAs. For instance, endothelial cells from patients suffering from diabetes mellitus II secrete MV with a decreased amount of miR-126 and miR-26a, compared to healthy subjects. MiR-126 promotes the regeneration of endothelial cells and has a protective effect. It was shown that hyperglycaemia reduces the packaging of miR-126 and miR-26a into microparticles (Jansen et al. 2013). MVs have been shown to transfer miRNAs (miR-1228-3p, miR-1246-5p, miR-1308-5p, miR-149-3p, miR-455-3p, miR-638-5p and miR-923-5p) from resistant to sensitive cell lines. Those miRNAs were implicated in pathways in relation with drug resistance (Jaiswal et al. 2012; Kanada et al. 2016; Akers et al. 2013).

2.5.3.2 Apoptotic bodies

When a cell undergoes apoptosis, the chromatin condenses and the membrane starts to bleb. The cell ends up disintegrating the cellular content and encapsulates it into distinct membrane enclosed vesicles, the apoptotic bodies. They contain DNA fragments, histones and organelles, and their size varies from 50 nm to 5 µm (Akers et al. 2013). Zernecke and colleagues showed that, during atherosclerosis, apoptotic bodies from endothelial cells were enriched in miR-126. Recipient cells having taken up those apoptotic bodies showed an increase in the transcription of CXCL12, a cytokine implicated in anti-apoptotic response (Zernecke et al. 2009). Another study demonstrated that apoptotic bodies were able to rescue apoptosis-deficient bone marrow mesenchymal stem cells, via the reuse of apoptotic bodies-derived miR-328-3p (and ubiquitin ligase RNF146). The miRNA could inhibit Axin1 and rescue the impaired cells (Liu et al. 2018; Zhu et al. 2017).

2.6 miR-373-3p, miR-887-3p, miR-122-5p and miR-129-5p

During the course of this work, we have taken interest in four microRNAs: hsa-miR-373-3p, hsa-miR-887-3p, hsa-miR-122-5p and hsa-miR-129-5p. For ease of reading, the prefix “hsa” will be omitted.

2.6.1 miR-373-3p

MiR-373-3p was first identified in embryonic stem cells (Suh et al. 2004). Since the -3p form is preferentially expressed, it’s the -5p that is marked with an asterisk in papers with the old nomenclature. MiR-373-3p is located in chromosome 19q13.4. It belongs to a cluster of miRNAs: the miR-371-3 cluster, which gives four mature miRNAs (miR-371, miR-372,

miR-373-3p and miR-373-5p). In addition, miR-373-3p is also part of a family of miRNA clusters sharing the same seed sequence, the miR520/373 family, consisting of three clusters: miR-302/367, miR-371/372/373, and miR-520. MiR-373-3p is regulated by HCV in hepatocytes. The effects of the upregulation of miR-373-3p are beneficial to the virus, because it decreases the expression of important factors of the Interferon signalling pathway: Jak1 (Janus Kinase 1) and IRF9 (IFN regulating factor 9) (Mukherjee et al. 2015).

2.6.1.1 MiR-373-3p in cancer

Mir-373-3p is a miRNA with many implications in cancer. It has been presented as tumour suppressor or oncogene, depending on the studies (**fig. I 14**).

MiR-373-3p has first been identified as an **oncogene** in testicular germ cell tumours. There, its overexpression induced the proliferation and tumorigenesis of primary human cells, by repressing the expression of the tumour suppressor LATS2 (Voorhoeve et al. 2007). MiR-373-3p, among other miRNAs, has been found increased in serum exosomes from patients suffering from epithelial ovarian cancer. However, the circulating level of miR-200b and miR-200c was found to better discriminate between healthy and sick patients than miR-373-3p (Meng et al. 2016). MiR-373-3p has been found to be upregulated in HeLa and MCF7 cancer cells under hypoxia in a HIF-1α (hypoxia-inducible factor-1 alpha) dependent manner. The miRNA would then impair the DNA damage repair system by down-regulating

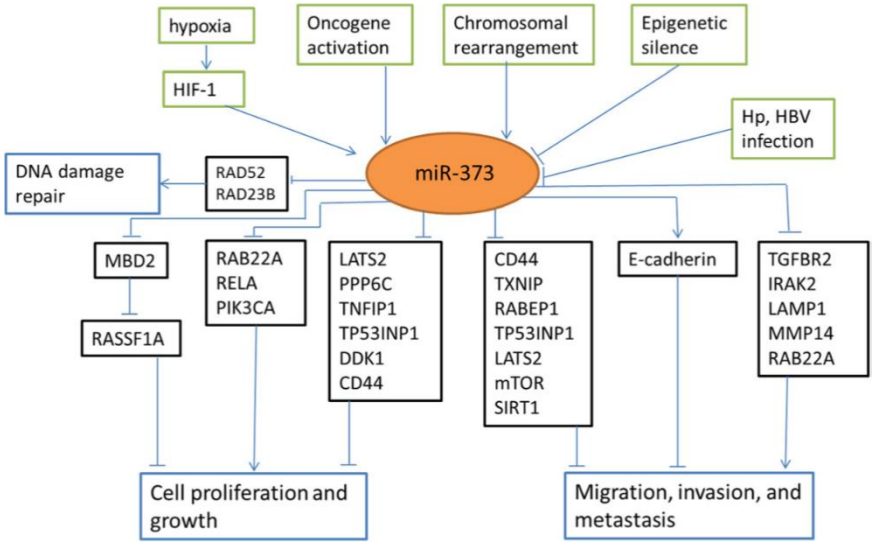

Figure I 14. ***Regulation network of miR-373-3p****. Green boxes: upstream regulators of miR-373, black boxes: functional targets of miR-373-3p, and blue boxes, the correspondingly involved cellular processes. miR-373-3p is involved in regulation of cell proliferation and growth, cell migration, invasion and metastasis, and DNA damage repair. Figure adapted from Wei et al. 2015.*

RAD23B and RAD52, two proteins implicated in homologous recombination repair. MiR-373-3p would then promote genetic instability and mutations (Crosby et al. 2009).

The miRNA can also act as a **tumour suppressor**. For instance, miR-373-3p is targeted by the oncogenic lncRNA HOTAIR. In ovarian cancer, HOTAIR would act as a sponge for miR-373-3p and decrease the plasma level of the miRNA by a competitive endogenous RNA mechanism (Zhang et al. 2016). In contrast to other studies, miR-373-3p here acted as a tumour suppressor by regulating the level of Rab22a, implicated in cell proliferation and EMT (Zhang et al. 2016). Epigenetic modifications are another way to silence miR-373-3p. Indeed, the re-expression of the miRNA improved the lung cancer cells response to cisplatin, inducing apoptosis and restricting cell migration. MiR-373-3p was found to repress RELA and PIK3CA (Adi Harel et al. 2015). Interestingly, the miR520/373 family members target RELA and TGFβR2 in breast cancer cells, influencing the NFκB and TGF-β signalling pathways. Inhibition of RELA led to a decreased secretion of IL-6 and IL-8, two pro-inflammatory cytokines. The downregulation of TGFβR2 cancelled breast cancer cells invasion in vitro and intravasation in vivo (Keklikoglou et al. 2012).

The role of miR-373-3p in **epithelial-mesenchymal transition** seems to be controversial. Mir-373-3p has been demonstrated to promote metastasis. Huang and colleagues have transduced MCF7 breast cancer cells with 450 miRNA vectors, and performed trans-well cell migration assays to identify which miRNAs stimulate cell migration. They discovered that miR-520c and miR-373-3p induced a strong migratory and invasion phenotype *in vitro*, and metastasis *in vivo*. They found that those effects were due, at least partially, to the downregulation of CD44 by the miRNAs. They validated CD44 as a specific target of miR-373-3p and miR-520c (Huang et al. 2008). Furthermore, it was later found that miR-373-3p stimulates metastasis and promotes EMT by decreasing the level of TXNIP (thioredoxin-interacting protein). It also activates the HIF1α-Twist signalling. This triggers a positive feedback loop, since Twist induces miR-373-3p expression. TXNIP is a metastasis suppressor gene, identified in melanoma (Yan et al. 2011; Chen et al. 2015). However, miR-373-3p has also been shown to induce the expression of the EMT suppressing gene e-cadherin. In prostate cancer cells, the miRNA was able to enhance the expression of its direct target e-cadherin and CSDC2 (cold-shock domain-containing protein C2). E-cadherin is a well-known protein of the epithelial phenotype, and its loss is a marker of EMT. Here miR-373-3p promotes the epithelial phenotype (Place et al. 2008).

With the data taken together, miR-373-3p seems to present paradoxical functions, sometimes promoting tumorigenesis, proliferation and metastases, sometimes triggering the

opposite effects. This is probably due to the cell context, the characteristics of the cancer cells and the tumour microenvironment (Wei et al. 2015).

2.6.2 miR-887-3p

Today, the potential roles and functions of miR-887-3p are still largely unknown. It is located on the 5p15.1 region of the genome. Its sequence is 5' GUGAACGGGCGCCAUCCCGAGG 3'. Only a handful of studies have mentioned this miRNAs. In prostate cancer, miR-887 was shown to target the 3'UTR of MDM4. Specifically, it targets the C-allele of the rs4245739 SNP (A>C). This SNP is associated with lower prostate cancer risk than the A-allele. MiR-887-3p, by inhibiting MDM4, decreased the viability of the cells (Stegeman et al. 2015). One study showed that the level of miR-887 was lower in Jurkat cells after a 7-days treatment with TNF-α (Lai et al. 2017). In another, its level of expression was increased 20h after high-dose ionizing-radiation of human peripheral blood mononuclear cells (Beer et al. 2014). However, those two studies did not state if the miRNA was miR-887-3p or 5p.

2.6.3 miR-122-5p

MiR-122-5p was first discovered in 2002 in mice as a liver-specific miRNA (Lagos-Quintana et al. 2002). Indeed, in hepatocytes, miR-122-5p is present at above 50 000 copies per cell, making up to 70% of the total miRNA population (Hu et al. 2012). Nevertheless, it has been detected in rare cases in other cell types such as endothelial cells and breast cancer cells (Stanzione et al. 2017), and in low level in spleen, gall bladder and veins (Ludwig et al. 2016). It is located on chromosome 18 and forms a cluster with miR-122b-5p. Its sequence is 5' UGGAGUGUGACAAUGGUGUUUG 3'.

2.6.3.1 MiR-122-5p in liver function

Physiology. Well-regulated in hepatocyte differentiation and liver development, its expression is carefully tuned by four liver-enriched transcription factors. The miRNA is able to induce the expression of hepatocyte functional genes by targeting CUTL1, a transcriptional repressor (Xu et al. 2010). A positive feedback loop was also found between miR-122-5p and the liver-enriched transcription factor HNF6 (Laudadio et al. 2012). MiR-122-5p is implicated in lipid metabolism. For instance, its depletion by antagomir led to a decreased cholesterol plasma level (Elmén et al. 2008). However, the regulatory mechanisms of lipid metabolism are still not clear.

Pathologies. One of the most interesting effect of miR-122-5p is its stimulation of HCV (hepatitis C virus) replication. MiR-122-5p acts in an unusual way for miRNAs. By binding to the 5'-noncoding region of the virus, the miRNA is able to stimulate the virus replication. When miR-122-5p is sequestered, the virus loses its autonomous replication capacity (Jopling et al. 2005). It was shown that miR-122-5p would bind two sites on the 5'-noncoding region of the virus, which would switch the internal ribosome entry site to an open conformation. This way, the miRNA could enhance the association of ribosomes with the viral RNA (Díaz-Toledano et al. 2009). Finally, another peculiar mechanism implicating Ago2 was demonstrated by Shimakami and colleagues. As previously described, the RISC usually acts by repressing the translation of mRNAs. However, it seems that, in this context, miR-122-5p/Ago2 is able to stabilize viral RNA and reduce its decay, protecting it from 5' exonuclease activities of the host cell (Shimakami et al. 2012). It is noteworthy to mention that an LNA inhibitor of miR-122-5p (miravirsen) has been evaluated in a phase II clinical trial. It showed no severe adverse events nor escape mutations in the viral genome, and the HCV RNA was decreased in a dose-dependent manner (Janssen et al. 2013). A role for miR-122-5p in hepatitis B virus (HBV) was also reported, this time inhibiting the virus replication (Hu et al. 2012).

In hepatocellular carcinoma (HCC), several studies showed that loss of miR-122-5p expression was associated with poor prognosis and metastasis (Kutay et al. 2006; Coulouarn et al. 2009). MiR-122-5p tends to act as a tumour suppressor in those cells. Its target genes, such as cyclin G1, ADAM10, CUTL1, Pkm2, Wnt1 or c-myc, are involved in hepatocarcinogenesis, angiogenesis and EMT (Nakao et al. 2014). In HCC again, the overexpressed lncRNA HOTAIR has recently been shown to regulate negatively miR-122-5p expression. It seems like HOTAIR was able to induce the methylation of miR-122-5p DNA, hence silencing the tumour suppressor miRNA (Cheng et al. 2018). In addition, overexpression of miR-122-5p was able to sensitize HCC cells to vincristine and adriamycin by regulating several genes implicated in multidrug resistance (Xu et al. 2011). It was also able to sensitize them to doxorubicin by targeting cyclin G1 (Fornari et al. 2009).

2.6.3.2 miR-122-5p in other cancers

Apart from liver cancer, miR-122-5p plays various role in different cancer cell types. In breast cancer, the MDA-MB-231 cell line secreted exosomes with high level of miR-122-5p. This circulating miR-122-5p was responsible for lowering the glucose intake of other cell types and favour the tumour cells. This way, miR-122-5p could take part in the

preparation of metastatic niches (Fong et al. 2015). A study on circulating miRNAs after chemotherapy neoadjuvant against breast cancer showed that there was an increase of circulating miR-122-5p and miR-34a following the chemotherapy. Those miRNAs would originate from both the tumour and the non-tumour tissues (Frères et al. 2015). In gastric cancer, a decreased in miR-122-5p was associated with aggressive clinicopathological features in patients. CREB1 was negatively correlated with miR-122-5p and was identified as one of its direct targets (Rao et al. 2017).

2.6.4 miR-129-5p

MiR-129-5p was first identified in mice (Lagos-Quintana et al. 2002). The mature sequence of miR-129-5p (5' CUUUUUGCGGUCUGGGCUUGC 3') actually represents a family of two miRNAs: miR-129-1-5p and miR-129-2-5p, which originate from distinct genomic regions. MiR-129-1-5p is located in chromosome 7q32, close to a specific fragile genomic site. MiR-129-2-5p is located in 11p11.2 (Calin et al. 2004). The RNA binding protein KSRP has recently been shown to bind to pri-miR-129-1-5p and regulate its processing in myeloid cells. KSRP is necessary for granulocyte differentiation of myeloid cells, while its attenuation is mandatory for monocyte differentiation. The authors showed that miR-129-5p inhibited monocyte differentiation but promoted granulocyte differentiation, acting downstream of KSRP and regulating the expression of the transcriptional regulator RUNX1 (Zhao et al. 2017). It has also been shown to be a regulated by the lncRNA MALAT1 (Xiong et al. 2018) and UCA1(Wang et al. 2018).

MiR-129-5p has been mainly studied in cancer, and has been considered a tumour suppressor in several cancer types. Its low expression has been associated with poor outcome in several cancers such as bladder cancer (Dyrskjøt et al. 2009), endometrial cancer (Huang et al. 2009), gastrointestinal cancer (Fesler et al. 2014), prostate cancer (Xu et al. 2016) or papillary thyroid cancer (Brest et al. 2011). This low expression seems to be due, at least partially, to hypermethylation of the miR-129-5p promoters. The targets of miR-129-5p include GALNT1 and SOX4 (Dyrskjøt et al. 2009; Huang et al. 2009), SOX2 (Xiong et al. 2018) or CDK6 (Fesler et al. 2014). Nevertheless, miR-129-5p has sometimes been shown to act as an oncogene, for instance regulating the tumour suppressor protein APC in laryngeal squamous cell carcinoma (Li et al. 2013; Gao et al. 2016).

Regarding drug resistance, miR-129 has been demonstrated to target the pro-apoptotic protein BCL2, and to enhance the cytotoxic effects of 5-fluorouracil in advanced colorectal cancer (Karaayvaz et al. 2013). In breast cancer, it was shown to target SOX2 and suppress

Adriamycin resistance (A. Zeng et al. 2018). It has recently been shown that the lncRNA UCA1 was acting like a sponge for miR-129 in ovarian cancer. The expression of this lncRNA was upregulated in paclitaxel-resistant ovarian cancer. One of the direct targets of miR-129 being ABCB1 (or MDR1), the downregulation of UCA1 induced a better availability of miR-129, which could in turn downregulate ABCB1. This mechanism led to the restoration of sensitivity to paclitaxel (Wang et al. 2018). Interestingly, a miR-129 mimic modified with a 5'fluorouracyl instead of a normal uracil has been shown to efficiently prevent colon cancer metastasis in vivo (Wu et al. 2010).

Transfer of miRNAs via EVs in now considered as a new mode of intercellular communication. This specific mode of miRNA transfer, the particularity of this type of vesicles and their implication in cancer is described in the next chapter.

III. Extracellular vesicles and exosomes

First in 1983, two groups visualized the release of small vesicles in vitro in rat reticulocytes (Harding et al. 1983) and sheep reticulocytes (Pan & Johnstone 1983). They were given the name exosomes four years later (Johnstone et al. 1987).

For years, they were considered, without much interest, as a way for cells to evacuate their proteins and debris. It wasn't until the beginning of the 2000's that some scientists started studying them again. In 2007, a major breakthrough was made with the discovery that exosomes carried nucleic acids (Valadi et al. 2007). This triggered a wave of interest for those vesicles, and they are now considered as major players in cellular communication, secreted by virtually all cell types and present in every biological fluid.

Since the discovery of the different kinds of extracellular vesicle (EV), the classification of the different types of EVs hasn't stopped evolving. A clear and consensual way to characterize the population being studied still needs to be found. Interestingly, all living cells, eukaryotes and prokaryotes alike, appear to secreted nano-sized membrane vesicles (Kim et al. 2015). Apoptotic bodies and microvesicles are released from the plasma membrane by dying cells and living cells respectively. They are both larger than 100 nm. Exosomes, however, are nano-sized vesicles smaller than 150 nm, surrounded by a lipid bilayer and of endocytic origin. Isolation techniques vary and are mostly based on sequential centrifugation, filtration or immunoaffinity-based isolation, or a combination of these. Each method has flaws and assets, which won't be discussed here. However, the methods of isolation cannot usually guarantee the purity of the preparation, and other types of non-exosomes vesicles can be contaminants. Various markers have been used to further characterize the preparations. In this work, we chose to use the term "exosome", for our material seems to match with the described characteristics (Kowal et al. 2016). However, in the introduction, vesicles will be referred to as "EVs" or "exosomes" depending on the terms used by the authors in the original papers.

3.1 Biogenesis

The major characteristic of exosomes is their biogenesis. Unlike the other extracellular vesicles, they are born from the endocytic pathway (Hessvik & Llorente 2018).

The first step of exosomes formation is the inward budding of late endosomes: the limiting membrane buds into their lumen. This creates what is called multivesicular bodies (MVBs), containing intra-luminal vesicles (ILVs) (Keller et al. 2006). The ILVs can sequester specifically sorted proteins, lipids and nucleic acids. The MVBs can follow various fates. Firstly, they can fuse with lysosomes, acidic compartment filled with hydrolases. This triggers the degradation of their content. MVBs can also be recycled via the trans-Golgi network. Finally, they can fuse with the plasma membrane and release their vesicles in the extracellular space. Once outside the cell, the vesicles are called exosomes (**fig. I 15**).

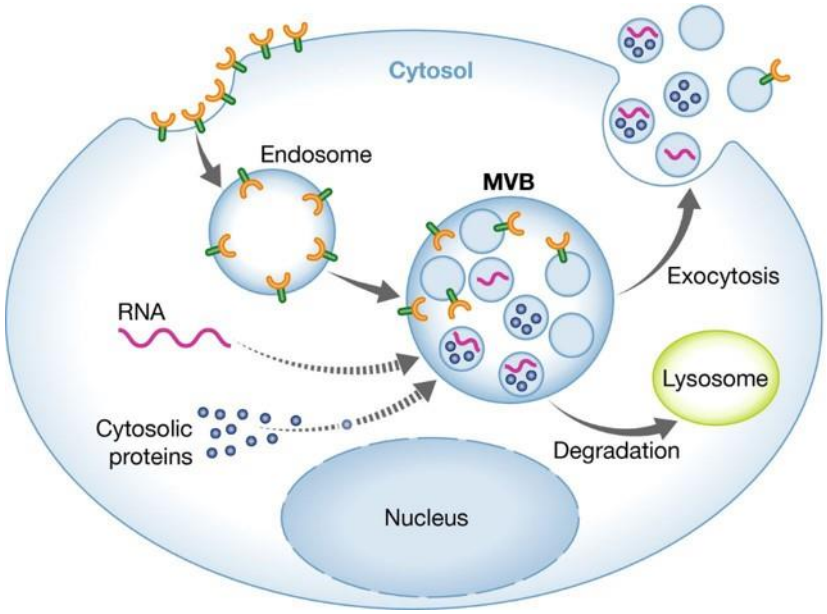

Figure I 15. ***Exosomes biogenesis****. Endosomes formed at the plasm membrane fuse into primary endosomes. Inward budding of the primary endosome produces ILVs. The resulting MVB can be fated for degradation by fusion with lysosomes, or directed towards the plasma membrane. Upon fusion with the membrane, the MVB releases the exosomes into the extracellular milieu. Figure adapted from Schorey et al. 2014.*

Several studies suggest the existence of several subpopulation of MVBs, their composition regulating their fate. MVBs with high cholesterol are more prone to fuse with the plasma membrane (Möbius et al. 2002), and those containing lysobisphosphatic acid (LBPA) more likely to be degraded (White et al. 2006). Moreover, it has been shown that exosomes secreted from the apical or basolateral side of polarized cells have different protein content (Chen et al. 2016).

Studies suggest that there is not one kind of exosomes biogenesis, but multiple mechanisms. It is still not known whether they can all act together, or if they rule over specific subpopulation of MVBs. The best-described mechanism is the one relying on the endosomal sorting complex required for transport (ESCRT). This machinery consists of four

different complexes: ESCRT-0, -I, -II, –III and some associated proteins. At first, the ubiquitinated transmembrane proteins are first recognized at the endosomal membrane and bound by the ESCRT-0 complex. Since the proteins of the complex can bind multiple ubiquitin moieties, it has for effect to concentrate and cluster ubiquitinated cargo. Interestingly, not all proteins in exosomes are ubiquitinated. HRS, a key protein from the ESCRT-0, also associates with clathrin, and recruits TSG101 of the ESCRT-I. ESCRT-I and –II co-assemble, and are able to induce the budding of the membrane. They are present at the neck of the buds and stabilize them. They recruit ESCRT-III, which is responsible for membrane scission (Hurley & Hanson 2010). Finally, Vsp4 disassembles the ESCRT complexes by hydrolysing ATP, and recycles them back to the cytoplasm (**fig. I 16**) (Schmidt & Teis 2012).

Another mechanism implicates ALIX, an ESCRT accessory protein. Baietti and colleagues showed a mechanism in which the interactions between syndecan, syntenin and ALIX regulate the formation of ILVs and the sorting of some specific cargo. Syndecan can cluster and recruit syntenin and ALIX, which in turn will trigger the budding of the endosomal membrane (Baietti et al. 2012).

Independently of the ESCRT, the lipid composition of the vesicles is involved in an alternative pathway to generate ILVs. This mechanism implicates the coalescence of micro-domains with high concentrations of ceramides, into larger domains that promote the budding of the membrane (Trajkovic et al. 2008).

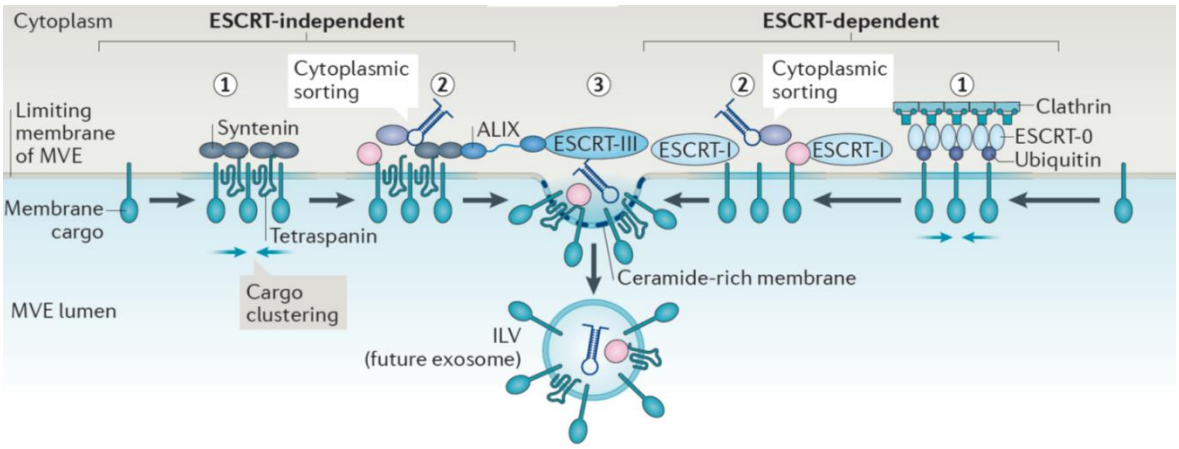

Figure I 16. ***Sorting mechanisms in exosomes biogenesis****. Several sorting machineries are involved in the generation of exosomes. Proteins and lipids are clustered in microdomains of the membrane of the MVB. They play a role in the recruitment of soluble components. The microdomains and additional machineries stimulates the budding of the membrane towards the lumen of the MVB. The mechanisms involved can be classified into ESCRT-dependent and ESCRT-independent mechanisms. Figure adapted from Van Niel et al. 2018.*

It has also been shown that the presence of proteins from the tetraspanin family (a family of membrane proteins) could influence the biogenesis of exosomes. For instance, the deletion of the tetraspanin CD63 would reduce the number of exosomes secreted (Hurwitz et al. 2016).

MVBs need to be transported to the plasma membrane for fusion. If the MVBs are intended for degradation by fusion with lysosomes, a retrograde transport on microtubule, towards the – end, occurs with the involvement of the protein Rab7 (a Rab-GTPase) and the motor protein dynein. In case of secretion-fated MVBs, the mechanism is not fully understood yet. It seems to also implicate Rab7, but with a different ubiquitination status. The MVBs are likely transported on microtubules towards the + end, and would also need Rab27a, Rab27b and the actin cytoskeleton (Mittelbrunn et al. 2015). The fusion itself is expected to be mediated by Snare proteins and synaptotagmin family members, two types of proteins respectively specialized in membrane fusion and calcium-dependent neurotransmitter release. Further work is still needed to improve the understanding of these mechanisms (van Niel et al. 2018).

3.2 Exosome composition

The exosomes have a composition that depends on their cell of origin to some extent, but that can also be influenced by different treatments or states of the secreting cells. In the last decade, an increasing amount of publications has proven the diversity of molecules present in this type of vesicles. The previous public database, compiling proteins and RNAs identified in exosomes, Exocarta (Mathivanan et al. 2012), has recently been replaced by a more comprehensive one: Vesipedia (Kalra et al. 2012).

3.2.1 Lipids

The lipid composition of exosomes depends on the cell of origin. However, analysis have shown that they are enriched in cholesterol, phosphatidylserine and sphingolipids such as ceramides and sphingomyeline (Vlassov et al. 2012). Lyso- bisphosphatidic acid (LBPA), a lipid present on MVBs fated to be degraded, is underrepresented in exosomes (Laulagnier et al. 2004). The specific lipid composition shows characteristics of lipid-rafts, such as enrichment of cholesterol and sphingomyelin, as well as lipid raft–associated proteins, GPI-anchored proteins and flotillin. These features could explain the resistance of exosomes to

detergents and contribute to their high stability. This may corroborate the implication of lipid-rafts to the biogenesis of exosomes (Wubbolts et al. 2003).

3.2.2 Proteins

More than 4000 different proteins had already been associated with exosomes in 2012 (Mathivanan et al. 2012). Today they are more than 9000 (http://www.exocarta.org/). Some are specific to the cell of origin or to the physiological or pathological state of the cell, while others are characteristic of those vesicles. Exosomes typically carry several types of tetraspanin (CD9, CD63, CD81, CD82), membrane dynamic and fusion proteins (GTPases, Annexins, flotillin), proteins necessary for the formation of MVBs (TSG101, ALIX) and heat shock proteins (Hsc70, Hsp 90). Cytoskeletal components (actin, tubulin), enzymes or signal transduction proteins can be present as well (**fig. I 17**). Some of those proteins are routinely used as positive markers of exosomes. However, recent studies have highlighted that some of those markers might be present in all extracellular vesicles, while some would be more specific to small EVs. They showed the presence of a subpopulation of small EVs containing CD9, CD63 and CD81 were also enriched in endosome markers, which fits the description of exosomes. TSG101 and syntenin-1 are also specific to the tetraspanins-enriched small EVs ("exosomes") (Bobrie et al. 2012; Kowal et al. 2016). In accordance with their cells of origin, MHC class II has been found on exosomes from antigen-presenting cells, and immunoglobulin-family members on vesicles from B cells (Théry et al. 2001). The protein content of exosomes, depending on the parent cell type and on changes in their states, has opened new opportunities in the field of biomarker researches (Sandfeld-Paulsen et al. 2016).

Interestingly, exosomes do not have protein markers from the nucleus, the mitochondria, the endoplasmic reticulum or the Golgi apparatus (Théry et al. 2002).

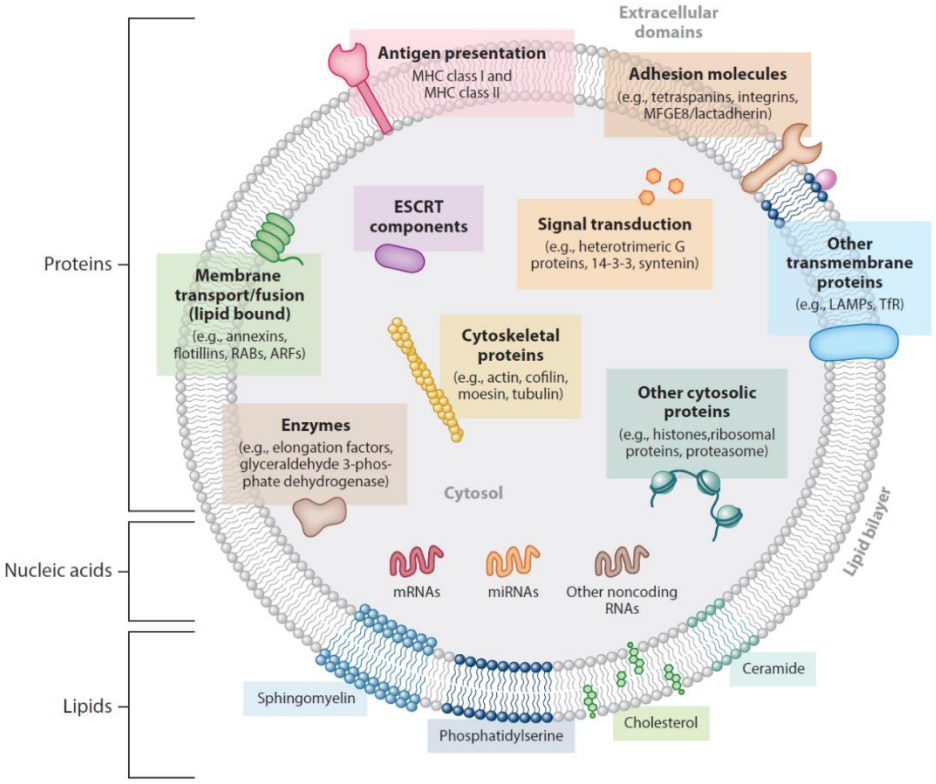

Figure I 17. ***Overall composition of small extracellular vesicles****. EV are composed of various types of proteins, lipids and nucleic acids. Some components may be present in some subtypes and not in others. ARF, ADP ribosylation factor; ESCRT, endosomal sorting complex required for transport; LAMP, lysosome-associated membrane protein; MHC, major histocompatibility complex; MFGE8, milk fat globule-epidermal growth factor-factor VIII; RAB, Ras-related proteins in brain; TfR, transferrin receptor. Figure adapted from Colombo et al. 2014.*

3.2.3 Nucleic acid composition

In 2007, Valadi and his team published a paper proving that exosomes contained nucleic acids (Valadi et al. 2007). Since then, it has been shown that the various nucleic acids are protected from degradation when encapsulated in small vesicles, and can be transferred in recipient cells, inducing modification in their phenotype.

3.2.3.1 DNA

Only a handful of studies have detected DNA in exosomes and EVs. Exosomal DNA in blood could provide another perspective to the studies of circulating DNA in cancer. Small EVs have been reported to contain mitochondrial DNA (Guescini et al. 2010). DNA found in exosomes from healthy and pancreatic cancer patients is mainly double-stranded, but fragmented (Cai et al. 2013; Kahlert et al. 2014). The presence of genomic dsDNA, often carrying the mutation of the cancer cell of origin, makes them useful tools to screen for genetic alterations (Kalluri & LeBleu 2016).

3.2.3.2 RNA

RNAs are the most widely studied molecule classes in exosomes, especially miRNAs. Ten years ago, it was shown that mARNs were present in exosomes, and that they could be translated into proteins after transfer to recipient cells. The same group also revealed that exosomes were carrying miRNAs (Valadi et al. 2007). Although some full length mARNs can be found (in rare occurrences), the vast majority of coding RNAs is fragmented. Those fragments seem to be enriched in 3'UTR (Wei et al. 2017; Batagov & Kurochkin 2013). In a recent study by our laboratory, it was proposed that the 3'UTR fragments, rich in miRNA-binding sites, were increased in exosomes to attenuate the effect of complementary miRNAs (Pérez-Boza et al. 2018).

miRNAs represent another significant category of RNAs discovered in exosomes. Those small non coding RNAs induce the repression of their target mRNA by base complementarity. Interestingly, the miRNAs are transferred horizontally via exosomes (Pegtel et al. 2010). They appear to be sometimes specifically enriched in exosomes, compared to the parent cells, and have been proven to maintain their functionality once inside recipient cells (Montecalvo et al. 2012; Bovy et al. 2015). Today still, the mechanism by which specific sequences of miRNA are incorporated into exosomes remain unclear. So far, a few studies have shown that specific sequences within miRNA were recognized by ribonucleoproteins and, therefore, encapsulated into vesicles (Villarroya-Beltri et al. 2013; Shurtleff et al. 2016). But a general mechanism, if it exists, has yet to be discovered.

Among the non-coding RNAs, miRNAs are the main focus, but perhaps not the most abundant population. Several deep-RNA sequencing have been performed on the RNA content of exosomes. They have revealed the presence of various species of small, and long non-coding RNAs, such as piwiRNA, snRNA, snoRNA, tRNA, vaultRNA, and yRNA. From our recent study, it appears that the long non-coding RNAs are the most abundant populations in exosomes (Nolte'T Hoen et al. 2012; Pérez-Boza et al. 2018).

Currently, there is a lack of standard methods to obtain pure and well-characterized exosomes. Depending on the purification method, different populations of vesicles are purified. Immunocapture techniques present the risk to select a subpopulation, while precipitation-based methods usually precipitate many contaminants (Colombo et al. 2014). Ultracentrifugation-based techniques, immunoprecipitation and density gradient have shown different results in term of composition and purity of the preparations (Van Deun et al. 2014). In addition, evidence have recently started to accumulate showing that different subpopulations of exosomes coexist within the population isolated from the same batch of

cells (Ferguson & Nguyen 2016). For instance, Kowal and colleagues have shown that a subpopulation of small EVs was lacking CD63 and CD81, but presenting CD9. This suggested that CD9 might be more ubiquitous (Kowal et al. 2016). Therefore, using beads coupled to antibodies against CD63 may exclude a subpopulation from a study. Regarding the miRNA content of exosomes, a model has been proposed in which only a few exosomes from the same cells are enriched in miRNA (Chevillet et al. 2014). It would then be interesting to manage to isolate this miRNA-enriched subpopulation (**fig. I 18**).

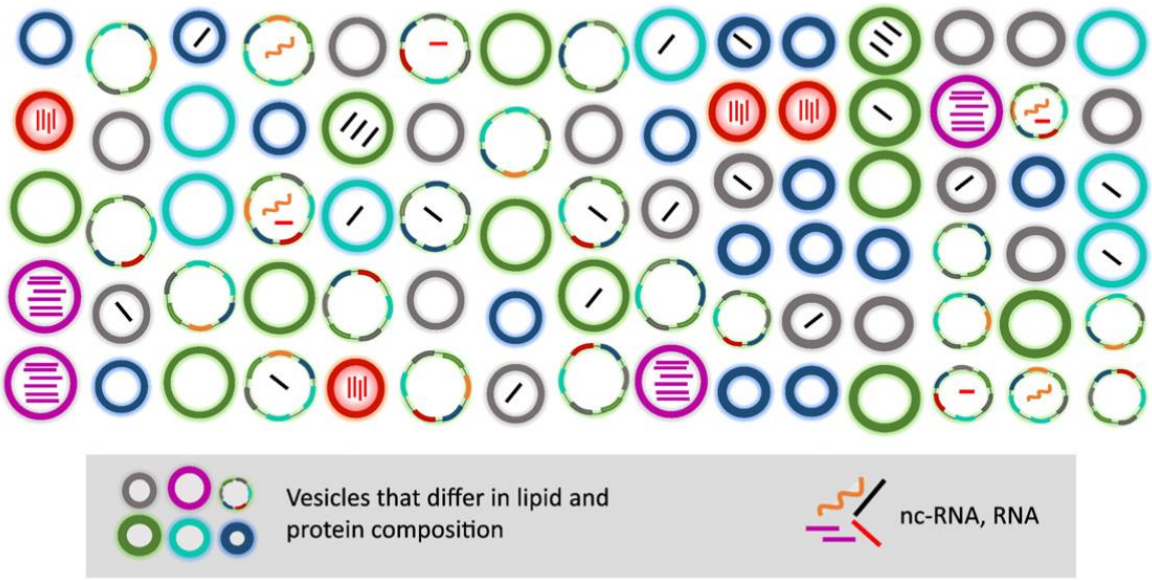

Figure I 18. ***Proposed model of exosomal composition and subpopulations.*** *Different subspecies exist within exosomes isolated from the same batch of cells. Exosomes can have diverse lipid, protein, and miRNA composition. In purple and red are depicted exosomal subspecies enriched with a high number of miRNAs. Other exosomes may contain low number of copy, or even be devoid of nucleic acids. Figure adapted from Ferguson & Nguyen 2016.*

Given the heterogeneity of the population, it seems important to take care of characterizing the extracellular vesicles preparation. In order to promote a rigorous EV science, the International Society for Extracellular Vesicles (ISEV) just released new guidelines on how vesicles should be characterised and analysed. The authors have updated the previous guidelines from 2014, based on new discoveries and developments within the field. They give advises on basic information requirement for collection and pre-processing of samples. They also recapitulate the evolution of characterisation and quantification methods, and recommend the use of positive and negative markers of EVs subtypes. Finally, the authors provides recommendations on functional studies, to avoid over-interpretations or artefacts (Théry et al. 2018). To support the transparency in EVs researches, a knowledgebase has been created to encourage researchers to share the methodological specifications of their EV experiments (Van Deun et al. 2017).

3.3 Transfer of information

When released in extracellular space, exosomes might be taken up by neighbouring recipient cells or end up in the circulation, where they would quickly be taken up by other recipient cells. The molecular mechanism of interaction between exosomes and recipient cells still remains unclear (**fig. I 19**). Data have shown that exosomes were easily taken up by monocytes or macrophages. This could be due to their strong phagocytic capacity (Feng et al. 2010), or due to some level of opsonisation of the vesicles (Van Der Meel et al. 2014). It seems like the combination of tetraspanins and their association with integrin at the surface of the vesicle might play a role in the targeting of recipient cells (Rana et al. 2012). The proteins on the surface of the target cell is also important to interact with the exosomes. Specific receptor-ligand interactions between different types of recipient cells and circulating vesicles have already been observed (McKelvey et al. 2015).

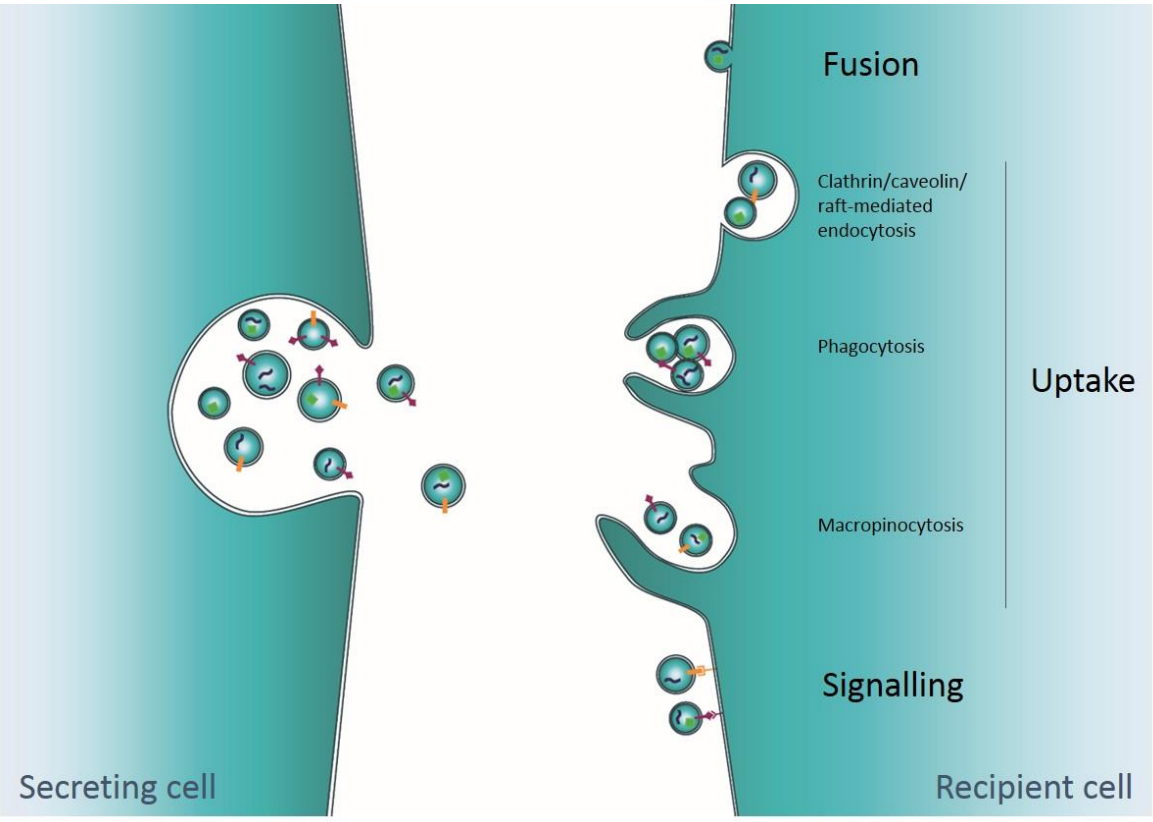

Figure I 19. ***Exosomes internalisation****. Exosomes released in the circulation can be taken up by recipient cells via various mechanisms, depending in particular on the cell type, the interaction of exosomal surface proteins and cellular receptors. The exosome may fuse with the plasma membrane and release its content into the cytoplasm; bind to surface antigens outside the cell; or be endocytosed by various mechanisms.*

Once the exosome is interacting with the membrane of its recipient cell, different possibilities may arise. Exosomes can stay attached to the cell surface. This may happen preferentially for cells with weak endocytic capacity. They can also dissociate from the cell,

directly fuse with the plasma membrane, or be internalized through distinct endocytic pathway (Raposo & Stoorvogel 2013). In the last two cases, the content of the vesicle gets released in the recipient cell. Direct fusion of the exosomes with the plasma membrane has been shown using exosomes labelled with a lipophilic dye, which got transmitted to the cytoplasmic membrane of the target cells (Montecalvo et al. 2012). The content of the exosomes is then directly released inside the cytoplasm of the cell. Several studies have assessed the internalisation of exosomes via clathrin-mediated endocytosis and macropinocytose (Tian et al. 2014; Fitzner et al. 2011). Svensson and colleagues have shown that exosomes from glioblastoma cells were taken up by endothelial cells by a mechanism relying on lipid raft and cholesterol, independent of clathrin (Svensson et al. 2013). The mechanism by which the content of exosomes is then released in the recipient cell depends on the type of endocytic pathway. It should be noted that recipient cells may incorporate exosomes from the same origin using multiple mechanisms (Escrevente et al. 2011).

3.4 Exosomes in Cancer

The broad range of molecules they carry and their presence in virtually every biological fluid have made exosomes important actors of cell to cell communication. Their implication has been shown in many diseases. We will focus here on their roles in various steps of cancer development.

Being the closest to the cancer cells, the **tumour microenvironment** plays an important role in the tumour development. In particular, the effects of tumour cell-derived exosomes (TDEs) has been intensively studied on cancer-associated fibroblasts (CAFs). For example, TGF-β, one of the CAFs activator, is frequently found in TDEs. It can be transferred to fibroblasts and induce the expression of α-SMA to differentiate them into myofibroblasts (Webber et al. 2010). Extracellular vesicles in cancer can be secreted by tumour cells, but also by cells of the micro-environment. CAFs-derived exosomes have been shown to promote tumour growth, by assisting in the reprogramming of tumour metabolism (Zhao et al. 2016) or promoting proliferation and drug-resistance (Richards et al. 2017). Exosomes from endothelial cells, while in a tumour-like environment, produced a bigger amount of exosomes than in normal conditions. Compared to endothelial cells in a normal environment, they were enriched in miR-503-5p, a tumour-suppressor miRNA (Bovy et al. 2015).

It is well-known that **angiogenesis** is a major step in tumour growth. Upon hypoxia, tumour cells stop proliferating. So in order to override this limitation, they send messengers

to endothelial cells and trigger the angiogenic switch, stimulating the proliferation and formation of new blood vessels (Carmeliet & Jain 2000). The role of exosomes in mediating tumour angiogenesis has been reported by several studies. For instance, one has shown that membrane-associated EGFR could be delivered to endothelial cells via EVs from A431 human squamous cell carcinoma cell line. This would elicit the activation of MAPK and Akt pathways, and initiate an autocrine activation of the VEGF-VEGFR cascade (Al-Nedawi et al. 2009). It has also been shown that exosomes from leukaemia cells K562 were transferring miR-92a to Human Umbilical Vascular Endothelial Cells (HUVECs), which resulted in enhanced endothelial cell migration and tube formation (Umezu et al. 2013). Moreover, miRNA-carrying exosomes promote the dissemination of cancer cells by disturbing tight junction between endothelial cells (Zhou et al. 2014).

More than just facilitating the migration of tumour cells, exosomes seem to be able to induce **pre-metastatic niches** in distant organs from the primary tumour. Exosomes from tumour cells can reprogram and educate stromal cells into the formation of metastatic sites through the MET oncoprotein (Peinado et al. 2012). Interestingly, integrin at the surface of tumour exosomes have been shown to determine the organotropism, and prepare the pre-metastatic niche (Hoshino et al. 2015). On the other hand, exosomes can also prevent the formation of metastasis by reinforcing immune surveillance through patrolling monocytes and other immune cells. This mechanism is dependent on proteins present on the outer membrane of the exosomes (Plebanek et al. 2017). Interestingly, it was suggested that cancer cells could get rid of tumour-suppressor miRNAs by encapsulating them in exosomes. Once the miRNAs are discarded, the cells would be able to acquire a metastatic phenotype (Ostenfeld et al. 2014).

The progression of tumour growth involves **immune regulation**. Exosomes from tumours appear to promote mainly immune evasion. For instance, they can impair the differentiation of bone marrow dendritic cells by inducing IL-6 (Yu et al. 2007) or via the activation of Stat3 by exosome-bound Hsp72 (Chalmin et al. 2010). Moreover, TDEs could suppress T-cell proliferation and inhibited NK cell cytotoxicity as well, which would promote an immunosuppressive environment at pre-metastatic niche (Wen et al. 2016). On the other hand, exosomes from NK cells have been shown to present toxic activity against different types of cancer cell lines, and activated immune cells (Lugini et al. 2012).

Overcoming **drug resistance** has been one of the major challenges in chemotherapy treatment those past years. Since exosomes have appeared as interesting players in the development of cancer, it was only a matter of time before the scientists started to investigate

their role in that process. Today, three main mechanisms are considered to be responsible for exosome-mediated drug resistance. The first one is the export of the drug via the exosome pathway, namely the capacity of the cell to pack the drug and send it away in vesicles. In 2005, studies already showed that cells were using the exosomal export pathway to get rid of cisplatin (Safaei et al. 2005) or mitoxantone (Ifergan et al. 2005). In the last case, the implication of ABC transporters at the membrane of the vesicles seems to be responsible for the accumulation of the drugs inside the exosomes during their formation (Ifergan et al. 2005). A second mechanism relies on TDEs to neutralize antibody-based drugs. Exosomes carry molecules that can be targeted by antibodies, such as CD20 (Aung et al. 2011) or HER2 (Ciravolo et al. 2012). Those TDEs would neutralize part of the antibody against HER2 (Trastuzumab) and, consequently, lower the amount of antibody available for binding on the cancer cells. Interestingly, those TDEs showed no effect on the tyrosine kinase inhibitor Lapatinib (Ciravolo et al. 2012). Finally, the last and most studied mechanism implicates the transfer of molecules via exosomes. Several studies have proven the transfer of MDR1, an ABC transporter implicated in multidrug resistance, from resistant to sensitive cells (Lv et al. 2014; Corcoran et al. 2012). TDEs can transfer proteins, but also nucleic acids implicated in drug resistance (Bouvy et al. 2017). The transfer of miR-221/222 from resistant to sensitive MCF7 cells was able to increase their resistance to tamoxifen (Wei et al. 2014). But cells from the microenvironment are also responsible for the development of resistance. CAFs are naturally resistant to gemcitabine, and are able to increase the level of Snail, a chemoresistance-inducing factor, in recipient cells (Richards et al. 2017). In the same way, EVs from bone marrow mesenchymal stromal cells were showed to help leukemic cells to evade drug-induced apoptosis (Crompot et al. 2017). But apart from transmitting resistance, it seems possible to re-sensitive resistant cells with miRNA-enriched exosomes (O'Brien et al. 2015). A study in our lab has shown that, upon treatment with epirubicin or paclitaxel, endothelial cells would secrete exosomes with an increased level of miR-503-5p, which would in turn act as a tumour-suppressor in breast cancer cells (Bovy et al. 2015).

3.5 Exosomes as therapeutic tools in cancer

3.5.1 As biomarker

Circulating exosomes are virtually present in all biological fluids and their composition reflects their cell of origin. Moreover, their good stability makes them good potential candidates as biomarkers of diagnosis and prognosis in many diseases. In cancer, analysis of a panel of 8 miRNAs from circulating exosomes allowed to discriminate between

patients suffering from benign ovarian disease, ovarian cancer, and healthy patients (Taylor & Gercel-Taylor 2008). Since there is a need to determine if patients are good responders to chemotherapy, various combinations of miRNAs have been implicated in the response of patients to different kind of treatments. In patients with colorectal cancer, variation of the circulating level of miR-126 could predict the tumour response to the treatment with chemotherapy and bevacizumab (Hansen et al. 2015). Likewise, the combination of circulating miR-133a and miR-133b could predict the chemosensitivity of oesophageal squamous carcinoma tumour cells to paclitaxel (Chen et al. 2014). However, the field is still in dire need of standardization regarding procedures before generalising this approach.

3.5.2 As therapeutic agent

Exosomes are currently being studied as potential therapeutic tools. They present some interesting properties. They have low immunogenicity, innate stability, but also high delivery efficiency and they fuse easily with plasma membranes. Scientifics are studying their potential to deliver treatments. Kim and colleagues have developed a platform to load exosomes from macrophages with paclitaxel, and managed to successfully deliver them to a murine model, where it showed potent anticancer effects (Kim et al. 2016). EVs could also be used to carry membrane proteins in their native conformation, allowing them to keep their activity (Yang et al. 2018). Self-derived exosomes have been engineered to deliver siRNA to the brain of mice (Alvarez-Erviti et al. 2011). Phase I clinical trials have already been performed to assess the potential of exosomes to activate the immune system of melanoma (Escudier et al. 2005) and lung cancer (Morse et al. 2005) patients by treating them with exosomes from their own dendritic cells. Since TDEs can be harmful to the patient, another approach has been to remove exosomes from the circulation with a dialysis-based device (Marleau et al. 2012).

Aim of the study

Aim of the study

The interaction between tumour cells and their microenvironment is an essential aspect of cancer development. Therefore, understanding how this tumour microenvironment communicates with tumour cells is crucial for the development of new anti-cancer therapies. Exosomes are small vesicles released by cells into the extracellular environment. They mediate cell-cell communication by their specific content. They carry miRNAs, which are able to regulate a wide range of functions in cells. In the context of cancer, exosomes are potentially secreted by all cell types that compose the tumour microenvironment, and participate in the tumour response to treatment.

Previous work in the laboratory has demonstrated that endothelial cells were able to communicate with cancer cells and modify their function via exosomal miRNAs. MDA-MB-231 cells (triple-negative breast carcinoma) were particularly efficient in internalizing exosomes from the endothelial cells and the miRNAs they carried. In a medium mimicking the tumour environment, the endothelial cells secreted a decreased level of an anti-tumour miRNA, miR-503-5p, in exosomes. However, the level of exosomal miR-503-5p increased after exposure of the cells to chemotherapy drugs (Bovy et al. 2015). The two drugs (epirubicin and paclitaxel) are those currently used to treat patients suffering from breast cancer. The aim of this study is to determine if other miRNAs are regulated by chemotherapy drugs in exosomes from endothelial cells, and their potential effects of breast cancer. In the first part of this thesis, we determined the profile of microRNAs in HUVECS cells treated with the chemotherapeutic drugs and compared it to untreated cells. This analysis highlighted four microRNAs that were further studied in relation to tumour properties.

In the second part of this work, we asked if the effects of the exosomes released by endothelial cells upon chemotherapeutic drugs treatment were conserved in cells resistant to those treatments. Indeed, several studies have reported that repeated chemotherapy induced resistance in cancer cells (Housman et al. 2014). Thanks to our collaboration with Dr Sharon Gorski and Dr Melanie Spears, we received breast cancer cells resistant to epirubicin or paclitaxel, respectively. In this part, we analysed if the miRNAs identified in the first part still affected the tumour properties of the resistant cells.

Materials & Methods

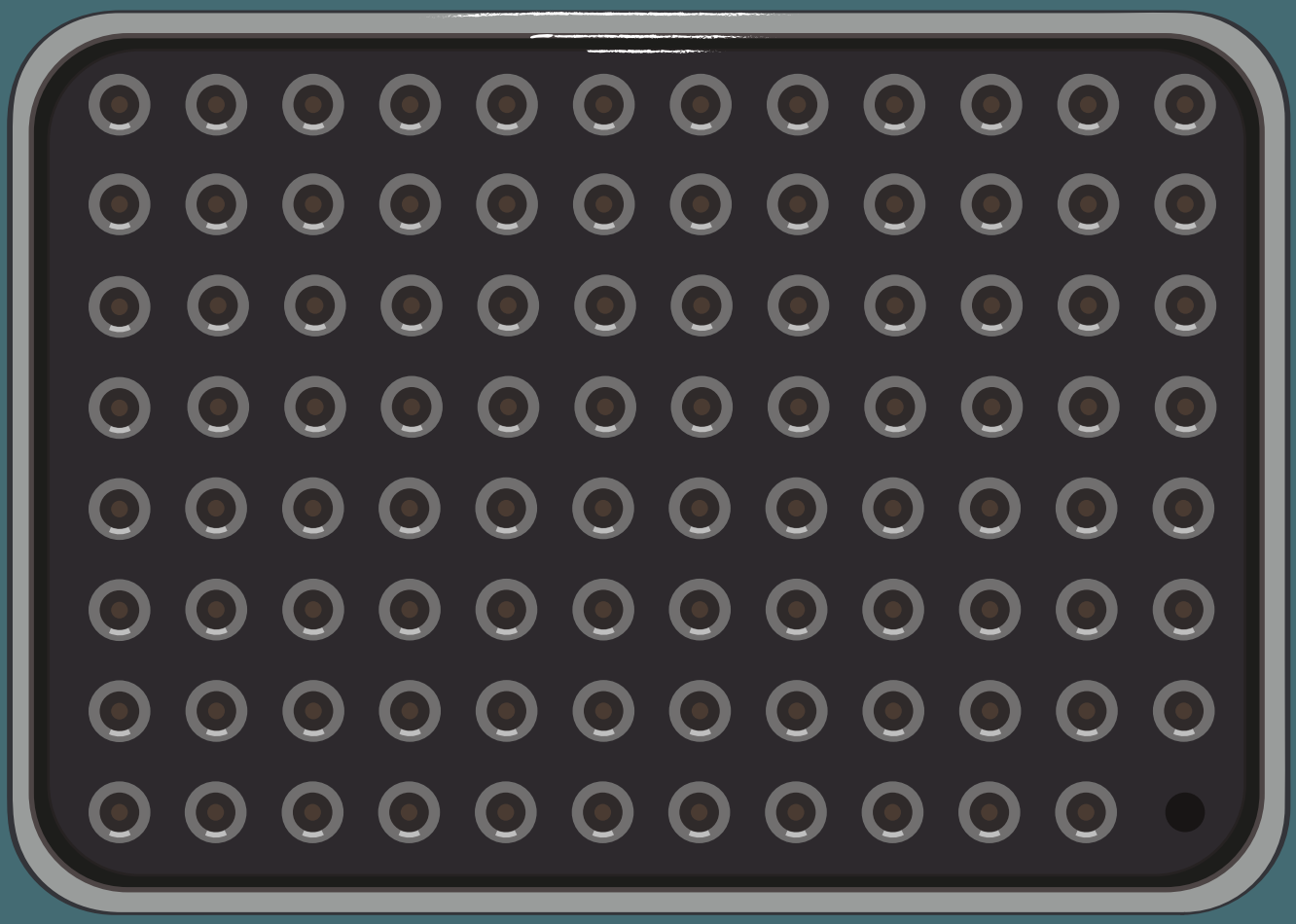

Materials and methods

I. Cell culture

1.1 Cell lines

1.1.1 HUVEC primary human cells (Lonza, Germany)

HUVEC (human umbilical vein endothelial cells) are endothelial cells extracted from human umbilical vein. HUVECs were grown in EBM-2 media (Lonza) implemented with 5% (v/v) Foetal Bovine Serum (FBS)(Lonza) and the kit "EGM-2 SingleQuots" (Lonza), and 1% of a mix of antibiotic (penicillin 10 000 units/ml, streptomycin 10 000 µg/ml (Life technologies, Carlsbad, USA)). Cells were cultivated up to passage 10, in an incubator at 37°C with 5% CO_2.

1.1.2 MDA-MB-231 cells

MDA-MB-231 cells (ATCC, Manassas, USA) are adenocarcinoma epithelial cells from human mammary gland. They were grown in DMEM medium (Gibco, Waltham, USA) with 4.5 g/l glucose, 110 mg/l sodium pyruvate, 584 mg/l L-glutamine, implemented with 10% (v/v) FBS (Lonza), and 1% (v/v) of a mix of antibiotic (penicillin 10 000 units/ml, streptomycin 10 000 µg/ml (Life technologies)). Cells were cultivated in an incubator at 37°C with 5% CO_2.

MDA-MB-231 resistant to epirubicin (MDA-MB-231/Epi). Courtesy of Dr Sharon Gorski, BC Cancer agency, Vancouver, Canada. Cells were grown in the same DMEM medium as described above for non-resistant MDA-MB-231 cells. 100 nM of epirubicin (Accord Healthcare, UK) was added in the medium. Experiments were performed in drug-free medium.

MDA-MB-231 resistant to paclitaxel (MDA-MB-231/Pacli). Courtesy of Dr Melanie Spears, MaRS Centre, Toronto, Canada. Cells were grown in the same DMEM medium as described above for non-resistant MDA-MB-231 cells. 25 nM of paclitaxel (Accord Healthcare) were added in the medium. Experiments were performed in drug-free medium.

The media were called "exosome free" when the exosomes from the serum had been removed. The serum was diluted 1:1 in culture medium then the mix was centrifuged 18 h at 110 000g, 4°C. The supernatant was then filtered through a 0.22 µm filter (Millipore, Burlington, USA) before being added to the rest of the medium, at the defined concentration.

II. Exosomes analysis

2.1 Exosomes purification

HUVECs were cultured in EGM2 (Lonza) without heparin and supplemented with 5% exosome-free serum for 72h. The supernatant was then recovered and exosomes were purified by sequential ultracentrifugation: the medium was first centrifuged at 2000 g for 20 minutes at 4°C to remove unattached cells and cell debris. It was followed by a second round of centrifugation at 12,000 g, 45 minutes at 4°C, to remove remaining cell debris and larger vesicles. The supernatant was then collected and passed through a 0.22 μm filter (Millipore) and centrifuged at 110,000 g for 2h at 4°C to pellet exosomes (Beckman Coulter Optima L-90K, Rotor SW32 Ti). The pellet was washed with PBS to remove any possible co-precipitated protein complexes, and underwent a final centrifugation at 110,000 g for 2h at 4°C. The pellet was then recovered and stored in PBS at -80°C.

2.2 Preparation of protein lysates and protein quantification

Cultured cells were washed with PBS and RIPA buffer was added to lysate the cells. The plates/flasks were then scratched and the homogenate was centrifuged at 10.000g and 4°C for 15 minutes. The supernatant was recovered and the pellet (cellular debris) discarded. The quantification of the protein from cell lysates was performed with the BCA Protein Assay Kit (Pierce Biotechnology) following manufacturer's instructions, with an incubation time of 30 minutes at 60°C. Standard curve was made of Bovine Serum Albumin (BSA) ranging from 0 to 2 μg/ml. For exosomes, the samples were lysed with Exosome Lysis buffer. Then they were incubated with the BCA kit at 60°C for 60 minutes, with a BSA curve from 0 to 100 ng/ml. The absorbance was measured at 562 nm, using a spectrophotometer (2030 Multilabel Reader VICTOR X3, Perkin Elmer).

2.3 Exosomes characterization

2.3.1 Dynamic Light Scattering (DLS)

DLS analysis allows to measure the size of particles in from 1 to 500 nm. It analyses the scattering of light in a sample of particles subjected to Brownian motion in a suspension. Exosomes were suspended in PBS (Lonza) and analysed with a Zetasizer Nano ZS (Malvern Instruments Ltd).

2.3.2 Transmission lectron microscopy

Exosomes were plated on a nickel grid covered by a thin layer of carbon for 1h, washed three times with PBS then fixed with 2% paraformaldehyde (PFA) for 10 min. After three washes, the grids were post-fixed 10 min with 2.5% glutaraldehyde. The samples were contrasted 10 min with 2.5% uranyl acetate. The samples were washed four times, then the grids were incubated 10 min in lead citrate. The grids are finally washed four times with deionized water and analysed with a transmission electron microscope JEM-1400 (JEOL) at 80 kV.

2.3.3 Floatation into iodixanol gradient

Exosomes were first purified following the protocol described above. Then, the amount of protein was measure and exosomes were further purified using an OptiPrep (Sigma-Aldrich) density gradient (protocol adapted from (Van Deun et al. 2014)). Briefly, a discontinuous iodixanol gradient was prepared by diluting a stock solution of OptiPrep (60% w/v) with 0.25 M sucrose/10 mM Tris, pH 7.5 to generate 40%, 20%, 10% and 5% w/v iodixanol solutions. With care, the discontinuous iodixanol gradient was generated by sequentially layering 3 ml each of 40, 20 and 10% (w/v) iodixanol solutions, followed by 2.5 ml of the 5% iodixanol solution in centrifuge tubes (Beckman Coulter). 500 µl containing 100 µg of exosomes was overlaid on the discontinuous iodixanol gradient and centrifuged using a SW 40 Ti rotor for 16 hours at 100,000 g at 4°C. Fractions of 1 mL were collected from the top of the gradient and analysed with DLS. Fractions 4 to 9 were diluted to 10 ml in PBS and centrifuged at 100,000 g for 2 hours at 4°C with a SW 40 Ti rotor. The resulting pellets were resuspended in 100 µl PBS.

III. Transfection

In order to assess the effects of the four miRNAs that were selected, we chose to use a transfection with pre-microRNAs. This method allows the modification of the content of miRNAs in cells during several days, without changing their genetic material. Pre-miRNAs (Ambion, Waltham, USA) are miRNAs precursors, they increase the cellular concentration of a given miRNA. The cells were transfected with Dharmafect-4 (Dharmacon, Lafayette, USA) following the manufacturer's instruction, at the time of seeding.

In a T-25 flask, 1 µl of Dharmafect-4 was added to 266 µl of RPMI-1640 (Lonza) without serum, and incubated 10 min at RT. 5 µl of Pre-miRNA at a concentration of 10 µM

were diluted in the same medium for a volume of 300 µl. Both solutions were mixed and incubated 20 min at RT, before being added into the flask. 800 000 cells (in 1.4 ml of complete DMEM medium) were seeded in the flask, and incubated at 37°C. The final pre-miRNA concentration was then 25 nM in 2 ml. After 16h, the transfection medium was removed and fresh complete DMEM was added.

The volumes of transfection were adapted to the size of the culture plates/flasks and the number of cells.

IV. Functional assays

4.1 Survival assay

2000 cells were seeded in a 96 wells plate, in 100 µl of complete medium. The cells were grown in the incubator at 37°C, 5% CO_2, for a specific time. The cells treated with chemotherapies were incubated after 16h in complete medium. After the treatment, the cells were gently washed with PBS and complete EGM2 or DMEM (for HUVECs or MDA-MB-231, respectively) was added. 1h before the endpoint, 10 µl of WST1 reagent (Roche, Switzerland) was added to the wells, including 3 control wells. Difference in absorbance at 450 nm was measured after 30 min using the VICTOR X3 Multilabel Reader (PerkinElmer). WST1 reagent is a colorimetric assay that is based on the cleavage of a tetrazolium salt, MTS, by mitochondrial dehydrogenases to form formazan in viable cells. The bigger the number of viable, metabolically active cells, the greater the amount of formazan product produced following the addition of WST-1.

4.2 Proliferation assay with BrdU

When the cells were transfected with pre-miRNAs, they were directly seeded in the wells of a 48 wells plate, 15 000 cells/well in 300 µl of transfection medium.

In other cases, 2000 MDA-MB-231 were seeded in a 96 wells, in 100 µl of complete DMEM. After 16h, the medium is replaced by DMEM 2% (v/v) FBS. 4h before the endpoint, 10 µM of BrdU were added to the medium. After that time, the culture was stopped. The level of proliferation was analysed by measuring the incorporation of BrdU with the kit *Cell Proliferation ELISA BrdU (Colorimetric)* (Roche), following the manufacturer's instructions. Absorbance at 355 nm was measured with the VICTOR X3 Multilabel Reader (PerkinElmer). This test allows the detection of the brdU incorporated in genomic DNA of dividing cells by using antibodies and colorimetry.

4.3 Annexin V-PI assay

The proportion of cells undergoing apoptosis was measured by flow cytometry using the kit *Roche Annexin-V-Fluos Staining Kit* (Roche). The cells were seeded in 6 cm cell culture dish (Greiner) with 4 ml of complete EGM2. After treatment with chemotherapy or control medium, the cells were incubated in exosome-free EGM2. 72h later, the culture medium was removed and kept, and the cells were gently detached with trypsin. The culture medium and detached cells were pooled. The cells were stained following the manufacturer's instructions with Annexin V – fluorescein and Propidium Iodide (PI) and analysed on the FACSCalibur (BD Biosciences). 3 controls were made: the buffer alone, the Annexin V – fluorescein only, and the PI alone. The Annexin V is the ligand of phosphatidylserine, which are express on the surface of dying cells. Viable cells with intact membranes exclude PI, whereas the membranes of dead and damaged cells are permeable to PI. By combining the two dyes, it allows to discriminate between living cells (Annexin V -, PI -) and cells in the early (Annexin V +, PI -) or late (Annexin V +, PI +) state of apoptosis.

4.4 Adhesion assay

The wells of a 96-wells plate were coated with 20 µg/ml Fibronectin (BD Biosciences) 1h at 37°C, then blocked with 3% BSA, 1h at 37°C. The cells were then counted and resuspended in serum-free medium, 0.1% BSA, at a concentration of 100 000 cells/ml. 100 µl of the mix was added per well of the coated plate (5 wells/condition), and the cells were left to adhere in an incubator at 37°C, 5% CO_2. After 1h, the medium was removed and the wells were washed with DPBS (Lonza). The cells, including 3 control blank wells, were then fixed with 8% glutaraldehyde (Sigma-Aldrich) and stained with 0.1% crystal violet (Sigma-Aldrich). After removing the staining solution, the cells were washed twice with water to remove the excess of solution. Eventually, the staining was dissolved in 10% Acetic Acid. The absorbance at 562 nm was read with the VICTOR X3 Multilabel Reader (PerkinElmer).

4.5 Colony forming assay

MDA-MB-231 were transfected in 6-wells plate. The next day, the transfection media were changed for complete DMEM. After 24 h, the cells were detached with trypsin and carefully counted. For each condition, cells were resuspended in complete DMEM at a concentration of 50 cells/ml. 2 ml of the suspension were plated in each well of a 6-wells plate, carefully to ensure that the cells were homogenously dispersed in the well. The cells were incubated for 12 days (MDA-MB-231) to 21 days (MDA-MB-231/Epi) at 37°C and

5% CO_2, the medium changed every 7 days. Then the medium was removed and the colonies were gently washed with DPBS and fixed and stained using a solution of 6.0% glutaraldehyde, 0.5% crystal violet. The plates were dried in the open air at RT overnight. Images were taken of each well and the number of colonies was counted with ImageJ.

4.6 Spheroid assay

48h after transfection, MDA-MB-231 were detached with trypsin and carefully counted. 1000 cells/well were seeded in 200 µl of a mix of 3:2 (v/v) EGM2/Methylcellulose 1.2% (Sigma-Aldrich, Cat-No: M0512-100G), in a 96 well suspension culture plate (Greiner). The cells were incubated 48h at 37°C and 5% CO_2. Once the spheroids were formed, they were collected and centrifuged to remove the remaining culture mix. They were delicately resuspended in a solution of 1:1 collagen (BD Biosciences) - pepsin/methylcellulose 1.2% and plated in the wells of a 48-wells plate. 6 spheroids were plated per well, in 300 µl of the collagen-pepsin/methylcellulose solution. Bubbles were removed and, after 30 min of polymerization, 500 µl of DMEM 2% FBS was added on each well. The spheroids were incubated 24h at 37°C and 5% CO_2. Images of each spheroid were taken using a microscope Olympus CKX41 (Olympus Life Science), and the area of the spheroids and the area of invasion were measured with ImageJ software.

4.7 Migration assay in Boyden Chamber

The Boyden Chambers consist of a membrane pierced with 8 µm micropores. Cells seeded on top of the membrane can be attracted by molecules present in the other side of the chamber, and migrate by chemotaxis through the pores of the membrane. 600 µl of complete DMEM were added on the bottom of the well of a 24-wells plate. The inserts were then added to the wells (3422, Corning) and filled with 30 000 cells (MDA-MB-231 transfected 2 days prior) in 300 µl of DMEM 1 g/ml Glucose without serum (Gibco). After a 24-h incubation at 37˚C and 5% CO_2, the inserts were emptied and the cells were fixed with glacial methanol in -20°C for 30 min. The methanol was removed and the inserts were left to dry overnight at RT. The next day, the cells were stained with 4% Giemsa (Merck, Germany) for 30 min. The inserts were washed three times with water and the non-invaded cells present in the inserts were removed with a cotton swab. The membranes were detached from the inserts and mounted on microscope slides. Images of the membrane were taken on a microscope Olympus CKX41 (Olympus Life Science) and the stained cells were counted with ImageJ.

V. RNA extraction from cells or exosomes

The purification of RNA from cellular sources was performed using the *miRNEAsy Mini kit* (Qiagen, Germany), following the manufacturer's instructions. The RNA was suspended in RNAse-free water and quantified by Nanodrop (ThermoFisher, USA). The same kit was used to extract RNA from exosomes, with a few modification: five volumes of Qiazol (Qiagen) were added to the exosomes and the volume of chloroform and ethanol were adjusted accordingly. RNA was suspended in RNAse-free water too and quantified with the *Quant-it Ribogreen RNA assay kit* (ThermoFisher) on black 96-well plates. The emitted fluorescence was assessed using a spectrophotometer (2030 Multilabel Reader VICTORTM X3, Perkin Elmer) at 592nm.

VI. Quantitative analysis of genes and microRNA expression by qRT-PCR

Three different approaches were used to measure the level of different RNAs.

6.1.1 mRNAs (Coding Genes)

RELA, TGFβR2, ABCB1, MDH2, POR, TOP2A, GADD45A, SIRT6, PCNA.

The synthesis of cDNA was performed with the *iScript DNA synthesis kit* (Biorad) following the manufacturer's instructions, starting from 250 to 1000 ng of total RNA. The cDNAs produced were used for the quantitative PCR reaction, using the *SYBR Green system* (Takyon Eurogentec, Belgium). The thermal cycles were performed on a PCR cycler Applied Biosystem 7900 HT (Applied Biosystem). For each experiment performed, two negative controls were done: one sample without cDNA (H_2O instead), and one submitted to the reverse transcription without the reverse transcriptase enzyme (RT-). The relative level of mRNA was quantified using the $2^{-\Delta Ct}$ method and was normalized compared to two housekeeping genes: β2-microglobuline (B2M) and Peptidylprolyl Isomerase A (PPIA). The primers were made so that they overlap exon-exon junctions to avoid detection of genomic DNA.

CD44, SLUG, ZEB1

The cDNAs of CD44, SLUG and ZEB1 were obtain after reverse transcription with the *cDNA synthesis First Strand kit* (Roche) with the *LightCycler480 Probes Master kit* and the *Universal Probe Library* (Roche) as previously described in (Suarez-Carmona et al. 2015).

6.1.2 miRNAs

The synthesis of cDNAs from miRNAs was performed using 15 to 200 ng of RNA with the *qScript microRNA cDNA Synthesis Kit* (Quanta Biosciences, Beverly, USA), following the manufacturer's instructions. Briefly, the synthesis happens in 2 steps. The first one allows the polyadenylation of the miRNAs. The second step consists of the synthesis of cDNA using the miRNA and poly(A) tail as template. The cDNAs were then used for the quantitative PCR reaction with SYBR green (Takyon Eurogentec), and two primers. The first primer was specific of the miRNA, the second one called Universal Primer and used for all miRNAs detection. The thermal cycles were performed on a PCR cycler Applied Biosystem 7900 HT (Applied Biosystem). For each experiment performed, two negative controls were done: one sample without cDNA (H_2O instead), and one submitted to the reverse transcription without the reverse transcriptase enzyme (RT-). The relative level of mRNA was quantified using the $2^{-\Delta Ct}$ method and was normalized compared to two internal control: SNORD44 and SNORD48 for RNA from cultured cells. For exosomal RNA, the normalization was made with two miRNAs that were among the less variable ones from the miRNA profiling: miR-23a-3p and miR-24-3p.

VII. Western Blot

Samples were denaturated by boiling at 95°C for 5 min in Loading Buffer, under non-reducing condition for antibody against CD63, CD81 or CD9. For all other antibodies, reducing condition applied. Equal amount of protein lysates were separated by electrophorese on SDS-PAGE with a concentration ranging from 8 to 15% of acrylamide. Separated proteins were then transferred to a polyvinylidene fluoride membrane (Milipore) using a wet transfer system. The membrane was blocked 1h at RT with a solution of Tris, 8 % powdered milk and 0.1 % Tween 20 and then incubated overnight at 4°C with the primary antibody. The antigen-antibody complexes were detected with a secondary antibody coupled to horseradish peroxidase (HRP) and the fluoro-chemoluminescent system ECL (Pierce Biotechnology).

VIII. miRNA profiling

Total RNA was extracted with the *miRNeasy Mini kit* (Qiagen) following manufacturer's instruction, and quantified using the *Quant-it Ribogreen RNA assay kit* (ThermoFisher). 20 ng of RNA was used per condition. Reverse transcription was performed using the kit *miRCURY LNA™ Universal RT microRNA PCR* (Exiqon, South Korea). cDNAs were mixed with the *ExiLENT SYBR green PCR Master mix* and loaded to each well of a 384 wells PCR plate *microRNA Ready-to-Use PCR panel 1* (Exiqon) pre-coated with LNA primers set for the detection of 372 different miRNAs. PCR amplification and detection was performed on Applied Biosystem 7900 HT (Applied Biosysems). In-plate controls comprise inter-plate calibrators, reference genes and negative control. A miRNA was considered "undetermined" when the Ct was superior to 40.

IX. Small RNA sequencing

Two independent biological replicates were prepared per condition. Total RNA was extracted with the *miRNeasy Mini kit* (Qiagen) following manufacturer's instruction, and quantified using the *Quant-it Ribogreen RNA assay kit* (ThermoFisher). Small RNA libraries were generated using *TruSeq Small RNA Library Prep Kit* (IRS-200-0012, llumina, San Diego, USA) for cellular and exosomal samples using 1µg and 15ng of RNA respectively. The libraries were purified using a 6% Novex TBW polyacrylamide gel (EC6265BOX, Invitrogen) and the sequences ranging in size from 145 to 160 nt were selected. Libraries were prepared following manufacturer's instructions. Libraries were then analysed on an Agilent Bioanalyzer DNA 1000 and quantified by qPCR using the Kapa kit (Kapa Biosystems). Sequencing was performed using an Illumina HiSeq 2000 (75 pb single-end reads) generating 25 million reads per sample.

All the raw sequence files underwent a quality control analysis using FastQC v.0.11.5. Remaining adaptor sequences of small RNA libraries were removed using Trimmomatic (Bolger et al. 2014). Reads shorter than 16 nt post trimming were discarded. The Small RNA libraries were mapped against the miRNOME (Kozomara & Griffiths-Jones 2014), for the detection of microRNAs. The mapping was performed by Bowtie2 using the mode "end-to-end" to ensure no clipping of the sequences. Only the best microRNA mapping to the reads was considered. The count of reads per gene was assessed using an in-house script (Pérez-Boza et al. 2018).

X. Transcriptomic analysis by high throughput sequencing

Three independent biological replicates were prepared per condition. Total RNA was extracted with the *miRNeasy Mini kit* (Qiagen) following manufacturer's instruction, and quantified using the *Quant-it Ribogreen RNA assay kit* (ThermoFisher). Libraries were prepared by the core facility using the TruSeq Stranded mRNA HT Sample Prep Kit (RS-122-2103, Illumina). Sequencing was performed using an Illumina HiSeq 2000 (75 pb single-end reads) generating 20 million reads per sample. Reads were trimmed to remove adapters. Correct removal of adapters and sequence quality were checked using fastQC v.0.11.5 (Andrews 2010) and MultiQC (Ewels, 2016). RNA sequences were then aligned on the hg38 human reference genome using STAR v2.4.0 (Dobin et al. 2013) with default parameters and removal of the noncanonical unannoted junctions. The number of reads mapping a gene were counted using HTSeq-count (Anders et al. 2015). We used DESeq2 package (v1.18.1) (Love et al. 2014) for read count normalization and differential expression analysis.

XI. Statistical analysis

All experiments were performed a minimal of 3 times otherwise stated. The values plotted represent the mean of the biological replicates ± the standard deviation (SD), the technique used is specified for each case in the figure's legend. The statistical significances of the results were assessed using an unpaired t-test. For high throughput sequencing, the statistical significance is given as the adjusted p-value, q-value, representing the p-value corrected to the multiple testing.

XII. Buffers, primers and antibodies

12.1 Buffers

Buffer	Composition
Exosome lysis buffer	10% triton, 1% SDS, PBS
Electrophoresis buffer	250 mM Tris HCl, 250 mM H3BO3, 1 mM EDTA
4x loading buffer	30 mM Tris HCl, 5% SDS, 5% glycerol, 0.002% bromophenol blue, 2.5% β-mercaptoethanol, pH=6.8

4x non-reducing loading buffer	30 mM Tris HCl, 5% SDS, 5% glycerol, 0.002% bromophenol blue, pH=6.8
RIPA buffer	50 mM Tris pH 7.5, 150 mM NaCl, 10 mM CaCl2, 0.5% NP40, 0.25% Sodium deoxycholate, 0.1% SDS
Trypsin-EDTA	0.5% trypsin (Difco, Detroit, MI, USA); 0.2% EDTA; PBS; pH=7.6

12.2 Primers for qRT-PCR (5' → 3')

Gene	Forward	Reverse
B2M	GAGTATGCCTGCCGTGTG	AATCCAAATGCGGCATCT
PPIA	CCAACACAAATGGTTCCCAGT	CCATGGCCTCCACAATATTCA
TGFβR2	CGCACGTTCAGAAGTCGGTTA	TCTGGTTGTCACAGGTGGAAAA
RELA	CTCCTGTGCGTGTCTCCAT	TTTCTCCTCAATCCGGTGA
ABCB1	TGCATTTGGAGGACAAAAGA	AGCAGGAAAGCAGCACCTAT
MDH2	GACCTGTTCAACACCAATGC	TGAAAACTTCTGCTGTGATGG
POR	CGGCTGAAGAGCTACGAGA	AGTCCGAGATGTCCAATTCC
TOP2A	GGATCCACCAAAGATGTCAA	CCAGTTTCATCCAACTTGTCC
GADD45A	GAGCTCCTGCTCTTGGAGAC	CCCGGCAAAAACAAATAAGT
SIRT6	GCAGTCTTCCAGTGTGGTGT	CTCTCAAAGGTGGTGTCGAA
PCNA	TAAAATGCGCCGGCAATG	TCTCCTGGTTTGGTGCTTCAA
GSK3A	GCCAAGTTGACCATCCCTAT	GTGGATGTAGGCCAAGCTG
CD44	ACCCTACTGATGATGACGTGAGCA	TGGAATGTGTCTTGGTCTCTGGTA
SLUG	ACAGCGAACTGGACACACAT	GATGGGGCTGTATGCTCCT
ZEB1	GAATGCCCAAACTGCAAGAAACGC	TTCTTGGTCGCCCATTCACAGGT
TBP	GACTCCCATGACCCCCAT	CAACCAAGATTCACTGTGGATAC

12.3 Primers for miRNA qRT-PCR (5' → 3')

miRNA	sequence
miR-373-3p	GCTTCGATTTTGGGGTGTAAAA
miR-887-3p	GCCATCCCGAGGAAAAA
miR-122-5p	TGGAGTGTGACAATGGTGTTTG
miR-129-5p	CTTTTTGCGGTCTGGGCTTG
miR-23a-3p	ACATTGCCAGGGATTTCCAA
miR-24-3p	TGGCTCAGTTCAGCAGGAACAG
Universal primer	GCATAGACCTGAATGGCGGTA

12.4 Pre-miRNAs

Pre-miRNAs	Brand	ref
Hsa-miR-373-3p	Ambion	PM11024
Hsa-miR-887-3p	Ambion	PM12954
Hsa-miR-122-5p	Ambion	PM11012
Hsa-miR-129-5p	Ambion	PM10195
Pre-miR miRNA Precursor negative control	Ambion	AM17110

12.5 Antibodies

Protein	host	brand	ref
CD9	Mouse	Santa Cruz	sc20048
CD81	Mouse	Invitrogen	10630D
CD63	Mouse	Invitrogen	10628D
CYC	Rabbit	Oncogene research	PC333
TSG101	Mouse	GeneTex	GTX70255
CD31	Mouse	Dako	M0823
TGFβR2	Goat	R&D System	AF-241-NA
RELA	Rabbit	Santa Cruz	sc-109-G
Anti-mouse FC-HRP	Horse	Cell signaling	7076
Anti-rabbit FC-HRP	Goat	Cell signaling	7074
Anti-goat FC-HRP	Rabbit	Dako	PO449

Results

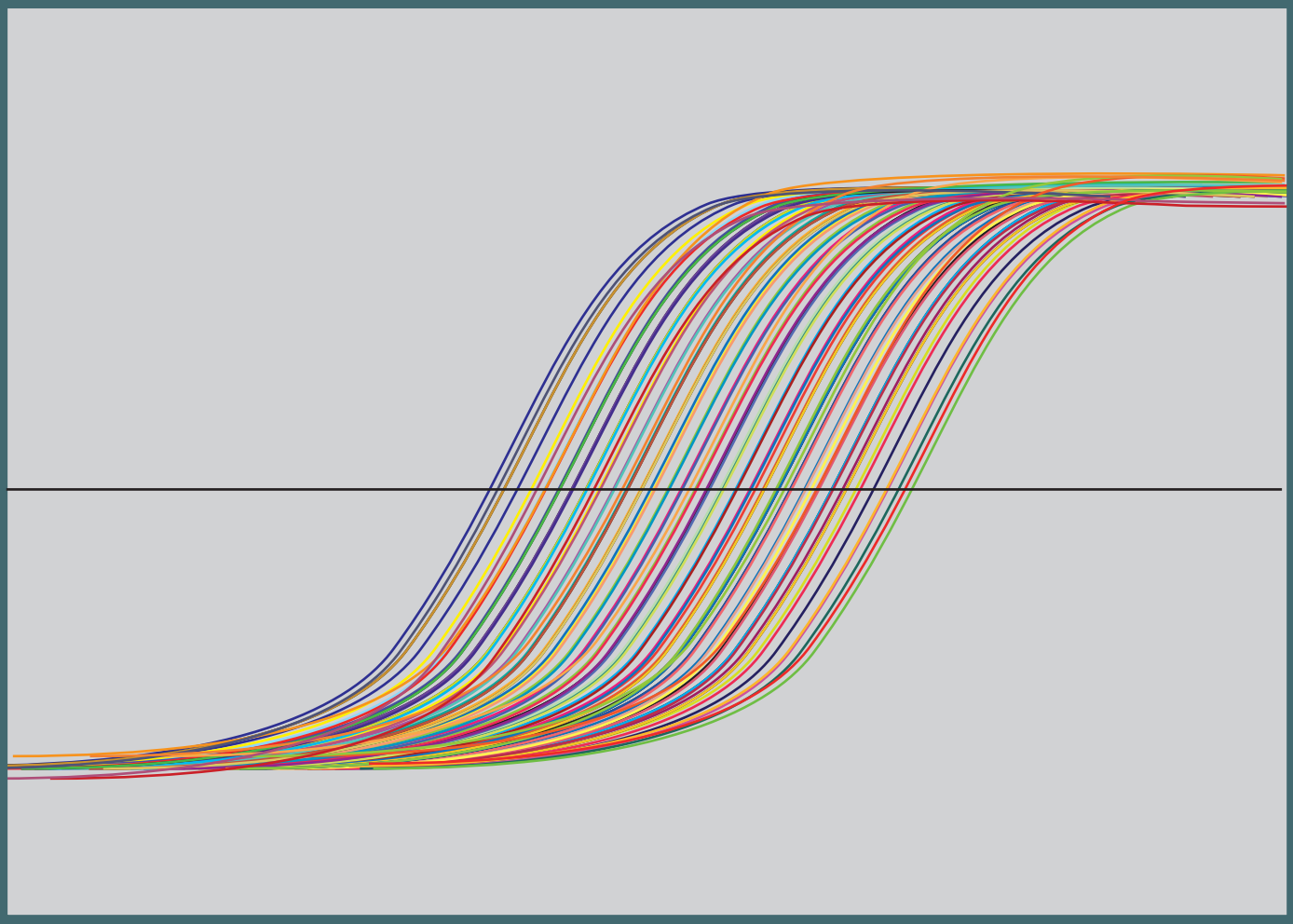

Results

I. Transfer of miRNAs via exosomes

Previous work in the lab has shown that a tumour mimicking media lowers the secretion and levels of miR-503-5p, a miRNA with anti-tumour properties, in the exosomes from endothelial cells. Exosomes from endothelial cells were able to transfer miRNAs to tumour cells (fig. S 55-56). Interestingly, they showed that the chemotherapy drugs epirubicin and paclitaxel induced an increase of the exosomal content of that miRNA. Exosomes loaded with miR-503-5p could then affect the tumour growth (Bovy et al. 2015). In the present work, we wanted to assess if the chemotherapy drugs alters the secretion of other miRNAs in exosomes by endothelial cells. In that case, we also wanted to determine how those miRNAs would affect the tumour cells.

1.1 Determination of the concentration of drugs to use for the production of exosomes by HUVECs

We aimed to produce exosomes from endothelial cells treated by epirubicin or paclitaxel. Since the drugs are toxic for the endothelial cells, we decided to use a dose that would not affect the survival of more than 50% of the cells. In order to determine the drugs concentration to be used on HUVECs, we performed a WST1 survival assay based on colorimetry. The HUVECs were incubated in complete media for 72h to mimic the conditions of exosomes purification. Results showed that when the HUVECs were incubated for 2h with epirubicin 1 µg/ml (1.84 µM) or paclitaxel 20 ng/ml (23.4 nM), half of the cells survived after 72h (**Fig. R 20**).

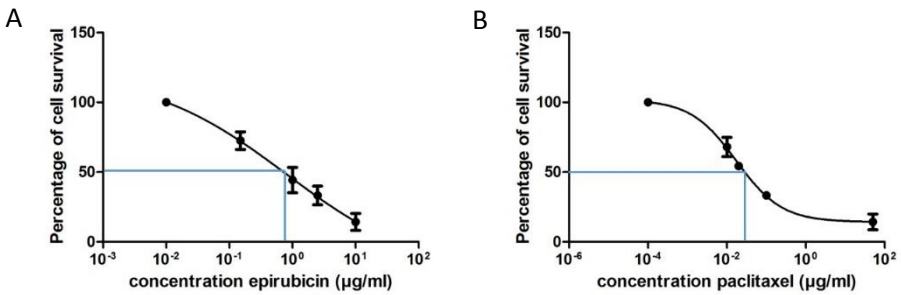

Figure R 20. ***Survival of HUVECs upon treatment with epirubicin or paclitaxel.*** *HUVECs were incubated 2h with concentrations ranging from 0 to 10 µg/ml (18.4 µM) of epirubicin (A), or from 0 to 50 µg/ml (58.5µM) of paclitaxel (B). The percentage of survival was assessed after 72h in complete media by addition of WST1 reagent and measuring absorbance. Data are represented as mean ± SD from three independent experiments.*

The level of apoptosis and necrosis in drug-treated HUVECs was measured by flow cytometry by staining for Annexin V and Propidium iodide (**fig. R 21**). Briefly, the living cells are negative for the two stainings, and are found in the lower left quadrant. Cells in early apoptosis are stained by Annexin V but not by PI, and are found in the lower right quadrant. Finally, late apoptosis and dead cells appear in the upper right quadrant, stained with both Annexin V and PI. The results showed that the treatments with paclitaxel induced a slight increase in apoptosis (11%) compared to the control (8.5%). We considered that the concentrations selected above did not induce to a drastic increase in cell apoptosis, which could lead to a major contamination by apoptotic bodies and cell debris in the purified extracellular vesicles. To verify the sensibility of cancer cells to the drugs, we applied the same concentration of drugs on MDA-MB-231 breast cancer cells. The drugs only slightly affected the proliferation and the survival of the cells (**fig. S 1**). The decrease of the proliferation was significant when the cells were treated with epirubicin.

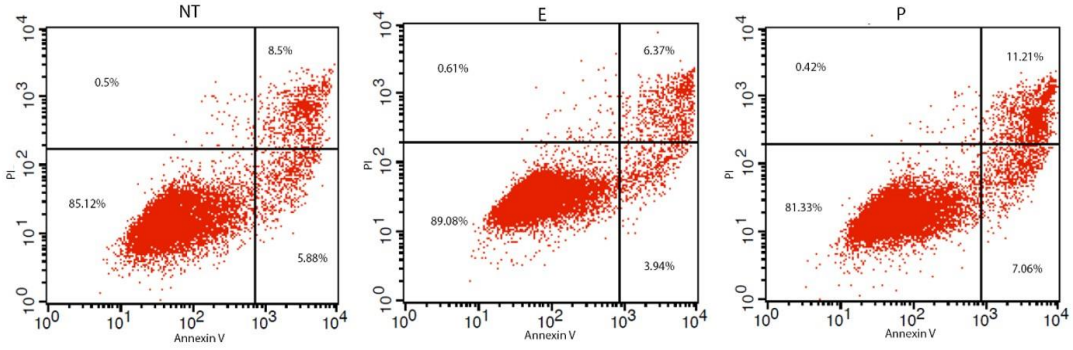

Figure R 21. ***Annexin V – PI staining of HUVECs incubated with epirubicin or paclitaxel.*** *The HUVECs were seeded, then incubated 2h with epirubicin 1 µg/ml (E) or paclitaxel 20 ng/ml (P). After 72h in complete medium, the cells were harvested and stained with annexin V and PI (Propidium Iodide) to differentiate living cells from those in apoptosis. Lower left, live cells; lower right, early apoptosis; upper right, late apoptosis; upper right, necrosis. The cells were then analysed by flow cytometry. (NT: untreated cells).*

1.2 Characterization of the extracellular vesicles

We produced exosomes by differential ultracentrifugation from cells incubated 2h with epirubicin 1 µg/ml or paclitaxel 20 ng/ml, based on the guidelines from Lötval et al (2014), a position paper from the International Society for Extracellular Vesicles. The size of the purified extracellular vesicles was assessed by Dynamic Light Scattering (DLS), and their size and morphology by Transmission Electron Microscopy.

As shown in the figure R 22, the vesicles display a diameter of around 140 nm, with no differences due to the drug treatment (**fig. R 22A**). Transmission Electron Microscopy

confirmed that the vesicles ranged between 30 and 150 nm, and that they presented a cup-shaped morphology with a lipid bilayer associated with exosomes (**fig. R 22B, fig. S 53, 54**).

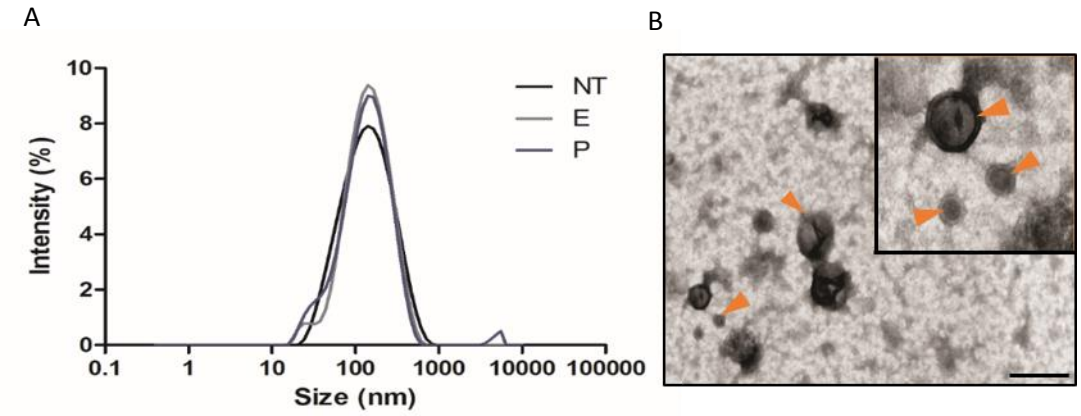

Figure R 22. ***Size and morphology of extracellular vesicles****. EVs were isolated from HUVECs supernatant and purified by ultracentrifugation. (A) HUVECs were incubated 2h with 1 µg/ml epirubicin (E), 20 ng/ml paclitaxel (P), or untreated (NT). The size of extracellular vesicles was assessed by DLS for the three conditions. (B) Purified extracellular vesicles from HUVECs untreated by transmission electron microscopy. The arrows show vesicles with a lipid bilayer. In collaboration with Pr. M. Thiry. Upper right: zoom; scale bar: 200 nm.*

We also evaluated the relative protein abundance of Cytochrome C (CYC), CD31, TGS101, CD63, CD81 and CD9 in the vesicles and in HUVECs by Western Blotting (**fig. R 23A**). As expected, the endothelial marker CD31 was present in both the endothelial cells and their vesicles. CYC, a mitochondrial protein, can be found in apoptotic bodies but not in exosomes. Our results showed that the vesicles were indeed devoid of CYC. The tetraspanins CD63, CD81 and CD9, considered to be exosome markers, were enriched in the vesicles. TSG101, a component of the ESCRT implicated in the biogenesis of exosomes, was found in both cells and vesicles, but it was enriched in the cellular compartment. We found no marked difference induced by the drug treatments, except for CD81, which was slightly increased in vesicles purified from epirubicin-treated HUVECs. The mechanisms behind this enrichment would be interesting to study in further research.

The purified exosomes obtained by differential ultracentrifugation were then separated by floatation on a density gradient made of sucrose/iodixanol cushions (**fig. R 23B**). After centrifugation and formation of the gradient, the resulting fractions were analysed by Western Blotting with antibodies for the exosomes markers CD9, CD81 and CD63. CD9 and CD63 can be found on multiple types of EVs, but in vesicles purified by centrifugation at 100 000g (light vesicles), they are markers of exosomes. CD81 is found in light vesicles only (Kowal et al. 2016). All three proteins were found in the same fraction, with no

contamination in other fractions, which shows that the exosomes purified by differential ultracentrifugation were not contaminated by other vesicles.

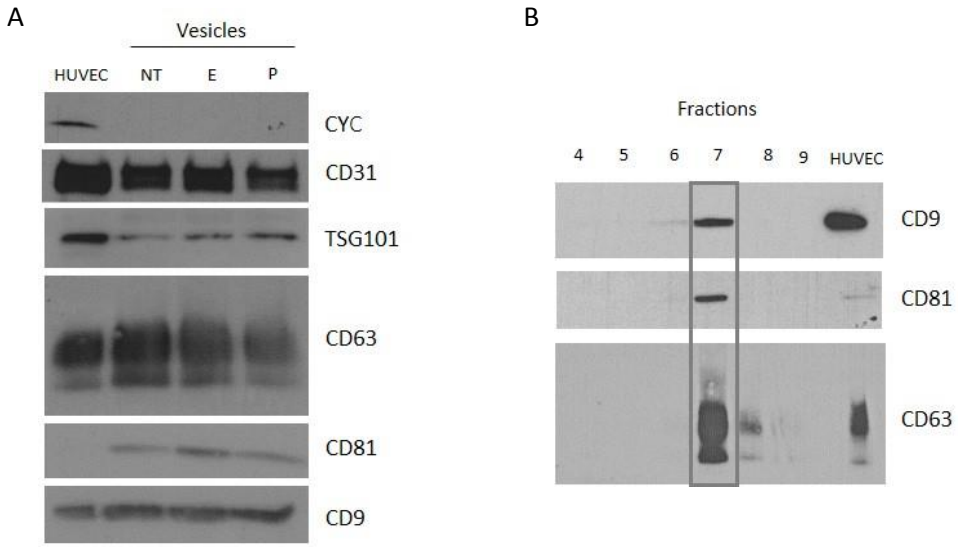

Figure R 23. ***Protein composition and density characterization of extracellular vesicles****. (A) 10 µg of proteins from HUVEC lysates or purified extracellular vesicles from untreated (NT) or epirubicin (E) – or paclitaxel (P) -treated HUVECs were separated by SDS-PAGE and subjected to Western blotting using the indicated antibodies. (B) After purification, extracellular vesicles were further separated using a sucrose/iodixanol density gradient. The resulting fractions were loaded into a polyacrylamide gel and the relative level of the exosomal protein markers CD9, CD81 and CD63 was assessed by Western Blotting.*

The size and protein profile of the extracellular vesicles imply that the preparation is strongly enriched in exosomes. Therefore, the extracellular vesicles purified by this methods will be further referred to as exosomes.

1.3 Analyses of the miRNA content of exosomes by miRNA sequencing

We then wanted to determine if the miRNA content of the exosomes was affected by the drugs. Based on the previous study on miR-503-5p, we hypothesized that their content would be different from the exosomes from untreated HUVECs. We wanted to compare the miRNA content of the exosomes, and also compare the miRNA in the endothelial cells after treatment with the drugs to see if the variations were similar in cells and in exosomes. In order to evaluate the miRNA composition, we performed a Next Generation Sequencing (NGS) analysis with small RNA libraries prepared from exosomal and cellular samples of HUVECs, untreated or incubated with epirubicin or paclitaxel.

We evaluated the distribution of the miRNAs in the different groups by Principal Component Analysis (PCA) (**fig. R 24A**). The cellular samples were well discriminated between the three conditions. However, the exosomal replicates presented too much variations between samples from the same condition, rendering further analysis difficult and

data barely exploitable (**fig. R 24B**). Only two miRNAs out of the 778 miRNAs detected presented a variation between conditions in exosomes, and the variation between samples was too important to produce significant results (**table R 1**).

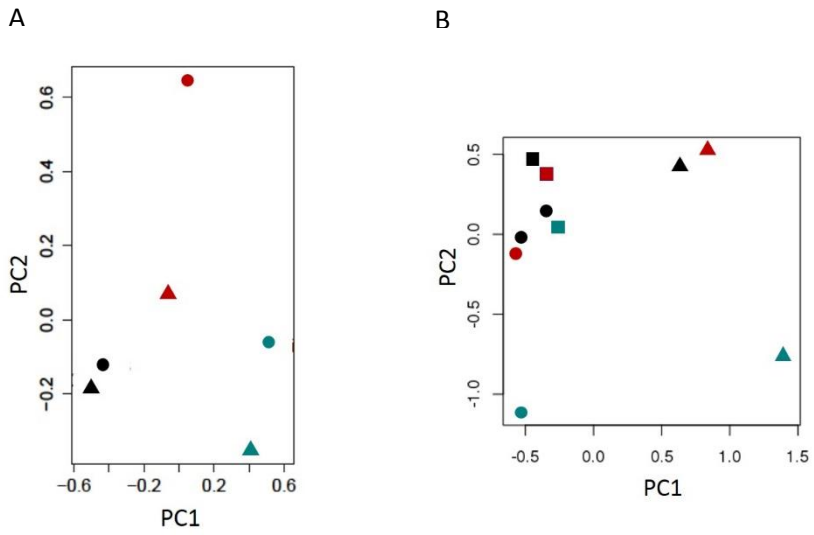

Figure R 24. ***Principal Component Analysis.*** *(A) Distribution of the cellular samples, in two experiments, and (B) of exosomal samples in three experiments. Exosomal controls were present in four experiments. Each colour represents a condition (black, control; red, epirubicin; green, paclitaxel) and each symbol represents a biological replicate.*

Comparison	Total miRNAs	Q value ≠ 1	miRNAs Q value < 0.05	Fold change	Q value
NT vs E	778	2			
NT vs P	778	24	miR-182-5p	11.85	0.0069
			miR-486-6p	0.09	0.0069

Table R 1. ***Summary of the results from the miRNA sequencing****. NT, exosomes from untreated HUVECs; E, exosomes from epirubicin-treated HUVECs; P, exosomes from paclitaxel-treated HUVECs.*

The high variability between the samples is probably due to the low concentration of exosomal RNA (15ng of RNA in exosomal samples, and 1µg in cellular samples). The technique may thus not be optimal yet for such small amount of RNA. We then decided to use another approach, the qRT-PCR array, which has already been proven successful in the laboratory.

1.4 Analyses of the miRNA content of exosomes by qRT-PCR profiling assay

We performed a qRT-PCR array on HUVECs and on exosomes from HUVECs. We incubated the cells with epirubicin or paclitaxel and compared them to untreated cells, and did the same for the exosomes. The total number of miRNAs detected was slightly lower in

exosomes than in cells. We noticed that, in cells and exosomes, the majority of miRNAs are common in all three conditions. Still, some miRNAs are specific to one condition (**fig. R 25**).

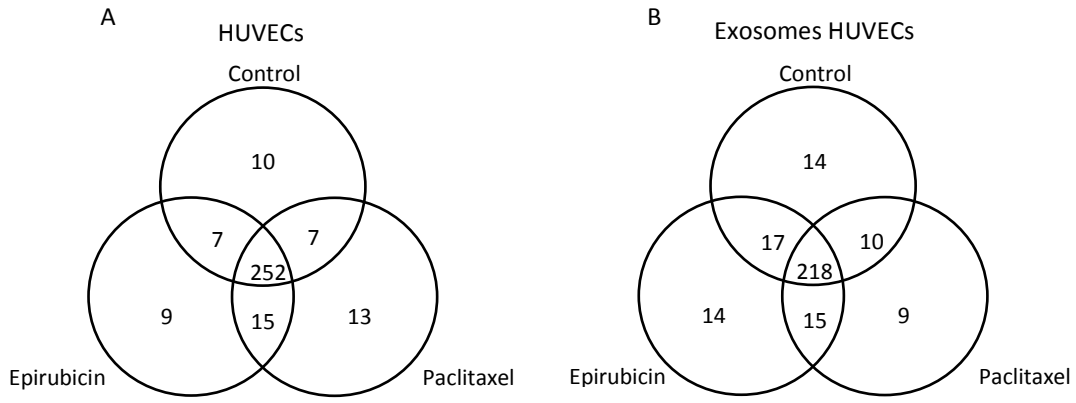

Figure R 25. ***Venn diagram of the miRNA content of HUVECs and exosomes is affected by the drugs.*** *The miRNA profile of HUVECs control, incubated with 1 µg/ml epirubicin or 20 ng/ml paclitaxel, and the respective exosomes, was analysed using the Exiqon miRCURY LNA Universal PCR system. Diagram representing the number of miRNAs in the different conditions, in cells (A) and in exosomes (B). Two cellular samples per condition; three exosomal samples per condition*

We searched for miRNAs that would be elevated in exosomes from drug-treated HUVECs. 14 miRNAs were detected only in exosomes from untreated cells, 14 miRNAs only in exosomes from epirubicin-treated HUVECs, and 9 were found in exosomes from paclitaxel-treated cells only (**fig. R 25**, **table S 8**). The level of miRNA detected in exosomes was compared between the untreated and epirubicin condition (235 miRNAs), and between the untreated and paclitaxel condition (228 miRNAs) (**fig. R 26, table S 10 and S 11**). The volcano plots represent the relative level of the miRNAs in relation to the p value. We wanted to identify miRNAs that were increased in exosomes after treatment with both drugs. We selected miR-887-3p and miR-373-3p, the most elevated miRNAs in both drug-treated conditions, for further research (**fig. R 26**). Moreover, we selected two miRNAs, miR-122-5p and miR-129-5p, that were not found in the exosomes from untreated HUVECs, but were detected in exosomes from epirubicin-treated and paclitaxel-treated HUVECs (**table S 8**). In the endothelial cells, miR-373-3p was not detected in drug-treated cells, miR-887-3p was slightly increased with drugs treatment, miR-122-5p was not detected in untreated cells, and miR-129-5p was not detected at all (**table S 9, S 12 and S 13**).

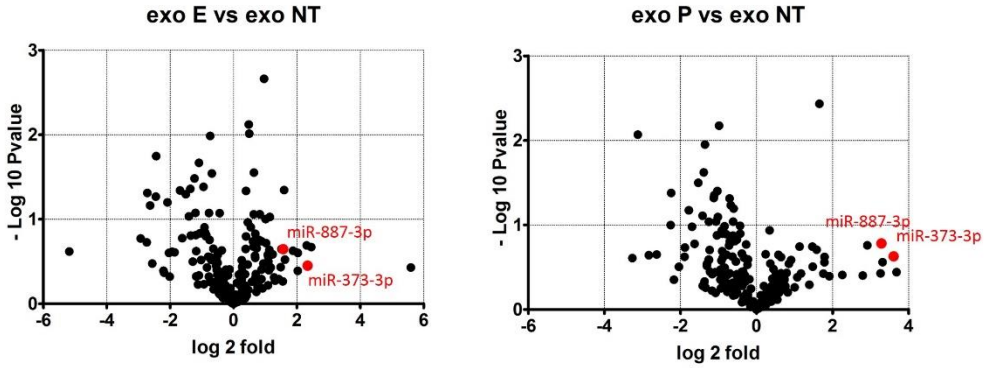

Figure R 26. ***The miRNA profile of exosomes from HUVECs treated with chemotherapy drugs is different than exosomes from untreated cells****. Volcano plot representing the level of secretion of miRNAs in exosomes from epirubicin-treated (E) and paclitaxel-treated (P) cells compared to untreated (NT). Results are normalized by the total mean of all the Ct.Results from one profiling experiment by qRT-PCR (n = 2 cellular samples per condition; n = 3 exosomal samples per condition).*

Our hypothesis is that the miRNAs specifically enriched in exosomes after treatment with epirubicin and paclitaxel could be implicated in the response of the endothelium to chemotherapy, and involved in the communication between the endothelial cells and the tumour cells. We then verified by qRT-PCR if the selected miRNAs were increased in exosomes from cells incubated with epirubicin or paclitaxel (**fig. R 27**).

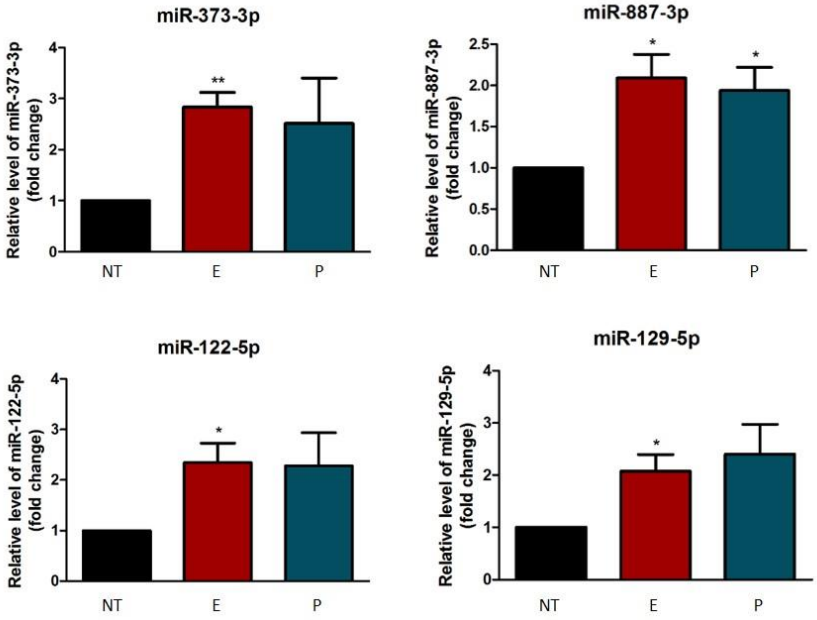

Figure R 27. ***Regulation of the miRNAs identified in the profile in exosomes produced by endothelial cells****. RNAs are extracted from exosomes produced by HUVECs incubated 2h with 1 µg/ml epirubicin (E), 20 ng/ml paclitaxel, or untreated (NT). The level of miR-373-3p, miR-887-3p, miR-122-5p and miR-129-5p in exosomes are expressed as fold change of their level in the untreated condition, 72h after the drug treatment. The values are normalized to the mean Ct of miR-23a-3p and miR-24-3p. Data are expressed as mean ± SD from five independent experiments (*, p<0.05; **, p<0.01).*

Curiously, we observed different results in cells analysed by qRT-PCR. We saw no change or a decrease in the expression of those four miRNAs in the endothelial cells after treatment with the drugs. This suggests that the miRNAs would not be loaded into exosomes via passive diffusion only (**fig. R 28**). Based on these observations, we decided to further study the role of these four miRNAs in tumour cells processes.

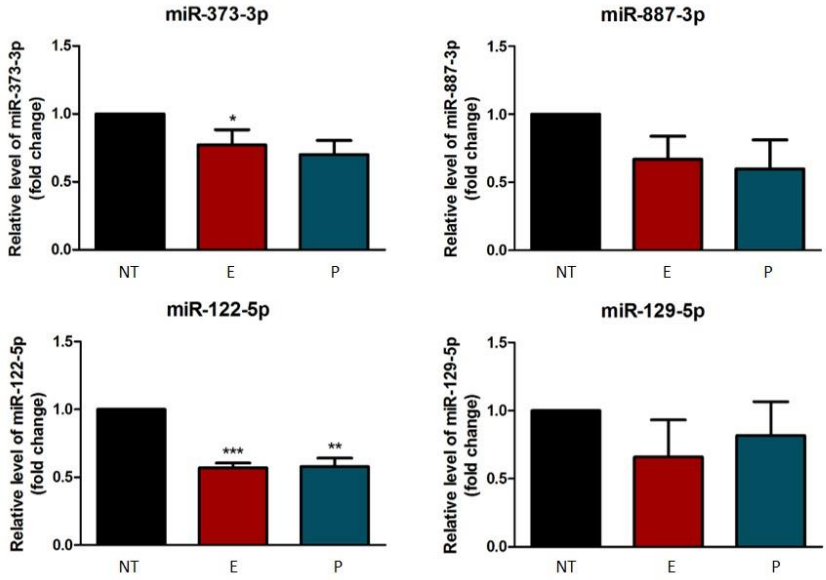

Figure R 28. ***miRNAs identified the profile of HUVEC treated with the drugs****. RNAs were extracted from HUVECs incubated 2h with 1 µg/ml epirubicin (E), 20 ng/ml paclitaxel, or untreated (NT), 48h after treatment. The level of expression of miR-373-3p, miR-887-3p, miR-122-5p and miR-129-5p are represented as fold change of their level in the untreated condition. The values are normalized to the mean Ct of RNU44 and RNU48. Data are expressed as mean ± SD from five independent experiments (*, p<0.05; **, p<0.01; ***, p<0.001).*

1.5 Functional effects of miR-373-3p, miR-887-3p, miR-122-5p and miR-129-5p overexpression in MDA-MB-231

We further studied the effects of miR-373-3p, miR-887-3p, miR-122-5p and miR-129-5p in breast cancer cells, to determine how exosomes carrying those miRNAs could affect the tumour functions. To determine their effects, we transiently overexpressed the miRNAs in MD-MB-231 by transfection with synthetic miRNAs designed to mimic endogenous mature miRNAs (**table S 14**). These transfected cells were then used to perform various functional assays. We analysed the capacity of the miRNAs to regulate cancer cells behaviour, and important functions such as proliferation, survival, migration, invasion or adhesion of the breast cancer cells. Results of BrdU incorporation showed that none of the four miRNAs influences proliferation (**fig. R 29A**). Survival assays with WST1 showed that miR-373-3p overexpression led to a very small increase of survival of MDA-MB-231 after

24h, but not anymore after 48h or 72h. After 72h, the overexpression of miR-122-5p and miR-129-5p resulted in a small decrease of survival of the breast cancer cells (**fig. R 29B**). It can be inferred that overexpressing either of the four miRNAs has only little effect on the MDA-MB-231 proliferation and survival.

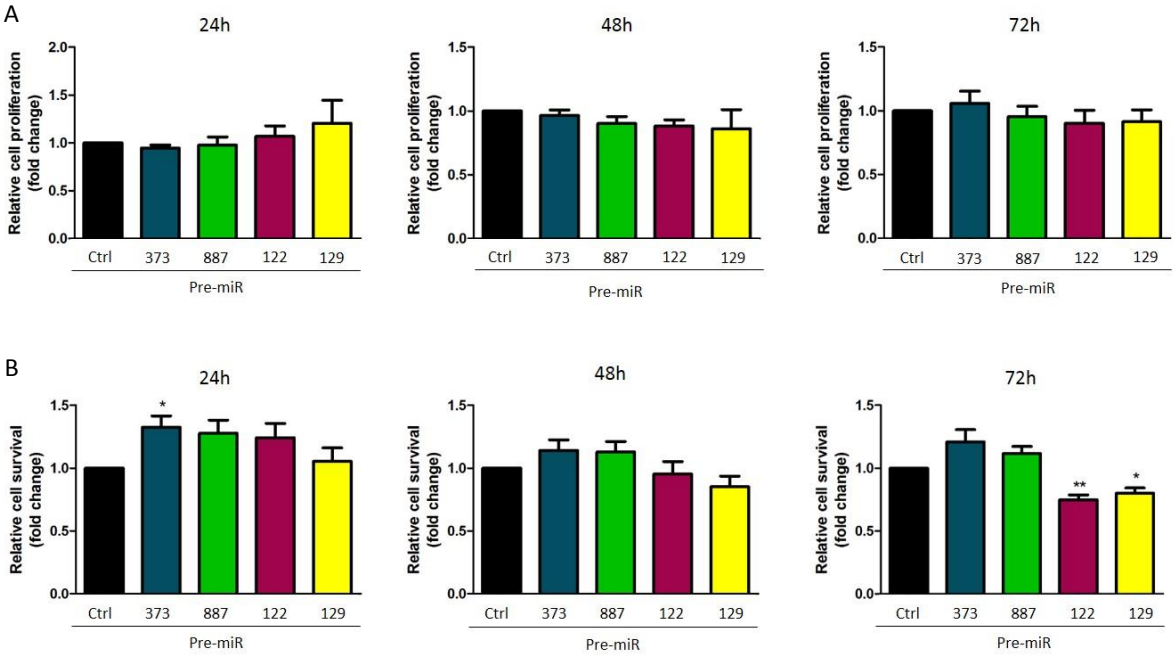

Figure R 29. ***MiR-373-3p, miR-887-3p, miR-122-5p and miR-129-5p overexpression has no effect on proliferation, and very few effect on breast cancer cells survival.*** *MDA-MB-231 were transfected with 25 nM of pre-miR-373-3p, pre-miR-887-3p, pre-miR-122-5p or pre-miR-129-5p, and the control. (A) The proliferation was assessed by the measure of the incorporation of BrdU during 4h. (B) Analysis of the survival capacity of the cells. The reagent substrate WST1 was added to the cells and the absorbance of the product was measured after 1h. The pre-miR control consists of a random nucleotide sequence with no effect on any known mRNA expression. Data are expressed as mean ± SD from at least three independent experiments (*, p<0.05; **, p<0.01).*

The potential of the miRNAs to modulate cell migration and invasion was assessed in Boyden Chamber and Spheroids assays. Migration results of miR-887-3p and miR-129-5p showed a tendency to increase the migratory capacity of the breast cancer cells (**fig. R 30A-B**). The overexpression of miR-373-3p induced a decrease in the invasive potential of the MDA-MB-231, as showed in the 3D culture model of spheroids (**fig. R 30E-F**). MiR-373-3p also increased the adhesion ability of those cells on a fibronectin matrix (**fig. R 30G**). In the long term, the transient overexpression of miR-373-3p or miR-129-5p led to an increase in the number of colonies of MDA-MB-231 formed on the plastic surface (**fig. R 30C-D**). Out of the four miRNAs, miR-373-3p appeared to regulate cancer cells the most, by decreasing invasion and increasing adhesion and the formation of colonies.

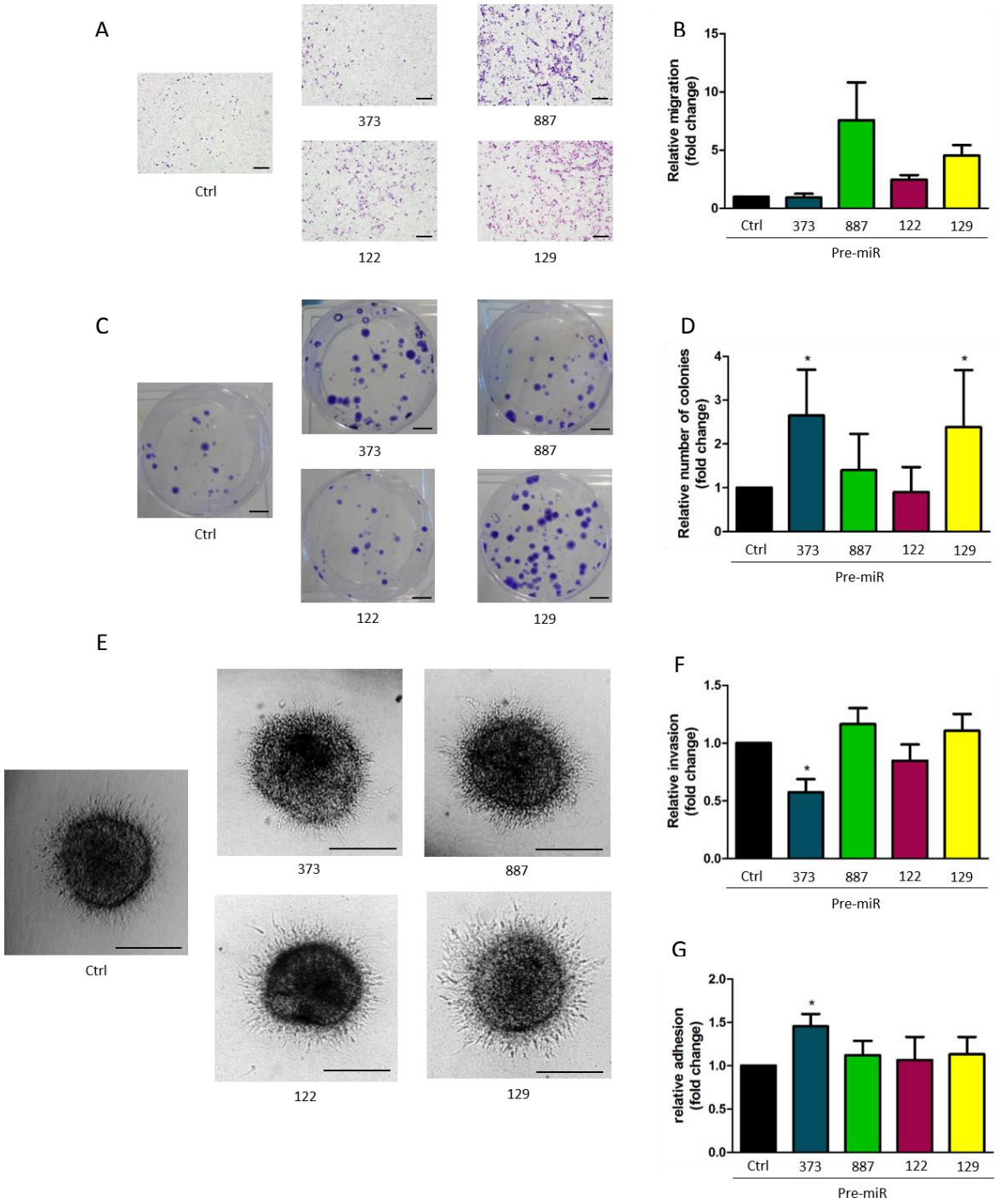

Figure R 30. ***Regulation of tumour cells migration, invasion, adhesion and capacity to form colonies by miR-373-3p, miR-887-3p, miR-122-5p and miR-129-5p****. MDA-MB-231 were transfected with 25 nM of pre-miR-373-3p, pre-miR-887-3p, pre-miR-122-5p or pre-miR-129-5p, and the control. (A) After transfection, cells were seeded in Boyden chambers and allowed to migrate for 16h. The cells were then fixed and the membrane removed and stained with Giemsa. Scale bar = 200 µm. (B) The migrating cells were counted and reported on a graph. (C) Colony forming assay. Transfected MDA-MB-231 were seeded in 6 wells plate and incubated for 12 days. After staining, the number of colonies were counted Scale bar = 5mm. (D) Relative number of colonies. (E) 3D spheroid invasion assay. Transfected MDA-MB-231 were seeded in collagen to form spheroid. Picture taken after 24h of incubation, scale bar = 200 µm. (F) Relative invasion, calculated with the formula (area of sprout-central area)/central area. (G) Adhesion on a fibronectin matrix. After transfection, the tumour cells were seeded on fibronectin (20 ng/ml). The cells were washed after 1h and the adherent cells stained and measured by absorbance. The pre-miR control consists of a random nucleotide sequence with no effect on any known mRNA expression. Data are expressed as mean ± SD from at least three independent experiments, and compared to the control (Ctrl) (*, p<0.05).*

1.6 Identification of miR-373-3p targets in MDA-MB-231

Based on our functional results and on the literature, we decided to deepen our understanding of miR-373-3p action in MDA-MB-231 cells. For that purpose, we performed a Deep-RNA Sequencing on MDA-MB-231 either transfected with the pre-miR-control or with the pre-miR-373-3p. This method allows to determine which mRNAs are affected by the overexpression of the miRNA, and to extrapolate the pathways involved in the cellular response. The overexpression of miR-373-3p led to a clear separation of the samples by principal component analysis (**fig. R 31A**). Of the 13,823 RNAs identified by the sequencing, 652 were found to be differentially regulated between the two conditions, with a fold change ± 2 the level of the control samples and with a q-value inferior to 0.05 (**fig. R 31B**).

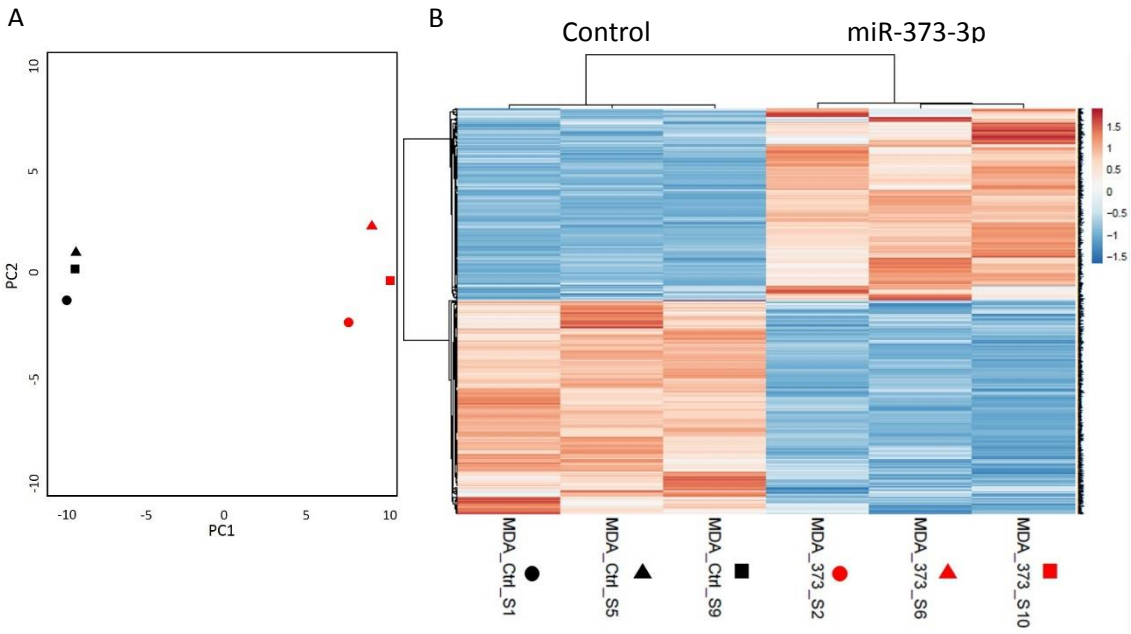

Figure R 31. ***The overexpression of miR-373-3p in MDA-MB-231 cells led to a clear discrimination of the samples based on the level of expression of the mRNAs****. MDA-MB-231 were transfected with 25 nM of either pre-miR-Control or pre-miR-373-3p. 48h later, the cells were harvested and the RNAs was extracted to produce TruSeq mRNA libraries, which were then sequenced. (A) Principal Component Analysis. Distribution of the samples, in triplicates. Each colour represents a condition (black, MDA-MB-231 transfected with the pre-miR-control; red, MDA-MB-231 transfected with the pre-miR-373-3p), each symbol represents a biological replicate. (B) Heat map representation of differentially regulated mRNAs by overexpression of miR-373-3p in each sample. Only the mRNAs differentially expressed with a fold change of ± 2 and a q-value < 0.05 are shown on the map.*

Among these 652 mRNAs differentially regulated, 308 were upregulated and 344 were downregulated (**fig. R 32**).

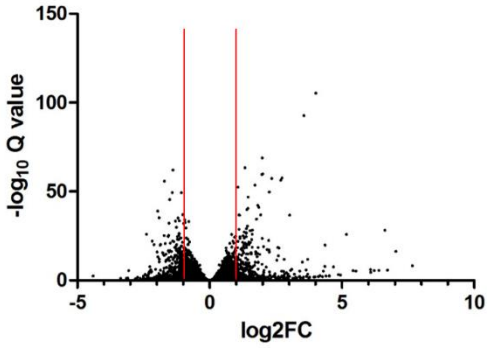

Figure R 32. ***The mRNA profile of MDA-MB-231 overexpressing miR-373-3p is different from the control.*** *Volcano plot representing the level expression of mRNAs in MDA-MB-231 48h after transfecting the cells with pre-miR-373-3p, compared to MDA-MB-231 transfected with a pre-miR control. Dots outside the red bars represent mRNA with a fold change lower than twice (left) or superior to twice (right) their level of expression in the control samples. Results from one RNA sequencing experiment with each condition in triplicate. Log2FC, log2 of the fold change.*

1.6.1 GSEA and pathways

We then selected the mRNAs differentially regulated with a q-value inferior to 0.05 and used them as input for the software GSEA. GSEA is a program which provides a list of regulated pathways based on a pre-ranked list of differentially expressed genes. It then uses this database to compare the genes to a group of genes associated to specific pathways.

A

Hallmark	NES	FDR q-val
MYC targets V1	4.709	0
MTORC1 signalling	3.093	0
Oxidative Phosphorylation	2.875	0
MYC targets V2	2.604	2.50E-04
E2F targets	2.521	5.22E-04
Unfolded protein response	2.382	0.00347333
DNA repair	2.244	0.00568277
Epithelial mesenchymal transition	2.149	0.00694739
KRAS signalling DN	2.077	0.0095004
UV response UP	2.037	0.01140466
Glycolysis	1.915	0.02283976
Myogenesis	1.776	0.04270349

B

Hallmark	NES	FDR q-val
TNFA signalling via NFkB	-3.018	0
KRAS signalling UP	-2.711	3.28E-04
Interferon gamma response	-2.169	0.01200139
Interferon alpha response	-2.092	0.01364591

C

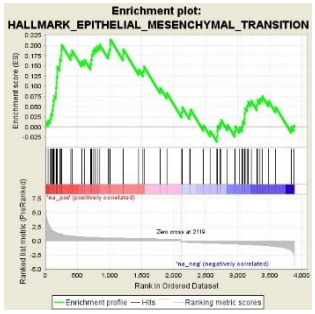

Figure R 33. ***GSEA analysis of the pathways regulated by the overexpression of miR-373-3p, with an enrichment of members of the EMT pathway****. Pathway with a FDR q-value < 0.05 are showed (A) Pathways significantly upregulated by miR-373-3p in MDA-MB-231 cells. (B) Pathways significantly downregulated by miR-373-3p in MDA-MB-231. NES, normalized enrichment score; FDR, False Discovery Rate. (C) Enrichment plot of the EMT pathway.*

Interestingly, some of the most upregulated pathways in cells overexpressing miR-373-3p

were pathways related to survival, DNA repair and stress response mechanisms (**fig. R 33**). Among those, the epithelial-mesenchymal transition (EMT) pathway was found to be of particular interest regarding the results from the functional assays. EMT is the transition from an epithelial, well-differentiated phenotype, towards a mesenchymal, less differentiated pro-migratory phenotype, which is related to tumour aggressiveness and circulating tumour cells. Indeed, the results showed that miR-373-3p regulated the invasion and adhesion properties of the MDA-MB-231, which are related to EMT.

1.6.2 MiR-373-3p targets regulation

We decided to look further into the EMT pathways by looking at the regulation of important factors by miR-373-3p. By qRT-PCR, we analysed the regulation of two important transcription factors implicated in EMT, SLUG and ZEB1 (**fig. R 34**). These two proteins support EMT by promoting the transcription of genes of mesenchymal phenotypes, such as the glycoprotein CD44. Interestingly, the level of SLUG, ZEB1 and CD44 are strongly decreased, corresponding to a diminution of EMT. The implications of these results need to be further investigated. Interestingly, CD44 is a direct target of miR-373-3p (Huang et al. 2008). It would be very interesting to look at the level of other proteins downstream the transcription factors to assess their level of expression and activity.

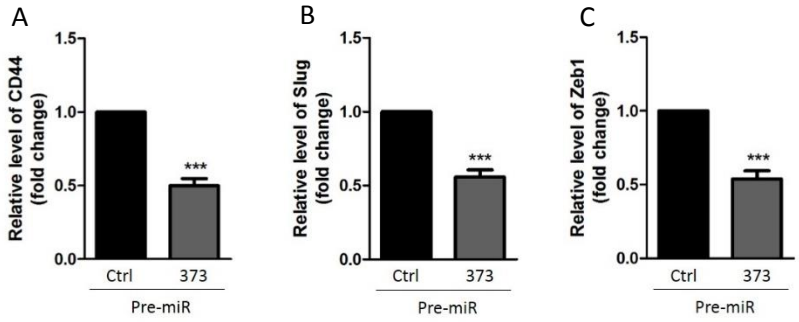

Figure R 34. ***MiR-373-3p inhibits the expression of CD44, SLUG and ZEB1 in breast cancer cells****. qRT-PCR analysis of the expression of CD44 (A), SLUG (B) and ZEB1 (C) from RNA extracted from MDA-MB-231 cells transfected with 25 nM of pre-miR-373-3p or the control. Results are normalized to the expression of TBP and GAPDH. In collaboration with Dr. Ch Gilles. Data are expressed as mean ± SD from four independent experiments (***, p<0.001).*

In order to further understand how miR-373-3p was affecting the cells, we used the *String* algorithm to look at the interactions between the 652 regulated mRNAs. *String* allows the creation of interaction webs by linking together proteins, based on their physical and functional interactions. The algorithm identified only 505 proteins out of the 652. As can be seen in **figures R 35A** and **35B**, lots of interactions are concentrated around proteins implicated in signalling, or transcription factors. The algorithm *Targetscan*, which gives a

list of predicted targets for a given miRNA, identified 51 direct targets of miR-373-3p among the 652 (**table S 15**). It helped us select 2 genes, RELA and TGFβR2. Those two genes are predicted direct targets of miR-373-3p and could potentially explain the effects previously observed in MDA-MB-231. As shown in **table R 2**, both targets are indeed regulated in the RNA seq results. We confirmed that the level of TGFβR2 and RelA are decreased in MDA-MB-231 after overexpressing miR-373-3p by qRT-PCR and Western blotting (**fig. R 36**). By its role in the signal transduction of the TGFβ growth factor, TGFβR2 is implicated in pathways related to metastasis, migration and invasion (Massagué 2008). The RELA transcription factor, also known as NFκB p65 subunit, is a very important regulator of cell metabolism. It also plays a crucial role in tumour development by regulating genes implicated in tumour growth, invasion and metastasis (Pires et al. 2017; Hoesel & Schmid 2013). Their regulation by miR-373-3p can have multiple implications for the cellular functions.

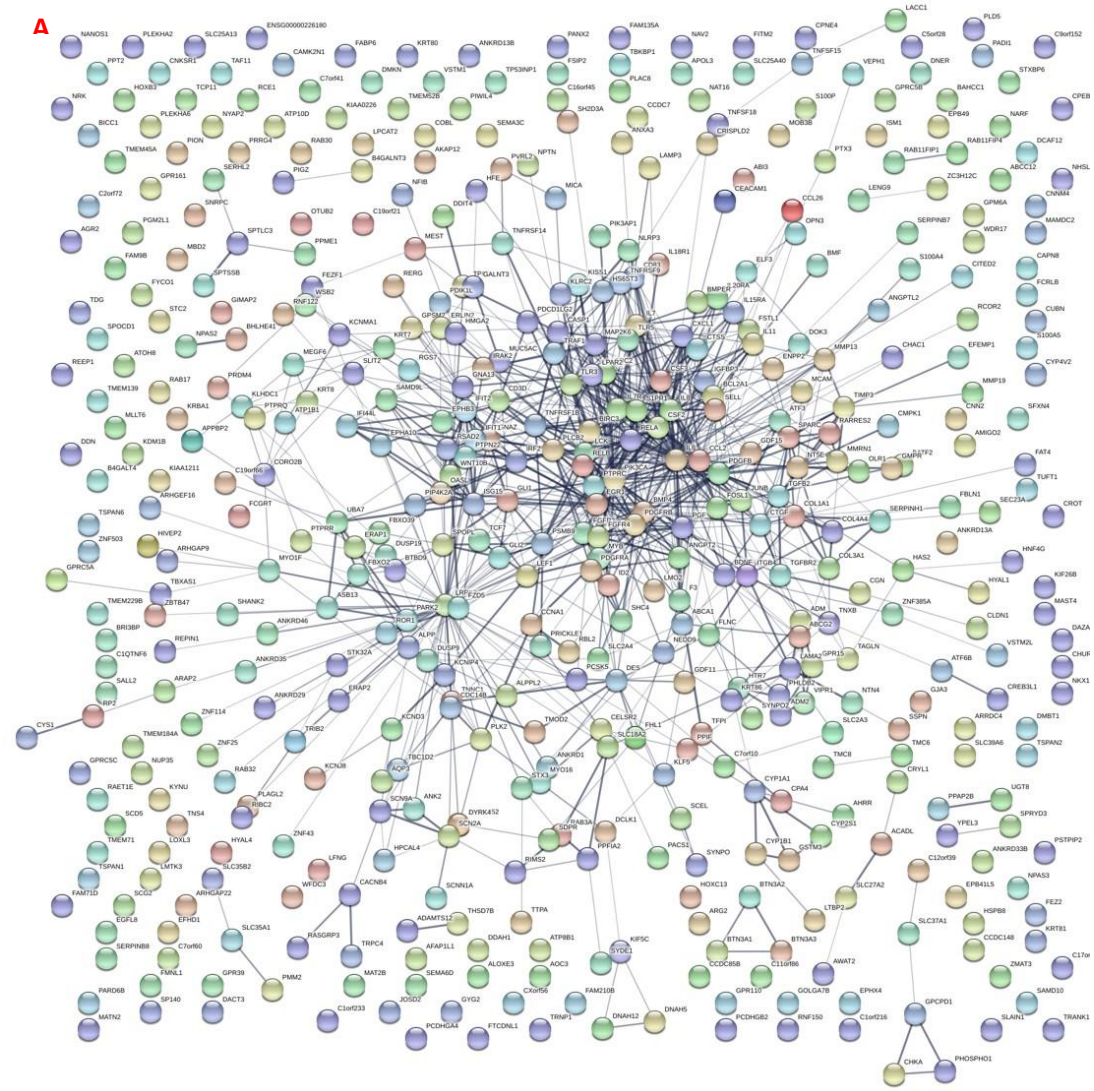

Figure 35. ***Analysis of the interactions between the 652 proteins potentially regulated by miR-373-3p****. (A) The 652 direct or indirect targets of miR-373 -3p are loaded into the algorithm. String recognized only 505 of them. (B) Zoom to the core of the interaction web. In a red circle, RELA and TFGBR2, two direct targets of miR-373-3p.*

Gene	Fold change	Q value
TFGβR2	0.27	6.67E-36
RELA	0.47	1.57E-24

Table R 2. ***Differential expression of mRNAs after overexpression of miR-373-3p in MDA-MB-231 cells, by RNA sequencing analysis****. Expressed in fold change of the expression level in the control.*

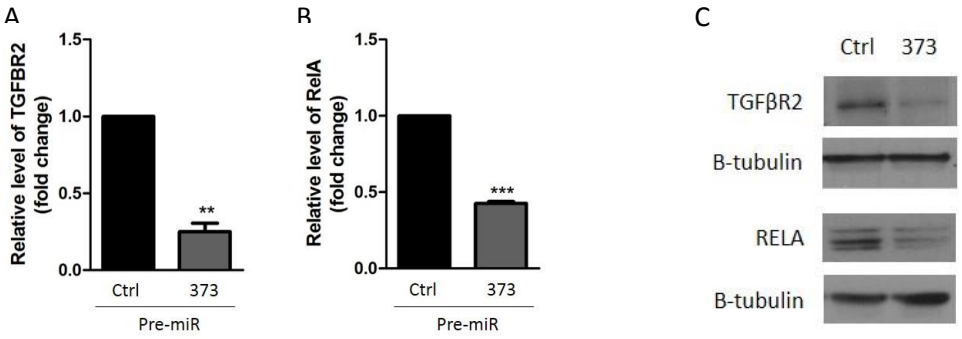

Figure R 36. ***MiR-373-3p inhibits the expression of TGFBR2 and RELA in breast cancer cells****. qRT-PCR analysis of the expression of TGFBR2 (A) and RELA (B) from RNA extracted from MDA-MB-231 cells transfected with 25 nM of pre-miR-373-3p or the control. (C) Decrease in protein level of TGFβR2 and RELA 72h after overexpressing miR-373-3p, analysed by Western Blotting. qRT-PCR results are normalized to the expression of PPIA and B2M. Data are expressed as mean ± SD from three independent experiments (**, p<0.01; ***, p<0.001).*

1.7 The exosomes influence the level of expression of TGFβR2 and RELA (preliminary results)

We then wanted to determine if exosomes from treated-HUVECs could impact MDA-MB-231 with the transfer of miR-373-3p. We added two different concentrations of exosomes on MDA-MB-231 in culture plates, and analysed the level of miR-373 and the expression level of TGFβR2 and RELA (**fig. R 37**) in the breast cancer cells. We observed that the level of miR-373-3p in MDA-MB-231 was higher in cells incubated with exosomes from epirubicin- or paclitaxel-treated HUVECs, compared to exosomes from untreated HUVECs. Curiously, the relative level of miR-373-3p increased less in cells treated with 50 µg/ml of exosomes than with 20 µg/ml. Since the level of miR-373-3p is increased in exosomes from drug-treated cells, this suggests that the miRNA can indeed be transferred from the exosomes to the breast cancer cells. Moreover, we looked at the level of expression of TGFβR2 and RELA, two targets of miR-373-3p, in the MDA-MB-231 after incubation with the exosomes. We saw that the incubation with exosomes from drug-treated HUVECs induced a decrease of their expression level, in a dose-dependent manner (**fig. R 37B-C**). Those results corroborate the hypothesis of a transfer of miRNA content from exosomes to cells. However, the experiment still needs to be repeated.

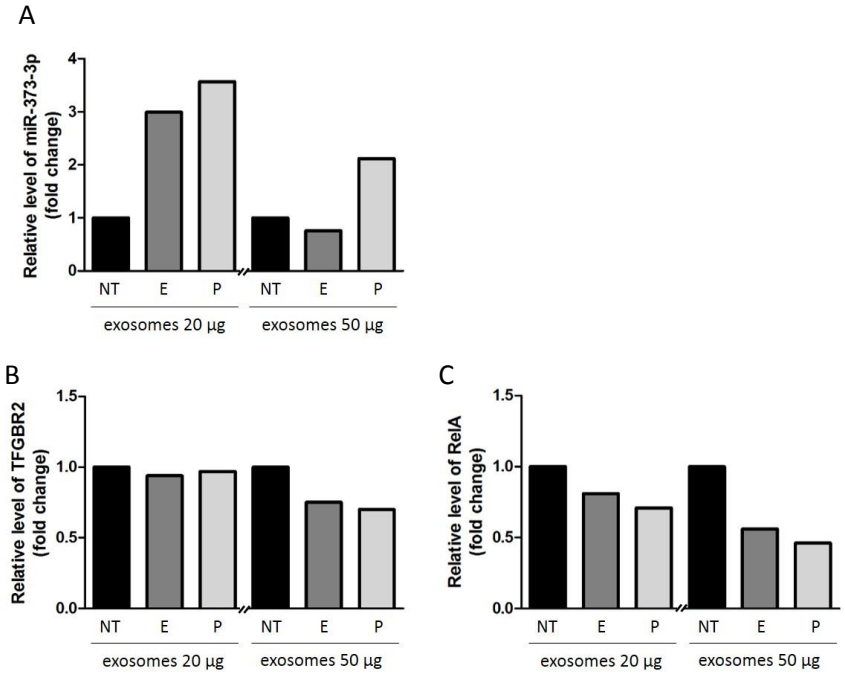

Figure R 37. ***Exosomes from drug-treated HUVECs induce the modulation of miR-373-3p, TGFβR2 and RELA in breast cancer cells****. Exosomes were purified from HUVECs untreated (NT), incubated 2h with 1 µg/ml epirubicin (E) or 20 ng/ml paclitaxel (P). 20 µg/ml or 50 µg/ml of exosomes were added to MDA-MB-231 in culture plates. After 16h, the RNA was extracted and the level of miR-373-3p (A), TGFβR2 (B) and RELA (C) were analysed by qRT-PCR. Result from one experiment, expressed as mean, relative to the NT condition.*

II. miR-373-3p in resistant cells

During the course of a chemotherapy treatment, cancer cells may acquire a resistance to the drugs. In this part of the work, we wondered whether the miRNA identified in the response to chemotherapeutic drug treatments in exosomes would be effective in cells with acquired resistance. To assess that, we obtained MDA-MB-231 resistant to epirubicin or paclitaxel, graciously provided by Dr Sharon Gorski (Genome Science Centre, Canada) and Dr Melanie Spears (Ontario Institute for Cancer Research, Canada) (**fig. R 38**). Polyclonal MDA-MB-231 resistant to epirubicin (MDA-MB-231/epi) were generated by growing in increasing concentrations of epirubicin (up to 100 nM) for one year (Chittaranjan et al. 2014). Polyclonal MDA-MB-231 resistant to paclitaxel (MDA-MB-231/pacli) were generated by growing in increasing concentration of paclitaxel (up to 25 nM) until a stable taxane resistant phenotype was acquired (Kenicer et al. 2014).

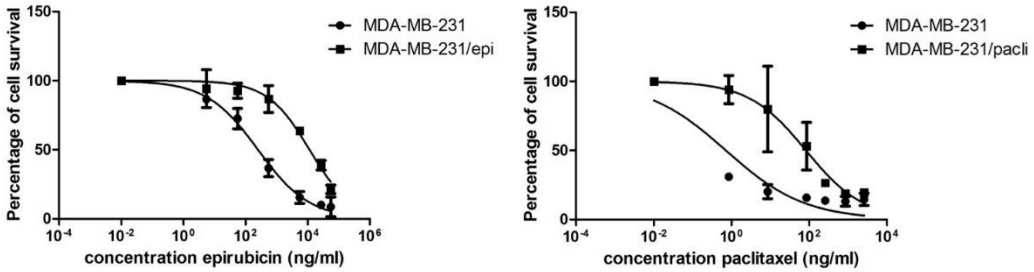

Figure R 38. ***Difference in sensibility to epirubicin or paclitaxel between MDA-MB-231 and MDA-MB-231 resistant to either epirubicin (MDA-MB-231/epi) or paclitaxel (MDA-MB-231/pacli)****. Cells were incubated with various concentration of the respective drugs for 48h, then their viability was assessed by measure of the absorbance after adding WST1. The IC50 relative to epirubicin exposure shifts from 252.2 ng/ml (560 nM) for sensitive MDA-MB-231 to 11 415 ng/ml (21 000 nM) in the resistant ones. The IC50 relative to paclitaxel exposure shifts from 0.71 ng/ml (0.8 nM) in sensitive MDA-MB-231 to 82.6 ng/ml (97 nM) in paclitaxel-resistant MDA-MB-231. Data expressed as mean ± SD from three (epirubicin) or two (paclitaxel) independent experiments.*

2.1 Functional effects of miR-373-3p, miR-887-3p, miR-122-5p and miR-129-5p overexpression in MDA-MB-231 resistant to epirubicin or paclitaxel

We wanted to determine if the four miRNAs previously identified in the exosomes from treated HUVECs (miR-373-3p, miR-887-3p, miR-122-5p and miR-129-5p) were able to induce similar effects in MDA-MB-231 resistant to either epirubicin or paclitaxel as in sensitive MDA-MB-231. As shown in **figures R 39A** and **R 40A**, the overexpression of the four miRNAs in breast cancer epirubicin-resistant cells did not much affect the proliferation and survival of the cells. Similar effects were observed in paclitaxel-resistant cells (**fig. R 39B** and **R 40B**). After 72h, the survival of the cells appeared to slightly decrease following

the overexpression of miR-122-5p and miR-129-5p, which was also observed in sensitive MDA-MB-231.

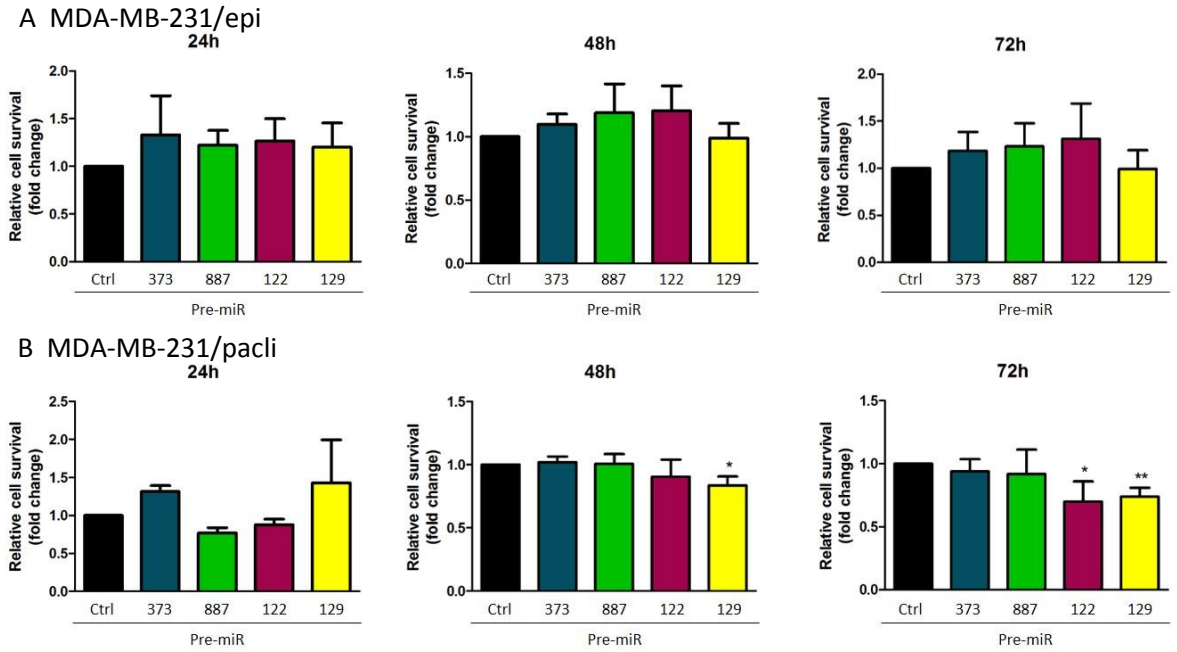

Figure R 39. ***MiR-373-3p, miR-887-3p, miR-122-5p and miR-129-5p overexpression has very few effect on survival of breast cancer cells resistant to epirubicin or paclitaxel****. MDA-MB-231/epi (A) or MDA-MB-231/pacli (B) were transfected with 25 nM of pre-miR-373-3p, pre-miR-887-3p, pre-miR-122-5p or pre-miR-129-5p, and the control. The reagent substrate WST1 was added to the cells and the absorbance of the product was measured after 1h. The pre-miR control consists of a random nucleotide sequence with no effect on any known mRNA expression. Data are expressed as mean ± SD from three independent experiments, and compared to the control (Ctrl) (*, p<0.05; **, p<0.01).*

In the epirubicin-resistant cells, miR-373-3p and miR-129-5p tended to decrease the migration, and miR-887-3p had no effect (**fig. R 41 A-B**). The overexpression of the miRNAs had no effect on the resistant cells invasion in the 3D spheroid assay (**fig. R 41E-F**). Likewise, none of the miRNA modified the capacity of the resistant cells to adhere to the fibronectin matrix (**fig. R 41G**). In the colony forming assay, both miR-373-3p and miR-129-5p lost their capacity to increase the number of colonies of MDA-MB-231/epi (**fig. R 41C-D**). Unfortunately, we were unable to repeat the assay more than once with paclitaxel-resistant cells, since the cells did not adhere well to the wells. In the migration assay, the paclitaxel-resistant cells showed the same tendency to as the sensitive one towards an increased migration when miR-887-3p and miR-129-5p were overexpressed (**fig. R 42A-B**). Overall, the overexpression of the miRNAs on resistant cells follows a tendency similar in sensitive MDA-MB-231, but the amplitude of these responses appears narrower. The resistant cells thus appear to be less able to respond to the miRNAs.

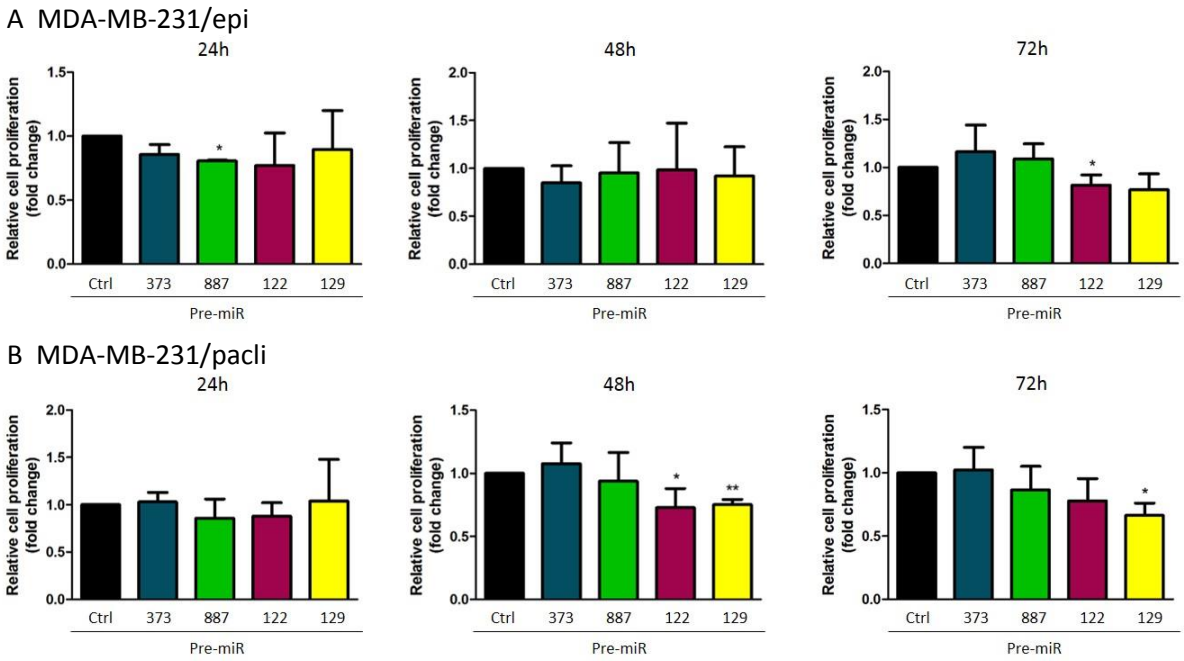

Figure 40. ***MiR-373-3p, miR-887-3p, miR-122-5p and miR-129-5p overexpression has almost no effect on proliferation of breast cancer cells resistant to epirubicin or paclitaxel****. MDA-MB-231/epi (A) or MDA-MB-231/pacli (B) were transfected with 25 nM of pre-miR-373-3p, pre-miR-887-3p, pre-miR-122-5p or pre-miR-129-5p, and the control. The proliferation was assessed by the measure of the incorporation of BrdU during 4h. The pre-miR control consists of a random nucleotide sequence with no effect on any known mRNA expression. Data are expressed as mean ± SD from three independent experiments, and compared to the control (Ctrl) (*, p<0.05; **, p<0.01).*

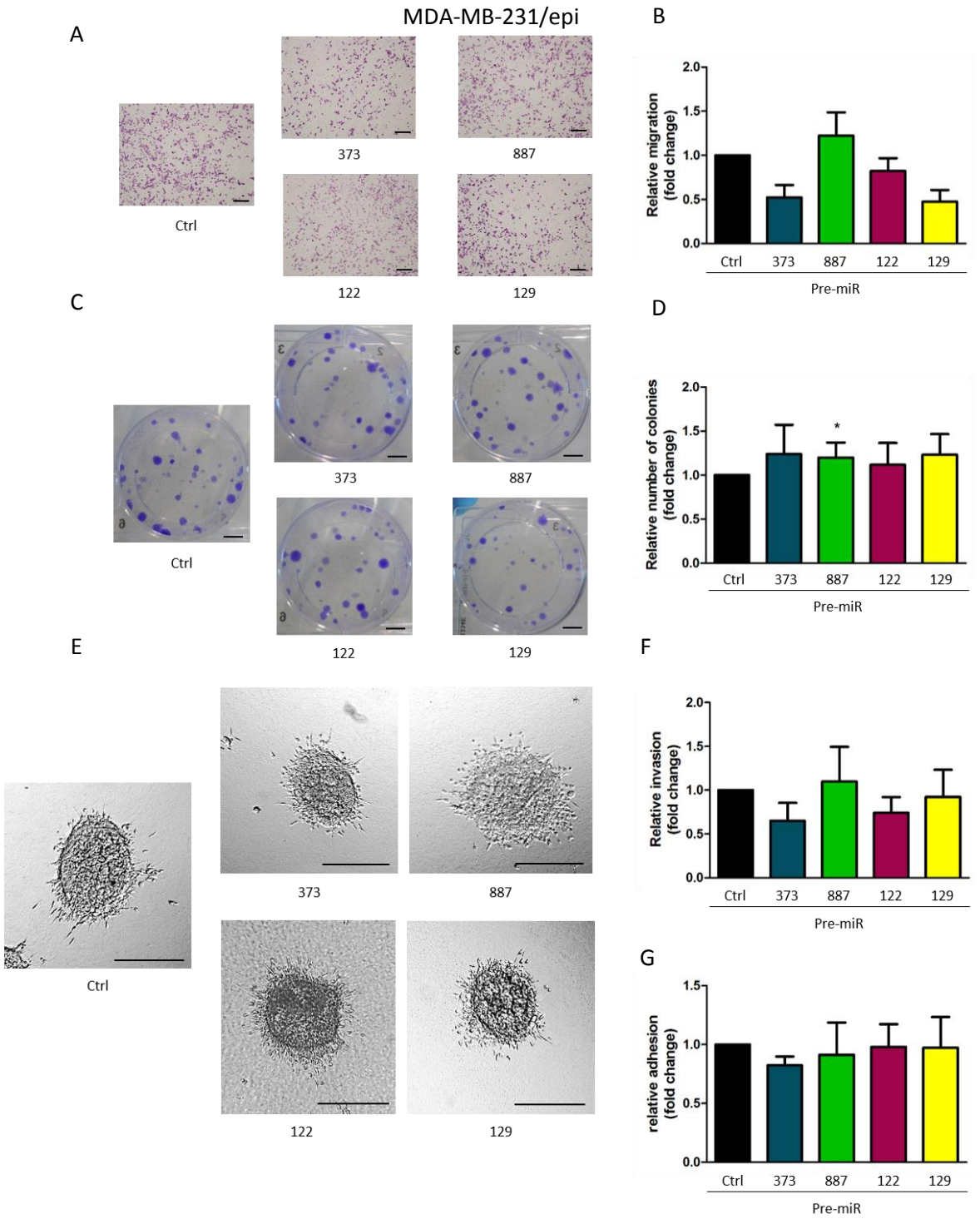

Figure R 41. ***Regulation of tumour cells migration, invasion, adhesion and capacity to form colonies by miR-373-3p, miR-887-3p, miR-122-5p and miR-129-5p.*** *MDA-MB-231/epi were transfected with 25 nM of pre-miR-373-3p, pre-miR-887-3p, pre-miR-122-5p or pre-miR-129-5p, and the control. (A) After transfection, cells were seeded in Boyden chambers and allowed to migrate for 16h. The cells were then fixed and the membrane removed and stained with Giemsa. Scale bar = 200 µm. (B) The migrating cells were counted and reported on a graph. (C) Colony forming assay. Transfected MDA/epi were seeded in 6 wells plate and incubated for 21 days. After staining, the number of colonies were counted Scale bar = 5mm. (D) Relative number of colonies. (E) 3D spheroid invasion assay. Transfected MDA/epi were seeded in collagen to form spheroid. Picture taken after 24h of incubation, scale bar = 200 µm. (F) Relative invasion, calculated with the formula (area of sprout-central area)/central area. (G) Adhesion on a fibronectin matrix. After transfection, the tumour cells were seeded on fibronectin (20 ng/ml). The cells were washed after 1h and the adherent cells stained and measured by absorbance. The pre-miR control consists of a random nucleotide sequence with no effect on any known mRNA expression. Data are expressed as mean ± SD from at least three independent experiments, and compared to the control (Ctrl) (*, p<0.05).*

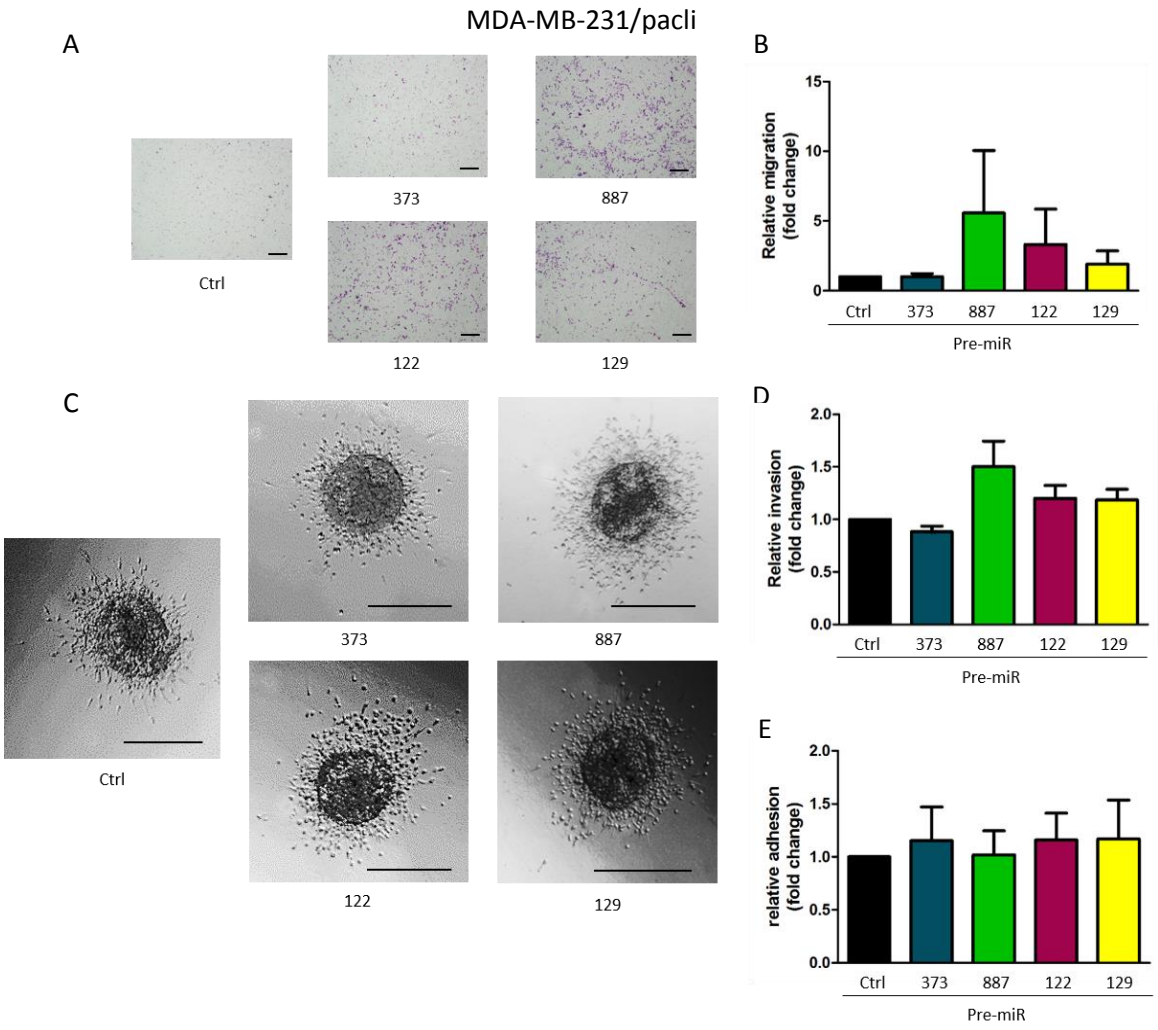

Figure R 42. ***Regulation of tumour cells migration, invasion and adhesion by miR-373-3p, miR-887-3p, miR-122-5p and miR-129-5p****. MDA-MB-231/pacli were transfected with 25 nM of pre-miR-373-3p, pre-miR-887-3p, pre-miR-122-5p or pre-miR-129-5p, and the control. (A) After transfection, cells were seeded in Boyden chambers and allowed to migrate for 16h. The cells were then fixed and the membrane removed and stained with Giemsa. Scale bar = 200 µm. (B) The migrating cells were counted and reported on a graph. (C) 3D spheroid invasion assay. Transfected MDA/pacli were seeded in collagen to form spheroid. Picture taken after 24h of incubation, scale bar = 200 µm. (D) Relative invasion, calculated with the formula (area of sprout-central area)/central area. (E) Adhesion on a fibronectin matrix. After transfection, the tumour cells were seeded on fibronectin (20 ng/ml). The cells were washed after 1h and the adherent cells stained and measured by absorbance. The pre-miR control consists of a random nucleotide sequence with no effect on any known mRNA expression. Data are expressed as mean ± SD from at least three independent experiments, and compared to the control (Ctrl).*

2.2 Analysis of the targets of miR-373-3p in MDA-MB-231 resistant to epirubicin

We wanted to understand if the resistant MDA-MB-231 were less responsive to the miRNA, or if the miRNAs had other targets and regulated the cells in a different way than the sensitive cells. For that, we performed a Deep RNA sequencing analysis on MDA-MB-231/epi transfected with a pre-miR control or a pre-miR-373-3p, submitted to the same conditions as the sensitive MDA-MB-231. The Principal Component Analysis (PCA) showed that the major differences between the samples were, first, between the breast cancer cells resistant or not to epirubicin, and second, between the cells overexpressing of miR-373-3p and the controls (**fig. R 43A**). The separation between the miRNA overexpression condition and the control is still present, but the difference between the two conditions is much smaller than in sensitive MDA-MB-231. Strikingly, only 95 of all the mRNAs identified in the sequencing were significantly up or downregulated when the miR-373-3p was overexpressed in cells, and three showed a fold change superior to ± 2 compared to the control (**fig. R 43B**).

A

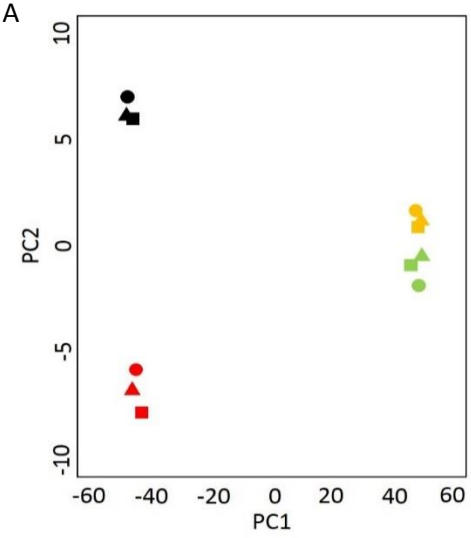

B

Gene	Fold change	Q value
SLC7A7	3.30	1.31E-05
DUSP9	2.27	1.01E-06
STEAP2	0.43	0.0464

Figure R 43. ***Discrimination of the RNA seq samples.*** *MDA-MB-231 and MDA-MB-231/epi were transfected with 25 nM of either pre-miR Control or pre-miR-373-3p. 48h later, the cells were harvested and the RNA was extracted to produce TruSeq mRNA libraries, which were then sequenced. (A) Principal component analysis of all the samples sequenced. Each colour represent a condition (black, MDA-MB-231 transfected with the pre-miR-control; red, MDA-MB-231 transfected with the pre-miR-373-3p; yellow, MDA-MB-231/epi transfected with the pre-miR-control; green, MDA-MB-231/epi transfected with the pre-miR-373-3p), and each symbol represents a biological replicate. Each condition in triplicate. (B) Three RNAs are regulated with a fold change ± 2 and a q value < 0.05 by miR-373-3p in MDA-MB-231/epi. Expressed in fold change of the expression level in the control.*

It can be seen on the volcano plot that almost all the dots representing the RNAs are confined within the red lines delimiting the ± 2 fold change (**fig. R 44**). Based on the mRNA sequencing profile, we assumed that the resistant breast cancer cells were less responsive to miR-373-3p than the sensitive ones.

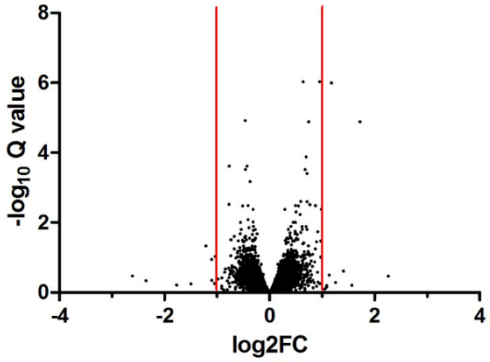

Figure R 44. ***RNA profile of MDA-MB-231/epi overexpressing miR-373-3p.*** *Volcano plot representing the level expression of mRNAs in MDA-MB-231/epi 48h after transfecting the cells with pre-miR-373-3p, compared to MDA-MB-231/epi transfected with a pre-miR control. Dots outside the red bars represent mRNAs with a fold change lower than twice (left) or superior to twice (right) their level of expression in the control samples. Results from one RNA sequencing experiment with each condition in triplicate. Log2FC, log2 of the fold change.*

2.2.1 MiR-373-3p targets and pathway regulation in MDA resistant to epirubicin

Since we had confirmed that TGFβR2 and RELA were important targets of miR-373-3p in sensitive MDA-MB-231, we checked if they were regulated in resistant cells as well. According to the sequencing data, TGFβR2 was still downregulated by miR-373-3p in resistant cells, but the effect on RELA was weaker (**table R 3**).

Gene	Fold change	Q value
TFGβR2	0.59	0.0002
RELA	0.82	0.1584
CD44	0.85	0.0211
SLUG	0.95	0.8511
ZEB1	0.76	0.4058

Table R 3. ***Differential expression of mRNAs after overexpression of miR-373-3p in MDA-MB-231/epi, by RNA sequencing analysis****. Expressed in fold change of the expression level in the control.*

Those results were confirmed by qRT-PCR(**fig. R 45A-B**). In view of the importance of the NFκB factors in tumour development, the loss of regulation by miR-373-3p could partly explain the weaker responses from the resistant breast cancer cells. Moreover, the

level of CD44, SLUG and ZEB1 were investigated as well. In the sequencing experiment, the level of all three mRNAs were very slightly decreased (**table R 3**). After confirmation by qRT-PCR, there was no difference in the level of CD44 and SLUG, and ZEB1 was indeed slightly decreased (**fig. R 45C-E**). The effects of the overexpression of miR-373-3p are strongly reduced in MDA-MB-231 resistant to epirubicin, which is in accordance with our previous observations.

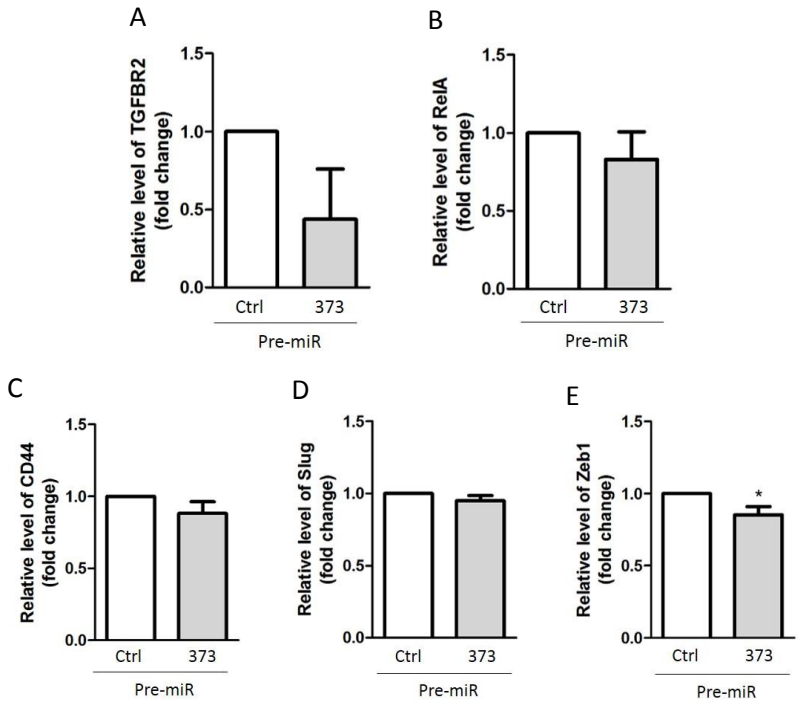

Figure R 45. ***MiR-373-3p loses its effects on the expression of TGFBR2, RelA, CD44 and Slug in breast cancer cells resistant to epirubicin****. qRT-PCR analysis of the expression of TGFBR2 (A), RELA (B), CD44 (C), SLUG (D) and ZEB1 (E) from RNA extracted from MDA-MB-231/epi cells transfected with 25 nM of pre-miR-373-3p or the control. Results are normalized to the expression of PPIA and B2M for TGFβR2 and RELA, and TBP and GAPDH for CD44, SLUG and ZEB1. Data are expressed as mean ± SD from three (TGFβR2 and RELA) and four (CD44, SLUG and ZEB1) independent experiments (*, p<0.05).*

2.3 Comparison of MDA-MB-231 and MDA-MB-231 resistant to epirubicin

After analysing the results from the overexpression of miR-373-3p in MDA-MB-231 sensitive and resistant to epirubicin, we were intrigued by the fact that the resistant cells seemed to have lost their capacity to respond to the miRNA. Considering that the major discriminating factor between samples in our analysis was the resistance (**fig. R 43**), we sought to determine the differences explaining our results. We found 5830 mRNAs statistically (q-value<0.05) differentially regulated between the control sensitive MDA-MB-231 and the control resistant cells, with a fold change superior to 2. The heat map was generated using the 300 most upregulated and 300 most downregulated RNAs from the 5830

(**fig. R 46**). They appeared to be well discriminating between the two cell types. Among the differentially regulated pathways, according to GSEA, EMT is strongly upregulated. This is in accordance to the fact that resistant cells tend to reach a cancer stem cell phenotype, which is linked to EMT (Mani et al. 2008; Morel et al. 2008).

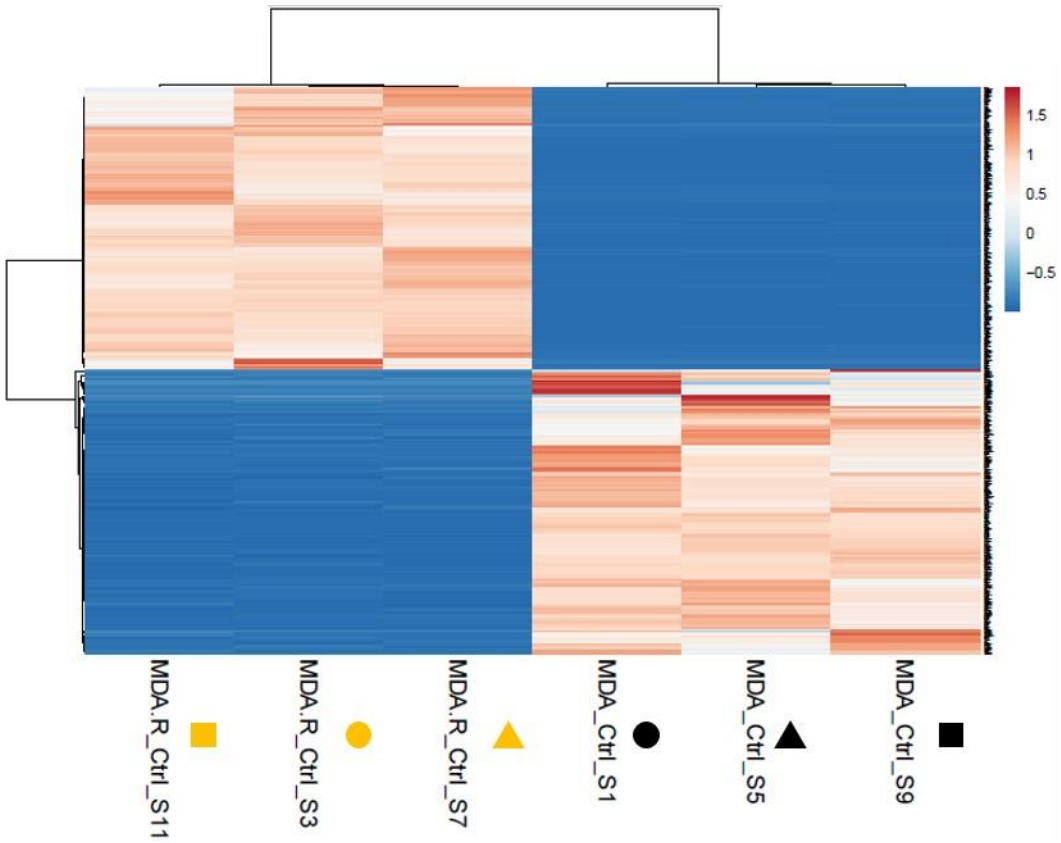

Figure R 46. ***Heat map representation of differentially regulated mRNAs by overexpression of miR-373-3p in MDA-MB-231 and MDA-MB-231/epi.*** *300 most downregulated and most upregulate RNAs in resistant breast cancer cells, compared to the sensitive cells, with a q-value < 0.05 and a fold change of at least ± 2. Each colour represent a condition (black, MDA-MB-231 transfected with the pre-miR-control; yellow, MDA-MB-231/epi transfected with the pre-miR-control), and each symbol represents a biological replicate*

A

Hallmark	NES	FDR q-val
Epithelial mesenchymal transition	3.857	0
Inflammatory response	3.081	6.35E-04
Apical junction	3.005	4.23E-04
Estrogen response early	2.824	3.17E-04
Interferon gamma response	2.708	2.54E-04
Angiogenesis	2.551	6.54E-04
TNFA signalling via NFκB	2.527	5.61E-04
KRAS signalling DN	2.521	4.91E-04
Interferon alpha response	2.432	0.001674
Estrogen response late	2.194	0.005678
Mitotic spindle	2.131	0.007378
Complement	2.130	0.006764
IL6 JAK STAT3 signalling	2.117	0.006533
Coagulation	2.093	0.006423
KRAS signalling UP	2.086	0.006494
Hedgehog signalling	1.795	0.03518
IL2 STAT5 signalling	1.794	0.033344
Allograph rejection	1.717	0.045875

B

Hallmark	NES	FDR q-val
MYC targets V1	-6.464	0
E2F targets	-6.050	0
G2M Checkpoint	-4.757	0
Oxidative phosphorylation	-3.996	0
MTORC1 signalling	-2.921	0
MYC targets V2	-2.858	8.89E-05
DNA repair	-2.586	3.54E-04
spermatogenesis	-2.543	3.10E-04
Fatty acid metabolism	-2.504	3.47E-04
adipogenesis	-2.380	5.25E-04
PI3K AKT MTOR signalling	-1.880	0.015203
Protein secretion	-1.856	0.015632

Table R 4. ***GSEA analysis of the pathways regulated in breast cancer cells resistant to epirubicin, compared to the sensitive breast cancer cells****. 5630 RNAs were significantly regulated with a fold change of two between sensitive and resistant breast cancer cells. Pathways with a FDR q-value < 0.05 are showed. (A) Pathways significantly upregulated in MDA-MB-231/epi, compared to MDA-MB-231. (B) Pathways significantly downregulated in MDA-MB-231/epi, compared to MDA-MB-231. NES, normalized enrichment score; FDR, False Discovery Rate.*

2.3.1 The identified targets of miR-373 are already regulated in resistant breast cancer cells

In order to determine if the low responses we observed were due to the targets being already regulated in resistant cells, we compared the level of expression of the mRNAs previously identified as targets between MDA-MB-231 and MDA-MB-231 resistant to epirubicin. We observed that, in the cases of TFGβR2 and RELA, the expression level of the genes were already lower in resistant cells compared to sensitive cells (**fig. R 47**). The overexpression of miR- 373-3p could only slightly decrease the level of the genes, which was already low. This could explain why we observe a weak response in resistant cells, for these two genes.

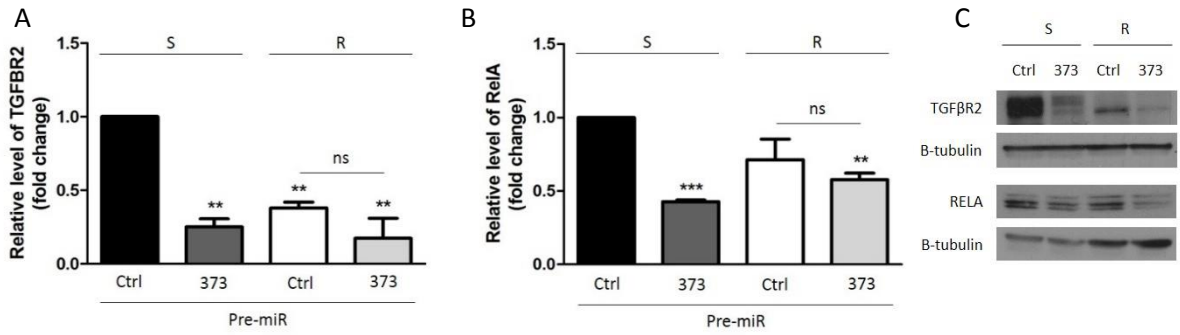

Figure R 48. ***Regulation of TGFβR2 and RELA by miR-373-3p****. qRT-PCR analysis of the expression of TGFBR2 (A) and RELA (B) from RNA extracted from MDA-MB-231 cells, sensitive or resistant to epirubicin, transfected with 25 nM of pre-miR-373-3p or the control. (C) Western blot analysis of the modulation of protein expression of TGFβR2 and RELA 72h after overexpressing miR-373-3p. Results are normalized to the expression of PPIA and B2M. S, sensitive MDA-MB-231; R, resistant MDA-MB-231/epi. Data are expressed as mean ± SD from three independent experiments (**, p<0.01; ***, p<0.001).*

Looking at the expression level of CD44, SLUG and ZEB1, we could observe two different cases. The expression of CD44 was three-times higher than in the sensitive MDA-MB-231, and SLUG was seven-time higher (**fig. R 47A-B**). MiR-373-3p appeared to have lost its regulatory capacity on the genes expression. The basal expression level of Zeb1 was just marginally higher in the MDA-MB-231 resistant to epirubicin (**fig. R 47C**). The overexpression of miR-373-3p led to the expression of Zeb1 at a level similar to the one of the sensitive breast cancer cells control level. It appeared that the capacity of miR-373-3p to regulate its direct or indirect targets was partly dependent on the basal expression level of the genes, depending on the target. This was the case for TGFβR2 and RELA. We also

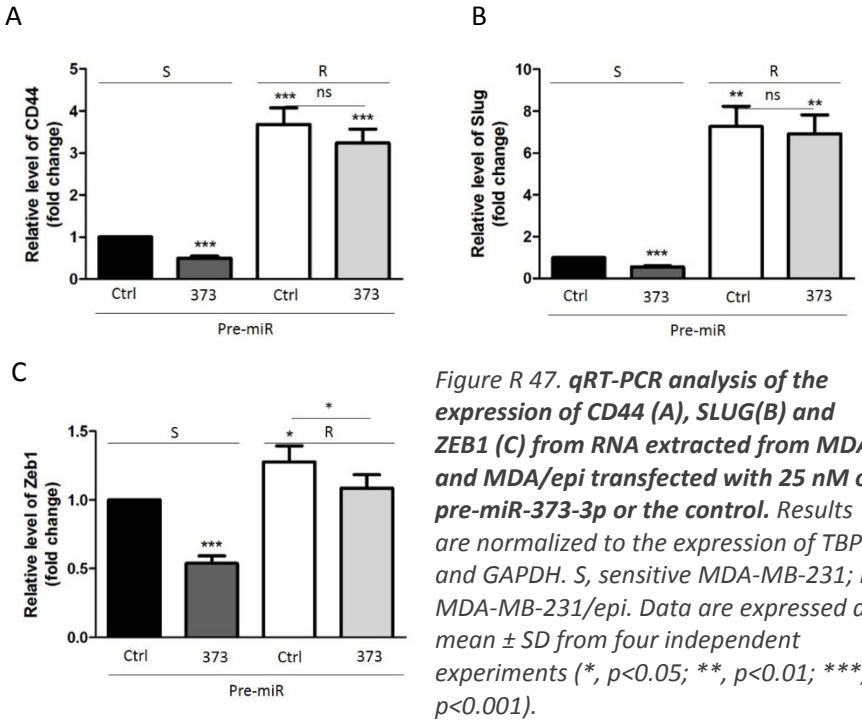

Figure R 47. ***qRT-PCR analysis of the expression of CD44 (A), SLUG(B) and ZEB1 (C) from RNA extracted from MDA and MDA/epi transfected with 25 nM of pre-miR-373-3p or the control.*** *Results are normalized to the expression of TBP and GAPDH. S, sensitive MDA-MB-231; R, MDA-MB-231/epi. Data are expressed as mean ± SD from four independent experiments (*, p<0.05; **, p<0.01; ***, p<0.001).*

observed that other genes, such as SLUG and CD44, or even ZEB1, were almost not regulated anymore in resistant cells. MiR-373-3p turned up to have lost, at least partially, its regulatory capacity on those genes.

III. Effects of exosomes on breast cancer cells

Since we wanted to study the transfer of miRNAs from cell to cell via exosomes, we analysed the impact of exosomes from HUVECs on MDA-MB-231.

3.1 The exosomes influence the level of expression of genes implicated in drug resistance

We wanted to determine if the exosomes from HUVECs treated with drugs used as chemotherapy agents could influence the development of resistance in cancer cells. For this purpose, we incubated MDA-MB-231 with exosomes from HUVECs treated with epirubicin or paclitaxel, or untreated. We then analysed the level of expression of genes that are known in the literature to influence the resistance to either one or both of these drugs in cancer cells. Interestingly, we observed that the exosomes from drug-treated HUVECs could decrease the level of those genes (**fig. R 49**). Some of the effects were induced by the exosomes from both the epirubicin- and paclitaxel-treated HUVECs, such as the regulation of MDH2 and SIRT6 (**fig. R 49 B** and **49F**). The modulation of the level of ABCB1 (**fig. R 49A**), the well-known MDR1 gene, appeared to only occur with exosomes from epirubicin-treated HUVECs. On the other hand, only exosomes from paclitaxel-treated endothelial cells induced a change in GADD45D level (**fig. R 49E**).

Since exosomes can be used by secreting cells to export drugs, the amount of epirubicin and paclitaxel was quantified in exosomes by high pressure liquid chromatography (HPLC). Results showed that the exosomes carry very small amounts of drugs (**table R 5**). It is unlikely that all the effects we have observed in MDA-MB-231 could be due only to such small amounts of drugs, and it suggests that other molecules such as miRNAs or proteins, composing or carried by exosomes, could take part in those gene expression modulations.

Exosomes (10 µg)	Concentration
Epirubicin	174.6 pg/ml
Paclitaxel	4.2 pg/ml

Table R 5. ***Concentration of epirubicin and paclitaxel in exosomes.*** *Concentration present in 10 µg of exosomes produced by HUVEC treated 2h with epirubicin 1 µg/ml or paclitaxel 20 ng/ml, respectively. Quantification by HPLC, in collaboration with Dr M. Fillet.*

Gene	description
ABCB1	Also known as MDR1, from the ABC transporter family. It is responsible for the export of various drugs outside the cell. It is frequently upregulated in paclitaxel and anthracyclines resistant cells (Villeneuve et al. 2006).
MDH2	The malate dehydrogenase 2 is a mitochondrial enzyme with a role in the citric acid cycle. It uses the NAD/NADH system to catalyze the reversible oxidation of malate to oxaloacetate. It is upregulated in doxorubicin-resistant cancer cells and inducing HIF1-α and metabolic reprogramming (Villeneuve et al. 2006; Ban et al. 2016).
POR	The cytochrome P450 oxydoreductase is a membrane-bound enzyme on the endoplasmic reticulum, and is required for electron transfer from NADPH to cytochrome P450. Its level has been found increased in doxorubicin-resistant cells, but has been shown to also increase the efficacy of various drugs (Villeneuve et al. 2006; Zanger & Schwab 2013).
TOP2A	The topoisomerase 2 α is one of the main target of epirubicin but is also found downregulated in paclitaxel-resistant cells (Eijdems et al. 1995; Villeneuve et al. 2006).
SIRT6	The sirtuin 6 is a stress responsive protein deacetylase, involved in DNA-damage repair and increased in epirubicin- and paclitaxel-resistant cells (Khongkow et al. 2013).
PCNA	PCNA is an essential protein for replication. It is used to evaluate the cellular proliferation capacity.
GADD45A	The Growth arrest and DNA-damage-inducible protein α is a stress response protein. Its expression has been found increased in paclitaxel- and anthracyclines resistant cells (Sherman-Baust et al. 2011; Villeneuve et al. 2006) but on the other hand promote genomic stability (Jin et al. 2003).

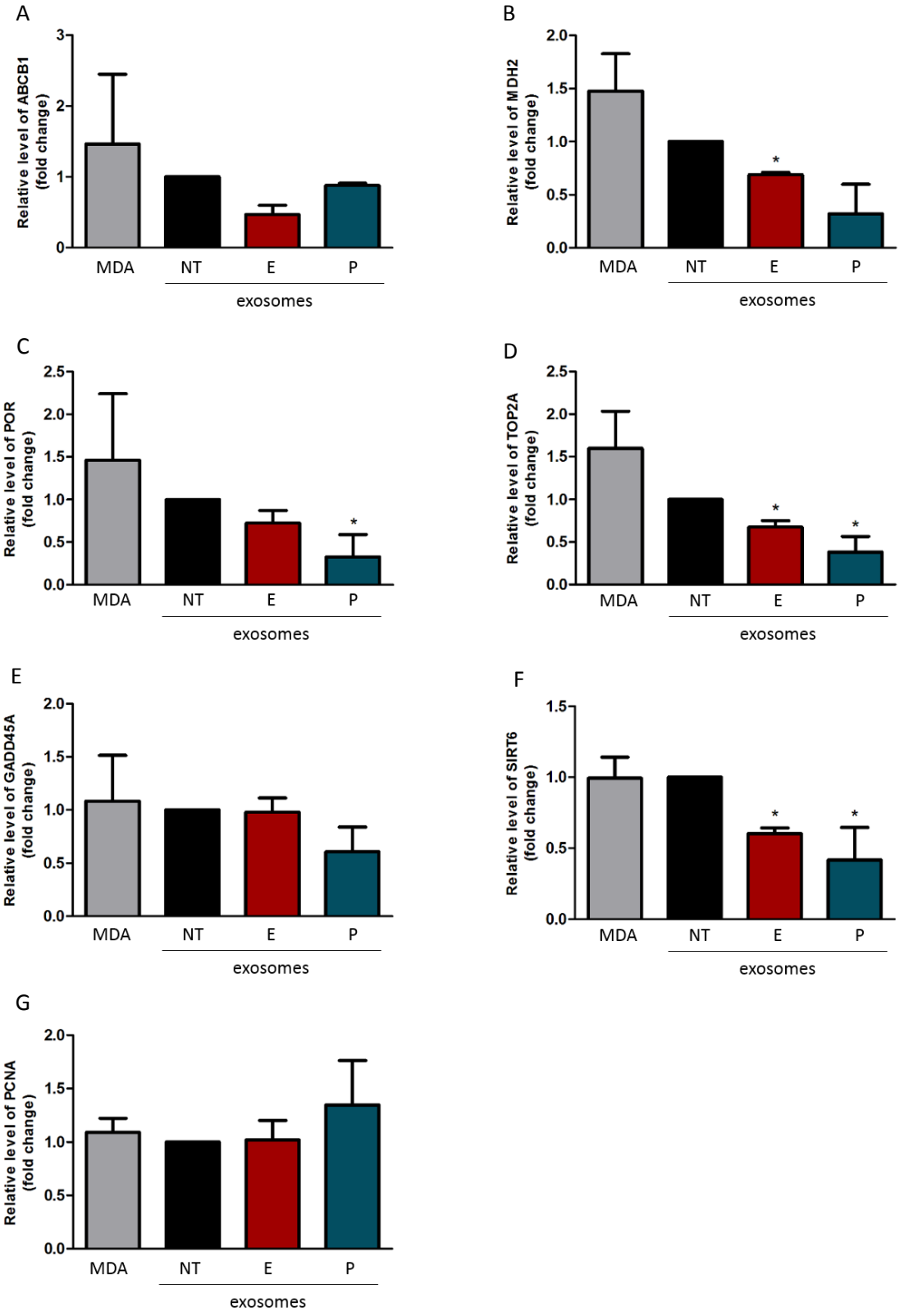

Figure R 49. ***Exosomes from chemotherapy-treated HUVECs induce the modulation of genes implicated in drug resistance in breast cancer cells****. Exosomes were purified from HUVECs untreated (NT), incubated 2h with 1 µg/ml epirubicin (E) or 20 ng/ml paclitaxel (P). 10 µg/ml of exosomes were added to MDA-MB-231 in culture plates, or PBS only (MDA). After 24h, the total RNA was extracted and the level of ABCB1 (A), MDH2 (B), POR (C), TOP2A (D), GADD45A (E), SIRT6 (F), PCNA (G) were analysed by qRT-PCR. Result from three experiments (ABCB1: two experiments) and are expressed as mean ± SD, relative to the NT condition (*, p<0.05).*

Discussion
Conclusion
Perspectives

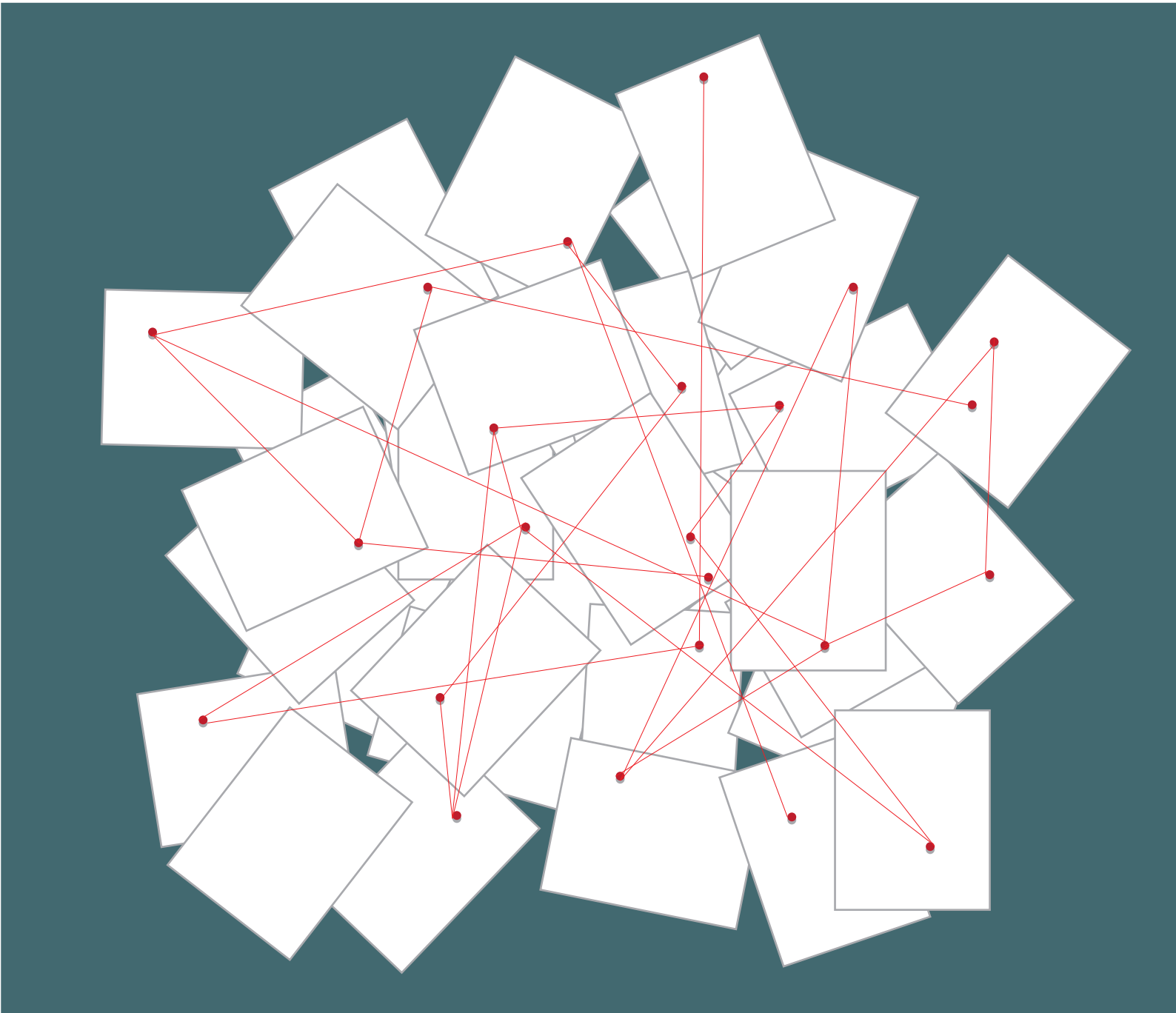

Discussion, conclusion and perspectives

In this work, we wanted to study how endothelial cells HUVECs respond to treatment by two chemotherapeutics drugs: epirubicin and paclitaxel. First, we needed to set up the treatment conditions. To do so, we analysed the effect of increasing concentration of the drugs in the same experimental setting than the one used to produce exosomes, i.e. treating the cells for a short period of time and then incubating them in drug-free media for 72h. The challenge was to minimize the risk of contamination of our vesicles preparation with apoptotic bodies while working with cytotoxic drugs, and a few cell death as unavoidable. We thus selected the condition affecting no more that 50% of the cells. Based on their survival rate, we chose to treat the HUVECs 2h with 1 µg/ml (1.84 µM) or paclitaxel 20 ng/ml (23.4 nM), and incubate them 72h in drug-free media. We noticed a small increase in the dead cells population after the treatment. We then characterized the vesicles produced by HUVECs in those conditions. The size and morphology were analysed by DLS and transmission electron microscopy, and are in agreement with the size of exosomes: 50 to 150 nm. The nature of the surface markers was analysed by Western blotting and we detected the endothelial cell marker CD31, from the cells of origin. We also observed the presence of CD63, CD81, CD9 and TSG101, markers associated with exosomes. We observed a small increase of CD81 in vesicles purified from epirubicin-treated HUVECs. It would be interesting to determine if it could be due to an enrichment in protein, or an increase in the production of a subpopulation of CD81-positive vesicles. Moreover, we couldn't detect Cytochrome c, which is associated with mitochondria and apoptotic bodies. This description corresponds to exosomes as described in the literature (Kowal et al. 2016), which suggests that our vesicles are in majority exosomes, though we cannot exclude that the samples contained a small proportion of other types of extracellular vesicles.

It has been shown that stress conditions could influence the composition of exosomes (de Jong et al. 2012). In particular, our laboratory showed that the secretion of miR-503-5p was increased in exosomes when the cells were treated with chemotherapy while its level was decreased in presence of growth factors (Bovy et al. 2015). In order to determine if the secretion of other miRNAs in exosomes was modified after treatment with epirubicin and paclitaxel, we first performed a small RNA sequencing analysis with the *truseq small RNA library preparation kit* from Illumina. As depicted by the PCA analysis, if the results were coherent for the cell samples, the exosomes samples were not consistent. Given the variation between the samples, we could not trust the results from the sequencing. Furthermore, our

positive control miR-503-5p was not confirmed in this experiment. Among the few miRNAs that were highlighted by the experiment, miR-486-5p could have been a good candidate, but we decided not to study this one since it has been described to be amplified by a bias in the sequencing technique (Huang et al. 2013). We tried to determine what went wrong in these experiments, and came to the conclusion that the method was not optimal for such small amount of small RNA. It is worth mentioning that successful miRNA sequencing from exosomes has been performed in the lab since then, using a different library preparation kit (from Clontech Laboratories). This kit relies on switching instead of ligation for the incorporation of the adapters to the miRNA sequence. This method seems to have better performances and less bias regarding very small amount of RNA than the Illumina kit that was used in this work.

We then turned towards a technique previously used successfully in our laboratory, the qRT-PCR array. The exosomes from drug-treated cells presented a different miRNA composition than those from the untreated condition. It can be seen from the volcano plot (**fig. R 26**) that many miRNAs were decreased in exosomes from drug-treated cells, especially with paclitaxel. We have decided to focus on miRNAs increased in exosomes by both epirubicin and paclitaxel treatments. The rationale behind this was that they would be important for cell communication during chemotherapy. We observed an increase in the level of miR-373-3p and miR-887-3p in both epirubicin and paclitaxel exosomes, and decided to further study their effects. Moreover, we also selected miR-122-5p and miR-129-5p, because they were detected in exosomes from drug-treated HUVECs, but not in the control exosomes. The level of miR-373-3p, miR-887-3p, miR-122-5p and miR-129-5p in cells were stable or decreased after the drug treatments, but their level in exosomes increased. This suggests that the loading of the miRNAs into the exosomes could be a specific process, which would not depend on passive diffusion only.

Other miRNAs were increased in drug-treated conditions, but only by one type of treatment, not both. The study of these specific miRNAs could be interesting regarding the specific mechanisms of action of the different drugs involved in this work.

We then wanted to determine if those microRNAs could impact the behaviour of tumour cells. To do so, we chose to further study the role of miR-373-3p, miR-887-3p, miR-122-5p and miR-129-5p by overexpressing them in the breast cancer cells using pre-miRNA mimic, and perform various functional assay.

MDA-MB-231		miR-373-3p	miR-887-3p	miR-122-5p	miR-129-5p
Migration		=	=	=	=
Spheroids		↘	=	=	=
Colony forming		↗	=	=	↗
Adhesion		↗	=	=	=
Proliferation	24h	=	=	=	=
	48h	=	=	=	=
	72h	=	=	=	=
Survival	24h	↗	=	=	=
	48h	=	=	=	=
	72h	=	=	↘	↘

Table D 6. ***Summary table of the functional effects of miR-373-3p, miR-887-3p, miR-122-5p and miR-129-5p on MDA-MB-231****.*

As shown in **table D 6**, miR-887-3p and miR-122-5p overexpression had barely any effect on the tumour cells. MiR-122-5p is usually considered as a liver specific miRNA, but has been shown to play various roles in cancer. For instance, miR-122-5p was shown to reverse acquired resistance to doxorubicin in hepatocellular carcinoma (Pan et al. 2016) and to inhibit the proliferation, migration and invasion of gastric cancer cells (Rao et al. 2017). Its role in exosomes from HUVECs still remained unknown in this work. MiR-129-5p overexpression seemed to have a small anti-tumour effect on MDA-MB-231, but also a long-term effect of promoting the formation of tumour colonies. The most interesting miRNA among the four ones was miR-373-3p, whose overexpression led to altered functions of the breast cancer cells. This miRNA has been studied in cancer already, but its role is considered to be pro- or anti-tumour depending on the cell type and context (Wei et al. 2015). Here we showed that short-term effects were anti-tumour by promoting the adhesion of the cells to the fibronectin matrix and by inhibiting cell invasion. MiR-373-3p could then regulate the aggressiveness of the cells and their capacity to form metastasis. Indeed, the formation of metastasis follows a sequential process starting with the loss of adhesion of tumour cells, and their invasion into the neighbouring tissue (Chaffer et al. 2016; Diepenbruck & Christofori 2016). However, we saw that, in a longer term assay such as the colony forming assay, the effect was largely pro-tumour, with a large amount of new and bigger colonies. We speculated that this increased number of colonies would happen as a reaction from the cells to the overexpression of the miRNA, since it is likely that the pre-miR-373-3p would have already been fully consumed and degraded by the cells. Moreover, as the miRNA increases the capacity of cells to adhere to the substrate, it would promote a better survival from the moment the cells are seeded. More cells would then be able to form colonies. It could be interesting to analyse the result of a long term exposition to the miRNA in other tests. Moreover, it is possible that some effects are hidden by the overexpression, but would

be revealed by inhibiting the miRNA. Indeed, the overexpression of miR-373-3p would have no effect on targets already strongly regulated by the miRNA in the normal state of the cells.

To better understand how miR-373-3p could alter breast cancer cells behaviour, we performed a transcriptomic analysis. The PCA showed that the transcriptome of the cells overexpressing miR-373-3p was different from the control. The effects of miR-373-3p were striking, with more than 600 modulated RNAs regulated upon miR-373-3p overexpression. Around half of the transcripts were upregulated, which suggest an indirect regulation. Though less common, we cannot remove the possibility that some direct targets of miR-373-3p were upregulated, as it has been shown in some cases for E-cadherin (Place et al. 2008). Of note, E-cadherin was not regulated in our analysis, and couldn't be detected in the sensitive cells by qRT-PCR. The downregulation of direct targets being the main mechanism of miRNA-mediated regulation, direct targets are more likely to be found in the other half of the regulated mRNAs (Huntzinger & Izaurralde 2011). We chose to analyse the transcriptome 48h after overexpressing miR-373-3p in order to obtain a global view of the modification happening in the cells, but an analysis after a much shorter period of time, such as 6h, would have given an overview of the most direct transcriptional modifications. Nevertheless, among the 344 downregulated targets, 45 of them are putative direct targets of miR-373-3p. We used Gene Set Enrichment Analysis (GSEA) to interpret the gene expression data (Subramanian et al. 2005). This method focuses on groups of genes sharing common biological functions. Among the most strongly upregulated pathways, part of them were related to responses to cell stress such as oxidative phosphorylation or UV, and DNA damage repair. These pathways have implications in drug resistance. For instance, mutations in the DNA damage repair pathways can help the cells to evade drug-induced apoptosis and escape the cytotoxicity (Salehan & Morse 2013). It could be interesting to evaluate the stress response of breast cancer cells overexpressing miR-373-3p to assess the general effect of the miRNA in these pathways. Another strongly regulated pathway caught our interest as a potential explanation of the functional responses, the epithelial-mesenchymal transition (EMT). EMT is firstly an important phenomenon in embryonic development, but more and more involved in cancer progression (Chaffer et al. 2016; Brabletz et al. 2018). By activating transcription factors such as the Snail, Twist or Zeb families, the cell switches from an epithelial, polarized, well-differentiated phenotype to a pro-invasion, pro-migration mesenchymal phenotype (Brabletz et al. 2018). The GSEA analysis suggests a general increase in genes related to EMT. However, results from the functional assays showed a decrease in invasion and an increase in adhesion, which would rather fit with an inhibition

of the pathway. We did not detect any effect of miR-373-3p in migration. To determine whether miR-373-3p could modulate the EMT process, we analysed its effect on the expression of well-known regulators and markers of EMT: SLUG, ZEB1 and CD44. We observed that the level of SLUG, ZEB1 and CD44 were decreased by a factor two. CD44, a glycoprotein, has been shown to be a direct target of miR-373-3p (Huang 2008). An increase of the glycoprotein is considered a marker of cancer stem cells and EMT, associated with aggressive tumour (Al-Hajj et al. 2003; Mallini et al. 2014). ZEB1 is a transcription factor promoting EMT and migration, and decreasing adhesion (Aigner et al. 2007). SLUG (also called SNAI2) is a transcription factor from the Snail family, a regulator of EMT and is important for wound healing (Ye & Weinberg 2015). The observed functional effects could be the results of the strong inhibition of the transcription factors. Moreover, our results showed a strong modulation of RELA and TGFβR2, two directs targets of miR-373-3p. RELA, or NFκB/p65, is a major component of the NFκB pathway. This leads us to consider that the observed effects may be linked to a strong regulation of the NFκB pathway, via a decrease in RELA, rather than a direct EMT modulation. It has been observed that NFκB blockade could partially revert EMT (Huber 2004). Moreover, blocking RELA in MDA-MB-231 impaired EMT and led to a decrease in invasiveness and migration, in part by failing to activate the expression of SLUG, TWIST1 and SIP1 (ZEB2) (Pires et al. 2017). Our data showed undeniably a decrease in SLUG expression. Data from the transcriptomic profiling revealed no change in E-cadherin level nor SIP1 level, and TWIST1 was not detected. E-cadherin is the major marker of epithelial cells. The TGF-β signalling pathway is also involved in EMT and cancer stemness (Massagué 2008; Smith & Bhowmick 2016). The stemness is a characteristic of cells expressing stem cells markers. It is related to EMT, and these cancer stem cells are highly tumorigenic (Morel et al. 2008). The pathway has been shown to lead to the transcription of genes implicated in cellular differentiation, by activating factors from the ZEB and SNAIL families (Thuault et al. 2006; Singh & Settleman 2010). Moreover, the TGF-β signalling could trigger EMT in breast cancer cells by activating NFκB (Neil & Schiemann 2008). In colon cancer, miR-373-3p has been shown to indirectly affect ID1 expression, which would repress metastatic activity, by targeting TGFβR2 (Ullmann et al. 2018). By downregulating TGFβR2, a major TGF-β receptor, miR-373-3p would impair the pro-invasion signalling cascade, and support the regulation by NFκB.

If miR-373-3p has been previously associated with promotion of EMT and metastasis in breast cancer cells (Huang et al. 2008; Chen et al. 2015), this is not always the case. Indeed, Keklikoglou and colleagues have demonstrated that miR-373-3p was considered as

a tumour suppressor and inhibitor of metastasis in MDA-MB-231 (Keklikoglou et al. 2012). They showed that miR-373-3p (and miR-520c-3p, from the same miR-520/373 family) targeted and downregulated RELA and TGFβR2. They observed the abrogation of the TNF-α-induced NFkB activity after overexpressing the miRNAs in breast cancer cells by measuring the decreased expression of the pro-inflammatory cytokines IL6 and IL8, two known NFκB targets. In our transcriptomic analysis, we found IL6 increased by a fold change of 1.68 (q value 0.0004) and a decrease by a fold change of 0.37 (q value 5.8e-14) in cells overexpressing miR-373-3p. However, we did not stimulate the cells with TNF-α in our experiments, which could explain the difference in IL6 regulation. They also demonstrated that the overexpression of miR-520c-3p or miR-373-3p reduced the invasive capacity of the MDA-MB-231 in invasion chamber, which is in accordance with our results of spheroid assay. Moreover, they showed that this effect on invasion was due to the downregulation of TGFβR2 by the miRNAs, and demonstrated a decrease of the phosphorylation of Smad2 and Smad3, two of the main transducers of extracellular TGF-β signalling. MiR-373-3p abrogated their translocation to the nucleus and the subsequent transcription of three downstream effectors of the TGF-β signalling, associated with metastasis formation. Our results are in accordance with the conclusions of this study, which provides further information about the mechanisms of miR-373-3p-regulated effects in the formation of metastasis. Furthermore, our results showed the implication of EMT-related factors such as the glycoprotein CD44 and the transcription factors SLUG and ZEB1, which highlight another mode of regulation of metastasis by miR-373-3p.

Moreover, preliminary results showed that adding exosomes from drug-treated HUVECs to MDA-MB-231 induced, like the overexpression of miR-373-3p, a regulation of TGFβR2 and RELA in a dose-dependent manner. If confirmed, those results support our hypothesis of a transfer of miRNA via exosomes from endothelial cells towards breast cancer cells, during treatment by chemotherapy. From the results of functional assays, and data from the sequencing of breast cancer cells overexpressing miR-373-3p, we could infer that the effects of the exosome-mediated transfer would tend towards tumour suppression, especially by repressing directly RELA and TGFβR2. This would lead indirectly to a decrease of expression of important transcription factors of EMT. The breast cancer cells would then present a less invasive and migratory behaviour. Our results support the observations previously made in the laboratory over the increased export of miR-503-5p during chemotherapeutic treatment (Bovy et al. 2015), and suggest a second, indirect, mechanism of action for the cytotoxic chemotherapeutic drugs epirubicin and paclitaxel. It would be

very interesting to reiterate functional assays with breast cancer cells treated with exosomes from drug-treated HUVECs instead of overexpressing miR-373-3p. Those experiments could also be performed by co-cultivating MDA-MB-231 with drug-treated HUVECs.

In the second part of the project, we wanted to study drug-resistant breast cancer cells. Indeed, the development of resistance is a major problem in the treatment of cancers. We then wanted to know if the effects of the four miRNAs that we had tested on sensitive MDA-MB-231 were conserved in resistant cells, or if they were only effective in drug-sensitive cells. MiR-373-3p was of particular interest, since we showed that it was acting as tumour-suppressor in breast cancer cells. Thanks to Dr Sharon Gorski and Dr Melanie Spears, we were able to obtain MDA-MB-231 resistant to either epirubicin or paclitaxel. The IC50 after exposure to the drugs confirmed that our breast cancer cells were indeed sensitive to lower amount of epirubicin and paclitaxel.

A

MDA-MB-231 resistant to epirubicin		miR-373-3p	miR-887-3p	miR-122-5p	miR-129-5p
Migration		=	=	=	=
Spheroids		=	=	=	=
Colony forming		=	↗	=	=
Adhesion		=	=	=	=
Proliferation	24h	=	↘	=	=
	48h	=	=	=	=
	72h	=	=	=	=
Survival	24h	=	=	↘	=
	48h	=	=	=	=
	72h	=	=	=	=

B

MDA-MB-231 resistant to epirubicin		miR-373-3p	miR-887-3p	miR-122-5p	miR-129-5p
Migration		=	=	=	=
Spheroids		=	=	=	=
Colony forming		=	=	=	=
Adhesion		=	=	=	=
Proliferation	24h	=	=	=	=
	48h	=	=	↘	↘
	72h	=	=	=	↘
Survival	24h	=	=	=	=
	48h	=	=	=	=
	72h	=	=	↘	↘

Table D 7. ***Summary tables of the functional effects of miR-373-3p, miR-887-3p, miR-122-5p and miR-129-5p on MDA-MB-231 resistant to epirubicin (A) or paclitaxel (B)****.*

The functional assays (**table D 7**) revealed that almost all the effects of the miRNA overexpression were lost in resistant cells, especially with miR-373-3p. Only miR-129-5p appeared to very slightly impair the proliferation and survival of paclitaxel-resistant breast cancer cells. This miRNA is often considered as a tumour-suppressor (Wu et al. 2010; H.

Zeng et al. 2018), and have been showed to restore sensitivity to paclitaxel (Wang et al. 2018). The results of the functional effects with miR-129-5p, though very slight, were in accordance to the anti-tumour effects described in the literature. However, we have not tested the chemosensitivity of the cells after overexpressing the miRNAs. As we had done with sensitive MDA-MB-231, we performed a transcriptional analysis on the epirubicin-resistant cells after overexpressing miR-373-3p. The transcriptome showed a striking discrimination between control sensitive and resistant cells. We observed the emergence of a phenotype associated with cancer stemness in the resistant cells, with an increased expression of SLUG, ZEB1 and CD44 (Al-Hajj et al. 2003; Morel et al. 2008). Resistant cells are often driven towards stemness, as a way to escape drug-induced cytotoxicity (Prieto-Vila et al. 2017; Vinogradov & Wei 2012). The second interesting result was the overall lower number of regulated genes following the overexpression of miR-373-3p. This correlates with the global absence of response to the miRNA from the resistant cells. The ensuing question is whether there is a general mechanism of resistance to miRNA regulation, or if the response inherent to miR-373-3p only is impaired. It has been shown that cancer cells tend to decrease their general expression of miRNAs, for instance by mutating the enzyme Dicer, because cancer cells favour less regulation (Kumar et al. 2007; Lu et al. 2005). On the other hand, RELA regulates the expression of a large number of genes (Gupta et al. 2001). If miR-373-3p is not able to downregulate RELA anymore, this could explain, at least partially, the absence of response. Aiming to determine why the regulation of miR-373-3p is lost in resistant cells, we analysed the sequencing data to determine if the target site for this miRNA in the RELA and TGFβR2 was mutated. We did not find any mutation in the RelA nor the TGFβR2 transcripts. A second possibility could be that some regions involved in the regulation of the expression of the RELA and TGFβR2 genes are mutated in the resistant cells. However, a deeper genomic sequencing would be needed to analyse potential mutations on the untranscripted regulatory sequences. Another possibility is that the transfection efficiency was altered in the resistant cells. Even though the transfection efficacy was lower in resistant cells, the level of miR-373-3p in transfected cell would still be high enough to saturate the free targets (**table S 14**). Moreover, an epigenetic modification of the targets promotor could be implicated to regulate their level of expression. Another mechanism could implicate the action of a long non coding RNA acting as a sponge to miR-373-3p, which would lower its availability in the cells. The lnc HOTAIR for instance has been shown to target miR-373-3p (Zhang et al. 2016). It is surprising that RELA was expressed at a slightly lower level in resistant cells than in sensitive breast cancer cells. However, we ought to look at the level of

activation of the complex, and the level of expression and of phosphorylation of the inhibitor IκB-α (Serasanambati & Chilakapati 2016).

In order to test if the decrease of response is a general mechanism for miRNA unresponsiveness rather than specific to miR-373-3p, we transfected sensitive and resistant breast cancer cells with another miRNA, miR-887-3p, and evaluated the level of expression of one predicted direct target, GSK3A (**fig. D 50**). We saw that GSK3A is expressed at a similar level between the two types of cells, and that the miRNA still inhibits its expression in the resistant cells. This result suggests that the loss of effect should be due to an impaired sensitivity to miR-373-3p regulation rather than a general mechanism inhibiting the action of all miRNAs.

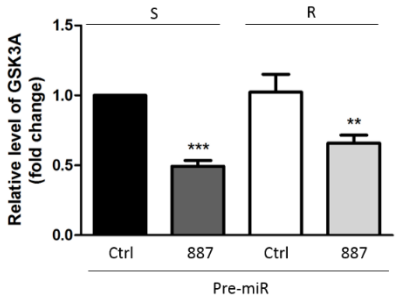

Figure D 50. ***MiR-887-3p regulates GSK3A in MDA-MB-231 sensitive as well as resistant to epirubicin****. RNA was extracted from cells transfected with 25 nM of pre-miR-887-3p or the control. The level of expression was analysed by qRT-PCR. Results are normalized to the expression of PPIA. S, sensitive MDA-MB231; R, MDA-MB-231 resistant to epirubicin. Data expressed as mean ± SD from four independent experiments (**, p<0.01; ***, p<0.001).*

Regarding the role of TGFβR2 in resistance to chemotherapy, the TGF-β signalling has been shown to be frequently re-organised in breast cancer to fit the needs of the cancer cells (Neuzillet et al. 2015). It is then possible that a small modification of its expression would not modify much the resistant cancer cells metabolism, or that the signal would be compensated by other actors of the signalling pathway. The expression of TGFBR2 was still lower in resistant cells overexpressing miR-373-3p, and we could still observe a tendency to decrease the cell migration. Overall, the results showed that miR-373-3p was able to influence breast cancer cells phenotype, but that this regulation would not be possible anymore if the cells present a resistant phenotype.

Finally in the last part of our thesis we showed that treating breast cancer cells with exosomes from drug-treated HUVECs induces the regulation of the expression of genes known to play a role in chemoresistance. Four mRNAs were decreased after treatment with exosomes from both types of chemotherapeutic drugs: MDH2, implicated in the citric acid

cycle, SIRT6, involved in DNA-damage repair, POR, a cytochrome P450 oxydoreductase, and TOP2A, one of the main target of epirubicin. ABCB1, the MDR1 transporter, was downregulated with epirubicin-exosomes, but not paclitaxel. The opposite was observed in the case of GADD45A. Finally, exosomes do not seem to affect the proliferation capacity of the cells, since PCNA did not vary. If it is quite complex to assign a mechanism of action to those exosomes, with such a variety of targets, the global effect of the exosomes on MDA-MB-231 breast cancer cells appears to be tumour-suppressive. This global action correlates with our finding that miR-373-3p in exosomes acts as tumour-suppressor in breast cancer cells. It would be interesting to assess the level of those genes in the resistant cell lines treated with exosomes from drug-treated endothelial cells, and see if the effects are conserved. If those findings were confirmed in resistant cells, exosomes could potentially be considered as treatment to avoid the development of resistance.

At the end of this thesis, we would like to propose the following model: chemotherapeutic drugs epirubicin and paclitaxel induce the preferential loading of miR-373-3p, miR-887-3p, miR-122-5p and miR-129-5p in exosomes in endothelial cells. Those exosomes transfer their miRNAs to cancer cells. MiR-373-3p, especially, regulates the cells adhesion and invasion capacities, via the downregulation of direct (TFGβR2, RELA, CD44) and indirect targets (SLUG, ZEB1). When the cells become resistant to the treatments, they would not respond to miR-373-5p anymore and present a phenotype of cancer stem cell, with marker of EMT such as CD44 highly expressed.

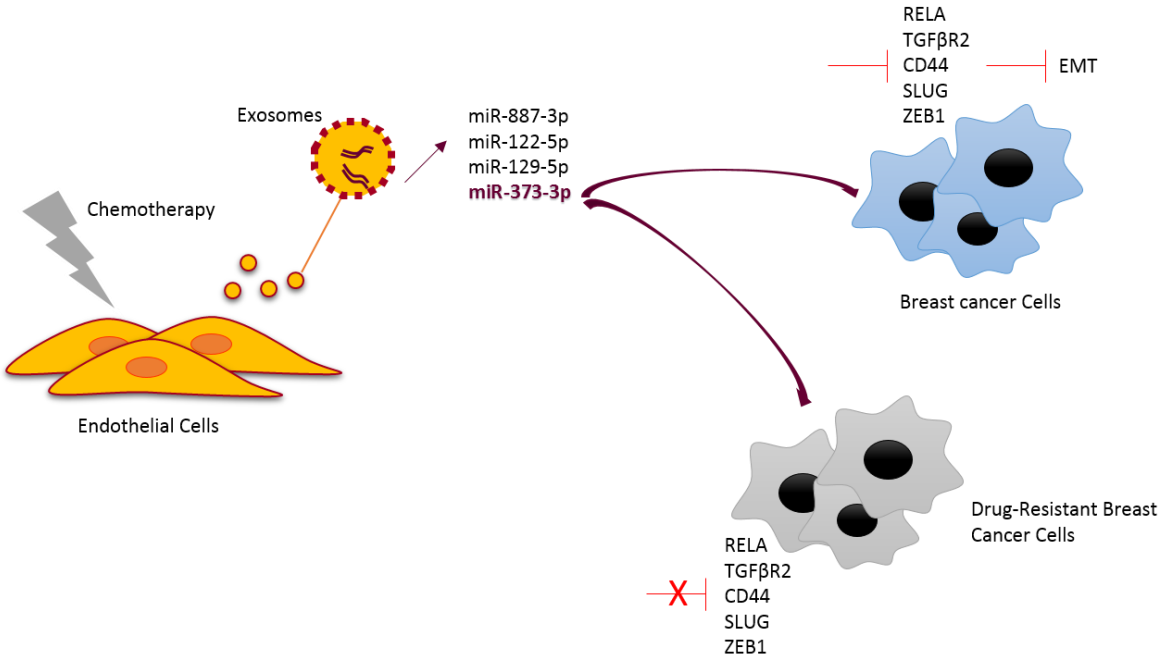

Figure D 51. ***Model of the regulation of tumour aggressiveness via exosomes loaded in miRNAs****. Endothelial cells undergoing chemotherapeutic treatment secrete exosomes loaded in miR-373-3p, miR-887-3p, miR-122-5p and miR-129-5p. MiR-373-3p decreases the invasive and adhesive properties of the breast cancer cells, by inhibiting RELA, TGFβR2, CD44, SLUG and ZEB1. Those effects are abolished in drug resistant cancer cells.*

Regarding the perspectives of this work, it would be very interesting to determine if exosomes keep their effects on resistant cells. It is possible that the modifications undergone by the resistant cells would impair they capacity to internalise exosomes. This could happen in paclitaxel-resistant cells in particular, since paclitaxel targets microtubules and they are involved in the transport of exosomes after internalization by recipient cells (McKelvey et al. 2015). Since we observed that the overexpression of miR-373-3p had less effects in resistant cells, we should also analyse their response to exosomes. Furthermore, the next step in assessing the response to miR-373-3p should be to analyse the level of expression of downstream effector in the TGF-β signalling and the NFκB pathway. This would allow us to get a better grasp in understanding the implications of such regulations in breast cancer cells. Moreover, we observed an increase in the number of colonies due to miR-373-3p. Tests need to be performed to determine if this could be due directly to miR-373-3p, or if it would rather result from a reaction of the cells to the overexpression of the miRNA. It could also be due to the increase of the cells adhesion capacity. The cells would then be able to adapt to substrate more rapidly, giving them better chances to survive from the moment they were seeded. Analyses of the cells state after a longer period should be made to better

understand this result. Besides, it would be quite interesting to look into the cumulative effect of the chemotherapeutic drugs and the exosomes/miR-373-3p.

Finally, analysis the role of endothelia-derived exosomes in a mouse model of cancer is, to our opinion, the most interesting. Several approaches are possible. We could generate mice overexpressing miR-373-3p in endothelial cells and study its role in the development of tumour xenograft. Alternatively, mice could be treated with chemotherapeutic drugs and the level of circulating miRNAs be assessed in the blood of those mice. Moreover, we could graft tumour cells while injecting exosomes from treated HUVECs, or from HUVECs transfected with pre-miR-373-3p, and determine the *in vivo* effect of those exosomes on tumour growth. The development of metastases should be of particular interest considering the results on EMT in vitro. Finally, high level of serum miR-373-3p has been associated with advanced clinical tumour stage, and increased after treatment with Lapatinib and Trastuzumab in HER2+ breast cancer (Müller et al. 2014). Since the effect of miR-373-3p appears to be context-dependant, we should consider measuring circulating miR-373-3p in patients suffering from triple-negative breast cancer treated with neoadjuvant chemotherapy to determine if the miRNA is overexpressed at a systemic level.

During the last decade, exosomes and other EVs have been widely studied for their potential as biomarkers of diagnosis and prognosis. Many studies have focussed on the miRNA content of EVs. miRNA as biomarkers are widely studied in biological fluids due to their high stability. An important question currently in the field is to determine whether there is an advantage to identified biomarkers in purified EV rather that in whole blood. Indeed, some studies have shown that miRNAs in whole plasma give better results in term of diagnostic potential when compared to miRNAs in EVs (Endzeliņš et al. 2017), other that the miRNA associated with the EVs gave better results (van Eijndhoven et al. 2016). With the development of new tools to analyse subpopulations of vesicles, there is a growing interest in determining if those diverse subpopulations could potentially provide more specific information. For instance, the development of a new multiplex bead-based platform to allow the identification of up to 39 markers in one sample could help find new association of membrane markers in EVs (Koliha et al. 2016). However, some of the main challenges in the development of EV-based biomarkers remain the lack of knowledge of pre-analytical factors and the need for standard operation procedures, which would increase the reproducibility (Clayton et al. 2001).

In that context, the results presented in this work would not appear to be directly related to the search for biomarkers. Indeed, we should first confirm *in vivo*, in mice, and preferentially in human, the increase of miRNAs we observed in the vesicles released from endothelial cells after treatment with chemotherapeutic drugs. Then we could seek to correlate the miRNA levels to a response from the patients. Moreover, it has been shown that a tumour mimicking media was able to influence the content of vesicles from endothelial cells. It is possible that resistant cells would trigger the secretion of a different content. Curiously, miR-373-3p was shown to be upregulated in exosomes produced by endothelial cells in a tumour-mimicking environment (Bovy et al. 2015). It would be interesting to test if that increase would be present when the cells are in the same environment, but supplemented with the drugs tested here, or tested in co-culture with resistant tumour cells.

Regarding the treatments by chemotherapy, studies have been performed on patients undergoing neoadjuvant chemotherapy with epirubicin and paclitaxel. Plasma level of miR-221 was associated with the hormone-receptor status of breast cancer patient after neoadjuvant chemotherapy (Zhao et al. 2011). It was also shown that there was an increase of the level of miR-34a and miR-122-5p in the plasma of patients after chemotherapy, especially anthracyclines (Frères et al. 2015). Interestingly, it was not increased in the tumour, suggesting a different origin. An increase in miR-122-5p appeared in our profiling of exosomes from drug-treated endothelial cells as well. However, miRNAs were analysed from the whole plasma. It is possible that responses would be different with EV-carried miRNAs, even more if we select a specific population such as the EVs from endothelial cells.

Using their capacity to target specific cell types thanks to their surface marker, their good stability in blood and low immunogenicity, EVs have also been proposed as new carrier to deliver pharmacological drugs (Pascucci et al. 2014; Bunggulawa et al. 2018). Combining the chemotherapeutic drugs and miRNAs able to increase the response to these drugs in the same carrier could potentially help avoiding drug resistance. However, they are still many challenges ahead before starting clinical use of engineered exosomes, such as large scale production and assessing the safety of procedures (Luan et al. 2017).

Supplementary Data

Supplementary data

I. Supplementary figures

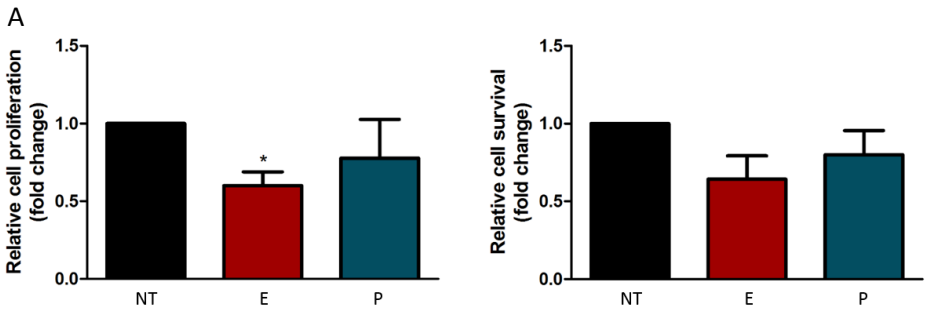

Figure S 52. ***Analysis of cell proliferation and cell survival of breast cancer cells upon treatment with chemotherapeutic drugs****. MDA-MB-231 cells were treated 2h with 1 µg/ml epirubicin (E) or 20 ng/ml paclitaxel (P). (A) Cell proliferation, measured by BrdU incorporation. (B) Cell survival, reflected by WST 1 reaction. NT, untreated cells. Data are expressed as mean ± SD from three independent experiments (*, p<0.05).*

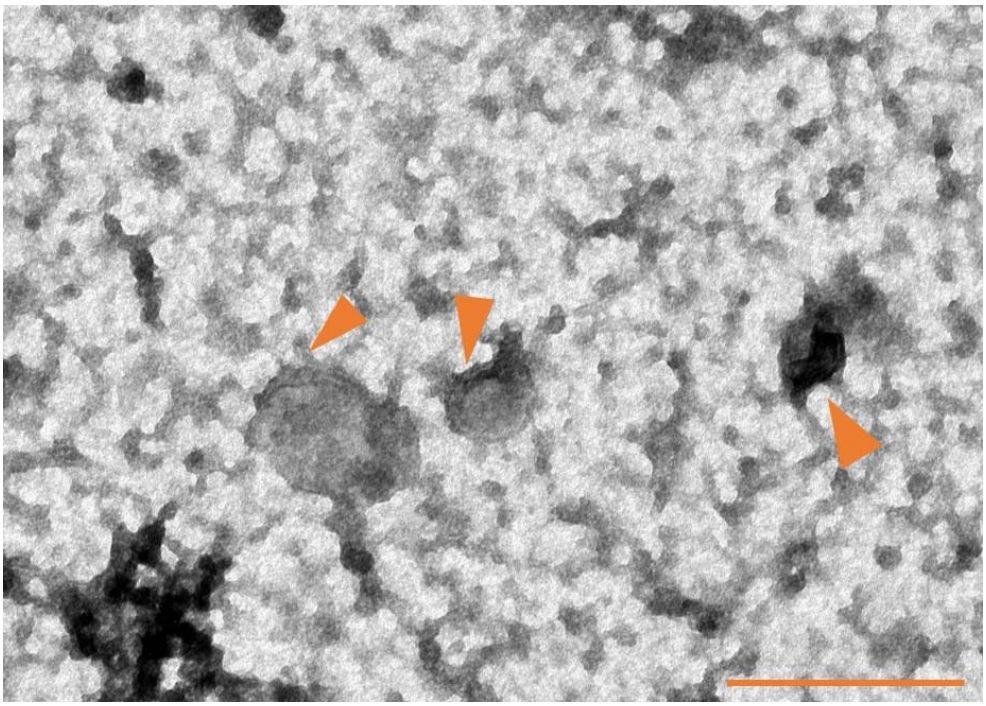

Figure S 53. ***Purified extracellular vesicles from HUVECs treated with epirubicin by transmission electron microscopy****. The arrows show vesicles with a lipid bilayer. In collaboration with Pr. M. Thiry. Upper right: zoom; scale bar: 200 nm.*

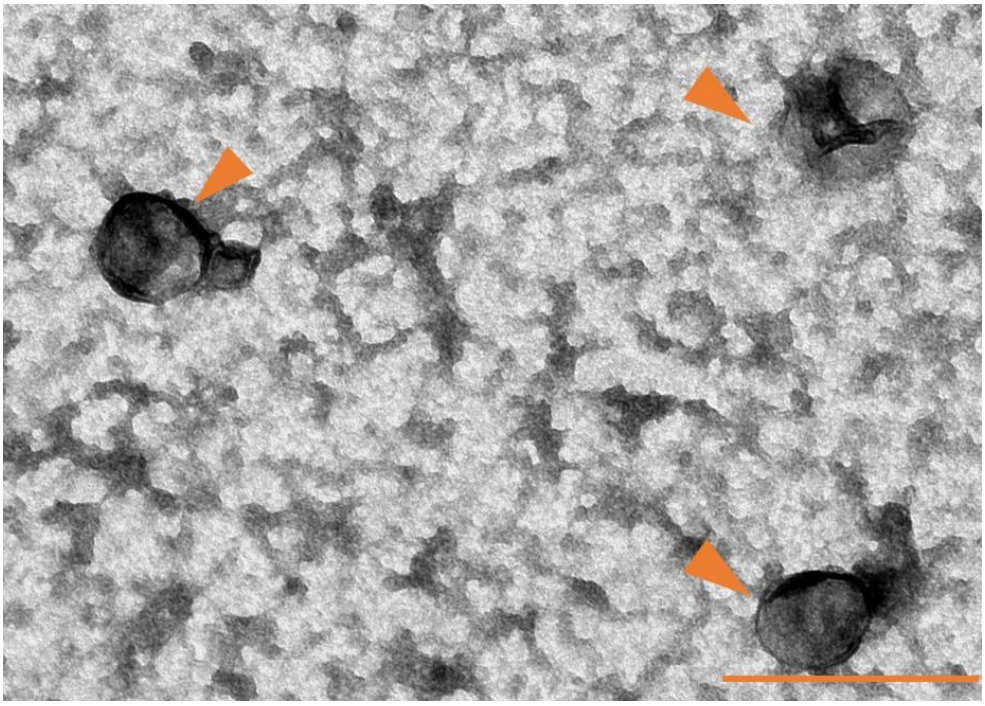

Figure S 54. ***Purified extracellular vesicles from HUVECs treated with paclitaxel by transmission electron microscopy****. The arrows show vesicles with a lipid bilayer. In collaboration with Pr. M. Thiry. Upper right: zoom; scale bar: 200 nm.*

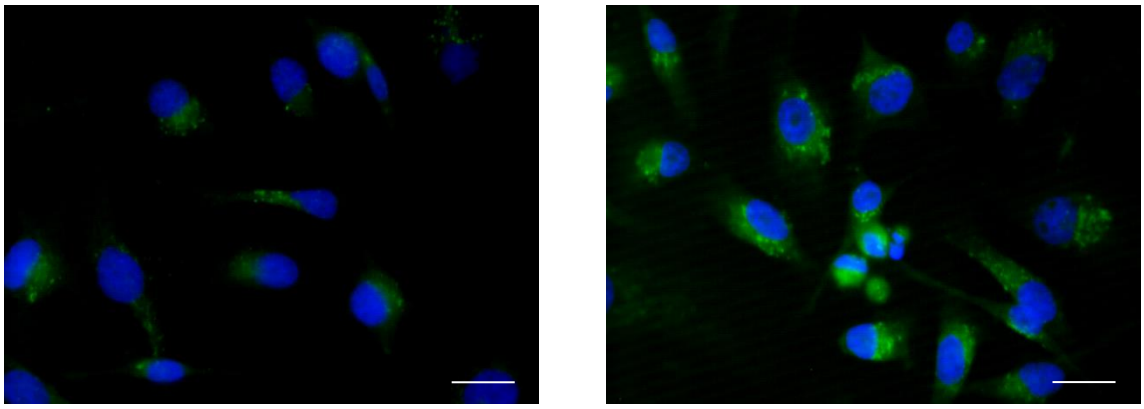

Figure S 55. ***Transfer of miR-503-5p from endothelial to breast cancer cells****. HUVECs were transfected with 50 nM of pre-miR control (PC) or pre-miR-503-5p coupled to the dye Cy3 (P503-Cy3). The pre-miRNA was coupled to the dye using the Label IT siRNA Tracker Cy3TM Kit (Mirus). They were co-cultured 24h in 0.22µm transwell with MDA-MB-231 in coverslips in 6 wells plate. Images were taken using the microscope Eclipse 90i (Nikon). scale bars = 25 µm (DAPI, blue; pre-miR-503-Cy3, green).*

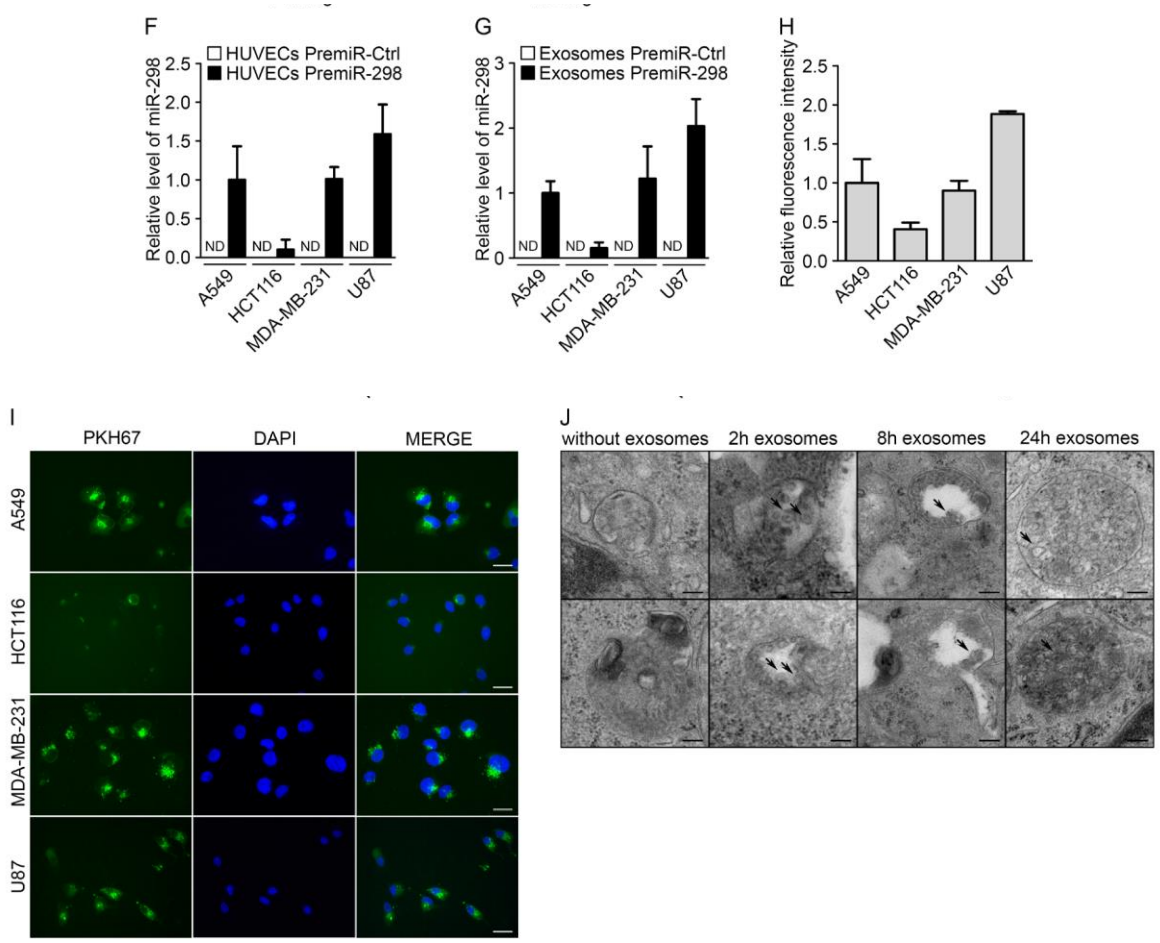

Figure S 54. ***Endothelial exosomes can transfer miRNAs to tumour cells.*** *(F) MiR-298 levels evaluated using qRT-PCR in cocultures either of tumour cells with HUVECs transfected with pre-miR-control or pre-miR-298 or (G) of tumor cells incubated with exosomes from HUVECs transfected with pre-miR-control or pre-miR-298. (H) Flow cytometry analysis of the uptake of exosomes (labeled with the green fluorescent PHK67 membrane linker) by tumor cells. (I) Fluorescence microscopy detection of the uptake of PHK67-labeled exosomes by tumor cells (DAPI, blue), scale bars = 25 µm. (J) Electron micrographs of MDA-MB-231 cell sections showing vesicles (arrows); after incubation with HUVEC exosomes for 0, 2, 8 and 24 hours, MDA-MB-231 cells showed larger multivesicular vesicles containing exosomes, scale bars = 100 nm. All data are the mean ± SD (n ≥ 3), vs. the respective control. Results from Bovy et al., 2015.*

II. Supplementary tables

miRNAs detected only in exosomes from epirubicin-treated HUVECs	miRNAs detected only in exosomes from paclitaxel-treated HUVECs	miRNAs detected only in exosomes from untreated HUVECs	miRNAs detected in exosomes from drug-treated HUVECs	miRNAs detected in all exosomes
miR-20b-3p, miR-590-5p, miR-873-5p, miR-548b-3p, miR-519d-3p, miR-184, miR-296-5p, miR-135a-5p, miR-26a-2-3p, miR-412-3p, miR-1, miR-299-3p, miR-576-5p, miR-340-5p	miR-129-5p, miR-494-3p, miR-658, miR-32-5p, miR-34b-3p, miR-498, miR-383-5p, miR-490-3p, miR-513a-5p	miR-374b-3p, miR-623, miR-509-3-5p, miR-524-3p, miR-452-5p, miR-589-5p, miR-302c-5p, miR-144-3p, miR-219a-5p, miR-518b, miR-514a-3p, miR-95-3p, miR-182-5p, miR-508-3p	miR-337-5p, miR-550a-5p, miR-181d-5p, miR-122-5p, miR-202-3p, miR-654-5p, miR-545-3p, miR-506-3p, miR-187-3p, miR-371a-5p, miR-298, miR-617, miR-216b-5p, miR-212-3p, miR-373-5p, miR-20b-3p, miR-590-5p, miR-873-5p, miR-548b-3p, miR-519d-3p, miR-184, miR-296-5p, miR-135a-5p, miR-26a-2-3p, miR-412-3p, miR-1, miR-299-3p, miR-576-5p, miR-340-5p, miR-129-5p, miR-494-3p, miR-658, miR-32-5p, miR-34b-3p, miR-498, miR-383-5p, miR-490-3p, miR-513a-5p	miR-7-5p, miR-217, miR-328-3p, miR-143-3p, miR-218-5p, miR-136-5p, miR-140-5p, miR-31-3p, miR-210-3p, miR-194-5p, let-7g-5p, miR-203a, miR-181a-3p, miR-137, miR-486-5p, miR-329-3p, miR-487b-3p, miR-191-5p, miR-103a-3p, miR-423-5p, miR-221-3p, miR-301b, miR-532-5p, miR-99a-5p, miR-16-5p, miR-98-5p, miR-185-5p, miR-25-3p, miR-765, miR-24-3p, miR-369-5p, miR-425-5p, miR-760, miR-574-3p, miR-130b-3p, miR-30c-5p, miR-133b, miR-23a-3p, miR-193b-3p, miR-501-5p, miR-130a-3p, miR-379-5p, miR-342-3p, miR-934, miR-101-3p, miR-539-5p, miR-331-3p, miR-330-3p, miR-570-3p, miR-26a-5p, miR-99b-5p, miR-431-5p, miR-23b-3p, miR-505-3p, miR-18a-5p, miR-92a-3p, miR-500a-5p, miR-887-3p, miR-423-3p, miR-126-3p, miR-421, miR-376b-3p, miR-625-3p, miR-339-5p, miR-323a-3p, miR-125a-5p, miR-20a-5p, miR-374b-5p, miR-346, miR-151a-3p, miR-493-3p, miR-99a-3p, miR-361-5p, miR-125b-5p, miR-503-5p, miR-204-5p, miR-30d-5p, miR-301a-3p, miR-362-5p, miR-29b-2-5p, miR-491-5p, miR-92b-3p, miR-665, miR-132-3p, miR-432-5p, miR-27a-3p, miR-376c-3p, miR-940, miR-22-5p, miR-224-5p, miR-885-5p, miR-320a, miR-18b-5p, miR-186-5p, miR-199a-5p, miR-155-5p, miR-107, miR-662, miR-485-3p, miR-337-3p, miR-631, miR-454-3p, let-7f-5p, miR-30e-5p, miR-34a-5p, miR-663a, miR-29b-3p, miR-572, miR-433-3p, miR-660-5p, let-7c-5p, miR-28-5p, miR-324-5p, miR-19b-3p, miR-215-5p, miR-30b-5p, miR-199a-3p, miR-335-5p, miR-21-5p, miR-26b-5p, miR-214-3p, miR-324-3p, miR-455-5p, miR-205-5p, miR-19a-3p, miR-150-5p, miR-15a-5p, let-7d-3p, miR-608, miR-671-5p, miR-497-5p, miR-877-5p, miR-187-5p, miR-10b-5p, let-7i-5p, miR-652-3p, miR-126-5p, miR-30e-3p, miR-152-3p, miR-93-5p, miR-365a-3p, miR-29c-3p, miR-595, miR-602, miR-223-3p, miR-410-3p, miR-17-5p, miR-376a-3p, miR-148b-3p, miR-127-3p, miR-598-3p, let-7d-5p, miR-495-3p, miR-299-5p, miR-34c-3p, miR-596, miR-744-5p, miR-145-5p, let-7a-5p, miR-615-3p, miR-128-3p, miR-766-3p, miR-206, miR-193a-5p, miR-192-5p, miR-29a-3p, miR-18a-3p, miR-142-5p, miR-197-3p, miR-326, miR-15b-5p, miR-196b-5p, miR-361-3p, miR-21-3p, miR-373-3p, miR-222-3p, miR-154-5p, let-7b-5p, miR-151a-5p, miR-502-5p, miR-345-5p, miR-509-3p, miR-134-5p, miR-382-5p, miR-30a-5p, miR-181b-5p, miR-195-5p, miR-874-3p, miR-146b-5p, miR-142-3p, miR-584-5p, miR-216a-5p, miR-424-5p, miR-140-3p, miR-181a-5p, miR-10a-5p, miR-106a-5p, miR-370-3p, miR-425-3p, miR-411-5p, miR-106b-5p, miR-22-3p, miR-483-3p, miR-582-5p, miR-193a-3p, let-7e-5p, miR-409-3p, miR-100-5p, miR-484, miR-518a-3p, miR-148a-3p, miR-146a-5p, miR-139-5p, miR-149-5p, miR-31-5p, miR-451a, miR-27b-3p, miR-374a-5p

Table S 8. ***miRNAs present in exosomes from HUVECs, control or incubated with epirubicin 1 µg/ml or paclitaxel 20 ng/ml.***

miRNAs detected only in epirubicin-treated HUVECs	miRNAs detected only in paclitaxel-treated HUVECs	miRNAs detected only in untreated HUVECs	miRNAs detected in drug-treated HUVECs	miRNAs detected in all conditions
miR-203a, miR-499a-5p, miR-371a-3p, miR-34b-3p, miR-147b, miR-518f-3p, miR-708-5p, miR-95-3p, miR-429	miR-524-3p, miR-885-5p, miR-184, miR-891a-5p, miR-518b, miR-223-3p, miR-512-5p, miR-596, miR-597-5p, miR-20b-5p, miR-375, miR-183-5p, miR-518a-3p	miR-20b-3p, miR-551b-3p, miR-200a-3p, miR-346, miR-549a, miR-595, miR-373-3p, miR-583, miR-153-3p, miR-523-3p	miR-203a, miR-499a-5p, miR-371a-3p, miR-34b-3p, miR-147b, miR-518f-3p, miR-708-5p, miR-95-3p, miR-429, miR-491-3p, miR-873-5p, miR-122-5p, miR-506-3p, miR-187-3p, miR-129-2-3p, miR-96-5p, miR-296-5p, miR-147a, miR-200c-3p, miR-135a-5p, miR-182-5p, miR-216b-5p, miR-642a-5p, miR-451a, miR-524-3p, miR-885-5p, miR-184, miR-891a-5p, miR-518b, miR-223-3p, miR-512-5p, miR-596, miR-597-5p, miR-20b-5p, miR-375, miR-183-5p, miR-518a-3p	miR-7-5p, miR-217, miR-337-5p, miR-328-3p, miR-374b-3p, miR-143-3p, miR-623, miR-218-5p, miR-136-5p, miR-127-5p, miR-140-5p, miR-31-3p, miR-210-3p, miR-199b-5p, miR-194-5p, let-7g-5p, miR-181a-3p, miR-137, miR-486-5p, miR-329-3p, miR-487b-3p, miR-191-5p, miR-103a-3p, miR-423-5p, miR-221-3p, miR-301b, miR-550a-5p, miR-532-5p, miR-99a-5p, miR-16-5p, miR-98-5p, miR-185-5p, miR-25-3p, miR-765, miR-24-3p, miR-369-5p, miR-425-5p, miR-590-5p, miR-760, miR-574-3p, miR-130b-3p, miR-30c-5p, miR-23a-3p, miR-193b-3p, miR-501-5p, miR-130a-3p, miR-379-5p, miR-452-5p, miR-589-5p, miR-141-3p, miR-342-3p, miR-668-3p, miR-934, miR-101-3p, miR-539-5p, miR-331-3p, miR-196a-5p, miR-330-3p, miR-570-3p, miR-188-5p, miR-26a-5p, miR-99b-5p, miR-431-5p, miR-23b-3p, miR-505-3p, miR-18a-5p, miR-92a-3p, miR-500a-5p, miR-887-3p, miR-423-3p, miR-126-3p, miR-421, miR-376b-3p, miR-625-3p, miR-339-5p, miR-323a-3p, miR-181d-5p, miR-125a-5p, miR-20a-5p, miR-374b-5p, miR-151a-3p, miR-493-3p, miR-99a-3p, miR-361-5p, miR-125b-5p, miR-503-5p, miR-204-5p, miR-30d-5p, miR-301a-3p, miR-362-5p, miR-654-5p, miR-545-3p, miR-29b-2-5p,miR-491-5p, miR-92b-3p, miR-665, miR-132-3p, miR-651-5p, miR-628-3p, miR-432-5p, miR-154-3p, miR-27a-3p,miR-376c-3p, miR-940, miR-22-5p, miR-224-5p, miR-320a, miR-18b-5p, miR-302c-5p, miR-548b-3p, miR-186-5p, miR-199a-5p, miR-155-5p, miR-107,miR-662, miR-485-3p, miR-337-3p, miR-494-3p, miR-16-1-3p, miR-631, miR-34c-5p, miR-454-3p, let-7f-5p, miR-30e-5p, miR-34a-5p, miR-663a, miR-29b-3p, miR-572, miR-433-3p, miR-660-5p, let-7c-5p, miR-28-5p, miR-324-5p, miR-219a-5p, miR-19b-3p, miR-215-5p, miR-30b-5p, miR-199a-3p, miR-335-5p, miR-21-5p, miR-26b-5p, miR-214-3p, miR-32-5p, miR-324-3p, miR-455-5p, miR-19a-3p, miR-150-5p, miR-15a-5p, let-7d-3p, miR-671-5p, miR-497-5p, miR-877-5p, miR-10b-5p, let-7i-5p, miR-652-3p, miR-126-5p, miR-30e-3p, miR-181c-5p, miR-152-3p, miR-93-5p, miR-365a-3p, miR-29c-3p, miR-602, miR-627-5p, miR-410-3p, miR-17-5p, miR-376a-3p, miR-514a-3p, miR-449a, miR-148b-3p, miR-127-3p, miR-598-3p, let-7d-5p, miR-135b-5p, miR-495-3p, miR-299-5p, miR-34c-3p, miR-744-5p, miR-145-5p, let-7a-5p, miR-185-3p, miR-615-3p, miR-128-3p, miR-766-3p, miR-206, miR-193a-5p, miR-192-5p, miR-29a-3p, miR-18a-3p, miR-142-5p, miR-197-3p, miR-326, miR-15b-5p, miR-196b-5p, miR-198, miR-361-3p, miR-21-3p, miR-222-3p, miR-154-5p, let-7b-5p, miR-151a-5p, miR-502-5p, miR-345-5p, miR-134-5p, miR-382-5p, miR-30a-5p, miR-181b-5p, miR-33a-5p, miR-195-5p, miR-874-3p, miR-26a-2-3p, miR-146b-5p, miR-299-3p, miR-338-3p, miR-584-5p, miR-377-3p, miR-216a-5p, miR-424-5p, miR-140-3p, miR-181a-5p, miR-10a-5p, miR-106a-5p, miR-370-3p, miR-576-5p, miR-425-3p, miR-450a-5p, miR-411-5p, miR-106b-5p, miR-22-3p, miR-212-3p, miR-542-5p, miR-576-3p, miR-483-3p, miR-582-5p, miR-33b-5p, miR-193a-3p, let-7e-5p, miR-409-3p, miR-100-5p, miR-629-5p, miR-484, miR-30c-2-3p, miR-340-5p, miR-381-3p, miR-148a-3p, miR-146a-5p, miR-139-5p, miR-373-5p, miR-149-5p, miR-31-5p, miR-27b-3p, miR-374a-5p

Table S 9. ***miRNAs present in HUVECs, control or incubated with epirubicin 1 µg/ml or paclitaxel 20 ng/ml***

miRNA	Fold	P value	Moyenne Ct Ctrl	Moyenne Ct Epi
miR-199b-5p	48.27	0.3724	39.84	33.63
miR-194-5p	5.47	0.2131	37.25	35.89
miR-373-3p	5.06	0.3541	39.26	38.54
miR-186-5p	4.96	0.2037	36.79	35.05
miR-572	4.08	0.2503	38.53	37.56
miR-422a	4.07	0.4081	39.18	36.76
miR-149-5p	3.66	0.2363	34.97	34.77
miR-432-5p	3.08	0.3006	34.14	33.97
miR-596	3.03	0.0452	37.49	36.09
miR-887-3p	2.98	0.2294	36.60	36.12
miR-595	2.94	0.5426	35.61	34.80
miR-323a-3p	2.85	0.2252	35.50	34.15
miR-500a-5p	2.81	0.3690	36.29	36.33
miR-330-3p	2.69	0.5109	35.96	35.93
miR-369-5p	2.48	0.5335	37.46	37.10
miR-491-5p	2.43	0.4884	35.94	34.37
miR-195-5p	2.35	0.2599	35.91	34.86
miR-16-1-3p	2.26	0.3725	39.64	38.34
miR-485-3p	2.23	0.2578	34.19	33.13
miR-92b-3p	2.21	0.0940	35.44	34.78
miR-139-5p	2.20	0.2378	33.53	33.11
miR-345-5p	2.19	0.2309	32.00	31.55
miR-539-5p	2.16	0.4016	35.82	34.68
miR-877-5p	2.14	0.3165	35.90	35.59
miR-425-3p	2.14	0.2785	36.23	35.56
miR-760	2.12	0.6049	36.04	36.25
miR-625-3p	2.11	0.2640	37.28	37.27
miR-431-5p	2.04	0.1916	36.86	35.21
miR-409-3p	2.02	0.0996	32.42	31.91
miR-193b-3p	1.95	0.0022	32.19	31.72
miR-602	1.92	0.3340	37.05	37.16
miR-29b-2-5p	1.89	0.6583	34.94	36.46
miR-223-3p	1.85	0.1827	30.63	30.35
miR-483-3p	1.85	0.3941	36.62	36.97
miR-200c-3p	1.84	0.5109	35.41	36.87
miR-629-5p	1.80	0.5144	37.41	36.67
miR-574-3p	1.77	0.0870	31.93	31.59
miR-154-5p	1.75	0.1761	33.87	33.64
miR-346	1.74	0.5448	38.37	38.14
miR-509-3p	1.69	0.6318	37.90	38.36
miR-145-5p	1.66	0.2205	33.68	33.09
miR-138-5p	1.65	0.7238	35.77	35.83
miR-210-3p	1.63	0.4454	33.69	33.29
miR-335-5p	1.61	0.4938	38.48	38.06
miR-127-3p	1.61	0.1486	31.53	31.35
miR-197-3p	1.61	0.2862	32.02	31.77
miR-940	1.60	0.2704	32.42	32.03
miR-125b-5p	1.56	0.0280	27.19	27.02
miR-320a	1.55	0.0876	29.39	29.26
miR-425-5p	1.54	0.2105	32.74	32.44
miR-342-3p	1.53	0.1825	32.58	32.51
miR-495-3p	1.50	0.5495	34.27	34.39
miR-99b-5p	1.46	0.1244	30.24	30.09
miR-125a-5p	1.41	0.0097	28.74	28.72
miR-92a-3p	1.40	0.0076	28.41	28.40
miR-518a-3p	1.38	0.6862	37.13	38.14
miR-25-3p	1.37	0.1087	31.61	31.62
miR-132-3p	1.36	0.3436	34.79	34.84
miR-584-5p	1.33	0.7958	35.64	36.89
miR-30c-5p	1.32	0.0461	29.55	29.63
miR-31-5p	1.31	0.1595	30.81	30.91
miR-449b-5p	1.30	0.2251	39.63	39.98
miR-301b	1.29	0.8597	34.41	34.36
let-7g-5p	1.29	0.4465	32.25	32.24
miR-26b-5p	1.28	0.7404	35.17	34.85
miR-491-3p	1.28	0.6093	39.01	38.50
miR-615-3p	1.28	0.8098	36.54	38.06
miR-204-5p	1.28	0.7367	33.78	34.13
miR-433-3p	1.26	0.7175	36.23	35.99
miR-410-3p	1.25	0.6378	35.43	35.61
miR-100-5p	1.24	0.4343	27.76	27.88
miR-193a-5p	1.24	0.6426	34.19	34.32
miR-339-5p	1.22	0.4534	31.03	31.23
miR-665	1.22	0.6415	31.46	31.30
miR-31-3p	1.22	0.7394	32.88	33.29
miR-151a-3p	1.21	0.3660	32.60	32.78
miR-361-5p	1.20	0.5185	31.12	31.40
let-7f-5p	1.20	0.3055	32.68	32.88

miRNA	Fold	P value	Moyenne Ct Ctrl	Moyenne Ct Epi
miR-331-3p	1.19	0.6140	31.49	31.82
miR-374b-5p	1.19	0.7287	34.27	34.27
miR-484	1.18	0.5613	32.12	32.43
miR-99a-5p	1.16	0.4391	29.04	29.30
miR-142-5p	1.15	0.8278	36.56	37.40
miR-30d-5p	1.15	0.6042	31.14	31.42
miR-140-3p	1.15	0.8385	33.28	33.83
miR-222-3p	1.14	0.5390	28.46	28.74
miR-10b-5p	1.14	0.5348	31.07	31.40
miR-224-5p	1.14	0.8217	35.68	35.36
miR-134-5p	1.13	0.8587	32.73	33.40
miR-187-5p	1.13	0.9073	37.09	36.80
miR-423-3p	1.13	0.5757	30.69	31.02
miR-23a-3p	1.12	0.4525	26.69	26.97
miR-217	1.12	0.7895	32.56	32.67
miR-324-3p	1.11	0.8504	32.90	33.61
miR-598-3p	1.10	0.9466	34.10	34.79
miR-299-5p	1.10	0.9107	36.04	34.99
miR-205-5p	1.10	0.8794	33.78	33.86
miR-362-5p	1.10	0.8654	36.16	36.32
miR-16-5p	1.08	0.5669	28.48	28.83
miR-106b-5p	1.08	0.9295	32.81	33.99
miR-199a-5p	1.06	0.9496	34.27	34.59
miR-379-5p	1.05	0.9638	36.53	37.15
miR-381-3p	1.05	0.9646	35.53	35.37
miR-140-5p	1.05	0.9495	35.64	35.63
miR-631	1.04	0.9661	36.69	38.30
miR-23b-3p	1.04	0.7790	28.53	28.92
miR-21-3p	1.04	0.9328	35.14	35.36
miR-151a-5p	1.02	0.9309	31.19	31.62
miR-137	1.02	0.9897	36.76	35.56
miR-191-5p	1.01	0.9548	30.84	31.26
miR-155-5p	1.01	0.9800	30.99	31.57
miR-127-5p	1.01	0.9919	37.91	39.26
miR-423-5p	1.00	0.9986	31.21	31.84
miR-30a-5p	1.00	0.9964	31.49	31.91
miR-133b	1.00	0.9984	34.44	35.72
miR-103a-3p	0.99	0.9772	28.83	29.52
miR-934	0.98	0.9780	35.88	35.57
miR-99a-3p	0.98	0.9875	36.36	34.84
miR-24-3p	0.98	0.9153	27.71	28.17
miR-126-5p	0.98	0.9532	32.03	32.54
miR-126-3p	0.97	0.9232	25.48	25.97
miR-18b-5p	0.97	0.9368	32.24	32.79
miR-329-3p	0.95	0.9517	33.90	35.64
miR-671-5p	0.94	0.9292	35.67	36.04
miR-501-5p	0.94	0.9572	33.34	35.29
miR-214-3p	0.94	0.6540	33.53	34.12
miR-874-3p	0.93	0.8797	33.06	33.51
miR-107	0.93	0.7871	30.31	30.88
miR-30e-5p	0.92	0.8782	32.85	33.16
miR-337-3p	0.92	0.9207	34.60	35.23
miR-221-3p	0.92	0.3921	27.70	28.30
miR-30e-3p	0.91	0.8973	34.93	35.54
miR-218-5p	0.91	0.9287	35.47	34.98
miR-142-3p	0.90	0.8474	33.51	34.30
miR-766-3p	0.90	0.8899	34.99	35.43
miR-21-5p	0.89	0.6476	27.89	28.47
miR-93-5p	0.89	0.4601	29.60	30.26
miR-382-5p	0.88	0.8073	32.97	34.59
miR-744-5p	0.85	0.7390	37.12	37.81
miR-30b-5p	0.85	0.3945	31.83	32.55
miR-663a	0.84	0.6097	31.31	31.99
miR-376c-3p	0.83	0.6683	32.74	33.35
miR-181b-5p	0.83	0.4445	31.08	31.80
miR-18a-3p	0.83	0.8151	35.35	35.16
miR-98-5p	0.82	0.7732	37.18	37.78
miR-885-5p	0.81	0.8251	37.12	38.45
miR-376a-3p	0.81	0.5927	34.34	35.35
miR-27b-3p	0.80	0.5247	31.06	31.81
miR-106a-5p	0.80	0.4315	28.89	29.71
miR-338-3p	0.79	0.8544	37.35	36.76
miR-376b-3p	0.79	0.7999	35.23	37.25
let-7b-5p	0.77	0.2338	30.00	30.85
miR-101-3p	0.77	0.5054	33.60	34.44
miR-15b-5p	0.76	0.4726	34.49	35.28
miR-493-3p	0.74	0.7762	35.15	35.51
miR-424-5p	0.74	0.6848	32.73	33.70

miRNA	Fold	P value	Moyenne Ct Ctrl	Moyenne Ct Epi
let-7a-5p	0.74	0.0847	29.04	29.96
miR-146b-5p	0.74	0.6610	38.86	39.30
miR-660-5p	0.74	0.5626	34.32	34.66
miR-608	0.73	0.4896	38.62	39.05
miR-652-3p	0.73	0.4160	32.93	33.92
miR-215-5p	0.73	0.7551	37.09	38.04
let-7c-5p	0.73	0.5562	32.25	33.01
miR-196b-5p	0.72	0.6766	34.41	35.10
miR-152-3p	0.72	0.5243	34.40	35.32
miR-150-5p	0.72	0.5951	32.80	33.54
miR-505-3p	0.71	0.6736	35.51	35.31
miR-326	0.71	0.4549	33.67	34.71
miR-502-5p	0.71	0.4215	33.20	34.13
miR-181a-5p	0.71	0.2643	29.40	30.42
let-7e-5p	0.71	0.3282	30.66	31.73
miR-662	0.70	0.4511	37.09	38.10
miR-133a-3p	0.70	0.6916	36.20	36.25
miR-34a-5p	0.70	0.6054	32.21	33.03
miR-28-5p	0.70	0.3926	32.88	33.91
miR-15a-5p	0.69	0.3972	31.50	32.71
miR-365a-3p	0.69	0.2959	30.98	31.93
miR-532-5p	0.69	0.5949	34.02	35.31
miR-486-5p	0.68	0.3545	33.32	34.41
miR-503-5p	0.66	0.5538	34.31	35.33
miR-199a-3p	0.65	0.5864	34.88	35.62
miR-374a-5p	0.65	0.6757	36.24	36.42
miR-20a-5p	0.64	0.2233	29.63	30.66
miR-29c-3p	0.64	0.2882	32.55	33.66
miR-27a-3p	0.62	0.0287	31.38	32.55
miR-19a-3p	0.61	0.3026	31.68	32.79
miR-193a-3p	0.61	0.5590	38.10	38.98
miR-22-3p	0.60	0.2824	31.37	32.74
miR-181a-3p	0.60	0.5483	35.19	35.18
miR-7-5p	0.60	0.0103	34.17	35.38
miR-34c-3p	0.59	0.1755	35.82	36.94
let-7d-5p	0.58	0.0843	32.25	33.56
miR-10a-5p	0.58	0.4762	33.99	35.29
miR-185-5p	0.57	0.2767	31.73	33.27
miR-582-5p	0.56	0.3726	34.36	35.09
miR-18a-5p	0.55	0.1537	31.70	33.15
let-7d-3p	0.55	0.1590	31.25	32.69
miR-26a-5p	0.54	0.1443	32.44	33.76
miR-29a-3p	0.53	0.1245	30.46	32.00
miR-328-3p	0.53	0.1497	33.07	34.36
miR-454-3p	0.52	0.5875	34.50	36.05
miR-143-3p	0.52	0.0413	33.47	35.00
miR-146a-5p	0.49	0.3032	34.97	36.21
miR-19b-3p	0.48	0.1464	29.40	31.02
let-7i-5p	0.47	0.0215	32.52	34.15
miR-128-3p	0.47	0.4622	34.70	36.31
miR-181c-5p	0.46	0.5917	35.49	37.21
miR-542-5p	0.44	0.2380	34.96	37.50
miR-17-5p	0.44	0.4759	35.63	36.74
miR-216a-5p	0.44	0.1541	32.17	33.67
miR-487b-3p	0.44	0.0842	34.36	36.55
miR-130b-3p	0.43	0.0329	34.07	35.88
miR-324-5p	0.41	0.3171	32.72	34.18
miR-301a-3p	0.39	0.1559	34.35	35.59
miR-765	0.39	0.0438	35.43	37.43
miR-455-5p	0.38	0.0925	34.77	36.06
miR-451a	0.35	0.0507	30.42	32.54
miR-206	0.33	0.1678	37.47	39.98
miR-203a	0.31	0.0456	34.21	35.91
miR-130a-3p	0.28	0.2461	35.08	37.47
miR-148b-3p	0.26	0.2420	34.85	35.31
miR-570-3p	0.25	0.4786	34.21	36.67
miR-136-5p	0.24	0.2501	33.41	35.33
miR-29b-3p	0.24	0.0631	34.60	36.62
miR-30c-2-3p	0.22	0.4289	35.41	39.15
miR-192-5p	0.22	0.4072	35.76	39.76
miR-421	0.18	0.0179	34.34	35.54
miR-370-3p	0.18	0.0540	34.03	36.58
miR-200b-3p	0.17	0.3348	36.53	38.88
miR-411-5p	0.16	0.0687	34.45	35.74
miR-148a-3p	0.15	0.0489	35.70	38.02
miR-22-5p	0.15	0.1880	34.04	36.17
miR-361-3p	0.13	0.1687	35.29	36.84
miR-512-5p	0.03	0.2404	33.87	39.48

Table S 10. ***Results of the qRT-PCR array performed to compare miRNA level in exosomes from HUVECs treated with epirubicin or controls****. Data are expressed as fold change (Epirubicin vs Control) and their corresponding P-value. miRNAs are detected in at least one out of three replicates, with Ct lower than 40.*

miRNA	Fold	P value	moyenne Ct Ctrl	moyenne Ct pacli
miR-372-3p	12.83	0.3620	39.87	34.99
miR-373-3p	11.96	0.2358	39.26	37.21
miR-572	9.95	0.2749	38.53	36.58
miR-887-3p	9.62	0.1664	36.60	34.43
miR-346	9.59	0.3736	38.37	36.98
miR-192-5p	7.52	0.1737	35.76	34.18
miR-335-5p	6.93	0.3955	38.48	35.60
miR-369-5p	4.77	0.3897	37.46	35.66
miR-455-5p	3.77	0.4038	34.77	34.24
miR-98-5p	3.45	0.2385	37.18	36.02
miR-602	3.45	0.2757	37.05	36.39
miR-377-3p	3.38	0.3762	37.65	36.03
miR-660-5p	3.14	0.0037	34.32	32.94
miR-425-3p	2.99	0.1959	36.23	35.02
miR-625-3p	2.78	0.3118	37.28	36.14
miR-491-5p	2.77	0.1800	35.94	34.28
miR-194-5p	2.62	0.5095	37.25	35.89
miR-433-3p	2.25	0.3747	36.23	35.09
miR-615-3p	2.19	0.1800	36.54	36.30
miR-539-5p	2.10	0.4164	35.82	34.65
miR-765	2.00	0.5472	35.43	35.74
miR-15b-5p	1.88	0.2591	34.49	34.02
miR-34c-3p	1.80	0.2875	35.82	35.38
miR-301b	1.77	0.6260	34.41	35.05
miR-663a	1.73	0.3686	31.31	31.16
miR-218-5p	1.69	0.5286	35.47	35.06
miR-154-3p	1.68	0.5826	36.56	37.08
miR-193b-3p	1.66	0.4427	32.19	32.20
miR-500a-5p	1.62	0.4988	36.29	36.85
miR-199a-3p	1.62	0.4263	34.88	34.11
miR-152-3p	1.60	0.4158	34.40	34.08
miR-532-5p	1.56	0.2397	34.02	33.52
miR-362-5p	1.56	0.3725	36.16	35.59
miR-877-5p	1.56	0.5200	35.90	35.70
miR-30e-3p	1.51	0.4969	34.93	34.49
miR-142-5p	1.51	0.6332	36.56	36.25
miR-128-3p	1.50	0.6050	34.70	33.97
miR-92b-3p	1.49	0.5464	35.44	35.53
miR-126-5p	1.49	0.2254	32.03	31.71
miR-140-5p	1.47	0.5384	35.64	34.74
miR-330-3p	1.46	0.7654	35.96	34.98
let-7g-5p	1.46	0.4313	32.25	32.00
miR-345-5p	1.42	0.3897	32.00	31.99
miR-196b-5p	1.39	0.4653	34.41	34.39
miR-662	1.36	0.5500	37.09	37.10
miR-224-5p	1.36	0.3323	35.68	35.50
miR-432-5p	1.34	0.5500	34.14	34.63
miR-509-3p	1.33	0.7264	37.90	38.09
miR-193a-5p	1.33	0.4326	34.19	34.00
miR-185-3p	1.33	0.6181	38.88	38.81
miR-518a-3p	1.31	0.8028	37.13	36.36
miR-940	1.31	0.5998	32.42	32.24
miR-423-5p	1.31	0.5334	31.21	31.34
miR-431-5p	1.30	0.6810	36.86	35.76
miR-151a-3p	1.28	0.2864	32.60	32.55
miR-320a	1.27	0.1158	29.39	29.37
miR-302a-3p	1.26	0.5615	39.22	39.25
miR-17-5p	1.25	0.7932	35.63	35.20
miR-7-5p	1.24	0.6901	34.17	34.47
miR-874-3p	1.19	0.7219	33.06	33.07
miR-299-5p	1.19	0.8671	36.04	34.27
miR-126-3p	1.19	0.6402	25.48	25.59
let-7i-5p	1.19	0.6600	32.52	32.79
miR-127-3p	1.19	0.6548	31.53	31.73
miR-99a-3p	1.18	0.8877	36.36	35.92
miR-31-5p	1.18	0.2216	30.81	30.90
miR-25-3p	1.18	0.7180	31.61	32.00
miR-215-5p	1.16	0.9000	37.09	35.75
miR-148b-3p	1.15	0.8199	34.85	33.52
miR-409-3p	1.14	0.5282	32.42	32.52
miR-34a-5p	1.13	0.8202	32.21	32.03
miR-525-5p	1.13	0.8350	38.27	38.48
miR-425-5p	1.12	0.7765	32.74	32.79
miR-379-5p	1.12	0.9267	36.53	35.44
miR-337-3p	1.12	0.8971	34.60	34.98
let-7b-5p	1.11	0.6766	30.00	30.22

miRNA	Fold	P value	moyenne Ct Ctrl	moyenne Ct pacli
miR-188-5p	1.10	0.8677	38.45	38.85
miR-376a-3p	1.10	0.8339	34.34	34.80
miR-376b-3p	1.10	0.9085	35.23	35.31
miR-130a-3p	1.09	0.8800	35.08	34.98
miR-106b-5p	1.09	0.8828	32.81	33.44
miR-27a-3p	1.08	0.6787	31.38	31.62
miR-27b-3p	1.06	0.8386	31.06	31.24
let-7c-5p	1.05	0.9171	32.25	32.37
miR-410-3p	1.05	0.9163	35.43	35.72
miR-146a-5p	1.04	0.9295	34.97	35.00
miR-30e-5p	1.04	0.9419	32.85	32.88
miR-124-3p	1.04	0.9669	37.15	36.46
miR-99b-5p	1.03	0.8967	30.24	30.45
miR-744-5p	1.02	0.9676	37.12	37.49
miR-374b-5p	1.02	0.9769	34.27	34.75
miR-10a-5p	1.01	0.9887	33.99	34.38
miR-374a-5p	1.00	0.9996	36.24	35.59
miR-885-5p	1.00	0.9967	37.12	37.68
miR-26a-5p	0.98	0.9693	32.44	33.10
miR-502-5p	0.98	0.9496	33.20	33.48
miR-10b-5p	0.97	0.9287	31.07	31.64
miR-19a-3p	0.96	0.9197	31.68	32.04
miR-21-5p	0.95	0.8923	27.89	28.33
let-7f-5p	0.94	0.8013	32.68	33.11
miR-217	0.94	0.8864	32.56	32.76
miR-101-3p	0.94	0.9068	33.60	34.38
miR-181b-5p	0.92	0.7971	31.08	31.56
miR-187-5p	0.91	0.8916	37.09	37.55
miR-23a-3p	0.90	0.5668	26.69	27.14
miR-323a-3p	0.90	0.8964	35.50	35.16
miR-149-5p	0.89	0.9285	34.97	34.38
miR-140-3p	0.89	0.7868	33.28	33.61
miR-20a-5p	0.89	0.8316	29.63	30.38
miR-23b-3p	0.88	0.4383	28.53	29.02
miR-584-5p	0.87	0.8088	35.64	36.23
miR-665	0.86	0.8106	31.46	31.88
miR-125a-5p	0.86	0.2556	28.74	29.31
miR-139-5p	0.85	0.6638	33.53	34.28
miR-382-5p	0.85	0.7111	32.97	33.68
miR-92a-3p	0.85	0.2954	28.41	28.99
miR-15a-5p	0.84	0.6723	31.50	32.29
miR-29c-3p	0.83	0.6504	32.55	33.16
miR-324-3p	0.83	0.8013	32.90	35.29
miR-423-3p	0.83	0.1697	30.69	31.28
miR-151a-5p	0.81	0.4693	31.19	31.83
miR-24-3p	0.81	0.4172	27.71	28.30
miR-191-5p	0.81	0.3963	30.84	31.43
miR-18b-5p	0.80	0.7034	32.24	33.66
miR-222-3p	0.80	0.2441	28.46	29.09
miR-193a-3p	0.79	0.7491	38.10	38.70
miR-31-3p	0.78	0.4579	32.88	33.50
let-7d-3p	0.78	0.3542	31.25	31.90
miR-30d-5p	0.78	0.4522	31.14	31.86
miR-30a-5p	0.78	0.4654	31.49	32.12
miR-22-3p	0.77	0.5251	31.37	32.23
miR-141-3p	0.77	0.8207	36.05	38.26
miR-30b-5p	0.77	0.2176	31.83	32.56
miR-93-5p	0.77	0.3582	29.60	30.40
miR-154-5p	0.75	0.4533	33.87	34.91
miR-484	0.74	0.1269	32.12	32.92
miR-125b-5p	0.74	0.1024	27.19	27.95
miR-199a-5p	0.73	0.4963	34.27	35.56
miR-19b-3p	0.72	0.4763	29.40	30.32
miR-329-3p	0.70	0.5265	33.90	33.96
miR-146b-5p	0.70	0.6353	38.86	39.26
miR-197-3p	0.70	0.3822	32.02	32.76
miR-221-3p	0.70	0.1487	27.70	28.61
miR-185-5p	0.70	0.3989	31.73	32.77
miR-328-3p	0.69	0.5263	33.07	34.24
miR-106a-5p	0.69	0.2703	28.89	29.82
miR-18a-3p	0.68	0.6716	35.35	35.78
miR-145-5p	0.68	0.5403	33.68	34.33
miR-186-5p	0.68	0.6500	36.79	38.51
miR-103a-3p	0.67	0.1550	28.83	29.82
miR-503-5p	0.67	0.6314	34.31	35.70
miR-671-5p	0.67	0.6037	35.67	36.52

miRNA	Fold	P value	moyenne Ct Ctrl	moyenne Ct pacli
miR-99a-5p	0.66	0.0640	29.04	29.95
miR-485-3p	0.65	0.6828	34.19	34.39
miR-331-3p	0.65	0.0913	31.49	32.46
miR-107	0.65	0.1336	30.31	31.20
miR-148a-3p	0.65	0.6217	35.70	35.27
miR-370-3p	0.65	0.4825	34.03	34.43
miR-214-3p	0.64	0.2370	33.53	34.73
miR-29b-3p	0.64	0.4965	34.60	36.30
miR-16-5p	0.63	0.1355	28.48	29.56
miR-361-5p	0.63	0.0585	31.12	32.17
miR-361-3p	0.62	0.5934	35.29	35.54
miR-342-3p	0.62	0.1648	32.58	33.89
miR-216a-5p	0.61	0.3734	32.17	33.33
miR-505-3p	0.61	0.5629	35.51	36.52
miR-100-5p	0.61	0.1564	27.76	28.74
let-7a-5p	0.61	0.0486	29.04	30.11
miR-155-5p	0.61	0.1747	30.99	32.04
miR-424-5p	0.60	0.4971	32.73	33.73
miR-301a-3p	0.59	0.3898	34.35	34.99
miR-22-5p	0.59	0.6157	34.04	33.99
miR-365a-3p	0.58	0.2248	30.98	32.17
miR-210-3p	0.58	0.4914	33.69	34.80
miR-181a-5p	0.57	0.1282	29.40	30.66
miR-934	0.56	0.3202	35.88	36.97
miR-136-5p	0.56	0.4430	33.41	35.12
miR-574-3p	0.56	0.1036	31.93	33.18
miR-495-3p	0.56	0.4939	34.27	33.68
miR-376c-3p	0.54	0.2457	32.74	33.81
miR-28-5p	0.54	0.3300	32.88	34.61
miR-450a-5p	0.54	0.5373	34.73	36.42
miR-497-5p	0.53	0.2040	34.29	35.43
miR-608	0.53	0.1268	38.62	39.49
let-7e-5p	0.53	0.1158	30.66	31.98
miR-134-5p	0.53	0.2637	32.73	35.38
miR-760	0.52	0.5611	36.04	37.26
miR-21-3p	0.52	0.3376	35.14	35.48
miR-204-5p	0.52	0.4427	33.78	35.01
miR-483-3p	0.51	0.3665	36.62	38.04
miR-30c-5p	0.50	0.0067	29.55	30.87
miR-18a-5p	0.49	0.0805	31.70	33.14
let-7d-5p	0.49	0.0397	32.25	33.66
miR-421	0.49	0.1325	34.34	35.02
miR-652-3p	0.48	0.0910	32.93	34.31
miR-598-3p	0.47	0.6349	34.10	38.05
miR-324-5p	0.47	0.3627	32.72	33.83
miR-339-5p	0.46	0.0443	31.03	32.48
miR-29a-3p	0.46	0.0479	30.46	31.95
miR-501-5p	0.45	0.3806	33.34	34.99
miR-570-3p	0.44	0.5980	34.21	36.78
miR-181a-3p	0.43	0.3582	35.19	36.72
miR-411-5p	0.43	0.1972	34.45	35.20
miR-203a	0.42	0.2581	34.21	36.92
miR-487b-3p	0.42	0.0914	34.36	35.31
miR-26b-5p	0.42	0.2565	35.17	37.10
miR-596	0.41	0.2881	37.49	38.46
miR-493-3p	0.40	0.3039	35.15	37.47
miR-137	0.40	0.5497	36.76	36.42
miR-223-3p	0.39	0.0112	30.63	32.32
miR-631	0.39	0.4658	36.69	39.19
miR-130b-3p	0.38	0.0239	34.07	35.92
miR-595	0.38	0.5245	35.61	37.57
miR-486-5p	0.37	0.0777	33.32	35.33
miR-451a	0.35	0.0317	30.42	32.27
miR-206	0.32	0.1673	37.47	39.68
miR-142-3p	0.31	0.1048	33.51	36.36
miR-143-3p	0.29	0.0670	33.47	34.25
miR-150-5p	0.27	0.1849	32.80	34.76
miR-205-5p	0.27	0.2377	33.78	36.32
miR-454-3p	0.24	0.3120	34.50	36.36
miR-29b-2-5p	0.22	0.4438	34.94	37.90
miR-326	0.21	0.0418	33.67	35.65
miR-582-5p	0.21	0.1001	34.36	35.54
miR-195-5p	0.16	0.2234	35.91	37.86
miR-766-3p	0.14	0.2277	34.99	37.75
miR-132-3p	0.11	0.0085	34.79	37.80
miR-133b	0.10	0.2460	34.44	37.31

Table S 11. ***Results of the qRT-PCR array performed to compare miRNA level in exosomes from HUVECs treated with paclitaxel or controls****. Data are expressed as fold change (Paclitaxel vs Control) and their corresponding P-value. miRNAs are detected in at least one out of three replicates, with Ct lower than 40.*

miRNA	Fold	P value
miR-934	7.58	0.2678
miR-651-5p	7.14	0.1944
miR-668-3p	6.31	0.3830
miR-142-3p	4.80	0.3152
miR-339-5p	3.73	0.4254
miR-103a-3p	3.12	0.0668
miR-760	3.03	0.5638
miR-299-3p	2.90	0.0040
miR-138-5p	2.82	0.0782
miR-627-5p	2.55	0.5968
miR-146b-5p	2.49	0.0208
miR-491-3p	2.44	0.5256
miR-145-5p	2.35	0.0168
miR-598-3p	2.31	0.1415
miR-877-5p	2.23	0.1674
miR-132-3p	2.19	0.0546
miR-665	1.86	0.2074
miR-509-3p	1.82	0.4771
miR-192-5p	1.81	0.0988
miR-33b-5p	1.80	0.3780
miR-328-3p	1.78	0.2539
miR-149-5p	1.76	0.1771
miR-146a-5p	1.75	0.2689
miR-186-5p	1.68	0.0622
miR-654-5p	1.66	0.1722
miR-500a-5p	1.62	0.5126
miR-338-3p	1.61	0.1510
miR-195-5p	1.61	0.2875
miR-574-3p	1.59	0.1540
miR-373-5p	1.58	0.3878
miR-411-5p	1.57	0.3624
miR-199a-3p	1.57	0.4053
miR-542-5p	1.56	0.2357
miR-421	1.56	0.3987
miR-134-5p	1.55	0.5067
miR-181c-5p	1.55	0.1616
miR-514a-3p	1.53	0.1149
miR-194-5p	1.52	0.4574
miR-572	1.49	0.6272
miR-602	1.49	0.1315
miR-320a	1.48	0.2147
miR-196a-5p	1.47	0.7747
miR-301a-3p	1.47	0.2476
miR-431-5p	1.46	0.2409
miR-374b-3p	1.46	0.2046
miR-22-5p	1.45	0.2303
miR-450a-5p	1.44	0.3516
miR-485-3p	1.44	0.4165
miR-361-3p	1.41	0.2898
miR-34c-3p	1.40	0.0733
miR-181d-5p	1.40	0.3036
miR-628-3p	1.39	0.4930
miR-127-5p	1.36	0.6377
miR-539-5p	1.35	0.5274
miR-193a-5p	1.35	0.2915
miR-30e-5p	1.33	0.1933
miR-29c-3p	1.32	0.0874
miR-483-3p	1.32	0.2625
miR-31-5p	1.32	0.2280
miR-369-5p	1.32	0.6194
miR-330-3p	1.30	0.4563
miR-340-5p	1.30	0.7295
miR-744-5p	1.29	0.5406
miR-31-3p	1.29	0.2763
miR-423-3p	1.29	0.2363
miR-150-5p	1.29	0.0953
miR-323a-3p	1.28	0.7150
miR-152-3p	1.28	0.5586
miR-532-5p	1.28	0.3331
miR-887-3p	1.28	0.4148
miR-215-5p	1.28	0.1394
miR-34a-5p	1.26	0.4741
miR-214-3p	1.25	0.1839
miR-29a-3p	1.25	0.4278
miR-181a-5p	1.25	0.5983
miR-376c-3p	1.25	0.5848
miR-197-3p	1.24	0.4448
miR-127-3p	1.24	0.5263

miRNA	Fold	P value
miR-10a-5p	1.24	0.6293
miR-433-3p	1.23	0.7375
miR-139-5p	1.23	0.3315
miR-154-3p	1.23	0.0503
miR-374a-5p	1.22	0.4820
miR-486-5p	1.21	0.8276
miR-505-3p	1.21	0.6581
miR-196b-5p	1.20	0.5345
miR-423-5p	1.20	0.5910
miR-30d-5p	1.20	0.4863
miR-329-3p	1.20	0.7720
miR-23b-3p	1.19	0.4510
miR-125b-5p	1.19	0.5309
miR-26a-5p	1.19	0.2197
miR-151a-3p	1.19	0.3709
miR-502-5p	1.18	0.4002
miR-30a-5p	1.18	0.4119
miR-181b-5p	1.18	0.6673
miR-432-5p	1.18	0.4784
miR-23a-3p	1.18	0.4041
miR-425-3p	1.17	0.0237
miR-191-5p	1.17	0.6985
miR-221-3p	1.17	0.4282
miR-21-5p	1.16	0.5334
miR-181a-3p	1.16	0.7463
miR-107	1.16	0.4898
miR-30e-3p	1.15	0.6241
miR-582-5p	1.15	0.3951
miR-376b-3p	1.14	0.3226
miR-151a-5p	1.14	0.5050
miR-125a-5p	1.14	0.6568
miR-30c-5p	1.14	0.4859
miR-374b-5p	1.14	0.4362
miR-493-3p	1.14	0.3684
miR-337-3p	1.12	0.6162
miR-452-5p	1.12	0.5197
miR-98-5p	1.12	0.4829
miR-671-5p	1.12	0.0933
let-7e-5p	1.11	0.6309
miR-222-3p	1.11	0.6268
miR-30b-5p	1.11	0.5022
let-7c-5p	1.11	0.4046
miR-425-5p	1.11	0.7261
miR-27b-3p	1.11	0.5417
miR-21-3p	1.11	0.7509
miR-326	1.11	0.4600
miR-455-5p	1.11	0.7769
miR-22-3p	1.11	0.7186
miR-140-3p	1.10	0.5364
miR-193b-3p	1.09	0.6599
let-7a-5p	1.08	0.7353
miR-301b	1.08	0.7066
miR-494-3p	1.08	0.8688
let-7d-5p	1.07	0.5978
miR-204-5p	1.07	0.8421
miR-331-3p	1.07	0.6581
miR-940	1.06	0.6077
miR-299-5p	1.06	0.7219
miR-24-3p	1.05	0.8668
miR-379-5p	1.05	0.8489
miR-409-3p	1.04	0.8987
miR-16-5p	1.04	0.8755
let-7f-5p	1.04	0.8523
miR-10b-5p	1.03	0.7766
miR-99a-3p	1.03	0.7487
miR-27a-3p	1.03	0.8912
miR-26b-5p	1.03	0.8459
miR-362-5p	1.03	0.9379
miR-365a-3p	1.03	0.9358
miR-19b-3p	1.02	0.9292
miR-217	1.01	0.9407
miR-100-5p	1.01	0.9730
miR-491-5p	1.01	0.9871
let-7i-5p	1.00	0.9794
miR-130a-3p	1.00	0.9898
miR-424-5p	1.00	0.9845
miR-155-5p	1.00	0.9994
miR-590-5p	1.00	0.9919

miRNA	Fold	P value
miR-324-3p	0.99	0.9753
miR-185-5p	0.99	0.9748
miR-106a-5p	0.99	0.9479
miR-32-5p	0.99	0.8836
miR-454-3p	0.98	0.9183
miR-324-5p	0.98	0.9130
miR-370-3p	0.98	0.9075
miR-224-5p	0.98	0.9045
miR-342-3p	0.98	0.9226
miR-382-5p	0.97	0.9250
miR-663a	0.97	0.7958
miR-20a-5p	0.97	0.8445
miR-99b-5p	0.97	0.9012
miR-99a-5p	0.96	0.7927
miR-212-3p	0.96	0.2271
miR-137	0.96	0.7615
miR-187-5p	0.95	0.9221
miR-503-5p	0.95	0.8575
miR-92a-3p	0.95	0.7303
miR-345-5p	0.94	0.8210
miR-495-3p	0.94	0.6879
miR-410-3p	0.94	0.8381
miR-766-3p	0.94	0.6955
miR-377-3p	0.94	0.7838
miR-106b-5p	0.94	0.5813
miR-652-3p	0.93	0.8429
miR-337-5p	0.93	0.4815
miR-361-5p	0.93	0.3774
miR-18b-5p	0.93	0.6576
let-7d-3p	0.92	0.6912
miR-193a-3p	0.92	0.1585
miR-15b-5p	0.92	0.8320
miR-874-3p	0.91	0.7003
miR-25-3p	0.91	0.6320
miR-570-3p	0.91	0.8628
let-7g-5p	0.91	0.6856
miR-29b-3p	0.91	0.5634
miR-101-3p	0.91	0.4859
miR-126-3p	0.90	0.6297
miR-381-3p	0.90	0.5303
miR-199a-5p	0.90	0.5063
miR-210-3p	0.90	0.6800
miR-15a-5p	0.89	0.4408
let-7b-5p	0.88	0.5863
miR-148b-3p	0.88	0.5180
miR-93-5p	0.88	0.5802
miR-576-5p	0.87	0.4942
miR-28-5p	0.86	0.4215
miR-335-5p	0.86	0.8285
miR-298	0.86	0.6514
miR-140-5p	0.86	0.1137
miR-497-5p	0.85	0.6665
miR-130b-3p	0.85	0.6546
miR-29b-2-5p	0.85	0.7341
miR-660-5p	0.85	0.3100
miR-30b-3p	0.84	0.8318
miR-376a-3p	0.83	0.5012
miR-188-5p	0.83	0.3458
miR-19a-3p	0.83	0.0854
miR-18a-5p	0.82	0.3537
miR-17-5p	0.81	0.1053
miR-487b-3p	0.80	0.5422
miR-484	0.79	0.4419
miR-589-5p	0.78	0.6739
miR-216a-5p	0.78	0.1548
miR-501-5p	0.77	0.4985
miR-154-5p	0.76	0.1459
miR-92b-3p	0.74	0.0891
miR-545-3p	0.73	0.0414
miR-126-5p	0.72	0.4362
miR-7-5p	0.71	0.0944
miR-136-5p	0.71	0.0533
miR-34c-5p	0.68	0.6759
miR-218-5p	0.67	0.0275
miR-128-3p	0.66	0.0736
miR-141-3p	0.66	0.6345
miR-33a-5p	0.64	0.1529
miR-219a-5p	0.61	0.3050

miRNA	Fold	P value
miR-148a-3p	0.49	0.0230
miR-765	0.44	0.2722
miR-615-3p	0.39	0.2240
miR-550a-5p	0.34	0.0341
miR-662	0.29	0.0420
miR-185-3p	0.25	0.0568

miRNA	Fold	P value
miR-18a-3p	0.57	0.0561
miR-629-5p	0.57	0.2542
miR-30c-2-3p	0.56	0.2267
miR-16-1-3p	0.56	0.0413
miR-584-5p	0.54	0.2658
miR-625-3p	0.50	0.0017

miRNA	Fold	P value
miR-302c-5p	0.16	0.0094
miR-142-5p	0.15	0.0093
miR-623	0.14	0.0035
miR-26a-2-3p	0.08	0.0064
miR-199b-5p	0.04	0.0014

Table S 12. ***Results of the qRT-PCR array performed to compare miRNA level in HUVECs treated with epirubicin or controls****. Data are expressed as fold change (Epirubicin vs Control) and their corresponding P-values. miRNAs are detected in at least one out of two replicates, with Ct lower than 40.*

miRNA	Fold	P value
miR-668-3p	25.68	0.3551
miR-760	7.42	0.1780
miR-934	6.97	0.1199
miR-190a-5p	5.36	0.1643
miR-373-5p	4.84	0.4732
miR-665	4.12	0.2802
miR-141-3p	3.39	0.5498
miR-651-5p	3.06	0.5180
miR-572	3.01	0.5275
miR-146b-5p	2.86	0.3707
miR-103a-3p	2.86	0.0640
miR-192-5p	2.62	0.1263
miR-598-3p	2.49	0.0249
miR-150-5p	2.03	0.4632
miR-139-5p	1.99	0.0296
miR-542-5p	1.99	0.0760
miR-491-3p	1.95	0.3203
miR-330-3p	1.86	0.3064
miR-34c-3p	1.81	0.4707
miR-199b-5p	1.81	0.6205
miR-323a-3p	1.75	0.2285
miR-181d-5p	1.68	0.2096
miR-574-3p	1.68	0.1013
miR-450a-5p	1.65	0.0736
miR-132-3p	1.63	0.4835
miR-204-5p	1.62	0.2501
miR-485-3p	1.53	0.1125
miR-361-3p	1.53	0.0006
miR-411-5p	1.51	0.0586
miR-877-5p	1.50	0.1051
miR-299-3p	1.48	0.2727
miR-10a-5p	1.47	0.3467
miR-181c-5p	1.47	0.3966
miR-194-5p	1.47	0.0349
miR-195-5p	1.47	0.2026
miR-151a-3p	1.46	0.0805
miR-494-3p	1.45	0.5714
miR-505-3p	1.45	0.4144
miR-374a-5p	1.44	0.1579
miR-10b-5p	1.44	0.3776
miR-887-3p	1.43	0.4666
miR-654-5p	1.42	0.6473
miR-374b-5p	1.42	0.0671
miR-539-5p	1.40	0.2605
miR-146a-5p	1.39	0.1638
miR-326	1.39	0.4877
miR-421	1.38	0.1110
miR-193a-5p	1.37	0.1626
miR-151a-5p	1.36	0.0726
miR-27b-3p	1.36	0.0480
miR-26a-5p	1.36	0.1968
miR-301a-3p	1.34	0.0045
miR-127-3p	1.34	0.2587
miR-149-5p	1.33	0.0083
miR-125a-5p	1.31	0.1364
miR-140-3p	1.31	0.5317
miR-328-3p	1.30	0.1159
miR-148b-3p	1.29	0.5591
miR-320a	1.28	0.0536
miR-152-3p	1.27	0.0457
miR-299-5p	1.25	0.0739
miR-193a-3p	1.24	0.1429
miR-582-5p	1.24	0.2166
miR-455-5p	1.22	0.3654
miR-30d-5p	1.22	0.4668
miR-188-5p	1.22	0.5005
miR-301b	1.21	0.3165
miR-30c-5p	1.21	0.0586
miR-26b-5p	1.21	0.1939
miR-145-5p	1.21	0.2123
miR-30e-5p	1.20	0.4266
miR-196a-5p	1.20	0.8035
miR-196b-5p	1.20	0.5671
miR-30e-3p	1.19	0.2313
miR-338-3p	1.19	0.0330
let-7e-5p	1.18	0.4323
miR-501-5p	1.18	0.2416
miR-30a-5p	1.17	0.0856

miRNA	Fold	P value
miR-23a-3p	1.17	0.0527
let-7c-5p	1.16	0.0389
miR-744-5p	1.16	0.1016
miR-452-5p	1.16	0.7024
miR-20a-5p	1.15	0.0213
miR-425-5p	1.15	0.3754
miR-425-3p	1.15	0.0190
miR-23b-3p	1.14	0.3476
miR-940	1.14	0.7289
miR-369-5p	1.13	0.6201
miR-222-3p	1.13	0.4387
miR-545-3p	1.12	0.6391
miR-423-5p	1.12	0.3126
miR-362-5p	1.12	0.5591
miR-339-5p	1.11	0.3614
miR-345-5p	1.11	0.6375
miR-107	1.11	0.4642
miR-337-3p	1.11	0.6777
miR-181b-5p	1.10	0.0437
miR-99a-3p	1.10	0.5659
miR-98-5p	1.10	0.3541
miR-29c-3p	1.10	0.6801
let-7d-5p	1.09	0.6018
miR-31-5p	1.09	0.1498
miR-424-5p	1.09	0.5003
miR-181a-3p	1.08	0.8169
miR-214-3p	1.07	0.5676
miR-500a-5p	1.07	0.9056
let-7a-5p	1.06	0.7123
miR-191-5p	1.05	0.8725
miR-21-3p	1.05	0.6311
miR-19b-3p	1.05	0.8298
miR-454-3p	1.04	0.2646
miR-324-5p	1.04	0.4245
miR-331-3p	1.04	0.6417
miR-154-5p	1.04	0.7274
miR-99b-5p	1.03	0.3907
miR-17-5p	1.03	0.7976
miR-127-5p	1.03	0.9301
miR-15b-5p	1.03	0.9241
miR-31-3p	1.03	0.7917
miR-423-3p	1.03	0.8110
miR-21-5p	1.03	0.5117
let-7f-5p	1.02	0.6091
miR-532-5p	1.02	0.8991
miR-590-5p	1.02	0.8178
miR-126-5p	1.02	0.9139
miR-18b-5p	1.02	0.5388
miR-431-5p	1.02	0.9530
miR-340-5p	1.01	0.9262
miR-22-5p	1.01	0.9417
miR-210-3p	1.01	0.9764
miR-32-5p	1.01	0.9208
miR-432-5p	1.01	0.7902
miR-181a-5p	1.01	0.9038
miR-629-5p	1.00	0.9944
miR-101-3p	1.00	0.9973
miR-140-5p	1.00	0.9875
miR-24-3p	0.99	0.9653
miR-324-3p	0.99	0.7431
miR-19a-3p	0.99	0.8380
miR-125b-5p	0.99	0.9216
miR-30b-5p	0.99	0.9699
miR-34a-5p	0.99	0.9401
miR-197-3p	0.99	0.9259
miR-329-3p	0.98	0.8790
let-7g-5p	0.98	0.9335
miR-134-5p	0.98	0.8827
miR-342-3p	0.98	0.8584
miR-137	0.98	0.8377
miR-130a-3p	0.97	0.8660
miR-379-5p	0.97	0.8726
let-7b-5p	0.97	0.6336
miR-652-3p	0.97	0.8304
miR-376b-3p	0.96	0.7679
miR-126-3p	0.96	0.7960
miR-361-5p	0.96	0.7626
miR-493-3p	0.95	0.8476

miRNA	Fold	P value
miR-93-5p	0.95	0.7291
miR-874-3p	0.95	0.6957
miR-106a-5p	0.95	0.6170
miR-148a-3p	0.94	0.1919
miR-29a-3p	0.93	0.7121
miR-155-5p	0.93	0.0930
miR-27a-3p	0.93	0.4648
miR-199a-3p	0.92	0.0908
miR-376c-3p	0.92	0.4483
miR-16-5p	0.92	0.5958
miR-186-5p	0.92	0.0345
miR-365a-3p	0.91	0.6817
miR-99a-5p	0.91	0.6641
miR-25-3p	0.91	0.6676
miR-377-3p	0.90	0.5801
miR-221-3p	0.90	0.4977
miR-660-5p	0.89	0.5854
miR-502-5p	0.89	0.4317
miR-28-5p	0.89	0.3001
miR-215-5p	0.89	0.2156
miR-409-3p	0.89	0.1090
miR-106b-5p	0.89	0.1544
miR-382-5p	0.88	0.6783
miR-337-5p	0.88	0.0358
miR-335-5p	0.87	0.8758
miR-92b-3p	0.87	0.0188
miR-224-5p	0.87	0.5422
miR-193b-3p	0.87	0.5699
miR-433-3p	0.85	0.0998
miR-185-5p	0.85	0.4444
miR-18a-5p	0.85	0.2206
miR-92a-3p	0.84	0.4249
miR-491-5p	0.83	0.4960
miR-503-5p	0.83	0.2557
miR-199a-5p	0.83	0.2560
miR-381-3p	0.82	0.3513
miR-22-3p	0.82	0.4785
miR-376a-3p	0.82	0.1087
miR-100-5p	0.81	0.1711
let-7i-5p	0.81	0.0317
miR-484	0.80	0.2966
miR-29b-3p	0.79	0.3003
miR-663a	0.79	0.2586
miR-219a-5p	0.78	0.0254
let-7d-3p	0.78	0.3205
miR-216a-5p	0.77	0.1634
miR-217	0.77	0.0725
miR-15a-5p	0.76	0.0394
miR-130b-3p	0.76	0.2398
miR-18a-3p	0.76	0.0173
miR-218-5p	0.75	0.0043
miR-671-5p	0.75	0.0925
miR-410-3p	0.74	0.0250
miR-374b-3p	0.74	0.3029
miR-766-3p	0.73	0.2488
miR-7-5p	0.73	0.3363
miR-576-5p	0.71	0.1185
miR-29b-2-5p	0.71	0.3567
miR-370-3p	0.71	0.0793
miR-495-3p	0.69	0.2444
miR-589-5p	0.69	0.6797
miR-487b-3p	0.69	0.1944
miR-136-5p	0.69	0.2002
miR-497-5p	0.69	0.1537
miR-33a-5p	0.68	0.0967
miR-628-3p	0.66	0.0988
miR-627-5p	0.65	0.6012
miR-625-3p	0.64	0.0622
miR-30c-2-3p	0.64	0.4863
miR-363-3p	0.63	0.5926
miR-212-3p	0.62	0.5342
miR-584-5p	0.62	0.3530
miR-483-3p	0.60	0.3396
miR-34c-5p	0.58	0.5285
miR-9-5p	0.58	0.0493
miR-154-3p	0.55	0.0534
miR-514a-3p	0.55	0.0509
miR-550a-5p	0.55	0.4692

miRNA	Fold	P value
miR-142-5p	0.54	0.0831
miR-128-3p	0.51	0.0051
miR-124-3p	0.50	0.3617
miR-33b-5p	0.39	0.0988
miR-623	0.38	0.1432
miR-185-3p	0.33	0.0890

miRNA	Fold	P value
miR-662	0.27	0.0163
miR-570-3p	0.27	0.0965
miR-486-5p	0.26	0.0578
miR-608	0.23	0.0261
miR-26a-2-3p	0.21	0.0462
miR-16-1-3p	0.15	0.0034

miRNA	Fold	P value
miR-765	0.14	0.0046
miR-615-3p	0.13	0.0109
miR-302c-5p	0.13	0.0028
miR-602	0.09	0.0027
miR-518c-5p	0.03	0.0007

Table S 13. ***Results of the qRT-PCR array performed to compare miRNA level in HUVECs treated with paclitaxel or controls****. Data are expressed as fold change (Paclitaxel vs Control) and their corresponding P-values. miRNAs are detected in at least one out of two replicates, with Ct lower than 40.*

	MDA-MB-231	MDA-MB-231/epi	MDA-MB-231/pacli
miR-373-3p	651121	387814	849997
miR-887-3p	171.1	49054	7423
miR-122-5p	36635	529242	77261
miR-129-5p	61169	19416	2252

Table S 14. ***Transfection efficiency of miR-373-3p, miR-887-3p, miR-122-5p, miR-129-5p in sensitive and resistant MDA-MB-231****. Cells were transfected with 25 nM of pre-miR-373-3p, pre-miR-887-3p, pre-miR-122-5p or pre-miR-129-5p, and the control. Total RNAs were isolated 48h post transfection and their level assessed by qRT-PCR. Results are presented as mean of the fold change of the control, per cell type. The pre-miR control consist of a random nucleotide sequence with no effect on any known mRNA expression.*

Gene	Fold	Q value
SLC2A4	2.90	0.0052
ABCA1	2.55	0.0012
TP53INP1	2.26	0.0002
RNF150	2.23	0.0364
KCNJ8	2.12	0.0425
RAB11FIP1	2.02	0.0003
PLAGL2	0.50	1.36E-12
PRDM4	0.50	1.06E-37
NPAS3	0.50	8.73E-06
TBC1D2	0.50	1.69E-07
BICC1	0.49	5.86E-09
MLLT6	0.49	1.78E-14
DYRK4	0.49	1.67E-06
SLC39A6	0.48	2.08E-14
CMPK1	0.48	4.43E-20
SYDE1	0.47	1.18E-12
RELA	0.47	1.57E-24

Gene	Fold	Q value
IRF2	0.47	1.53E-16
FAT4	0.47	0.0343
ZNF385A	0.47	1.37E-06
NFIB	0.46	4.98E-12
PDCD1LG2	0.45	0.0056
DCAF12	0.45	4.12E-14
CAMK2N1	0.45	3.15E-13
PIP4K2A	0.45	6.09E-26
GPR161	0.44	1.13E-18
CPEB2	0.44	0.0002
COL4A4	0.43	0.0322
SPRYD3	0.43	8.79E-24
SCN2A	0.42	0.0005
FBXO39	0.41	0.0299
ATF6B	0.41	1.26E-14
SCD5	0.40	2.40E-19
HOXB3	0.39	0.0001

Gene	Fold	Q value
CROT	0.38	2.01E-12
DAZAP2	0.38	5.07E-50
ANKRD13B	0.37	3.59E-08
ZBTB47	0.37	6.15E-17
ZNF25	0.35	2.23E-17
GPM6A	0.35	2.19E-06
MBD2	0.35	3.36E-46
HIVEP2	0.35	2.34E-07
ANKRD52	0.35	1.46E-13
SLAIN1	0.34	1.15E-16
KIF26B	0.32	0.0016
KDM1B	0.32	2.05E-15
FYCO1	0.31	1.90E-21
GALNT3	0.30	7.63E-15
LEF1	0.30	3.38E-15
TGFBR2	0.27	6.67E-36
NTN4	0.26	1.13E-39

Table S 15. ***51 genes identified by the RNA sequencing and predicted to be directly targeted by miR-373-3p in MDA-MB-231.*** *The selected genes are predicted to be direct targets of miR-373-3p by the TargetScan algorithm and are regulated in MDA-MB-231 transfected with 25 nM of pre-miR-373-3p for 48h, compared to the cells transfected with pre-miR-Control. The pre-miR control consists of a random nucleotide sequence with no effect on any known mRNA expression. Genes regulated with a fold change superior to 2 and a q-value < 0.05 are represented. Data are expressed as fold change (miR-373-3p vs Control) and their corresponding q-value.*

References

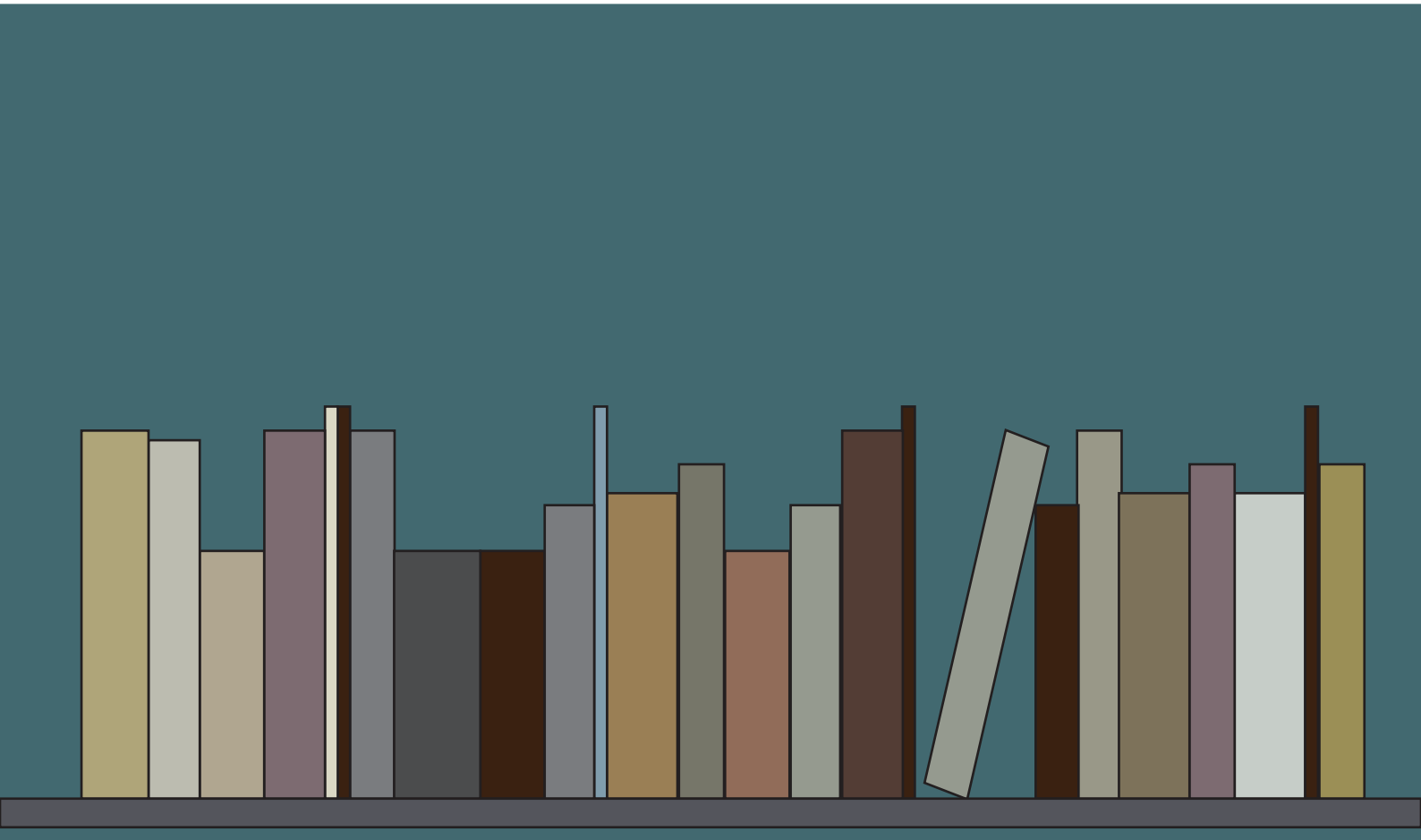

References

van ’t Veer, L.J. et al., 2002. Gene expression profiling predicts clinical outcome of breast cancer. *Nature*, 415(6871), pp.530–6.

Aas, T. et al., 1996. Specific P53 mutations are associated with de novo resistance to doxorubicin in breast cancer patients. *Nature Medicine*, 2(7), pp.811–814.

Adi Harel, S. et al., 2015. Reactivation of epigenetically silenced miR-512 and miR-373 sensitizes lung cancer cells to cisplatin and restricts tumor growth. *Cell death and differentiation*, 22(8), pp.1328–40.

Aigner, K. et al., 2007. The transcription factor ZEB1 (δEF1) promotes tumour cell dedifferentiation by repressing master regulators of epithelial polarity. *Oncogene*, 26(49), pp.6979–6988.

Akers, J.C. et al., 2013. Biogenesis of extracellular vesicles (EV): Exosomes, microvesicles, retrovirus-like vesicles, and apoptotic bodies. *Journal of Neuro-Oncology*, 113(1), pp.1–11.

Al-Hajj, M. et al., 2003. Prospective identification of tumorigenic breast cancer cells. *Proceedings of the National Academy of Sciences*, 100(7), pp.3983–3988.

Al-Nedawi, K. et al., 2009. Endothelial expression of autocrine VEGF upon the uptake of tumor-derived microvesicles containing oncogenic EGFR. *Proceedings of the National Academy of Sciences*, 106(10), pp.3794–3799.

Alvarez-Erviti, L. et al., 2011. Delivery of siRNA to the mouse brain by systemic injection of targeted exosomes. *Nature Biotechnology*, 29(4), pp.341–345.

Anampa, J. et al., 2015. Progress in adjuvant chemotherapy for breast cancer: An overview. *BMC Medicine*, 13(1), p.195.

Anders, S., Pyl, P.T. & Huber, W., 2015. HTSeq-A Python framework to work with high-throughput sequencing data. *Bioinformatics*, 31(2), pp.166–169.

Andrews, S., 2010. FastQC: a quality control tool for high throughput sequence data. Available at: http://www.bioinformatics.babraham.ac.uk/projects/fastqc.

Arroyo, J.D. et al., 2011. Argonaute2 complexes carry a population of circulating microRNAs independent of vesicles in human plasma. *Proceedings of the National Academy of Sciences of the United States of America*, 108(12), pp.5003–8.

Aung, T. et al., 2011. Exosomal evasion of humoral immunotherapy in aggressive B-cell lymphoma modulated by ATP-binding cassette transporter A3. *Proceedings of the National Academy of Sciences*, 108(37), pp.15336–15341.

Azuma-Mukai, A. et al., 2008. Characterization of endogenous human Argonautes and their miRNA partners in RNA silencing. *Proceedings of the National Academy of Sciences of the United States of America*, 105(23), pp.7964–9.

Baietti, M.F. et al., 2012. Syndecan–syntenin–ALIX regulates the biogenesis of exosomes. *Nature Cell Biology*, 14(7), pp.677–685.

Ban, H.S. et al., 2016. A novel malate dehydrogenase 2 inhibitor suppresses hypoxia-inducible factor-1 by regulating mitochondrial respiration. *PLoS ONE*, 11(9), pp.1–14.

Bartel, D.P., 2004. MicroRNAs: Genomics, Biogenesis, Mechanism, and Function. *Cell*, 116(2), pp.281–297.

Bartel, D.P., 2009. MicroRNAs: Target Recognition and Regulatory Functions. *Cell*, 136(2), pp.215–233.

Batagov, A.O. & Kurochkin, I. V, 2013. Exosomes secreted by human cells transport largely mRNA fragments that are enriched in the 3′-untranslated regions. *Biology Direct*, 8(1), p.12.

Beer, L. et al., 2014. High dose ionizing radiation regulates micro RNA and gene expression changes in human peripheral blood mononuclear cells. *BMC genomics*, 15(1), p.814.

Beg, M.S. et al., 2017. Phase I study of MRX34, a liposomal miR-34a mimic, administered twice weekly in patients with advanced solid tumors. *Investigational new drugs*, 35(2), pp.180–188.

Behm-Ansmant, I. et al., 2006. mRNA degradation by miRNAs and GW182 requires both CCR4:NOT deadenylase and DCP1:DCP2 decapping complexes. *Genes & development*, 20(14), pp.1885–98.

Bishop, J.F. et al., 1997. Paclitaxel as first-line treatment for metastatic breast cancer. The Taxol Investigational Trials Group, Australia and New Zealand. *Oncology (Williston Park, N.Y.)*, 11(4 Suppl 3), pp.19–23.

Bobrie, A. et al., 2012. Diverse subpopulations of vesicles secreted by different intracellular mechanisms are present in exosome preparations obtained by differential ultracentrifugation. *Journal of Extracellular Vesicles*, 1(0), pp.1–11.

Bolger, A.M., Lohse, M. & Usadel, B., 2014. Trimmomatic: A flexible trimmer for Illumina sequence data. *Bioinformatics*, 30(15), pp.2114–2120.

Bontenbal, M. et al., 1998. Doxorubicin vs epirubicin, report of a second-line randomized phase II/III study in advanced breast cancer. *British Journal of Cancer*, 77(12), pp.2257–2263.

Bouvy, C. et al., 2017. Transfer of multidrug resistance among acute myeloid leukemia cells via extracellular vesicles and their microRNA cargo. *Leukemia Research*, 62, pp.70–76.

Bovy, N. et al., 2015. Endothelial exosomes contribute to the antitumor response during breast cancer neoadjuvant chemotherapy via microRNA transfer. *Oncotarget*, 6(12), pp.10253–10266.

De Brabander, M. et al., 1981. Taxol induces the assembly of free microtubules in living cells and blocks the organizing capacity of the centrosomes and kinetochores. *Proceedings of the National Academy of Sciences*, 78(9), pp.5608–5612.

Brabletz, T. et al., 2018. EMT in cancer. *Nature Reviews Cancer*, 18(2), pp.128–134.

Braun, J.E. et al., 2012. A direct interaction between DCP1 and XRN1 couples mRNA decapping to 5′ exonucleolytic degradation. *Nature Structural and Molecular Biology*, 19(12), pp.1324–1331.

Brest, P. et al., 2011. MiR-129-5p is required for histone deacetylase inhibitor-induced cell death in thyroid cancer cells. *Endocrine-Related Cancer*, 18(6), pp.711–719.

Bunggulawa, E.J. et al., 2018. Recent advancements in the use of exosomes as drug

delivery systems. *Journal of Nanobiotechnology*, pp.1–13.

Burkhart, C.A. et al., 1994. Relationship between the structure of taxol and other taxanes on induction of tumor necrosis factor-alpha gene expression and cytotoxicity. *Cancer research*, 54(22), pp.5779–82.

Cai, J. et al., 2013. Extracellular vesicle-mediated transfer of donor genomic DNA to recipient cells is a novel mechanism for genetic influence between cells. *Journal of Molecular Cell Biology*, 5(4), pp.227–238.

Calin, G.A. et al., 2004. Human microRNA genes are frequently located at fragile sites and genomic regions involved in cancers. *Proceedings of the National Academy of Sciences of the United States of America*, 101(9), pp.2999–3004.

Carmeliet, P. & Jain, R.K., 2000. Angiogenesis in cancer and other diseases. *Nature*, 407(6801), pp.249–257.

Chabner, B.A. & Roberts, T.G., 2005. Timeline: Chemotherapy and the war on cancer. *Nature reviews. Cancer*, 5(1), pp.65–72.

Chaffer, C.L. et al., 2016. EMT, cell plasticity and metastasis. *Cancer and Metastasis Reviews*, 35(4), pp.645–654.

Chalmin, F. et al., 2010. Membrane-associated Hsp72 from tumor-derived exosomes mediates STAT3-dependent immunosuppressive function of mouse and human myeloid-derived suppressor cells. *The Journal of clinical investigation*, 120(2), pp.457–71.

Chen, D. et al., 2015. MiR-373 drives the epithelial-to-mesenchymal transition and metastasis via the miR-373-TXNIP-HIF1α-TWIST signaling axis in breast cancer. *Oncotarget*, 6(32), pp.32701–12.

Chen, G. et al., 2014. Combined downregulation of microRNA-133a and microRNA-133b predicts chemosensitivity of patients with esophageal squamous cell carcinoma undergoing paclitaxel-based chemotherapy. *Medical Oncology*, 31(11), pp.1–8.

Chen, J. et al., 2012. Down-regulation of microRNA-200c is associated with drug resistance in human breast cancer. *Medical oncology (Northwood, London, England)*, 29(4), pp.2527–34.

Chen, Q. et al., 2016. Different populations of Wnt-containing vesicles are individually released from polarized epithelial cells. *Scientific Reports*, 6(June), pp.1–10.

Chendrimada, T.P. et al., 2005. TRBP recruits the Dicer complex to Ago2 for microRNA processing and gene silencing. *Nature*, 436(7051), pp.740–4.

Cheng, D. et al., 2018. LncRNA HOTAIR epigenetically suppresses miR-122 expression in hepatocellular carcinoma via DNA methylation. *EBioMedicine*, 36, pp.159–170.

Chevillet, J.R. et al., 2014. Quantitative and stoichiometric analysis of the microRNA content of exosomes. *Proceedings of the National Academy of Sciences of the United States of America*, 111(41), pp.14888–93.

Chien, A.J. & Moasser, M.M., 2008. Cellular Mechanisms of Resistance to Anthracyclines and Taxanes in Cancer: Intrinsic and Acquired. *Seminars in Oncology*, 35(SUPPL. 2), pp.S1–S14.

Chikamori, K. et al., 2010. DNA Topoisomerase II Enzymes as Molecular Targets for Cancer Chemotherapy. *Current Cancer Drug Targets*, 10(7), pp.758–771.

Chittaranjan, S. et al., 2014. Autophagy inhibition augments the anticancer effects of epirubicin treatment in anthracycline-sensitive and -resistant triple-negative breast cancer. *Clinical Cancer Research*, 20(12), pp.3159–3173.

Christie, M. et al., 2013. Structure of the PAN3 Pseudokinase Reveals the Basis for Interactions with the PAN2 Deadenylase and the GW182 Proteins. *Molecular Cell*, 51(3), pp.360–373.

Christopher, A.F. et al., 2016. MicroRNA therapeutics: Discovering novel targets and developing specific therapy. *Perspectives in clinical research*, 7(2), pp.68–74.

Ciravolo, V. et al., 2012. Potential role of HER2-overexpressing exosomes in countering trastuzumab-based therapy. *Journal of Cellular Physiology*, 227(2), pp.658–667.

Clayton, A. et al., 2001. Summary of the ISEV workshop on extracellular vesicles as disease biomarkers , held in. *Journal of Extracellular Vesicles*, 7(1).

Colditz, G.A. & Bohlke, K., 2014. Priorities for the primary prevention of breast cancer. *CA: a cancer journal for clinicians*, 64(3), pp.186–94.

Colombo, M., Raposo, G. & Théry, C., 2014. Biogenesis, Secretion, and Intercellular Interactions of Exosomes and Other Extracellular Vesicles. *Annual Review of Cell and Developmental Biology*, 30(1), pp.255–289.

Conte, P.F. et al., 2000. Role of Epirubicin in Advanced Breast Cancer. *Clinical Breast Cancer*, 1(1), pp.S46–S51.

Corcoran, C. et al., 2012. Docetaxel-resistance in prostate cancer: evaluating associated phenotypic changes and potential for resistance transfer via exosomes. N. Kyprianou, ed. *PloS one*, 7(12), p.e50999.

Corrie, P.G., 2008. Cytotoxic chemotherapy: clinical aspects. *Medicine*, 36(1), pp.24–28.

Cougot, N., Babajko, S. & Séraphin, B., 2004. Cytoplasmic foci are sites of mRNA decay in human cells. *The Journal of cell biology*, 165(1), pp.31–40.

Coulouarn, C. et al., 2009. Loss of miR-122 expression in liver cancer correlates with suppression of the hepatic phenotype and gain of metastatic properties. *Oncogene*, 28(40), pp.3526–3536.

Crompot, E. et al., 2017. Extracellular vesicles of bone marrow stromal cells rescue chronic lymphocytic leukemia B cells from apoptosis, enhance their migration and induce gene expression modifications. *Haematologica*, 102(9), pp.1594–1604.

Crosby, M.E. et al., 2009. MicroRNA regulation of DNA repair gene expression in hypoxic stress. *Cancer research*, 69(3), pp.1221–9.

Crown, J., 2004. Docetaxel and Paclitaxel in the Treatment of Breast Cancer: A Review of Clinical Experience. *The Oncologist*, 9(suppl_2), pp.24–32.

Van Deun, J. et al., 2017. EV-TRACK: transparent reporting and centralizing knowledge in extracellular vesicle research. *Nature Methods*, 14(3), pp.228–232.

Van Deun, J. et al., 2014. The impact of disparate isolation methods for extracellular vesicles on downstream RNA profiling. *Journal of extracellular vesicles*, 3, pp.1–14.

Díaz-Toledano, R. et al., 2009. In vitro characterization of a miR-122-sensitive double-helical switch element in the 5' region of hepatitis C virus RNA. *Nucleic acids research*, 37(16), pp.5498–510.

Diepenbruck, M. & Christofori, G., 2016. Epithelial-mesenchymal transition (EMT) and metastasis: Yes, no, maybe? *Current Opinion in Cell Biology*, 43, pp.7–13.

Dobin, A. et al., 2013. STAR: ultrafast universal RNA-seq aligner. *Bioinformatics (Oxford, England)*, 29(1), pp.15–21.

Dumalaon-Canaria, J.A. et al., 2014. What causes breast cancer? A systematic review of causal attributions among breast cancer survivors and how these compare to expert-endorsed risk factors. *Cancer Causes and Control*, 25(7), pp.771–785.

Dyrskjøt, L. et al., 2009. Genomic profiling of microRNAs in bladder cancer: miR-129 is associated with poor outcome and promotes cell death in vitro. *Cancer Research*, 69(11), pp.4851–4860.

Early Breast Cancer Trialists' Collaborative Group (EBCTCG), 2015. Aromatase inhibitors versus tamoxifen in early breast cancer: patient-level meta-analysis of the randomised trials. *Lancet (London, England)*, 386(10001), pp.1341–1352.

Early Breast Cancer Trialists' Collaborative Group (EBCTCG) et al., 2012. Comparisons between different polychemotherapy regimens for early breast cancer: Meta-analyses of long-term outcome among 100 000 women in 123 randomised trials. *The Lancet*, 379(9814), pp.432–444.

Early Breast Cancer Trialists' Collaborative Group (EBCTCG) et al., 2011. Effect of radiotherapy after breast-conserving surgery on 10-year recurrence and 15-year breast cancer death: meta-analysis of individual patient data for 10,801 women in 17 randomised trials. *Lancet (London, England)*, 378(9804), pp.1707–16.

Eijdems, E.W. et al., 1995. Reduced topoisomerase II activity in multidrug-resistant human non-small cell lung cancer cell lines. *British journal of cancer*, 71(1), pp.40–7.

van Eijndhoven, M.A.J. et al., 2016. Plasma vesicle miRNAs for therapy response monitoring in Hodgkin lymphoma patients. *JCI Insight*, 1(19), pp.1–16.

Eliyatkin, N. et al., 2015. Molecular Classification of Breast Carcinoma: From Traditional, Old-Fashioned Way to A New Age, and A New Way. *Journal of Breast Health*, 11(2), pp.59–66.

Elmén, J. et al., 2008. LNA-mediated microRNA silencing in non-human primates. *Nature*, 452(7189), pp.896–899.

Elston, C.W. & Ellis, I.O., 1991. Pathological prognostic factors in breast cancer: experience from a large study with long-term follow-up. *Histopathology*, 19, pp.403–410.

Endzeliņš, E. et al., 2017. Detection of circulating miRNAs: comparative analysis of extracellular vesicle-incorporated miRNAs and cell-free miRNAs in whole plasma of prostate cancer patients. *BMC cancer*, 17(1), p.730.

Escrevente, C. et al., 2011. Interaction and uptake of exosomes by ovarian cancer cells. *BMC cancer*, 11(1), p.108.

Escudier, B. et al., 2005. Vaccination of metastatic melanoma patients with autologous dendritic cell (DC) derived-exosomes: results of thefirst phase I clinical trial. *Journal of Translational Medicine*, 3(1), p.10.

Eulalio, A., Behm-Ansmant, I. & Izaurralde, E., 2007. P bodies: At the crossroads of post-transcriptional pathways. *Nature Reviews Molecular Cell Biology*, 8(1), pp.9–22.

Fabbri, M. et al., 2012. MicroRNAs bind to Toll-like receptors to induce prometastatic inflammatory response. *Proceedings of the National Academy of Sciences of the United States of America*, 109(31), pp.E2110-6.

Farazi, T.A. et al., 2014. Identification of distinct miRNA target regulation between breast cancer molecular subtypes using AGO2-PAR-CLIP and patient datasets. *Genome biology*, 15(1), p.R9.

Feng, D. et al., 2010. Cellular Internalization of Exosomes Occurs Through Phagocytosis. *Traffic*, 11(5), pp.675–687.

Feng, H. et al., 2016. Epirubicin pretreatment enhances NK cell-mediated cytotoxicity against breast cancer cells in vitro. *American Journal of Translational Research*, 8(2), pp.473–484.

Ferguson, S.W. & Nguyen, J., 2016. Exosomes as therapeutics: The implications of molecular composition and exosomal heterogeneity. *Journal of controlled release : official journal of the Controlled Release Society*, 228, pp.179–190.

Ferlini, C. et al., 2003. Bcl-2 down-regulation is a novel mechanism of paclitaxel resistance. *Molecular pharmacology*, 64(1), pp.51–8.

Fesler, A., Zhai, H. & Ju, J., 2014. miR-129 as a novel therapeutic target and biomarker in gastrointestinal cancer. *OncoTargets and Therapy*, 7, pp.1481–1485.

Fitzner, D. et al., 2011. Selective transfer of exosomes from oligodendrocytes to microglia by macropinocytosis. *Journal of cell science*, 124(Pt 3), pp.447–58.

Fong, M.Y. et al., 2015. Breast-cancer-secreted miR-122 reprograms glucose metabolism in premetastatic niche to promote metastasis. *Nature cell biology*, 17(2), pp.183–94.

Fornari, F. et al., 2009. MiR-122/cyclin G1 interaction modulates p53 activity and affects doxorubicin sensitivity of human hepatocarcinoma cells. *Cancer Research*, 69(14), pp.5761–5767.

Frères, P. et al., 2015. Neoadjuvant Chemotherapy in Breast Cancer Patients Induces miR-34a and miR-122 Expression. *Journal of cellular physiology*, 230(2), pp.473–81.

Gallo, A. et al., 2012. The Majority of MicroRNAs Detectable in Serum and Saliva Is Concentrated in Exosomes K. Afarinkia, ed. *PLoS ONE*, 7(3), p.e30679.

Gao, Y. et al., 2016. MicroRNA-129 in Human Cancers: From Tumorigenesis to Clinical Treatment. *Cellular Physiology and Biochemistry*, 39(6), pp.2186–2202.

Gaudelot, K. et al., 2017. Targeting miR-21 decreases expression of multi-drug resistant genes and promotes chemosensitivity of renal carcinoma.

Gelderblom, H. et al., 2001. Cremophor EL: The drawbacks and advantages of vehicle selection for drug formulation. *European Journal of Cancer*, 37(13), pp.1590–1598.

Gnant, M., Harbeck, N. & Thomssen, C., 2017. St. Gallen/Vienna 2017: A Brief Summary of the Consensus Discussion about Escalation and De-Escalation of Primary Breast Cancer Treatment. *Breast Care*, 12(2), pp.102–107.

Gottesman, M.M., 2002. Mechanisms of Cancer Drug Resistance. *Annual Review of Medicine*, 53(1), pp.615–627.

Gray, J.M. et al., 2017. State of the evidence 2017: an update on the connection between breast cancer and the environment. *Environmental health : a global access science source*, 16(1), p.94.

Gregory, P.A. et al., 2008. The miR-200 family and miR-205 regulate epithelial to mesenchymal transition by targeting ZEB1 and SIP1. *Nature Cell Biology*, 10(5), pp.593–601.

Gregory, R.I. et al., 2005. Human RISC couples microRNA biogenesis and posttranscriptional gene silencing. *Cell*, 123(4), pp.631–640.

Griffiths-Jones, S. et al., 2006. miRBase: microRNA sequences, targets and gene nomenclature. *Nucleic acids research*, 34(Database issue), pp.D140-4.

Guescini, M. et al., 2010. C2C12 myoblasts release micro-vesicles containing mtDNA and proteins involved in signal transduction. *Experimental Cell Research*, 316(12), pp.1977–1984.

Gupta, S.C. et al., 2001. Inhibiting NF-κB activation by small molecules as a therapeutic strategy. *Biochimica et biophysica acta*, 1799(10–12), pp.775–87.

Ha, M. & Kim, V.N., 2014. Regulation of microRNA biogenesis. *Nature reviews. Molecular cell biology*, 15(8), pp.509–24.

Han, J. et al., 2006. Molecular Basis for the Recognition of Primary microRNAs by the Drosha-DGCR8 Complex. *Cell*, 125(5), pp.887–901.

Hanahan, D. & Weinberg, R.A., 2011. Hallmarks of cancer: The next generation. *Cell*, 144(5), pp.646–674.

Hansen, T.F. et al., 2015. Changes in circulating microRNA-126 during treatment with chemotherapy and bevacizumab predicts treatment response in patients with metastatic colorectal cancer. *British Journal of Cancer*, 112(4), pp.624–629.

Harding, C., Heuser, J. & Stahl, P., 1983. Receptor-mediated endocytosis of transferrin and recycling of the transferrin receptor in rat reticulocytes. *The Journal of cell biology*, 97(2), pp.329–39.

Hashiguchi, Y. et al., 2015. Chemotherapy-induced neutropenia and febrile neutropenia in patients with gynecologic malignancy. *Anti-Cancer Drugs*, 26(10), pp.1054–1060.

Hayes, J., Peruzzi, P.P. & Lawler, S., 2014. MicroRNAs in cancer: biomarkers, functions and therapy. *Trends in molecular medicine*, 20(8), pp.460–9.

He, L. et al., 2007. A microRNA component of the p53 tumour suppressor network. *Nature*, 447(7148), pp.1130–4.

Henke, J.I. et al., 2008. microRNA-122 stimulates translation of hepatitis C virus RNA. *The EMBO journal*, 27(24), pp.3300–10.

Hessvik, N.P. & Llorente, A., 2018. Current knowledge on exosome biogenesis and release. *Cellular and molecular life sciences : CMLS*, 75(2), pp.193–208.

Hoesel, B. & Schmid, J.A., 2013. The complexity of NF-κB signaling in inflammation and cancer. *Molecular Cancer*, 12(1), p.1.

Von Hoff, D.D. et al., 2013. Increased Survival in Pancreatic Cancer with nab-Paclitaxel plus Gemcitabine. *New England Journal of Medicine*, 369(18), pp.1691–1703.

Hoshino, A. et al., 2015. Tumour exosome integrins determine organotropic metastasis. *Nature*, 527(7578), pp.329–35.

Housman, G. et al., 2014. Drug resistance in cancer: an overview. *Cancers*, 6(3), pp.1769–92.

Hu, J. et al., 2012. MiR-122 in hepatic function and liver diseases. *Protein and Cell*, 3(5), pp.364–371.

Huang, Q. et al., 2008. The microRNAs miR-373 and miR-520c promote tumour invasion and metastasis. *Nature Cell Biology*, 10(2), pp.202–210.

Huang, X. et al., 2013. Characterization of human plasma-derived exosomal RNAs by deep sequencing. *BMC genomics*, 14(1), p.319.

Huang, Y.-W. et al., 2009. Epigenetic repression of microRNA-129-2 leads to overexpression of SOX4 oncogene in endometrial cancer. *Cancer research*, 69(23), pp.9038–46.

Humphries, B. et al., 2014. MicroRNA-200b targets protein kinase Cα and suppresses triple-negative breast cancer metastasis. *Carcinogenesis*, 35(10), pp.2254–2263.

Huntzinger, E. & Izaurralde, E., 2011. Gene silencing by microRNAs: contributions of translational repression and mRNA decay. *Nature reviews. Genetics*, 12(2), pp.99–110.

Hurley, J.H. & Hanson, P.I., 2010. Membrane budding and scission by the ESCRT machinery: it's all in the neck. *Nature Reviews Molecular Cell Biology*, 11(8), pp.556–566.

Hurwitz, S.N. et al., 2016. Nanoparticle analysis sheds budding insights into genetic drivers of extracellular vesicle biogenesis. *Journal of Extracellular Vesicles*, 5(1), p.31295.

Ifergan, I., Scheffer, G.L. & Assaraf, Y.G., 2005. Novel extracellular vesicles mediate an ABCG2-dependent anticancer drug sequestration and resistance. *Cancer Research*, 65(23), pp.10952–10958.

Ithimakin, S. & Chuthapisith, S., 2013. Neoadjuvant Chemotherapy for Breast Cancer. In *Neoadjuvant Chemotherapy - Increasing Relevance in Cancer Management*. InTech, pp. 43–50.

Jain, K.K. et al., 1985. A prospective randomized comparison of epirubicin and doxorubicin in patients with advanced breast cancer. *Journal of Clinical Oncology*, 3(6), pp.818–826.

Jaiswal, R. et al., 2012. Microparticle conferred microRNA profiles--implications in the transfer and dominance of cancer traits. *Molecular cancer*, 11, p.37.

Jansen, F. et al., 2013. Endothelial microparticle-mediated transfer of MicroRNA-126 promotes vascular endothelial cell repair via SPRED1 and is abrogated in glucose-damaged endothelial microparticles. *Circulation*, 128(18), pp.2026–38.

Janssen, H.L.A. et al., 2013. Treatment of HCV Infection by Targeting MicroRNA. *New England Journal of Medicine*, 368(18), pp.1685–1694.

Jin, S. et al., 2003. Gadd45a contributes to p53 stabilization in response to DNA damage. *Oncogene*, 22(52), pp.8536–8540.

Johnstone, R.M. et al., 1987. Vesicle formation during reticulocyte maturation. Association of plasma membrane activities with released vesicles (exosomes). *Journal of Biological Chemistry*, 262(19), pp.9412–9420.

de Jong, O.G. et al., 2012. Cellular stress conditions are reflected in the protein and RNA content of endothelial cell-derived exosomes. *Journal of Extracellular Vesicles*, 1(1),

pp.1–12.

Jopling, C.L. et al., 2005. Modulation of hepatitis C virus RNA abundance by a liver-specific MicroRNA. *Science (New York, N.Y.)*, 309(5740), pp.1577–81.

Jordan, M.A. et al., 1993. Mechanism of mitotic block and inhibition of cell proliferation by taxol at low concentrations. *Proceedings of the National Academy of Sciences of the United States of America*, 90(20), pp.9552–6.

Junttila, M.R. & De Sauvage, F.J., 2013. Influence of tumour micro-environment heterogeneity on therapeutic response. *Nature*, 501(7467), pp.346–354.

Kahlert, C. et al., 2014. Identification of double-stranded genomic DNA spanning all chromosomes with mutated KRAS and p53 DNA in the serum exosomes of patients with pancreatic cancer. *The Journal of biological chemistry*, 289(7), pp.3869–75.

Kalluri, R. & LeBleu, V.S., 2016. Discovery of Double-Stranded Genomic DNA in Circulating Exosomes. *Cold Spring Harbor symposia on quantitative biology*, 81, pp.275–280.

Kalra, H. et al., 2012. Vesiclepedia: A Compendium for Extracellular Vesicles with Continuous Community Annotation. *PLoS Biology*, 10(12), p.e1001450.

Kanada, M., Bachmann, M.H. & Contag, C.H., 2016. Signaling by Extracellular Vesicles Advances Cancer Hallmarks. *Trends in cancer*, 2(2), pp.84–94.

Karaayvaz, M., Zhai, H. & Ju, J., 2013. MiR-129 promotes apoptosis and enhances chemosensitivity to 5-fluorouracil in colorectal cancer. *Cell Death and Disease*, 4(6).

Kavallaris, M. et al., 1997. Taxol-resistant epithelial ovarian tumors are associated with altered expression of specific beta-tubulin isotypes. *Journal of Clinical Investigation*, 100(5), pp.1282–1293.

Keklikoglou, I. et al., 2012. MicroRNA-520/373 family functions as a tumor suppressor in estrogen receptor negative breast cancer by targeting NF-κB and TGF-β signaling pathways. *Oncogene*, 31(37), pp.4150–63.

Keller, S. et al., 2006. Exosomes: From biogenesis and secretion to biological function. *Immunology Letters*, 107(2), pp.102–108.

Kenicer, J. et al., 2014. Molecular characterisation of isogenic taxane resistant cell lines identify novel drivers of drug resistance. *BMC Cancer*, 14(1), pp.1–10.

Khongkow, M. et al., 2013. SIRT6 modulates paclitaxel and epirubicin resistance and survival in breast cancer. *Carcinogenesis*, 34(7), pp.1476–1486.

Khvorova, A., Reynolds, A. & Jayasena, S.D., 2003. Functional siRNAs and miRNAs exhibit strand bias. *Cell*, 115(2), pp.209–16.

Kim, D.K. et al., 2015. EVpedia: A community web resource for prokaryotic and eukaryotic extracellular vesicles research. *Seminars in Cell and Developmental Biology*, 40, pp.4–7.

Kim, M.S. et al., 2016. Development of exosome-encapsulated paclitaxel to overcome MDR in cancer cells. *Nanomedicine: Nanotechnology, Biology and Medicine*, 12(3), pp.655–664.

Kim, V.N., Han, J. & Siomi, M.C., 2009. Biogenesis of small RNAs in animals. *Nature Reviews Molecular Cell Biology*, 10(2), pp.126–139.

Koliha, N. et al., 2016. A novel multiplex bead-based platform highlights the diversity of extracellular vesicles. *Journal of extracellular vesicles*, 5(17), p.29975.

Kowal, J. et al., 2016. Proteomic comparison defines novel markers to characterize heterogeneous populations of extracellular vesicle subtypes. *Proceedings of the National Academy of Sciences of the United States of America*, 113(8), pp.E968-77.

Kozomara, A. & Griffiths-Jones, S., 2014. MiRBase: Annotating high confidence microRNAs using deep sequencing data. *Nucleic Acids Research*, 42(D1), pp.D68–D73.

Krol, J., Loedige, I. & Filipowicz, W., 2010. The widespread regulation of microRNA biogenesis, function and decay. *Nature reviews. Genetics*, 11(9), pp.597–610.

Krützfeldt, J. et al., 2005. Silencing of microRNAs in vivo with "antagomirs". *Nature*, 438(7068), pp.685–9.

Kuang, Y. et al., 2013. Repression of Dicer is associated with invasive phenotype and chemoresistance in ovarian cancer. *Oncology letters*, 5(4), pp.1149–1154.

Kumar, M.S. et al., 2007. Impaired microRNA processing enhances cellular transformation and tumorigenesis. *Nature Genetics*, 39(5), pp.673–677.

Kutay, H. et al., 2006. Downregulation of miR-122 in the rodent and human hepatocellular carcinomas. *Journal of cellular biochemistry*, 99(3), pp.671–8.

Kwok, J.C. & Richardson, D.R., 2002. Unexpected anthracycline-mediated alterations in iron-regulatory protein-RNA-binding activity: the iron and copper complexes of anthracyclines decrease RNA-binding activity. *Molecular pharmacology*, 62(4), pp.888–900.

Lagos-Quintana, M. et al., 2002. Identification of Tissue-Specific MicroRNAs from Mouse ated proteins from RNA degradation. These putative proteins may as well mediate the translational suppres-sion. The miRNA precursor processing reaction requires Department of Cellular Biochemistry Dic. *Current Biology*, 12(02), pp.735–739.

Lai, N.-S. et al., 2017. The role of aberrant expression of T cell miRNAs affected by TNF-α in the immunopathogenesis of rheumatoid arthritis. *Arthritis research & therapy*, 19(1), p.261.

Lam, S.W., Jimenez, C.R. & Boven, E., 2014. Breast cancer classification by proteomic technologies: current state of knowledge. *Cancer treatment reviews*, 40(1), pp.129–38.

Laudadio, I. et al., 2012. A feedback loop between the liver-enriched transcription factor network and miR-122 controls hepatocyte differentiation. *Gastroenterology*, 142(1), pp.119–129.

Laulagnier, K. et al., 2004. Mast cell- and dendritic cell-derived exosomes display a specific lipid composition and an unusual membrane organization. *The Biochemical journal*, 380(Pt 1), pp.161–71.

Lee, R.C., Feinbaum, R.L. & Ambros, V., 1993. The C. elegans heterochronic gene lin-4 encodes small RNAs with antisense complementarity to lin-14. *Cell*, 75(5), pp.843–54.

Lee, Y. et al., 2004. MicroRNA genes are transcribed by RNA polymerase II. *The EMBO journal*, 23(20), pp.4051–60.

Li, L. et al., 2012. Argonaute 2 Complexes Selectively Protect the Circulating MicroRNAs in Cell-Secreted Microvesicles D. T. Starczynowski, ed. *PLoS ONE*, 7(10), pp.1–9.

Li, M.H. et al., 2013. Down-Regulation of miR-129-5p Inhibits Growth and Induces Apoptosis in Laryngeal Squamous Cell Carcinoma by Targeting APC. *PLoS ONE*, 8(10), pp.1–10.

Lieberman, J., 2018. Tapping the RNA world for therapeutics. *Nature Structural & Molecular Biology*, 25(5), pp.357–364.

Lin, S. & Gregory, R.I., 2015. MicroRNA biogenesis pathways in cancer. *Nature reviews. Cancer*, 15(6), pp.321–333.

Liu, D. et al., 2018. Circulating apoptotic bodies maintain mesenchymal stem cell homeostasis and ameliorate osteopenia via transferring multiple cellular factors. *Cell research*, 28(9), pp.918–933.

Lombardi, D. et al., 2004. Long-term, weekly one-hour infusion of paclitaxel in patients with metastatic breast cancer: a phase II monoinstitutional study. *Tumori*, 90(3), pp.285–8.

Love, M.I., Huber, W. & Anders, S., 2014. Moderated estimation of fold change and dispersion for RNA-seq data with DESeq2. *Genome biology*, 15(12), p.550.

Lu, J. et al., 2005. MicroRNA expression profiles classify human cancers. *Nature*, 435(7043), pp.834–838.

Luan, X. et al., 2017. Engineering exosomes as refined biological nanoplatforms for drug delivery. *Nature Publishing Group*, 38(6), pp.754–763.

Ludwig, N. et al., 2016. Distribution of miRNA expression across human tissues. *Nucleic Acids Research*, 44(8), pp.3865–3877.

Lugini, L. et al., 2012. Immune Surveillance Properties of Human NK Cell-Derived Exosomes. *The Journal of Immunology*, 189(6), pp.2833–2842.

Lund, E. et al., 2004. Nuclear Export of MicroRNA Precursors. *Science*, 303(5654), pp.95–98.

Lv, M. meng et al., 2014. Exosomes mediate drug resistance transfer in MCF-7 breast cancer cells and a probable mechanism is delivery of P-glycoprotein. *Tumor Biology*, 35(11), pp.10773–10779.

Ma, L., Teruya-feldstein, J. & Weinberg, R.A., 2007. Tumour invasion and metastasis initiated by microRNA-10b in breast cancer. , 449(October).

Ma, Y. et al., 2013. Anticancer chemotherapy-induced intratumoral recruitment and differentiation of antigen-presenting cells. *Immunity*, 38(4), pp.729–741.

Macfarlane, L.-A. & Murphy, P.R., 2010. MicroRNA: Biogenesis, Function and Role in Cancer. *Current genomics*, 11(7), pp.537–61.

Mahn, R. et al., 2011. Circulating microRNAs (miRNA) in serum of patients with prostate cancer. *Urology*, 77(5), p.1265.e9-1265.e16.

Maia, J. et al., 2018. Exosome-Based Cell-Cell Communication in the Tumor Microenvironment. *Frontiers in Cell and Developmental Biology*, 6(6), p.18.

Malhotra, G.K. et al., 2010. Histological, molecular and functional subtypes of breast cancers. *Cancer Biology and Therapy*, 10(10), pp.955–960.

Mallini, P. et al., 2014. Epithelial-to-mesenchymal transition: What is the impact on breast cancer stem cells and drug resistance. *Cancer Treatment Reviews*, 40(3), pp.341–348.

Malone, K.E. et al., 2006. Prevalence and Predictors of BRCA1 and BRCA2 Mutations in a Population-Based Study of Breast Cancer in White and Black American Women Ages 35 to 64 Years. *Cancer Research*, 66(16), pp.8297–8308.

Mani, S.A. et al., 2008. The Epithelial-Mesenchymal Transition Generates Cells with Properties of Stem Cells. *Cell*, 133(4), pp.704–715.

Marleau, A.M. et al., 2012. Exosome removal as a therapeutic adjuvant in cancer. *Journal of Translational Medicine*, 10(1), p.134.

Martello, L.A. et al., 2003. Elevated levels of microtubule destabilizing factors in a Taxol-resistant/dependent A549 cell line with an alpha-tubulin mutation. *Cancer research*, 63(6), pp.1207–13.

Masoud, V. & Pagès, G., 2017. Targeted therapies in breast cancer: New challenges to fight against resistance. *World Journal of Clinical Oncology*, 8(2), p.120.

Massagué, J., 2008. TGFbeta in Cancer. *Cell*, 134(2), pp.215–30.

Mathivanan, S. et al., 2012. ExoCarta 2012: Database of exosomal proteins, RNA and lipids. *Nucleic Acids Research*, 40(D1), pp.1241–1244.

Matsen, C.B. & Neumayer, L.A., 2013. Breast cancer: A review for the general surgeon. *JAMA Surgery*, 148(10), pp.971–979.

McKelvey, K.J. et al., 2015. Exosomes: Mechanisms of Uptake. *Journal of Circulating Biomarkers*, 4, p.1.

Van Der Meel, R. et al., 2014. Extracellular vesicles as drug delivery systems: Lessons from the liposome field. *Journal of Controlled Release*, 195, pp.72–85.

Meng, X. et al., 2016. Circulating Cell-Free miR-373, miR-200a, miR-200b and miR-200c in Patients with Epithelial Ovarian Cancer. *Advances in experimental medicine and biology*, 924(13), pp.3–8.

Michell, D.L. & Vickers, K.C., 2016. Lipoprotein carriers of microRNAs. *Biochimica et biophysica acta*, 1861(12 Pt B), pp.2069–2074.

Michelotti, A. et al., 2000. Single agent epirubicin as first line chemotherapy for metastatic breast cancer patients. *Breast Cancer Res Treat*, 59(2), pp.133–139.

Minciacchi, V.R. et al., 2016. the Emerging Role of Large Oncosomes. *Semin Cell Dev Biol*, 40, pp.41–51.

Minotti, G., 2004. Anthracyclines: Molecular Advances and Pharmacologic Developments in Antitumor Activity and Cardiotoxicity. *Pharmacological Reviews*, 56(2), pp.185–229.

Mitchell, P.S. et al., 2008. Circulating microRNAs as stable blood-based markers for cancer detection. *Proceedings of the National Academy of Sciences of the United States of America*, 105(30), pp.10513–8.

Mittelbrunn, M., Vicente-Manzanares, M. & S??nchez-Madrid, F., 2015. Organizing polarized delivery of exosomes at synapses. *Traffic*, 16(4), pp.327–337.

Möbius, W. et al., 2002. Immunoelectron Microscopic Localization of Cholesterol Using Biotinylated and Non-cytolytic Perfringolysin O. *Journal of Histochemistry &*

Cytochemistry, 50(1), pp.43–55.

Montecalvo, A. et al., 2012. Mechanism of transfer of functional microRNAs between mouse dendritic cells via exosomes. *Blood*, 119(3), pp.756–66.

Mørch, L.S. et al., 2018. Contemporary hormonal contraception and the risk of breast cancer. *Obstetrical and Gynecological Survey*, 73(4), pp.215–217.

Morel, A.P. et al., 2008. Generation of breast cancer stem cells through epithelial-mesenchymal transition. *PLoS ONE*, 3(8), pp.1–7.

Morse, M.A. et al., 2005. A phase I study of dexosome immunotherapy in patients with advanced non-small cell lung cancer. *Journal of Translational Medicine*, 3(1), p.9.

Mukherjee, A., Di Bisceglie, A.M. & Ray, R.B., 2015. Hepatitis C Virus-Mediated Enhancement of MicroRNA miR-373 Impairs the JAK/STAT Signaling Pathway. *Journal of Virology*, 89(6), pp.3356–3365.

Müller, V. et al., 2014. Changes in serum levels of miR-21, miR-210, and miR-373 in HER2-positive breast cancer patients undergoing neoadjuvant therapy: a translational research project within the Geparquinto trial. *Breast Cancer Research and Treatment*, 147(1), pp.61–68.

Nakanishi, K., 2016. Anatomy of RISC: how do small RNAs and chaperones activate Argonaute proteins? *Wiley interdisciplinary reviews. RNA*, 7(5), pp.637–60.

Nakao, K., Miyaaki, H. & Ichikawa, T., 2014. Antitumor function of microRNA-122 against hepatocellular carcinoma. *Journal of gastroenterology*, 49(4), pp.589–93.

Narod, S.A., 2006. Modifiers of risk of hereditary breast cancer. *Oncogene*, 25(43), pp.5832–5836.

Neesse, A. et al., 2014. SPARC independent drug delivery and antitumour effects of nab-paclitaxel in genetically engineered mice. *Gut*, 63(6), pp.974–83.

Neil, J.R. & Schiemann, W.P., 2008. Altered TAB1:IκB kinase interaction promotes transforming growth factor β-mediated nuclear factor-κB activation during breast cancer progression. *Cancer Research*, 68(5), pp.1462–1470.

Neuzillet, C. et al., 2015. Targeting the TGFβ pathway for cancer therapy. *Pharmacology & therapeutics*, 147, pp.22–31.

Niculescu, L.S. et al., 2015. MiR-486 and miR-92a Identified in Circulating HDL Discriminate between Stable and Vulnerable Coronary Artery Disease Patients. K. Jeyaseelan, ed. *PloS one*, 10(10), p.e0140958.

van Niel, G., D'Angelo, G. & Raposo, G., 2018. Shedding light on the cell biology of extracellular vesicles. *Nature reviews. Molecular cell biology*, 19(4), pp.213–228.

Nolte'T Hoen, E.N.M. et al., 2012. Deep sequencing of RNA from immune cell-derived vesicles uncovers the selective incorporation of small non-coding RNA biotypes with potential regulatory functions. *Nucleic Acids Research*, 40(18), pp.9272–9285.

O'Brien, J. et al., 2018. Overview of MicroRNA Biogenesis, Mechanisms of Actions, and Circulation. *Frontiers in endocrinology*, 9, p.402.

O'Brien, K. et al., 2015. miR-134 in extracellular vesicles reduces triple-negative breast cancer aggression and increases drug sensitivity. *Oncotarget*, 6(32), pp.32774–32789.

Ørom, U.A., Nielsen, F.C. & Lund, A.H., 2008. MicroRNA-10a binds the 5'UTR of

ribosomal protein mRNAs and enhances their translation. *Molecular cell*, 30(4), pp.460–71.

Ostenfeld, M.S. et al., 2014. Cellular disposal of miR23b by RAB27-dependent exosome release is linked to acquisition of metastatic properties. *Cancer Research*, 74(20), pp.5758–5771.

Ouyang, M. et al., 2014. MicroRNA profiling implies new markers of chemoresistance of triple-negative breast cancer. P. Rameshwar, ed. *PloS one*, 9(5), p.e96228.

Paller, C.J. & Antonarakis, E.S., 2011. Cabazitaxel: A novel second-line treatment for metastatic castration-resistant prostate cancer. *Drug Design, Development and Therapy*, 5(5), pp.117–124.

Pan, B.T. & Johnstone, R.M., 1983. Fate of the transferrin receptor during maturation of sheep reticulocytes in vitro: Selective externalization of the receptor. *Cell*, 33(3), pp.967–978.

Pan, C. et al., 2016. MiR-122 reverses the doxorubicin-resistance in hepatocellular carcinoma cells through regulating the tumor metabolism. *PLoS ONE*, 11(5), pp.1–15.

Pan, X., Wang, Z.X. & Wang, R., 2010. MicroRNA-21: A novel therapeutic target in human cancer. *Cancer Biology and Therapy*, 10(12), pp.1224–1232.

Pang, B. et al., 2015. Chemical profiling of the genome with anti-cancer drugs defines target specificities. *Nature Chemical Biology*, 11(7), pp.472–480.

Pascucci, L. et al., 2014. Paclitaxel is incorporated by mesenchymal stromal cells and released in exosomes that inhibit in vitro tumor growth: A new approach for drug delivery. *Journal of Controlled Release*, 192, pp.262–270.

Paul Launchbury, A. & Habboubi, N., 1993. Epirubicin and doxorubicin: a comparison of their characteristics, therapeutic activity and toxicity. *Cancer Treatment Reviews*, 19(3), pp.197–228.

Pauley, K.M. et al., 2006. Formation of GW bodies is a consequence of microRNA genesis. *EMBO reports*, 7(9), pp.904–10.

Pegtel, D.M. et al., 2010. Functional delivery of viral miRNAs via exosomes. *Proceedings of the National Academy of Sciences of the United States of America*, 107(14), pp.6328–33.

Peinado, H. et al., 2012. Melanoma exosomes educate bone marrow progenitor cells toward a pro-metastatic phenotype through MET. *Nature Medicine*, 18(6), pp.883–891.

Pérez-Boza, J., Lion, M. & Struman, I., 2018. Exploring the RNA landscape of endothelial exosomes. *RNA*, 24(3), pp.423–435.

Perou, C.M. et al., 2000. Molecular portraits of human breast tumours. *Nature*, 406(6797), pp.747–52.

Petri, S. et al., 2011. Increased siRNA duplex stability correlates with reduced off-target and elevated on-target effects. *RNA*, 17(4), pp.737–749.

Piasecka, D. et al., 2018. MicroRNAs in regulation of triple-negative breast cancer progression. *Journal of Cancer Research and Clinical Oncology*, pp.1–11.

Pires, B.R.B. et al., 2017. NF-kappaB Is Involved in the Regulation of EMT Genes in Breast Cancer Cells. R. Samant, ed. *PloS one*, 12(1), p.e0169622.

Place, R.F. et al., 2008. MicroRNA-373 induces expression of genes with complementary promoter sequences. *Proceedings of the National Academy of Sciences of the United States of America*, 105(5), pp.1608–13.

Plebanek, M.P. et al., 2017. Pre-metastatic cancer exosomes induce immune surveillance by patrolling monocytes at the metastatic niche. *Nature Communications*, 8(1), p.1319.

Prieto-Vila, M. et al., 2017. Drug resistance driven by cancer stem cells and their niche. *International Journal of Molecular Sciences*, 18(12).

Rakha, E.A. & Green, A.R., 2017. Molecular classification of breast cancer: what the pathologist needs to know. *Pathology*, 49(2), pp.111–119.

Rana, S. et al., 2012. Toward tailored exosomes: The exosomal tetraspanin web contributes to target cell selection. *International Journal of Biochemistry and Cell Biology*, 44(9), pp.1574–1584.

Rao, M. et al., 2017. MicroRNA-122 inhibits proliferation and invasion in gastric cancer by targeting CREB1. *American journal of cancer research*, 7(2), pp.323–333.

Rao, S. et al., 1994. 3'-(p-azidobenzamido)taxol photolabels the N-terminal 31 amino acids of beta-tubulin. *The Journal of biological chemistry*, 269(5), pp.3132–4.

Raposo, G. & Stoorvogel, W., 2013. Extracellular vesicles: Exosomes, microvesicles, and friends. *Journal of Cell Biology*, 200(4), pp.373–383.

Richards, K.E. et al., 2017. Cancer-associated fibroblast exosomes regulate survival and proliferation of pancreatic cancer cells. *Oncogene*, 36(13), pp.1770–1778.

Robson, M. et al., 2017. Olaparib for Metastatic Breast Cancer in Patients with a Germline BRCA Mutation. *New England Journal of Medicine*, 377(6), pp.523–533.

Roswall, P. et al., 2018. Microenvironmental control of breast cancer subtype elicited through paracrine platelet-derived growth factor-CC signaling. *Nature Medicine*, 24(4), pp.463–473.

Rowinsky, E.K. et al., 1993. Clinical toxicities encountered with paclitaxel (Taxol). *Seminars in oncology*, 20(4 Suppl 3), pp.1–15.

Rowinsky, E.K. & Donehower, R.C., 1995. Paclitaxel (Taxol) A. J. J. Wood, ed. *New England Journal of Medicine*, 332(15), pp.1004–1014.

Safaei, R. et al., 2005. Abnormal lysosomal trafficking and enhanced exosomal export of cisplatin in drug-resistant human ovarian carcinoma cells. *Molecular cancer therapeutics*, 4(10), pp.1595–604.

Salehan, M.R. & Morse, H.R., 2013. DNA damage repair and tolerance: A role in chemotherapeutic drug resistance. *British Journal of Biomedical Science*, 70(1), pp.31–40.

Sandfeld-Paulsen, B. et al., 2016. Exosomal Proteins as Diagnostic Biomarkers in Lung Cancer. *Journal of Thoracic Oncology*, 11(10), pp.1701–1710.

Sandhu, H. & Maddock, H., 2014. Molecular basis of cancer-therapy-induced cardiotoxicity: introducing microRNA biomarkers for early assessment of subclinical myocardial injury. *Clinical Science*, 126(6), pp.377–400.

Sandhu, R. et al., 2010. Microarray-Based Gene Expression Profiling for Molecular Classification of Breast Cancer and Identification of New Targets for Therapy.

Laboratory Medicine, 41(6), pp.364–372.

Schiff, P.B., Fant, J. & Horwitz, S.B., 1979. Promotion of microtubule assembly in vitro by taxol. *Nature*, 277(5698), pp.665–667.

Schmidt, O. & Teis, D., 2012. The ESCRT machinery. *Current biology : CB*, 22(4), pp.R116-20.

Senkus, E. et al., 2015. Primary breast cancer: ESMO Clinical Practice Guidelines for diagnosis, treatment and follow-up. *Annals of Oncology*, 26(suppl 5), pp.v8–v30.

Serasanambati, M. & Chilakapati, S.R., 2016. Function of Nuclear Factor Kappa B (NF-kB) in Human Diseases-A Review. *South Indian Journal of Biological Sciences*, 2(4), p.368.

Sherman-Baust, C.A. et al., 2011. Gene expression and pathway analysis of ovarian cancer cells selected for resistance to cisplatin, paclitaxel, or doxorubicin. *Journal of Ovarian Research*, 4(1), pp.1–11.

Shimakami, T. et al., 2012. Stabilization of hepatitis C virus RNA by an Ago2-miR-122 complex. *Proceedings of the National Academy of Sciences of the United States of America*, 109(3), pp.941–6.

Shurtleff, M.J. et al., 2016. Y-box protein 1 is required to sort microRNAs into exosomes in cells and in a cell-free reaction. , pp.1–23.

Silversmit, G. et al., 2017. Cancer Incidence Projections in Belgium, 2015 to 2025. *Belgian Cancer Registry*.

Singh, A. & Settleman, J., 2010. EMT, cancer stem cells and drug resistance: An emerging axis of evil in the war on cancer. *Oncogene*, 29(34), pp.4741–4751.

Skog, J. et al., 2008. Glioblastoma microvesicles transport RNA and proteins that promote tumour growth and provide diagnostic biomarkers. *Nature Cell Biology*, 10(12), pp.1470–1476.

Smith, B. & Bhowmick, N., 2016. Role of EMT in Metastasis and Therapy Resistance. *Journal of Clinical Medicine*, 5(2), p.17.

Sondka, Z. et al., 2018. The COSMIC Cancer Gene Census: describing genetic dysfunction across all human cancers. *Nature Reviews Cancer*, 18(november).

Sotiriou, C. et al., 2003. Breast cancer classification and prognosis based on gene expression profiles from a population-based study. *Proceedings of the National Academy of Sciences of the United States of America*, 100(18), pp.10393–8.

de Souza, P.S. et al., 2015. Microparticles induce multifactorial resistance through oncogenic pathways independently of cancer cell type. *Cancer Science*, 106(1), pp.60–68.

Stanzione, R. et al., 2017. A Decrease of Brain MicroRNA-122 Level Is an Early Marker of Cerebrovascular Disease in the Stroke-Prone Spontaneously Hypertensive Rat. *Oxidative Medicine and Cellular Longevity*, 2017, pp.1–13.

Stegeman, S. et al., 2015. A genetic variant of MDM4 influences regulation by multiple microRNAs in prostate cancer. *Endocrine-related cancer*, 22(2), pp.265–76.

Suarez-Carmona, M. et al., 2015. Soluble factors regulated by epithelial-mesenchymal transition mediate tumour angiogenesis and myeloid cell recruitment. *Journal of Pathology*, 236(4), pp.491–504.

Subramanian, A. et al., 2005. Gene set enrichment analysis: A knowledge-based approach for interpreting genome-wide expression profiles. *Proceedings of the National Academy of Sciences*, 102(43), pp.15545–15550.

Suh, M.-R. et al., 2004. Human embryonic stem cells express a unique set of microRNAs. *Developmental biology*, 270(2), pp.488–98.

Sun, G. et al., 2009. SNPs in human miRNA genes affect biogenesis and function. *RNA (New York, N.Y.)*, 15(9), pp.1640–51.

Sun, J. et al., 2017. A systematic analysis of FDA-approved anticancer drugs. *BMC Systems Biology*, 11(Suppl 5), p.87.

Sun, T. et al., 2009. The role of microRNA-221 and microRNA-222 in androgen-independent prostate cancer cell lines. *Cancer research*, 69(8), pp.3356–63.

Svensson, K.J. et al., 2013. Exosome uptake depends on ERK1/2-heat shock protein 27 signaling and lipid raft-mediated endocytosis negatively regulated by caveolin-1. *Journal of Biological Chemistry*, 288(24), pp.17713–17724.

Tabet, F. et al., 2014. HDL-transferred microRNA-223 regulates ICAM-1 expression in endothelial cells. *Nature communications*, 5, p.3292.

Taylor, D.D. & Gercel-Taylor, C., 2008. MicroRNA signatures of tumor-derived exosomes as diagnostic biomarkers of ovarian cancer. *Gynecologic oncology*, 110(1), pp.13–21.

Théry, C. et al., 2018. Minimal information for studies of extracellular vesicles 2018 (MISEV2018): a position statement of the International Society for Extracellular Vesicles and update of the MISEV2014 guidelines. *Journal of Extracellular Vesicles*, 7(1), p.1535750.

Théry, C. et al., 2001. Proteomic Analysis of Dendritic Cell-Derived Exosomes: A Secreted Subcellular Compartment Distinct from Apoptotic Vesicles. *Journal of Immunology*, (166), pp.7309–7318.

Théry, C., Zitvogel, L. & Amigorena, S., 2002. Exosomes: composition, biogenesis and function. *Nature reviews. Immunology*, 2(8), pp.569–579.

Thuault, S. et al., 2006. Transforming growth factor-β employs HMGA2 to elicit epithelial-mesenchymal transition. *Journal of Cell Biology*, 174(2), pp.175–183.

Tian, T. et al., 2014. Exosome uptake through clathrin-mediated endocytosis and macropinocytosis and mediating miR-21 delivery. *The Journal of biological chemistry*, 289(32), pp.22258–67.

Trajkovic, K. et al., 2008. Ceramide triggers budding of exosome vesicles into multivesicular endosomes. *Science (New York, N.Y.)*, 319(5867), pp.1244–1247.

Turchinovich, A. et al., 2011. Characterization of extracellular circulating microRNA. *Nucleic Acids Research*, 39(16), pp.7223–7233.

Turchinovich, A. & Burwinkel, B., 2012. Distinct AGO1 and AGO2 associated miRNA profiles in human cells and blood plasma. *RNA biology*, 9(8), pp.1066–75.

Ullmann, P. et al., 2018. The miR-371~373 Cluster Represses Colon Cancer Initiation and Metastatic Colonization by Inhibiting the TGFBR2/ID1 Signaling Axis. *Cancer Research*, 78(14), pp.3793–3808.

Umezu, T. et al., 2013. Leukemia cell to endothelial cell communication via exosomal miRNAs. *Oncogene*, 32(22), pp.2747–2755.

Valadi, H. et al., 2007. Exosome-mediated transfer of mRNAs and microRNAs is a novel mechanism of genetic exchange between cells. *Nature cell biology*, 9(6), pp.654–659.

Vasudevan, S. & Steitz, J.A., 2007. AU-rich-element-mediated upregulation of translation by FXR1 and Argonaute 2. *Cell*, 128(6), pp.1105–18.

Viale, G., 2012. The current state of breast cancer classification. *Annals of Oncology*, 23(SUPPL. 10).

Vickers, K.C. et al., 2011. MicroRNAs are transported in plasma and delivered to recipient cells by high-density lipoproteins. *Nature Cell Biology*, 13(4), pp.423–435.

Villarroya-Beltri, C. et al., 2013. Sumoylated hnRNPA2B1 controls the sorting of miRNAs into exosomes through binding to specific motifs. *Nature communications*, 4, p.2980.

Villeneuve, D.J. et al., 2006. cDNA microarray analysis of isogenic paclitaxel- and doxorubicin-resistant breast tumor cell lines reveals distinct drug-specific genetic signatures of resistance. *Breast Cancer Research and Treatment*, 96(1), pp.17–39.

Vinogradov, S. & Wei, X., 2012. Cancer stem cells and drug resistance: the potential of nanomedicine. *Nanomedicine (London, England)*, 7(4), pp.597–615.

Vlassov, A. V. et al., 2012. Exosomes: Current knowledge of their composition, biological functions, and diagnostic and therapeutic potentials. *Biochimica et Biophysica Acta - General Subjects*, 1820(7), pp.940–948.

Volkova, M. & Russell, R., 2012. Anthracycline Cardiotoxicity: Prevalence, Pathogenesis and Treatment. *Current Cardiology Reviews*, 7(4), pp.214–220.

Voorhoeve, P.M. et al., 2007. A genetic screen implicates miRNA-372 and miRNA-373 as oncogenes in testicular germ cell tumors. *Advances in Experimental Medicine and Biology*, 604, pp.17–46.

Wagner, J. et al., 2013. Characterization of levels and cellular transfer of circulating lipoprotein-bound microRNAs. *Arteriosclerosis, Thrombosis, and Vascular Biology*, 33(6), pp.1392–1400.

Wang, J. et al., 2018. UCA1 confers paclitaxel resistance to ovarian cancer through miR-129/ABCB1 axis. *Biochemical and Biophysical Research Communications*, 501(4), pp.1034–1040.

Wang, K. et al., 2010. Export of microRNAs and microRNA-protective protein by mammalian cells. *Nucleic acids research*, 38(20), pp.7248–59.

Wang, P. et al., 2013. The serum miR-21 level serves as a predictor for the chemosensitivity of advanced pancreatic cancer, and miR-21 expression confers chemoresistance by targeting FasL. *Molecular oncology*, 7(3), pp.334–45.

Wani, M.C. et al., 1971. Plant Antitumor Agents.VI.The Isolation and Structure of Taxol, a Novel Antileukemic and Antitumor Agent from Taxus brevifolia2. *Journal of the American Chemical Society*, 93(9), pp.2325–2327.

Webber, J. et al., 2010. Cancer exosomes trigger fibroblast to myofibroblast differentiation. *Cancer research*, 70(23), pp.9621–30.

Wei, F. et al., 2015. Diverse functions of miR-373 in cancer. *Journal of Translational Medicine*, 13(1), p.162.

Wei, Y. et al., 2014. Exosomal miR-221/222 enhances tamoxifen resistance in recipient ER-positive breast cancer cells. *Breast cancer research and treatment*, 147(2),

pp.423–31.

Wei, Z. et al., 2017. Coding and noncoding landscape of extracellular RNA released by human glioma stem cells. *Nature Communications*, 8(1), p.1145.

Wellner, U., Brabletz, T. & Keck, T., 2010. ZEB1 in pancreatic Cancer. *Cancers*, 2(3), pp.1617–1628.

Wen, S.W. et al., 2016. The Biodistribution and Immune Suppressive Effects of Breast Cancer-Derived Exosomes. *Cancer research*, 76(23), pp.6816–6827.

White, I.J. et al., 2006. EGF stimulates annexin 1-dependent inward vesiculation in a multivesicular endosome subpopulation. *The EMBO journal*, 25(1), pp.1–12.

Wilson, R.C. & Doudna, J.A., 2013. Molecular mechanisms of RNA interference. *Annual review of biophysics*, 42(1), pp.217–39.

Winter, J. et al., 2009. Many roads to maturity: microRNA biogenesis pathways and their regulation. *Nature Cell Biology*, 11(3).

Wu, J. et al., 2010. miR-129 regulates cell proliferation by downregulating Cdk6 expression. *Cell Cycle*, 9(9), pp.1809–1818.

Wubbolts, R. et al., 2003. Proteomic and biochemical analyses of human B cell-derived exosomes. Potential implications for their function and multivesicular body formation. *The Journal of biological chemistry*, 278(13), pp.10963–72.

Xia, L. et al., 2008. miR-15b and miR-16 modulate multidrug resistance by targeting BCL2 in human gastric cancer cells. *International journal of cancer*, 123(2), pp.372–379.

Xiong, Z. et al., 2018. LncRNA MALAT1/miR-129 axis promotes glioma tumorigenesis by targeting SOX2. *Journal of Cellular and Molecular Medicine*, 22(8), pp.3929–3940.

Xu, H. et al., 2010. Liver-enriched transcription factors regulate MicroRNA-122 that targets CUTL1 during liver development. *Hepatology*, 52(4), pp.1431–1442.

Xu, S. et al., 2016. MiR-129 predicts prognosis and inhibits cell growth in human prostate carcinoma. *Molecular Medicine Reports*, 14(6), pp.5025–5032.

Xu, Y. et al., 2011. MicroRNA-122 sensitizes HCC cancer cells to adriamycin and vincristine through modulating expression of MDR and inducing cell cycle arrest. *Cancer Letters*, 310(2), pp.160–169.

Yager, J.D. & Davidson, N.E., 2006. Estrogen Carcinogenesis in Breast Cancer. *New England Journal of Medicine*, 354(3), pp.270–282.

Yan, G.R. et al., 2011. Global identification of miR-373-regulated genes in breast cancer by quantitative proteomics. *Proteomics*, 11(5), pp.912–920.

Yang, Y. et al., 2018. Extracellular vesicles as a platform for membrane-associated therapeutic protein delivery. *Journal of Extracellular Vesicles*, 7(1), p.1440131.

Ye, X. et al., 2014. Epigenetic silencing of miR-375 induces trastuzumab resistance in HER2-positive breast cancer by targeting IGF1R. *BMC Cancer*, 14(1), pp.1–12.

Ye, X. & Weinberg, R.A., 2015. Epithelial-Mesenchymal Plasticity: A Central Regulator of Cancer Progression. *Trends in Cell Biology*, 25(11), pp.675–686.

Yekta, S., Shih, I.H. & Bartel, D.P., 2004. MicroRNA-Directed Cleavage of HOXB8

mRNA. *Science*, 304(5670), pp.594–596.

Yin, S., Cabral, F. & Veeraraghavan, S., 2007. Amino acid substitutions at proline 220 of beta-tubulin confer resistance to paclitaxel and colcemid. *Molecular cancer therapeutics*, 6(10), pp.2798–806.

Yu, S. et al., 2007. Tumor exosomes inhibit differentiation of bone marrow dendritic cells. *Journal of immunology (Baltimore, Md. : 1950)*, 178(11), pp.6867–75.

Yue, W. et al., 2013. Estrogen receptor-dependent and independent mechanisms of breast cancer carcinogenesis. *Steroids*, 78(2), pp.161–170.

Zanger, U.M. & Schwab, M., 2013. Cytochrome P450 enzymes in drug metabolism: regulation of gene expression, enzyme activities, and impact of genetic variation. *Pharmacology & therapeutics*, 138(1), pp.103–41.

Zeng, A. et al., 2018. miR-129-5p targets Wnt5a to block PKC/ERK/NF-κB and JNK pathways in glioblastoma. *Cell Death & Disease*, 9(3), p.394.

Zeng, H. et al., 2018. microRNA-129-5p suppresses Adriamycin resistance in breast cancer by targeting SOX2. *Archives of Biochemistry and Biophysics*, 651, pp.52–60.

Zernecke, A. et al., 2009. Delivery of microRNA-126 by apoptotic bodies induces CXCL12-dependent vascular protection. *Science Signaling*, 2(100).

Zhang, Z. et al., 2016. LncRNA HOTAIR controls the expression of Rab22a by sponging miR-373 in ovarian cancer. *Molecular medicine reports*, 14(3), pp.2465–72.

Zhao, H. et al., 2017. KSRP specifies monocytic and granulocytic differentiation through regulating miR-129 biogenesis and RUNX1 expression. *Nature Communications*, 8(1), pp.1–18.

Zhao, H. et al., 2016. Tumor microenvironment derived exosomes pleiotropically modulate cancer cell metabolism. *eLife*, 5(FEBRUARY2016), pp.1–27.

Zhao, R. et al., 2011. Plasma miR-221 as a predictive biomarker for chemoresistance in breast cancer patients who previously received neoadjuvant chemotherapy. *Onkologie*, 34(12), pp.675–680.

Zhong, S. et al., 2016. MicroRNA expression profiles of drug-resistance breast cancer cells and their exosomes. *Oncotarget*, 7(15), pp.19601–19609.

Zhou, W. et al., 2014. Cancer-secreted miR-105 destroys vascular endothelial barriers to promote metastasis. *Cancer cell*, 25(4), pp.501–15.

Zhu, Z. et al., 2017. Macrophage-derived apoptotic bodies promote the proliferation of the recipient cells via shuttling microRNA-221/222. *Journal of leukocyte biology*, 101(6), pp.1349–1359.

Zhuang, G. et al., 2012. Tumour-secreted miR-9 promotes endothelial cell migration and angiogenesis by activating the JAK-STAT pathway. *The EMBO Journal*, 31(17), pp.3513–3523.

Ziebarth, J.D., Bhattacharya, A. & Cui, Y., 2012. Integrative Analysis of Somatic Mutations Altering MicroRNA Targeting in Cancer Genomes S. P. Chellappan, ed. *PLoS ONE*, 7(10), p.e47137.